Y. Ikeda

National Research Council Canada
Institute for Marine Dynamics

Conseil national de recherches Canada
Institut de dynamique marine

NRC·CNRC

4TH INTERNATIONAL SHIP STABILITY WORKSHOP

September 27th- 29th, 1998

St. John's, Newfoundland

Kerwin Place
P.O. Box 12093
Postal Station A
St. John's, Newfoundland
A1B 3T5

Fax: (709) 772-2462

Place Kerwin
C.P. 12093
Station postale A
St-Jean (Terre-Neuve)
A1B 3T5

Télécopieur : (709) 772-2462

Canada

List of Attendees
4th International Ship Stability Workshop
St. John's, Newfoundland, Canada
October 28 and 29, 1998

Tom Allan
Maritime & Coastguard Agency
Spring Place, Rm. 3/1
Southampton, Hants, UK
S015 1EG
+44-1703-329110
(Fax) +44-1703-329264

Don Bass
Memorial University of Newfoundland
St. John's, NF Canada
A1E 1G4
709-737-8950
(Fax) 709-737-4042
dbass@engr.mun.ca

Kate Armstrong
British Columbia Ferry Corporation
1112 Fort Street
Victoria, BC, Canada
V8V 4V2
250-978-1304
(Fax) 250-360-0217
kaper@uniserve.com

Vadim Belenky
National Research Institute of Fisheries
Ebidai, Hasaki
Kashima, Ibaraki, Japan
314-0421
+81-479-44-5942
(Fax) +81-479-44-1875
vadim@nrife.affrc.go.jp

Richard Birmingham
University of Newcastle Upon Tyne
Dept. of Marine Technology
England, UK
NE1 7RU
+44-191-222-6722
(Fax) +44-191-222-5491
r.w.birmingham@ncl.ac.uk

David Cumming
Institute for Marine Dynamics
National Research Council Canada
P.O. Box 12093, Station A
St. John's, NF Canada A1B 3T5
709-772-2266
(Fax) 709-772-2462
dcumming@minnie.imd.nrc.ca

Sander Calisal
University of British Columbia
Mechanical Engineering Dept.
Vancouver, BC
V6R 2T1
604-822-2836
(Fax) 604-822-2403
calisal@mech.ubc.ca

Ian Dand
BMT Seatech Ltd
Director of Hydrodynamics
Bldg. 144, Dera Haslar
Gosport, Hampshire, UK
PO12 2AG
+44-1705-335021
(Fax) +44-705-335018
ian@bmthaslr.demom.co.uk

Liangzi Cong
DalTech
Centre for Marine Vessel Dev.
Halifax, NS
B3J 2X4
902-420-7659
(Fax) 902-423-9734
liangzi.cong@dal.ca

Jan de Kat
MARIN
P.O. Box 28
Wageningen, Netherlands
6700 AA
+31-317-493405
(Fax) +31-317-493245
j.o.dekat@marin.nl

Chris Dicks
UK MOD
PE, Ash Oa #95
Bristol, England
BS34 8JH
0117-91-35073
(Fax) 0117-91-35943
na121a@dawn.pe.mod.uk

Mahmoud Haddara
Memorial University of Newfoundland
Faculty of Engineering & Applied Science
St. John's, NF, Canada
A1B 3X5
709-737-8900
(Fax) 709-737-3480
mhaddara@engr.mun.ca

Alberto Francescutio
University of Trieste
Trieste, Italy
34127
+39-040-6763425
(Fax) +39-040-6763443
francesc@univ.trieste.it

Masami Hamamoto
Osaka University
2-1 Yamada-oka
Suita, Osaka, Japan
565
+81-6-879-7587
(Fax) +81-6-879-7594
hamamoto@noe.eng.osaka-u.ac.jp

Charles Hsiung
DalTech
1360 Barrington Street, P.O. Box 1000
Halifax, NS
B3J 2X4
902-494-3918
(Fax) 902-423-6711
charles.hsiung@dal.ca

Yoshiho Ikeda
Osaka Prefectore University
Dept. of Marine System Engineering
1-1 Gakuen-cho
Sakai, Osaka, Japan
+81-722-54-9343
(Fax) +81-722-54-9114
ikeda@marine.osakafu-u.ac.jp

Shigesuke Ishida
Ship Research Institute
6-38-1 Shimkawa
Mitaka, Tokyo, Japan
181-0004
+81-422-41-3061
(Fax) +81-422-41-3056
ishida@stimot.go.jp

Anneliese Jost
Walter-Schuler
Hamburg, Germany
D22459
040-583886
(Fax) +49-40-361-497320
jt@germanlloyd.org

Mariusz Koniecki
Canadian Coast Guard
Fleet Services
200 Kent Street
Ottawa, ON, Canada K1A 0E6
613-998-1775
(Fax) 613-991-2497
konieckim@dfo-mpo.gc.ca

Jerzy Matusiak
Helsinki University of Technology
Ship Laboratory
P.O. Box 4100, Finland
02015 HUT
+358-0-4513480
(Fax) +358-004514173
Jerzy.Matusiak@hut.fi

Kevin McTaggart
Defence Research Establishment Atlantic
9 Grove St., P.O. Box 1012
Dartmouth, NS, Canada
B2Y 3Z7
902-426-3100 Ext.325
(Fax) 902-426-9654
mctaggart@drea.dnd.ca

Martin Renilson
Australian Maritime College
P.O. Box 986, Launceston
Tasmania, Australia, 7252
61-363-354-770
(Fax) 61-3-63-354720
m.renilson@mte.amc.edu.au

David Molyneux
Institute for Marine Dynamics
National Research Council Canada
P.O. Box 12093, Station 'A'
St. John's, NF, Canada, A1B 3T4
709-772-2481
(Fax) 709-772-2462
dmolyneux@minnie.imd.nrc.ca

Brad Rixmann
Marineering Ltd.
P.O. Box 277
Mount Pearl, NF, Canada A1N 2C3
709-747-3570
(Fax) 709-747-3590
brad_rixmann@marineering.com

David Murdey
Institute for Marine Dynamics
National Research Council Canada
P.O. Box 12093, Station 'A'
St. John's, NF, Canada, A1B 3T4
709-772-2481
(Fax) 709-772-2462
dmurdey@minnie.imd.nrc.ca

Olle Rutgersson
KTH
Naval Architecture Dept.
Stockholm, Sweden
16572
46 8790 7520
(Fax) 46 8790 6684
olle@fkt.kth.se

Apostolos Papanikolaou
NTVA - Ship Design Laboratory
9 Heroon Polytechniou
Athens-Zografou, Greece
15773
0030-1-7721416
(Fax) 0030-1-7721408
papa@deslab.ntua.gr

Kostas Spyrou
University College London
Gower Street
London, UK
WC1E 7AT
44 171 5042524
(Fax) 44 171 3800986
kspyrou@ucl.ac.uk

Andrew Peters
Dera Haslar
Haslar Road, Gospor
Hampshire, UK
PO12 2AG
+44-01705-335217
(Fax) +44-01705-5461
ships@faz.dera.gov.uk

Robert Tagg
Herbert Engineering Corp.
98 Battery Street, Suite 500
San Francisco, CA, USA
94111
415-296-9700
(Fax) 415-296-9763
rtagg@herbert.com

Andre Taschereau
Transportation Development Centre
800 Rene-Levesque Blvd. W.
Montreal, PQ H3B 1X9
514-283-0040
(Fax) 514-283-7158
taschea@tc.gc.ca

Kin Tue-Fee
Transport Canada Marine Safety
Ottawa, ON Canada K1A 0N8
613-998-0607
(Fax) 613-993-8196
tuefeek@tc.gc.ca

Osman Turan
University of Strathclyde, SSRC
801 Colville Bld.
Glasgow, Scotland, UK
G1 1XM
0044-141-548-4782
(Fax) 0044-141-548-4784
o.turan@strath.cc.uk

Dracos Vassalos
University of Strathclyde, SSRC
801 Colville Bld.
Glasgow, Scotland, UK
G1 1XM
0044-141-548-4780
(Fax) 0044-141-548-4784
d.vassalos@strath.ac.uk

Naoya Umeda
National Research Institute of Fisheries
Ebidai, Hasaki
Kashima, Ibaraki, Japan
314-0421
+81-479-44-5942
(Fax) +81-479-44-1875
umeda@nrife.attrc.go.jp

Piotr Waclawek
Institute for Marine Dynamics
National Research Council Canada
P.O. Box 12093, Station A
St. John's, NF Canada A1B 3T5
709-772-2266
(Fax) 709-772-2462
pwaclawek@minnie.imd.nrc.ca

4th International Ship Stability Workshop
St. John's, Newfoundland, Canada

October 28th and 29th, 1998

Summary of Discussion

Since its formation in 1995, the Ship Stability Workshop has presented a unique opportunity for experts in the field to gather together and present their latest research results. The Workshop provides an overview of the state of the art and the discussion developed from the presentations is an important part of the meeting. These notes are an attempt to summarize the discussion in each of the areas, but the very nature of the discussion leads in interesting directions, not necessarily tied in to the topic which initiated the thought. Therefore, there is some structure to these notes, but they certainly are not a verbatim record of the meetings, and they have been edited to make them more structured, since similar topics arose at different times during the meetings. The summaries are ordered in the same sequence as the presentation topics.

Numerical and Physical Modeling of Intact Stability

Discussion Leader, Prof. C. C. Hsiung, Dal-Tech University, Halifax, N. S.

The presentations made in this area highlighted several developments in the area of numerical modeling of intact and damaged stability. These are;

The development of hybrid models,
The use of numerical models,
The validation of numerical models,
The need for simple capsize criteria and
Data visualization.

The first area is the use of hybrid models, which are essentially linear, but with some non-linear capability. Professor Hamamoto presented a method for expanding strip theory type programs to include capsize due to loss of stability. Strip theory programs are well established for the prediction of seakeeping motions and loads, where the responses are essentially linearly dependent on wave height. The method works best for high frequency, low amplitude responses. The advantage of strip theory methods is the efficiency of computation. The method has been expanded into seemingly non-linear issues such as slamming and deck wetness. It has not been used for stability studies however.

Traditional strip theory programs do not consider the variation in ship stability with wave height, but use classical small angle stability in the linear regime. Professor Hamamoto's paper presented an alternative approach, which included change in GZ as a linear function roll angle. The revised equations of motion now result in unstable solutions, which allows for the prediction of capsize due to loss of stability. This method makes full advantages of the computational efficiency of strip theory, but enables it to be used for the study of ship capsizing.

Another attempt to deal with some of the problems of modeling ship motion behaviour in large waves was addressed by Dr. Umeda. In his paper, he points out that capsizing is a non-linear phenomenon. Traditional seakeeping programs deal with linear behaviour, as discussed by Prof. Hamamoto. Seakeeping predictions do not depend on initial conditions, because the motion is essentially stable. However, capsizing simulation does depend on the initial conditions, and starting a numerical experiment in the correct condition is critical. Different techniques for starting the simulation have been tired, such as the 'worst' condition of the ship relative to the wave, or by starting the simulation in a stable, periodic motion, and make a sudden change to the control system, such as the rudder. Dr. Umeda also discussed the use on non-linear system dynamics models and their use in conjunction with model experiments. Non-linear dynamics gives a much better assessment of the 'stability' of the situation than classical modeling approaches. In his paper he compares predictions made from numerical experiments with those made from non-linear analysis.

A very encouraging observation is that numerical models are being used for parametric studies. In this case, numerical experiments are carried out over a large parameter space and limiting conditions are established. The example given by Dr. McTaggart focused on ship stability, but other recent papers have also used this approach. It is encouraging to think that the output from relatively sophisticated numerical models is now at the point where it is accepted for the development of standards. The particular program used by Dr. McTaggart was FREDYN from MARIN. This approach has been used also in the area of damaged stability by Prof. Vassalos and others.

However, some of the computational methods can be very intensive. It is important to optimize the length of the numerical experiments, without compromising the accuracy. The approach taken by Dr. McTaggart was to fit probability distributions to observed data, and estimate extremes based on the fitted distributions, rather than on the measured results.

Validation of computer predictions against physical observations is an important part of their development. The experiments needed to validate computer codes require the measurement of different parameters from those which are used to predict overall system performance. The level of sophistication required in the measurement system is much higher, since the intention is to check hydrodynamic components, rather than the overall performance. Dr. de Kat presented a paper on some model experiments on a frigate hull, carried out in large waves. Extreme motions were observed in the form of surf riding, broaching and capsizing. The paper also compared the model experiments with numerical simulations.

Reduction of data into stability criteria continues to be an ongoing issue. The challenge is to take the complex problem of ship stability in waves, with all the associated aspects of non-linearity and random behaviour, and develop something which can be used as the basis for safety regulations or guidelines. Dr. Renilson presented a paper which outlines a single stability parameter, based on all wave slopes, speeds and wave headings. Whilst this method is attractive from a regulatory point of view, there was some concern that important information on the complex motions of ships would be lost.

An alternative approach to the presentation of motion data for ships is the use of video records for model experiments and animation for simulations. Several authors used video or animation during their presentation. Dr. de Kat, Dr. Umeda and Prof. Hamamoto showed videos of experiments on ship models. Whilst this can give a good overview of the results of a particular experiment, it can take many attempts to obtain a particular set of conditions that is required. Prof. Papanikolaou showed some animations of a damaged ferry capsizing. Animation certainly has some attractive potential for displaying the results of numerical simulations. However, whilst this method is very visual, it is difficult to use in the development of standards or regulations. The scientific approach to safety would be to analyze each ship in a representative range of wave conditions. A probabilistic approach to capsize would include the probability of capsize occurring on a given wave and the probability of that wave occurring.

Non-linear Dynamics and Ship Capsize

Discussion Leader; Prof. Don Bass, Memorial University of St. John's, NF.

The use of non-linear dynamics highlights the complexities involved in simulating a capsize. The advantage of this approach is that the numerical models are relatively simple and fully non-linear. The biggest disadvantage of this approach relates to the fact that the hydrodynamics are implicit rather than explicit. The strength of non-linear dynamics approach is in studying the 'big' picture of ship capsizing, in terms of wide ranges of ship and wave parameters. Work in this area continues to give new insights into the problems of ship capsizing.

Dr. Spyrou presented recent work on the dynamical systems approach to problems of ship stability in beam and following seas. He discussed the role of parametric excitation and roll damping at large roll amplitudes. The type of instability associated with parametric excitation epitomized by the Mathieu equation appeared to indicate capsize would take place in a number of cycles that was greater than the number observed by other researchers. Based on experiments, parametrically excited capsize took place in just 3 or 4 cycles of roll in following seas.

Dr. Spyrou pointed out that if it was necessary to take into account the non-linearities of the righting moment in evaluating large amplitude ship dynamics, it was equally important to model roll damping at large amplitudes given its significance in dynamic stability. He outlined a methodology for its evaluation. As was pointed out in discussions, large amplitude roll damping based on a simple (non-linear) roll equation is difficult to evaluate given other hydrodynamic factors associated with large heel angles, such as the effects of deck-edge immersion.

Bias is a significant factor in increasing the risk of capsize, as can be amply demonstrated using non-linear dynamics. It would seem however that it is not possible to demonstrate, at the present state of the art, that direction of bias is a significant factor in capsize vulnerability. Vessels biased to weather appear to have a greater risk of capsize.

In the wide ranging discussions following Spyrou's paper, auto-pilots were discussed . For example the question arose as to whether or not it was possible that a 'badly' designed auto-pilot could precipitate broaching (and possibly capsize). In severe stern seas, it was noted that the rudder and therefore the auto-pilot might be largely ineffective. Increasing the propeller race to increase the rudder effectiveness might have the adverse effect of instigating the dangerous regime of surf-riding. In severe seas, the rudder tended to shift from hard-over to port to hard-over to starboard. It was not clear whether a helmsman would do things much differently. A clearer understanding of the mechanism of broaching might make it feasible to design a 'more intelligent' auto-pilot, that was more able to avoid broaching situations.

Dr. Francescutto spoke on the identification of parameters in the non-linear equation of roll. Results based on a number of experiments with various vessels demonstrated the accuracy with which predictions agreed with tests in beam seas. Absolute roll versus relative roll equations were discussed. The roll damping derived from the relative roll equation differed from that derived in the absolute roll equation. Roll decay tests are to be carried out at some later date to determine which gave the better results.

Dr. Belenky presented work on a piece-wise linear approximation to non-linear roll dynamics. He demonstrated that the technique was able to produce results qualitatively very similar to those using the standard approach. He claimed the method was less tainted with numerical instabilities and uncertainties, since it provided an essentially analytical solution. However the main advantage of the method would appear to be its applicability to a probabilistic formulation of the notion of dynamic instability or capsize threshold.

Special Problems in Ship Stability

Discussion Leaders, Dr. Kevin McTaggart, DREA, Dartmouth, N.S. & Prof. C. C. Hsiung, Dal-Tech University, Halifax, N. S.

Papers in this session covered a wide range of topics. Most of them dealt with small vessels, including planing hulls. Small ships have special problems with regard to stability. For planing craft, stability comes from hydrodynamic forces, rather than hydrostatic ones. The hydrodynamics can induce some system instabilities, since the location of the centre of pressure can change. Porpoising (longitudinal instability) and chine walking (lateral instability) have both been frequently observed in planing hulls at some speed and loading conditions. Understanding these phenomena is critical to designing safe and effective ships. There were two papers on the stability of planing hulls. Full scale measurements on small ships are also challenging, and two papers presented were related to this topic. Finally, one paper was presented on the influence of dynamics on the stability of a flooded ship.

Professor Rutgersson's paper described a proposed series of full scale trials examining maneuvering properties of small naval craft in a seaway. The trials will assess the capability of ships to stay on course and avoid broaching in waves. The researchers propose that maneuvering performance in moderate seas will be a useful indicator of performance in more severe seas.

There was discussion on the feasibility of developing a broaching index. Among other factors, broaching is dependent among the amplitude of overshoot angles. There was considerable interest regarding the type instrumentation that will be used for the trials. An onboard GPS unit connected to a laptop computer will provide a record of ship course. Wave conditions will be measured using a wave buoy, which could be supplemented by relative

motion measurements at the bow. Video observations from a helicopter could also be available. Ship motions would be measured in 6 degrees of freedom.

It was only planned to study one ship loading condition for the Finnish ship, but it was possible that several loading conditions could be studied for a Swedish vessel, 20 m LOA.

Professor Hamamoto gave a brief description of some model scale zig-zag maneuvering tests being planned in Japan.

Dr. Dand's presentation on damage stability experiments provided interesting physical insights and generated much discussion. Dr. Dand defined dynamic stability as the ability of a floating body to return to its original position after being disturbed. The behaviour of a damaged ship was shown to be sensitive to the shape of the damage opening and to heel bias. The validity of the IMO damage opening was challenged, since real damage is much more ragged. Also, whether the damage is trapezoidal or rectangular has an effect on the flooding process. Bias was found to have a large influence on experimental results. Values as small as 0.1 degrees were found to significantly increase the wave height survived by the model.

The occurrence of capsize can be quite dependent on the vessel drift motions after damage occurs. In the case of the European Gateway, it had a residual drift speed of 4-6 knots after separation from its colliding vessel. This effect could be particularly important for high speed craft. Considering that high speed ferries are becoming common, more attention should be given to damage stability after high speed collisions.

The session on Tuesday morning began with a short presentation from Dal-Tech on work they had done on the influence of water trapped on deck , and its influence on ship motions. The numerical model includes water shipping onto the deck and water draining off, over the bulwarks. Results of some simulations were presented.

Professor Ikeda presented a paper on experiments to determine hydrodynamic forces and moments (six components) on a planing hull. The model was towed at different yaw angles, heel angles and trim angles. These data will be used to develop an understanding of the forces acting on a planing hull during a turn.

Professor Kijima also presented the results of an experimental study on planing hulls. The objective of this paper was to determine ways of improving the transverse stability of planing hulls. Stability was improved by the use of spray strips. The strips had little effect on the resistance. The model heels, as forward speed increases, due to asymmetry in the pressure distribution, rather than a dynamic reduction in static stability.

Dr. Birmingham presented a paper on the challenging aspects of determining the stability of small boats, for which there was no technical information. The paper presented a method which in theory, would give the necessary information, by moving weights horizontally and vertically on the ship and comparing the roll periods for each condition. However, it was found that the accuracy required to measure roll period is beyond the practical limits of resolution in a working environment. Discussion stimulated by this paper focused on alternative methods, such as developing the hull lines from stereo photography. There was also some concern about the size of the weights that needed to be moved. The practical movement of weight means that the technique is only applicable to small boats, but this is the area where the most data is missing. Also, in practice it is difficult to induce pure roll, without inducing heave and trim.

Numerical and Physical Modeling of Damaged Stability

Discussion Leader, Prof. Sander Calisal, UBC, Vancouver, B. C.

The five papers presented in this session all dealt with different aspects of the problem of water accumulation on the deck of a flooded RO-RO Ferry. This topic has received a great deal of discussion since the sinking of the Estonia and the introduction of the Stockholm Convention. A major step forward has been to specifically include water on the deck of a damaged RO-RO ship when assessing its stability. However, there are competing models for the amount of water, and their merits are the subject of academic discussion.

Professor Vassalos presented a paper studying the effect of degrees of freedom on

flooding the deck of a RO-RO ferry model. After the presentation there was discussion concerning the location of the damage and the resulting worst case scenario. All experiments had been carried out with midships damage and level trim. Forward damage and bow down trim was suggested as being a case for further study. There was also discussion over the type of wave used. All experiments were carried out with long-crested waves. For long crested waves, the motion of the model is in phase with the waves, whereas for short crested waves, the model moves less, and may be considered to be more static (and more likely to flood). Also wind will influence the results, assuming that the waves are wind generated and the directions coincide. This will result in an increase in the drift velocity and a subsequent reduction in encounter frequency. This was studied by the author and it was found to have little effect on the results.

Mr. Molyneux presented some work done for Transport Canada, reanalyzing model test data to compare it with the Static Equivalent Method, proposed by Dr. Vassalos. There was some discussion over the use of the term 'Static Equivalency' and it was noted that the Stockholm Agreement had taken a different approach. Based on experiment results, it was found to be difficult to determine a critical volume of water on the deck.

There was also discussion over the form of the equation for the SEM, where

$$h_{crit} = A * Hs^{B}$$

The author's original intention had been to expand this relationship to include the effect of freeing ports, but the IMD data was too scattered to develop a meaningful relationship. There was some discussion on the benefits of freeing ports (open and flapped) and no consensus was reached on the benefits of fitting them.

Mr. Koniecki presented some more work done for Transport Canada, also related to predicting the amount of water on the deck of a flooded RO-RO ship. The SEM takes no account of how water gets onto the RO-RO Deck. His paper attempted to develop a method for predicting the amount of water on deck, based on the height of the free surface above sea level and the relative motion of the ship. This can now be expanded to include freeing ports, irregular shaped openings etc. Discussion focused on the use of a weir model for flow onto the deck, ability of the model to drift and the availability of experiment data in the public domain.

Mr. Ishida presented a paper which looked at the influence of wave period, initial heel angle and the relationship between critical height of water on deck and critical wave height to cause a capsize. The findings of the research showed that it is possible for ships to survive the values of Hs in excess of those given by the SEM, provided that the modal period was increased to values associated with deep water rather than coastal spectra. The discussion prompted by this presentation focused on the influence of wave period and the assessment of the volume of water on deck.

Ms. Jost presented the results of a study to better define the critical height of water on the deck, as defined by the Stockholm Agreement. Model data for three different ferries were discussed, with different residual freeboards. Each design was built to different stability standards, due to the year of construction. Design modifications of bulkheads and side casings were studied for each ship. Most of the discussion focused on the experiment techniques used. Also, there was some discussion on the most cost effective ways to improve survivability of existing ships. Residual freeboard was found to be a very important factor influencing survivability, but subdivision below the main deck is prohibitively expensive after construction. The alternatives are side casings and bulkheads on the main deck.

Application to Ship Design and Operation

Discussion Leader, Mr. David Murdey, Institute for Marine Dynamics, St. John's, NF.

This session covered some specialized areas of ship design in relation to stability. It was more general in nature than the previous sessions. Three papers were presented, by Professor Calisal, on a viscous flow model for water discharge, Professor Papanikolaou on design for survivability of warships and merchant ships and Professor Vassalos on the concept of a secure RO-RO ship. Mr. Alan also presented a wrap up of the Workshop, from the perspective of a regulator. His notes have been included.

Professor Calisal attempted to take our understanding of water discharge through freeing ports to the next level. Models given in other presentations at the workshop simplified the problem of water discharge to a weir flow model, which did not include a rigorous treatment of viscous flow. Professor Calisal presented a two dimensional viscous flow model which simulated the water profile as a function of space and time. The results from the simulation were compared with data measured during experiments. The discussion questioned the importance of surface tension in the model. The model experiments were conducted with a sprung freeing port, which was 12 inches long by 4 inches high. This was typical of ports used on fishing vessels. However, the nature of the trap door was criticized, since it did not bear much relationship to flapped freeing ports.

Professor Papanikolaou discussed various design aspects of survivability for surface warships and merchant ships, using a common probabilistic approach. Warships have unique problems associated with survivability, due in part to the lack of regulations. Generally there is a lack of data for naval vessels. Existing survivability prediction programs require considerable detail and so the design has to be well developed before they are appropriate. Also there is a lack of statistics for probability based methods. Also included in the presentation was an animation of a passenger vessel capsizing, which visualized the results of a numerical simulation.

Professor Vassalos presented a paper on the concept of a 'capsize proof' RO-RO ferry. The study included alternative methods of draining water off the deck, such as combinations of freeing ports, positive and negative sheer, and positive and negative camber. These systems have the advantage that they do not obstruct the car deck with side casings or bulkheads. There was some concern about the ability of this system to handle deck washing systems. There was also some discussion over the use of the term 'safe haven'. It is used within the Offshore Industry, as the safest place within an offshore structure. The term is not strictly applicable to a ship, since the ship can sink, but the concept of 'design-for-safety' was very much appreciated, and studies like this help to clarify the boundaries established by 'conventional' thinking.

Wrap-Up Session

Tom Allan made the final presentation. His notes are given below.

Speaking at the close of a workshop such as this is not easy, particularly after listening to words of some of the most accomplished academic naval architects in the world. I have to admit to, at times, being slightly lost when listening to some of the more theoretical postulations. It is because of this that I have a few simple requests and it goes beyond the question asked by Dr. Spyrou; "What is the motivation in what you are trying to do?" I would make the question a little simpler; "What is the end result of what you are trying to achieve - will it assist the design naval architect to improve or make safer the design of a particular type of ship or even ship design in general?"

Will your work provide additional information to assist the master - to help him to operate his ship in a safer manner? I would ask that each of you have these few basic principles in mind at all times as you carry out or develop research projects such as those you have discussed over the past two days.

So "Have we got it right?" is my main question - have we addressed everything that needs to be addressed? In this instance I am thinking particularly of the future designs of high density passenger ships. Currently we have designs for 3500-4000 persons - can we afford a disaster where in excess of 3000 persons may be lost? How do we evacuate this number of persons from the ship in the event of fire or, in your specific area of expertise, after a collision?

A few other questions I would ask you to ponder again under the theme " Have we got it right?"; collisions of high speed craft at speed; and to address a subject which has been debated extensively at this workshop - when carrying out damage model tests, are we using the correct or most appropriate damage opening.

It is my belief that the current opening used in the damage model tests for acceptance under the Stockholm Agreement is <u>not</u> the most appropriate. For these tests we use the SOLAS defined damage opening. For the deterministic method of calculation I would agree that this opening is appropriate in that it ensures an adequate spacing of transverse watertight

bulkheads. However for physical model tests, as I said, it is not appropriate - it does not reflect the type of damage openings caused by collision and during the model tests themselves the SOLAS opening probably allows more water to exit the hull than would normally be expected.

What is the most appropriate shape of damage opening that we should be using for physical model tests? From a safety point of view it should be the most onerous shape of opening for the ship - but I have to ask you; "What should that shape be?"

On the same subject I have been fascinated by the amount and diversity of work you are all carrying out on the aspect of "water on the car deck" of ro-ro passenger ships. I don't think that Hartmut Hormann (Germany), Iwao Watanabe (Japan) nor I realized what we were releasing into the world of Naval Architecture after our initial meeting in Tokyo in January 1995 as part of re-assessment of ro-ro passenger ships with the IMO Panel of Experts. I just trust that we are not entering a phase of "academic nit picking" on the subject and that some useful criteria will eventually be developed.

There were two papers that I would ask each of you to consider seriously for a solution which would assist industry. First the paper by Richard Birmingham on "The Stability Assessment of Small Working Craft without Reference to Hydrostatic Data" which is looking for a simple formula to assess the stability of small workboats when no basic hydrostatic information is available. The second paper was that presented by Martin Renilson proposing a standard presentation method with a limiting KG envelope curve. Both of these papers, if solutions can be found, would be of great benefit to the industry.

In closing I would like, on behalf of myself and IMO, to thank each of you for the efforts made to improve the science of Naval Architecture and from that base the improved safety of ships of all types.

Conclusions

Organizer, David Molyneux, Institute for Marine Dynamics

There are tremendous benefits to be gained from organizing a Workshop like this. The bringing together of experts in the field for a free and frank exchange of ideas is an essential part of the development of a scientific approach to ship stability. Each workshop has had a core of committed participants, but also each year new faces are added to the mix, depending on the location. It is a unique opportunity for researchers, regulators and practicing designers and operators to discuss problems from their own perspective, and in turn gain a better understanding of the topics.

Form an organizational point of view, the workshop should continue to evolve. The original idea for the Workshop resulted from collaboration between the United Kingdom and Japan. The strength of the idea has been confirmed since now we have had half the workshops within the original organizers and half outside. As new organizers are invited to participate, it is important that the original idea is allowed to grow in natural directions. The publication of the proceedings of the four Workshops to date as a book is important recognition of the value of the work presented. However, it is important to keep open discussion and freedom to present new and challenging ideas as an essential part of the process. Hopefully the potential conflict between publication for posterity and exploring challenging ideas can be addressed by the next organizers. We certainly wish them luck in organizing the next even. I am sure that it will be as rewarding for them as organizing the fourth workshop was for us.

Based on the discussion for each of the papers and Tom Allan's notes, I would like to take the opportunity to summarize the areas where I feel we should move forward. Hopefully at the next Workshop in Trieste, in 2000, we will see some interesting new developments in these and other areas.

Validation of numerical models against model and full scale data

Integration of non-linear dynamics with conventional 'structural' models

Operational limits for ships using dynamic lift, such as planing hulls

Data reduction into a format for simple but meaningful regulation

Consolidation of results for water on deck of a flooded RO-RO ship

There is a general shift from prescriptive regulations for preventing the loss of ships to a safety case management approach. This will result in the need for more sophisticated analysis at the design stage than is the current practice. The need for educating Naval Architects in the results of the latest research on ship stability continues to grow. The Ship Stability Workshops should continue to contribute towards this goal for many years to come.

Finally I would like to thank all the presenters and discussion leaders. It is a risky business to stand before your peers and discuss research results which are partially complete or challenge accepted practices. However, this open mindedness helps to accelerate the development of new ideas, which will eventually result in safer ships. This is the goal that we must all be aiming for.

Ro-ro Passenger Vessels Survivability - a study of three different hull forms considering different Ro-ro-deck subdivisions.

by
Anneliese E. Jost, Germanischer Lloyd and Dr. Peter Blume, HSVA

Synopsis:

Based on the newly defined Stockholm Agreement's water on deck criteria model tests where carried out aiming at a better understanding of the critical water height on the ro-ro deck.

For this purpose three differently aged vessel types with respectively different operating freeboards have been included in this study. The results achieved are shown and discussed.

1. Background

Legislative Activities have finally calmed down that had been pushed forward by the tragic losses of ro-ro passenger the most recent of which had been the Estonia. The drastic measures newly required are being put into place now. Once they will be completely in place, time will proof their effectiveness.

Legislative tools dedicated to ro-ro passenger vessels cover other than a set of 1995 SOLAS Amendments, IMO Resolutions requiring the upgrading of shell doors scantlings and their securing as well as a Regional Agreement on a specific damage stability standard applicable to ships travelling in the North and Baltic Seas.

With regard to damage survivability it should be noted that the amended SOLAS [1] requirements and the Regional agreement [2] enforce an increase in standard that will become mandatory to both new and existing passenger vessels. One of the newly installed criteria is a survivability standard that requires to show sufficient residual stability even with accumulating water on the damaged ro-ro deck. The respective legislation does allow to chose showing compliance with this standard either by calculation or by model tests. In both cases the regional agreement does give detailed procedures which are to be complied with.

The scope of this research project (sponsored by BMBF[1]) was to find a better understanding of the critical amount of water on deck relative to the existing trading practice and eventual upgrading of the ship types. Thus three existing hull forms that had been built in accordance with different subdivision and survivability standards due to their individual keel laying and or reconstruction dates were chosen as sample ships. It was anticipated that some kind of subdivision of the ro-ro deck would become necessary during the course of the proposed upgrading and the effect of such subdivision on the survivability of these hull forms was to be studied.

[1] German Ministry for Research and Technology

2. Hydrostatic Evaluation of the Sample Ships

Today's subdivision standard is based on the SOLAS 1974 requirement that has been considerably amended after 1988. Up to 1988 for any passenger ship compliance had to proven with existing intact stability criteria the requirement of floodable lengths and certain damage stability criteria. Usually the damage stability requirements would be the crucial criteria and the designs freeboard. Both the intact stability criteria and the floodable length requirement have not been reconsidered while the damage stability criteria had been amended by a requirement of a residual stability standard. As usual this new standard became applicable to new ships and showed a remarkable influence on the designs.

Ro-ro passenger ferries operating in the Baltic and North sea areas are required to comply with a survivability standard that includes the flooding of the ro-ro (bulkhead) deck. The requirement is that acceptable residual stability standards are to be maintained even with a certain flooding height ($h_{ww} \leq 0.5m$). Compliance with this standard can either shown by model testing or calculation.

Technically, two different survivability standards for new and existing ro-ro passenger ferries can not be justified. Consequently the amended standard became mandatory also to existing vessels.

The vessels chosen for this project are considered to be typical representatives of the kind used in this area:

1. Ship A

   This ship was built in accordance with SOLAS 74/83 standard. Her subdivision below the

bulkhead deck consists of a relative high number of transverse bulkheads combined with some longitudinal subdivision. The operating freeboard is minimised by making use of cross flooding that decrease or eliminate heeling angles in damaged condition. In this case the criteria of non-submerging the margin was the governing criteria as residual stability standards had not been imposed.

2. Ship B

   Although this ship had been built prior to ship A, with regard to survivability standards she presents a later design standard since she was completely re-built when entering a different service after the 1988 SOLAS amendments came into force. With this conversion in accordance with SOLAS 74/88 she features a very similar subdivision below the bulkhead deck, the operating freeboard was remarkably increased due to the requirement of a minimum heeling lever curve in damaged condition.

3. Ship C

   This vessel was only designed when the new standard had already been established. Her subdivision below the bulkhead deck is governed by longitudinal bulkheads located at B/5 measured from the shell. Not all of these are equipped with cross flooding ducts. Respectively heeling angles in the damaged water lines are not eliminated although they are legally limited.

The main dimensions of the vessels and some general remarks regarding the damage stability calculations are:

Main Dimensions:	Ship A	Ship B	Ship C
length L_S [m]	151.46	177.21	179.5
beam B [m]	29.00	26.00	27.2
height D [m]	8.10 /16.20	8.0 /	8.7 /
draught t [m]	6.40/ 6.20 / 5.90	5.75	6.0
trim [m]	0.0	-1.0 /0.0 / +1.0	-1.0 /0.0 / +1.0
modelled damaged Compartments	9/10 and 11/12	7/8 and 11/12	6/7 and 10/11

All three vessels are narrow and evenly subdivided below the bulkhead deck [figures 1]. All three ships had in their original configuration non watertight divided ro-ro decks.

Each one was subjected to a SOLAS 90 damage stability calculation in order to establish a governing double compartment that was taken into account regarding the "water on deck" criteria.

The Stockholm agreement requires that unless the governing criteria is located within 10% of the mid-length a second double compartment located within this margin has to be demonstrated. Taking this into account the models of all three vessels were built to cover two SOLAS damages over the length. Where the crucial condition turned out to be within the a.m. mid length part the second damage was chosen to be near the vessels shoulder.

For vessels B and C, where the operating freeboard was considered rather large, it was understood that further increase of freeboard would only effect the survivability to become more favourable by allowing for less GM_0 values. In those cases the introduction of trim was considered to be of more interest.

Generally, for all three vessels three different ro-ro deck versions were investigated. Starting point was

Version A the open deck configuration.

In the course of this project. By calculation a variety of different deck subdivision alternatives were considered. Within the scope of this project only two further versions could be expanded on in model testing:

Version E2 with 2 full height bulkheads in transverse ship direction and

Version F with side casings.

In terms of compliance with "SOLAS 90" standard, in the damage stability investigation the side casing version was the version that seemed to best cope with the criteria.

Summarising the scope the research project covered variations of damage location, subdivision on the ro-ro deck and GM as well as draughts and trims respectively.

	Ship A			Ship B			Ship C		
	draught variations			trim variations			trim variations		
	6.4 m	6.2 m	5.9 m	-1.0 m	0.0 m	+1.0 m	-1.0 m	0.0 m	+1.0
GM variations	X	X	X	X	X	X	X	X	X
Sea State realisations	X	X	X	X	X	X	X	X	X

3. Model testing

Within the model tests the model is subjected to a long-crested irregular seaway. The damaged model is free to drift and is placed in beam seas with the damage hole facing the oncoming waves.

The survival criteria in these model tests are such that at least five experiments for each peak period need to be carried out. The test duration shall be such that a stationary state has been reached and a minimum of 30 min. in full scale time are proven. The model is considered to survive when the angles of roll do not reach more than 30° against a vertical axis occurring more frequently than 20%

of the rolling cycles or the steady heeling angle becomes greater than 20°.

To cover the scope of these tests the model has to be such that the hull is thin enough in the damaged areas and the main design features such as watertight bulkheads, air escapes permeabilities and etc. above and below the bulkhead deck can be modelled to represent the real situation.

Each of the models used in this project was built accordingly in GRP and the interior for two damage locations was mostly built of ply wood in suitable size. These two damage locations were chosen in accordance with the SOLAS damage stability as described above. The damage holes were opened successively. Each one sized in accordance with the SOLAS damage and a penetration depth of B/5. Both of the damage locations per ship were subjected to draught or trim variations and to address the critical wave height the GM_L was continuously decreased in order to find the boarder line between safe and capsizing.

This borderline is of course subject to uncertainties that are usually involved in methods that include statistics. The results cover for each tested GM_L the observation survived/ not survived. This statement of result does not cover the residual margin that might exist versus an exact limiting condition on the edge of capsizing. For this reason it would be necessary to evaluate many more runs in testing such capsizing margins to finally achieve the answer to a question of critical "water on deck"-height.

4. Computer Simulations

The scope of this investigation covered also a computer simulation of the relative motions of the damaged ro-ro passenger vessels in the seaway. The software utilised in this respect is based on methodologies developed at the Institut für Schiffbau, Hamburg. (Kröger [3] and Petey [4]) which was expanded and adapted to such model tests by Chang [5]

As an example table 4 and 5 cover the results of simulations for ship A, tables 6 and 7 ship B and tables 8 and 9 ship C respectively. The simulation confirm the outcome of the model testing.

In order to get an improved understanding of the boarder line between safe and unsafe in this context the simulations covered the same scope of GM variations, only in much smaller steps.

5. Conclusions

The realisation of the seaway and the accumulated water on deck is shown in figures2 and 3. Due to the a.m. uncertainties the measured accumulated water heights can not be considered representing the critical water height on deck. The scheme of water height measurements are shown in figures 3a.

Figure 2 shows a typical time history of a capsizing. Obviously, the identification of the "critical" water height on deck is judgmental.

In order to produce a better understanding of such critical height of water and in conjunction with earlier survivability test made at the HSVA model basin, it is proposed that the residual stability lever curve is employed to help judge the residual stability margin. It is proposed that the residual area of the heeling lever curve of the respective damage case beyond the measured heeling and rolling angle is used to represent survivability borders. (figure 4)

With regard to improving safety of such existing vessels, and in order to limit the necessary increase in GM to a practicable margin further subdivision versions on the ro-ro deck were investigated. As described above three versions per ship were tested.

As an example the scope of the tested configurations is shown in the following table:

Initial draught	Original configuration Version A		With additional bulkheads Version E2		With side casings Version F	
	L 11/12 GM_L	L9/10 GM_L	L 11/12 GM_L	L9/10 GM_L	L 11/12 GM_L	L9/10 GM_L
6.4 m	-	4.2 m	-	2.3 m	-	2.4 m
6.2 m	3.5 m	4.2 m	1.3 m	2.0 m	1.8 m	2.4 m
5.9 m	2.6 m	3.2 m	1.4 m	1.7 m	1.6 m	1.9 m

The conclusion to be drawn from such result can be summarised as follows:

- the increase in freeboard effects a drastic decrease in GM requirement of the damage case.
- For this vessel not built in accordance with "SOLAS 90" standard the requirement in GM in the original configuration becomes impracticably high.
- Any subdivision introduced on the ro-ro deck significantly influences the survivability of the vessel in damaged condition.
- Other than the calculation the test show better results by the introduction of the proposed two full height bulkheads.

A graphical evaluation of the maximum allowable KG-values are shown in figure 5, 6 and 7.

In case of ship B and ship C the freeboard effect was not considered of the same predominance. A result of the trim variations, however is that obviously small trim angles do have some effect on the GM-requirement.

This is shown for ship B:

Initial trim	Original configuration Version A		With additional bulkheads Version E2		With side casings Version F	
	L 11/12 GM_L	L 7/8 GM_L	L 11/12 GM_L	L 7/8 GM_L	L 11/12 GM_L	L 7/8 GM_L
-1.0 m	2.73 m	-	0.78 m	-	1.54 m	-
0.0 m	2.30 m	1.13 m	1.11 m	1.21 m	1.19 m	1.29 m
1.0 m	-	1.37 m	-	0.96 m	-	1.60 m

The evaluation of Ship C had the following outcome:

Initial trim	Original configuration Version A		With additional bulkheads Version E2		With side casings Version F	
	L 10/11 GM_L	L 6/7 GM_L	L 10/11 GM_L	L 6/7 GM_L	L 10/11 GM_L	L 6/7 GM_L
1.06 m	0.71 m	1.92 m	0.54 m	-	1.11 m	-
0.0 m	1.02 m	1.94 m	1.07 m	1. 24 m	1.20 m	1.83 m
-1.07 m	-	2.10 m	-	1.29 m	-	2.00 m

An overview of the survivability results are shown in table 1, table 2 and table 3

The ship motion, the relative motion between the damage opening and the water surface and the water height on deck were measured during the tests. The most important information is the roll-response which indicates whether or not the vessels is regarded as capsizing or not. Figures 3a show as a section of the measured time and water height records such a typical capsizing. Encountering a group of high waves the vessel is forced to heel to a rather large angle by the load introduced by the collected water on deck. In the following calmer period the vessels recovers very slowly to a more upright position. Another group of larger waves approaching again increases the heeling continuously to lead to the eventually observed capsize. Provided the initial GM is slightly larger the vessel shows better recovering times before encountering the next group of high waves.

Once the critical KG/GM values had been generated as describing the limit between safe and unsafe, the residual stability parameters were calculated. Accordingly the respective maximum lever arms and stability ranges were derived.

The results indicate clearly that the "open deck" Version iterates a larger requirement of residual stability. Both of the subdivided Versions (side casings and two transverse bulkheads), however, showed requirements in a similar order.

Based on the known dependency of the stability parameters on B/T and the observation that the deck area involved (i.e. length and beam of the wetted ro-ro cargo area) and trim have large impact. Therefore, it is proposed to use these geometric features to describe the residual stability characteristic.

$$GZ = GZ_{MAX} * \frac{T}{B} * \frac{1}{(1.368 - \exp((A_{RO}/bL)^2)) * (0.2 + \exp((573 * \Delta T/L)^2))}$$

$$F_b^* = (F_b + B/2 * \sin\Phi_{Stat})/\zeta_{\omega sig}$$

For Version A all three hulls are shown in figure 4a versus the freeboard.

6. Nomenclature

A_{RO}	flooded area on RoRodeck
B	beam
b	breadth of the damaged compartment on deck
D	height up to freeboarddeck
dT	initial trim (undamaged)
ΔT	trim in damaged condition
E	area under the righting lever arm curve
F_b	residual freeboard at damage location
GM_o	metacentric height in the initial condition
GM_L	metacentric height in damaged condition
GZ	righting lever
L_{pp}	length between perpendiculars
T	draught
T_p	wave period
V	buoyant volume
$\zeta_{\omega\ sig}$	significant wave elevation
ϕ	heeling angle

7. References

[1] The International Convention for the Safety of Life at Sea (SOLAS) 1974 including all relevant amendments

[2] Regional Agreement concerning specific stability requirements for ro-ro passenger ships ("Stockholm Agreement") published as IMO Circ. Letter 1891 dated 29th April 1996.

[3] Kröger, H.P., Rollsimulation von Schiffen, Schiffstechnik 33 (1986)

[4] Petey, F., Ermittlung der Kentersicherheit lecker Schiffe im Seegang, Schiffstechnik 35 (1988), 155-172

[5] Chang Bor-Chau, On the capsizing safety of damaged ro-ro ships by means of motion simulation in waves, Int. Symposium Ship Safety in a Seaway: Stability, Manoeuverability, Nonlinear Approach, Kaliningrad 1995

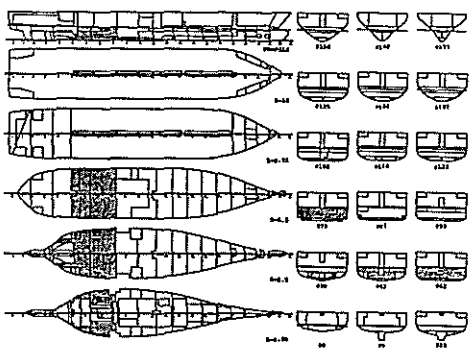

Figure 1A: Subdivision of Ship A Version A Damage Case 11/12

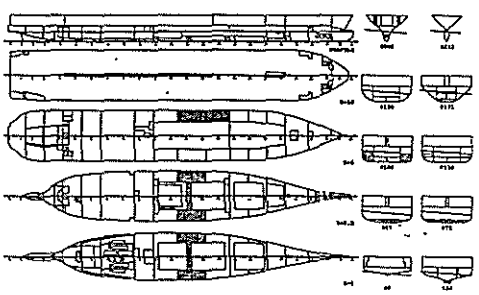

Figure 1B: Subdivision of Ship B Version A Damage Case 7/8

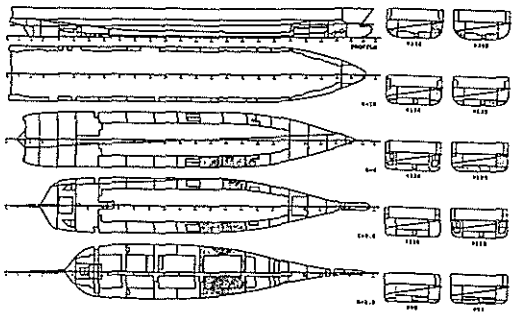

Figure 1 C: Subdivision of Ship C Version A Damage Case 6/7

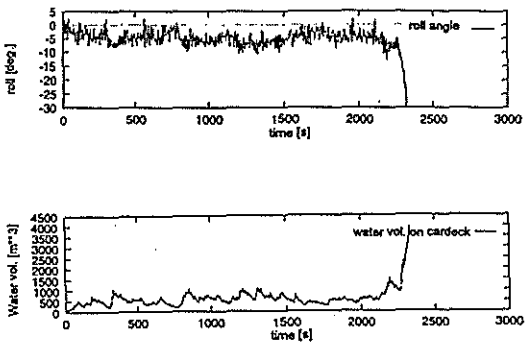

Figure 2: Typical Capsize Scenario

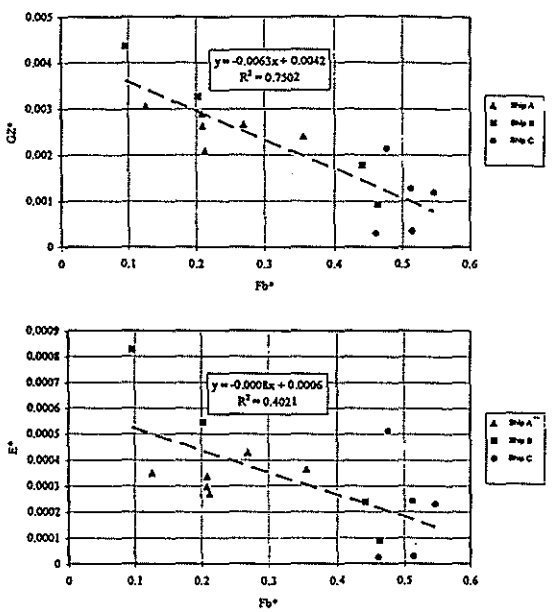

Figure 4a: Standardised maximum lever arm and area curves demonstrated as a function of freeboard

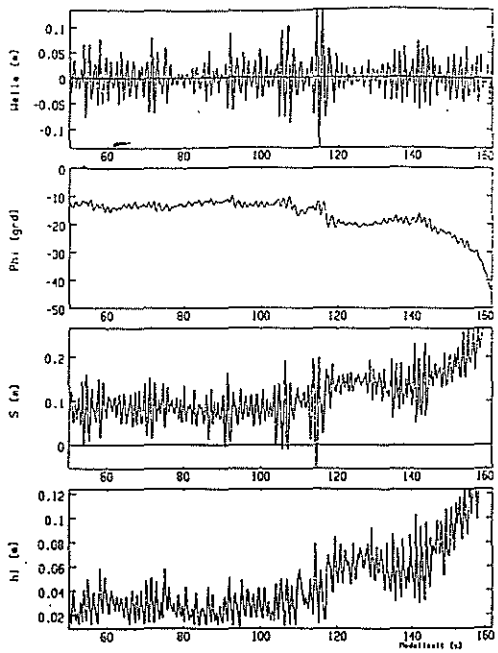

Figure 3a.1: Section of time records measured for a capsizing situation

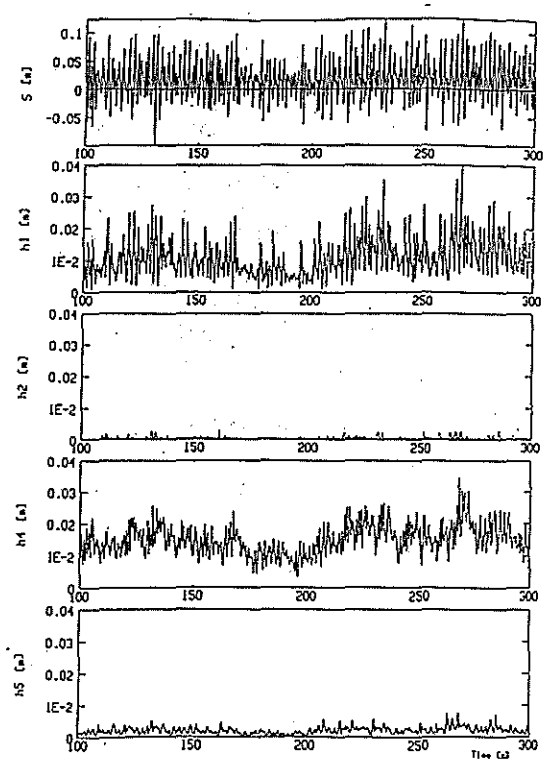

Figure 3a.2: Section of time records of water height

Table 4: Number of tests resp. simulation runs N and number of observed capsizing incidents N_c Ship A; damage case 9/10; no trim

initial draught T [m]	damage GM_t	Test N	Test N_c	Simulation N	Simulation N_c	Test N	Test N_c	Simulation N	Simulation N_c
	Open deck					(Version A)			
5.9	3.83	2	-	2	-	-	-	4	-
	3.45	2	-	2	-	-	-	4	-
	3.23	2	-	4	-	-	-	4	1
	3.22	-	-	4	1	-	-	4	1
	3.17	-	-	8	1	-	-	4	2
	3.13	-	-	4	1	-	-	8	4
	3.08	1	1	8	1	-	-	8	5
	3.03	-	-	4	2	-	-	8	-
6.2	4.44	2	-	4	-	-	-	4	-
	4.14	-	-	8	-	-	-	8	-
	4.09	2	1	4	2	-	-	4	2
	4.05	-	-	8	3	-	-	8	2
	4.00	-	-	4	1	-	-	4	2
	3.95	1	1	4	3	-	-	4	2
	3.73	1	1	4	4	-	-	4	4
6.4	4.20	-	-	4	-	-	-	4	-
	4.15	-	-	8	1	-	-	8	-
	4.10	-	-	-	-	-	-	4	4
	4.05	1	-	4	4	-	-	4	4
	4.10	1	1	4	4	-	-	4	4
	3.60	1	1	4	4	-	-	4	4
	3.03	1	1	4	4	-	-	4	4
	Side casings					(Version F)			
5.9	2.52	2	-	4	-	-	-	4	-
	2.17	2	-	4	-	-	-	4	-
	1.78	2	1	4	-	-	-	8	-
	1.69	-	-	8	-	-	-	8	-
	1.64	-	-	4	2	-	-	8	-
	1.59	-	-	-	-	-	-	8	1
	1.44	-	-	4	2	-	-	-	-
6.2	2.69	2	-	4	-	-	-	4	-
	2.35	2	1	4	-	-	-	4	-
	2.20	-	-	8	-	-	-	4	-
	2.10	-	-	4	-	-	-	8	-
	2.00	-	-	8	-	-	-	8	-
	1.90	-	-	8	1	-	-	8	-
	1.85	-	-	8	1	-	-	8	1
6.4	2.82	2	-	4	-	-	-	4	-
	2.82	2	-	4	-	-	-	4	-
	2.40	2	-	4	-	-	-	4	-
	2.30	-	-	8	-	-	-	8	-
	2.10	-	-	8	-	-	-	8	-
	2.00	-	-	8	-	-	-	8	-
	1.95	-	-	8	1	-	-	8	1
	With transverse bulkheads					(Version E)			
5.9	2.08	2	-	4	-	-	-	4	-
	1.91	-	-	8	-	-	-	8	-
	1.66	-	-	8	2	-	-	4	3
	1.81	-	-	4	3	-	-	4	3
	1.74	2	-	8	3	-	-	4	4
	1.78	-	-	4	3	-	-	4	4
	1.65	-	-	4	2	-	-	4	-
	1.65	1	1	4	1	-	-	4	4
	1.45	-	-	4	4	-	-	4	-
6.2	2.70	2	-	4	-	-	-	4	-
	2.37	2	-	4	-	-	-	4	-
	2.28	-	-	8	-	-	-	8	-
	2.23	-	-	4	2	-	-	4	1
	2.13	-	-	4	4	-	-	4	4
	2.04	2	-	4	4	-	-	4	4
	1.90	1	1	4	4	-	-	4	4
6.4	2.81	2	-	4	-	-	-	4	-
	2.67	2	-	8	-	-	-	4	-
	2.46	-	-	8	-	-	-	8	-
	2.40	-	-	8	3	-	-	8	1
	2.34	2	-	4	4	-	-	4	4
	2.10	1	1	4	4	-	-	4	4

Table 5: Number of tests resp. simulation runs N and number of observed capsizing incidents N_c Ship A; damage case 11/12; no trim

initial draught T [m]	damage GM_t	Test N	Test N_c	Simulation N	Simulation N_c	Test N	Test N_c	Simulation N	Simulation N_c
	Open deck					(Version A)			
5.9	4.45	2	-	4	-	2	-	4	-
	3.24	2	-	4	-	2	-	4	-
	2.85	5	-	8	-	5	-	8	-
	2.60	-	-	8	-	-	-	-	-
	2.55	-	-	8	2	-	-	-	-
	2.49	5	1	8	4	5	-	8	-
	2.45	-	-	-	-	-	-	8	-
	2.40	-	-	-	-	-	-	8	3
6.2	3.76	2	-	4	-	-	-	4	-
	3.65	-	-	8	-	-	-	-	-
	3.60	-	-	4	1	-	-	-	-
	3.55	-	-	4	2	-	-	-	-
	3.45	-	-	4	4	-	-	-	-
	3.33	2	1	4	4	-	-	8	-
	3.30	-	-	-	-	-	-	4	3
	2.48	1	1	4	4	-	-	4	4
	Open deck					(Version A)			
	1° additional heeling towards the inside								
5.9	3.24	2	-	4	-	2	-	4	-
	2.95	-	-	8	-	-	-	-	-
	2.90	-	-	8	2	-	-	-	-
	2.85	2	1	4	1	2	-	8	-
	2.80	-	-	-	-	-	-	8	-
	2.75	-	-	-	-	-	-	8	1
	Side casings					(Version F)			
5.9	1.93	2	-	4	-	-	-	4	-
	1.67	-	-	8	-	-	-	-	-
	1.62	2	-	4	3	-	-	8	-
	1.57	-	-	-	-	-	-	8	2
	1.48	2	1	4	3	-	-	4	2
6.2	2.42	-	-	4	-	-	-	-	-
	2.22	-	-	8	-	-	-	-	-
	2.17	-	-	4	3	-	-	8	-
	2.12	2	-	4	4	-	-	4	2
	1.83	2	-	4	4	-	-	4	4
	1.40	-	-	4	4	-	-	-	-
	With transverse bulkheads					(Version E)			
5.9	2.32	2	-	4	-	-	-	4	-
	1.94	2	-	4	-	-	-	4	-
	1.56	2	-	4	-	-	-	4	-
	1.45	2	-	4	-	-	-	4	-
	1.39	-	-	8	-	-	-	-	-
	1.34	-	-	8	-	-	-	8	-
	1.29	-	-	8	1	-	-	8	-
	1.24	-	-	-	-	-	-	4	2
6.2	1.66	2	-	4	-	-	-	4	-
	1.57	-	-	8	-	-	-	8	-
	1.52	-	-	8	2	-	-	4	2
	1.47	-	-	4	3	-	-	4	3
	1.37	2	-	4	3	-	-	4	4
	1.09	1	1	4	4	-	-	4	4

Table 6: Number of tests resp. simulation runs N and number of observed capsizing incidents N_c
Ship B; damage case 11/12; initial draught t = 5,75m

initial trim d T [m]	damage GM_L	Test N	Test N_c	Simulation N	Simulation N_c
	Open deck				(Version A)
0.	2.44	-	-	8	-
	2.39	-	-	8	2
	2.34	5	-	8	3
	2.26	2	2	8	8
	2.19	1	1	8	7
-1.0	3.02	2	-	8	-
	2.87	2	-	8	-
	2.77	-	-	8	-
	2.74	-	-	8	2
	2.71	2	1	8	3
	Side casings				(Version F)
0.	1.94	2	-	8	-
	1.64	2	-	8	-
	1.44	-	-	8	-
	1.39	-	-	8	5
	1.34	2	-	8	5
	1.16	1	1	8	8
-1.0	2.47	2	-	8	-
	2.24	2	-	8	-
	2.02	2	-	8	-
	1.79	2	-	8	-
	1.67	-	-	8	-
	1.62	-	-	8	4
	1.57	2	-	8	5
	1.30	1	1	8	8
	With transverse bulkheads				(Version E)
0.	1.77	3	-	8	-
	1.47	2	-	8	-
	1.17	2	-	8	-
	1.07	-	-	8	-
	1.02	1	1	8	1
-1.0	1.38	2	-	8	-
	1.16	2	-	8	-
	0.93	2	-	8	-
	0.83	-	-	8	-
	0.78	-	-	8	-
	0.73	2	-	8	4
	0.65	1	-	8	5

Table 7: Number of tests resp. simulation runs N and number of observed capsizing incident N_c
Ship B; damage case 7/8; initial draught t = 5,75m

initial trim d T [m]	damage GM_L	Test N	Test N_c	Simulation N	Simulation N_c
	Open deck				(Version A)
0.	2.31	5	-	8	-
	1.72	2	-	8	-
	1.67	-	-	8	-
	1.62	-	-	8	8
	1.44	2	-	8	7
	1.38	2	-	8	8
+1.0	2.10	2	-	8	-
	1.79	2	-	8	-
	1.74	-	-	8	-
	1.69	-	-	8	-
	1.64	-	-	8	5
	1.49	1	1	8	8
	Side casings				(Version F)
0.	2.27	2	-	8	-
	1.96	2	-	8	-
	1.77	2	-	8	-
	1.68	-	-	8	-
	1.63	-	-	8	2
	1.58	2	1	8	4
+1.0	2.27	2	-	8	-
	1.89	2	-	8	-
	1.68	-	-	8	-
	1.63	-	-	8	2
	1.58	1	1	8	7
	With transverse bulkheads				(Version E)
0.	2.13	2	-	8	-
	1.75	2	-	8	-
	1.44	2	-	8	-
	1.29	2	-	8	-
	1.19	-	-	8	-
	1.14	-	-	8	5
+1.0	1.55	2	-	8	-
	1.31	2	-	8	-
	1.11	-	-	8	-
	1.06	-	-	8	6
	1.01	2	-	8	8

Table 8: Number of tests resp. simulation runs N and number of observed capsizing incidents N_c
Ship C; damage case 10/11; initial draught t = 6,0m

initial trim d T [m]	damage GM_L	Test N	Test N_c	Simulation N	Simulation N_c
	Open deck				(Version A)
0.	2.16	5	-	8	-
	1.62	2	-	8	-
	1.48	-	-	8	-
	1.43	-	-	8	2
	1.33	-	-	8	3
	1.23	-	-	8	2
	1.08	2	-	8	2
	0.3	2	1	8	5
+1.04	1.53	2	-	8	-
	1.12	2	-	8	-
	0.75	-	-	8	-
	0.70	-	-	8	2
	0.11	2	-	8	4
	Side casings				(Version F)
0.	1.90	2	-	8	-
	1.42	2	-	8	-
	1.37	-	-	8	1
	1.27	-	-	8	7
	1.17	2	2	8	7
+1.04	1.78	2	-	8	-
	1.54	2	-	8	-
	1.14	2	-	8	-
	1.09	-	-	8	-
	1.04	-	-	8	5
	With transverse bulkheads				(Version E)
0.	2.03	2	-	8	-
	1.74	2	-	8	-
	1.35	2	-	8	-
	1.25	-	-	8	-
	1.15	-	-	8	-
	1.05	-	-	8	-
	1.00	-	-	8	-
	0.95	-	-	8	1
+1.04	1.68	2	-	8	-
	1.31	2	-	8	-
	0.56	2	-	8	-
	0.51	-	-	8	-
	0.46	-	-	8	3

Table 9: Number of tests resp. simulation runs N and number of observed capsizing incidents N_c
Ship C; damage case 6/7; initial draught t = 6,0m

initial trim d T [m]	damage GM_L	Test N	Test N_c	Simulation N	Simulation N_c
	Open deck				(Version A)
0.	2.49	5	-	8	-
	2.05	2	-	8	-
	1.95	-	-	8	-
	1.90	-	-	8	2
	1.77	1	1	8	2
+1.08	2.33	2	-	8	-
	2.07	2	-	8	-
	1.90	1	1	8	-
	1.78	-	-	8	-
	1.68	-	-	8	-
	1.63	-	-	8	-
	1.58	-	-	8	1
-1.07	2.47	2	-	8	-
	2.24	2	-	8	-
	2.15	-	-	8	-
	2.08	1	1	8	2
	Side casings				(Version F)
0.	2.31	2	-	8	-
	2.12	2	-	8	-
	2.01	-	-	8	-
	1.96	2	-	8	2
	1.85	2	1	8	3
-1.07	2.29	1	-	8	-
	2.19	-	-	8	1
	2.14	-	-	8	3
	2.09	2	-	8	5
	1.95	1	1	8	6
	With transverse bulkheads				(Version E)
0.	2.00	2	-	8	-
	1.82	2	-	8	-
	1.63	2	-	8	-
	1.43	-	-	8	-
	1.38	-	-	8	-
	1.33	-	-	8	1
-1.07	2.20	2	-	8	-
	2.00	2	-	8	-
	1.83	2	-	8	-
	1.65	2	-	8	-
	1.45	-	-	8	-
	1.40	-	-	8	-
	1.35	-	-	8	3

4th INTERNATIONAL SHIP STABILITY WORKSHOP,
September 27th - 29th, 1998

SESSION 1: NUMERICAL AND PHYSICAL MODELLING OF INTACT STABILITY

Monday, September 28, 08:45-11:15

Discussion Leader: Professor C. Hsuing, Memorial University of Newfoundland

1. M. Hamamoto and A. Munif
   A Mathematical Model to Describe Ship Motions Leading to Capsize in Severe Astern Waves

2. J.O. de Kat and W.L. Thomas III
   Broaching and Capsize Model Tests for Validation of Numerical Ship Motion Predictions

3. K. McTaggart
   Ongoing Work Examining Capsize Risk of Intact Frigates Using Time Domain Simulation

4. M. Renilson and M. Hamamoto
   A Standard Method for Presentation of Capsize Data

5. N. Umeda
   New Remarks on Methodologies for Intact Stability Assessment

SESSION 2: NON-LINEAR DYNAMICS AND SHIP CAPSIZE

Monday, September 28, 11:45-15:45 (includes break for lunch)

Discussion Leader: Professor D. Bass, Memorial University of Newfoundland

6. K. Spyrou
   Ship Capsize Assessment Based on Nonlinear Dynamics

7. A. Francescutto and G. Contento
   The Modelling of the Excitation of Large Amplitude Rolling in Beam Waves

8. V.L. Belenky
   Piecewise Linear Approach to Non-linear Ship Dynamics

SESSION 3: SPECIAL PROBLEMS OF SHIP STABILITY

Monday, September 28, 16:15-17:15

Discussion Leader: Professor M. Haddara, Memorial University of Newfoundland

9. O. Rutgersson
   Full scale Trials – An Important Element in the Research on High-Speed Ship Performance in Following Seas

10. I.W. Dand
    Some Effects of Dynamics on Damage Stability

19:00 for 19:30 WORKSHOP DINNER

Tuesday, September 29, 08:30-10.00

Discussion Leader: Professor C. Hsiung, Dal-Tech University

11. Y. Ikeda, H. Okumura and T. Katayama
    Stability of Planing Craft in Turning Motion

12. Y. Washio, K. Kijima and T. Nagamatsu
    An Experimental Study on the Improvement of Transverse Stability at Running for High-Speed Craft

13. R. Birmingham
    The Stability Assessment of Small Working Craft without Reference to Hydrostatic Data

SESSION 4: NUMERICAL AND PHYSICAL MODELLING OF DAMAGE STABILITY

Tuesday, September 29, 10.30-13:00

Discussion Leader: Professor S. Calisal, University of British Columbia

14. D. Vassalos and O. Turan
    Water Accumulation on the Vehicle Deck of a Damaged Ro-Ro Vessel and Proposal of Survival Criteria

15. A. Kendrick, D. Molyneux, A. Taschereau and T. Pierce
    Exploration of the Applicability of the Static Equivalency Method Using Experimental Data

16. M. Pawlowski, M. Koniecki and M. Barbahan
    Analytical Studies for Water on Deck Accumulation

17. T. Haraguchi, S. Ishida and S. Murashige
    On the Critical Significant Wave Height for Capsizing of a Damaged RO-RO Passenger Ship

18. A. Jost
    RO-RO Passenger Vessels Survivability - A Study of Three Different Hull Forms Considering Different RO-RO-Deck Subdivisions.Ritical Height for Water on RO-RO Deck

SESSION 5: APPLICATIONS TO SHIP DESIGN AND OPERATION

Tuesday, September 29, 14.30-17:00

Discussion Leader: Mr. D. Murdey, Institute for Marine Dynamics

19. S.M. Calisal, M.J. Rudman, A. Akinturk, A. Wong and B. Tasevski
Water Discharge from an Opening in Ships

20. K. Hasegawa, K. Ishibashi and Y. Yasuda
Modelling and Computer Animation of Damage Stability

21. A. Papanikolaou and E. Boulougouris
Design Aspects of Survivability of Surface Naval and Merchant Ships

22. D. Vassalos
A Realisable Concept of a Safe Haven RO-RO Design

23. T. Allan
Expected Developments at IMD

4th INTERNATIONAL SHIP STABILITY WORKSHOP,
September 27th - 29th, 1998

INTERNATIONAL COMMITTEE MEMBERS

Prof. Alberto Francescutto
University of Trieste, Institute of Naval Architecture, Italy

Prof. Yoshiho Ikeda
Osaka Prefecture University, Japan

Prof. M. Hamamoto
Osaka University, Japan

Prof. Katsuro Kijima
Kyushu University, Japan

Mr. David Molyneux
National Research Council, Institute for Marine Dynamics, Canada

Prof. Apostolos Papanikolaou
National Technical University of Athens, Department of Naval Architecture & Marine Engineering, Greece

Dr. Naoya Umeda
National Research Institute of Fisheries Engineering, Japan

Prof. Dracos Vassalos
University of Strathclyde, Ship Stability Research Centre, Scotland

Dr. Iwao Watanbe
Ship Research Institute, Japan

LOCAL COMMITTEE MEMBERS

Prof. Mahmoud Haddara
Memorial University of Newfoundland, Canada

Dr. Kevin McTaggart
Defence Research Establishment Atlantic, Canada

Mr. David Molyneux
National Research Council, Institute for Marine Dynamics, Canada

Ms. Joanne Myrick-Harris
Conference Planning Consultant, Memorial University of Newfoundland, Canada

A Mathematical Model to Describe Ship Motions Leading to Capsize in Severe Astern Waves

by
Masami HAMAMOTO and **Abdul MUNIF**
Osaka University

ABSTRACT

A reasonable method used in prediction of ship motions leading to capsize in severe waves is developed on the basis of strip method. In this method the variation of metacentric height in waves is taken into account. Several simulations were conducted to predict the stability against capsizing of a container carrier 15000GT in severe waves due to parametric rolling. Finally the stable and unstable areas of the ship running in severe astern seas are computed

1. INTRODUCTION

As well known a linearized dynamic-hydrodynamic analysis of ship motion in waves has been successfully obtained in the strip method. The strip method now provides a workable design tool for predicting the average seakeeping performance of a ship early in the design process. The Performance which has been successfully described by linear procedures are ship motions, structural loads and even occurrence of seemingly nonlinear large amplitude phenomena such as the frequency of slamming and bow immersion. However, the strip method has partially developed for predicting stability against capsizing due to the parametric resonance, pure loss of stability and broaching-to of a ship running through astern seas, because the strip method has been mainly concerned with small amplitude periodic motion in a higher frequency range. By taking into account the variation of metacentric height based on the right arm curve of a ship in waves, it is useful to review some of the features of linear motion theory in hopes that its results may provide some guidance and insight into ship motion leading to capsizing. When a ship is running through waves with a constant forward speed U and encounter angle χ to waves, the linearized equations of motion with respect to heaving displacement ζ_G, pitching angle θ, swaying displacement η_G, yawing angle ψ and rolling angle ϕ, are described by:

$$\begin{aligned} m\ddot{\zeta}_G &= Z(Rad)+Z(Dif)+Z(FK)+W \\ I_{yy}\ddot{\theta} &= M(Rad)+M(Dif)+M(FK) \\ m\ddot{\eta}_G &= Y(Rad)+Y(Dif)+Y(FK) \\ I_{zz}\ddot{\psi} &= N(Rad)+N(Dif)+N(FK) \\ I_{xx}\ddot{\phi} &= K(Rad)+K(Dif)+K(FK)-W\overline{GM}\phi \end{aligned} \qquad (1)$$

where m is the mass of ship, and, I_{yy}, I_{zz} and I_{xx} the mass moments of inertia of ship about y,z and x axes as shown in Fig.1, $Z(Rad)$ and $Y(Rad)$ the radiation forces of heaving and swaying motions, $M(Rad), N(Rad)$ and $K(Rad)$ the radiation moments of pitching, yawing and rolling motions, $Z(Dif)$ and $Y(Dif)$ the diffraction forces of incident waves, $M(Dif), N(Dif)$ and $K(Dif)$ the diffraction moments of incident waves, $Z(F.K)$ and $Y(F.K)$ the Froude-Krylov forces including the hydrostatic forces, $M(F.K), N(F.K)$ and $K(F.K)$ the Froude-Krylov moments including the hydrostatic moments W the ship weight and $\overline{GM}$ the metacentric height.

In these linearized equations, the radiation, diffraction and Froude-Krylov forces acting on a section of the ship in the equilibrium position, can be computed by the ordinary strip method, but the linearized restoring moment is computed for the equilibrium position can not be used for a ship with metacentric height varies with respect to the relative position of ship to waves and wave steepness. As pointed out by Paulling[1) 2)], the variation of metacentric height is caused by the change of water plane area in the flare of fore and aft parts of ship hull plane with respect to the relative position of a ship to a wave. In order to take into account the effect of the variation, the linearized restoring moment of a ship in astern seas should be described by:

$$W\overline{GM}\left[1+\frac{\Delta\overline{GM}}{\overline{GM}}\cos(\omega_e t - k\xi_0)\right]\phi \qquad (2)$$

instead of $W\overline{GM}\phi$ in the last equation of Eq.(1).

where $\Delta\overline{GM}$ is the variation of metacentric height, ω_e the encounter frequency of ship to waves, k the wave number and ξ_0 the initial position of ship to waves.

The problem here is how to predict the variation of metacentric height consisting of the wave height to length ratio, H/λ, wave length to ship length ratio λ/L, encounter angle of ship to waves χ and the geometry of ship hull. The purpose of this study is to investigate the insight of parametric resonance taking into account the variation of metacentric height of a contain carrier running with constant forward speed U.

2. VARIATION OF METACENTRIC HEIGHT

In general the matacentric height $\overline{GM}$ can be obtained from the righting arm curve which is given by a nonlinear function of rolling angle ϕ. When a ship is displaced in a regular wave with rolling angle ϕ and encounter angle χ of ship to waves, the Froude-Krylov moment *K(F.K)* including the hydrostatic buoyancy with respect to the rolling about the center of gravity G is described as follows:

$$K(F.K) = -\int_L dx \iint \left[y\left(\frac{\partial p}{\partial z}\right) - (z-\overline{OG})\left(\frac{\partial p}{\partial y}\right)\right] dydz \qquad (3)$$

where:

$$\frac{\partial p}{\partial y} = \rho g \sin\phi + \rho g a k e^{-k\sigma d} \sin\phi \cos k\Theta$$
$$- \rho g a k e^{-k\sigma d} \cos\phi \sin\chi \sin k\Theta$$
$$\frac{\partial p}{\partial z} = \rho g \cos\phi + \rho g a k e^{-k\sigma d} \cos\phi \cos k\Theta \qquad (4)$$
$$+ \rho g a k e^{-k\sigma d} \sin\phi \sin\chi \sin k\Theta$$
$$\Theta = \xi_G + x\cos\chi - (y\cos\phi - z\sin\phi)\sin\chi - ct$$

ρ is water density, g the gravitational acceleration, a the amplitude of a regular wave, k wave number, ξ_G the position of ship to wave, c phase velocity of a wave, σ the sectional area ratio of x coordinate, t time, d draft in equilibrium, $\overline{OG}$ the position of center of gravity measured from the origin of body coordinate system $O-x,y,z$ in which the x is directed forward, the z axis directed downward and y axis directed to starboard as shown in Fig.1. In this computation, the integrals are taken over all volume up to the instantaneous submerged surface and the relative position of ship to wave is defined at t =0 by the ratio of ξ_G to the wave length λ.

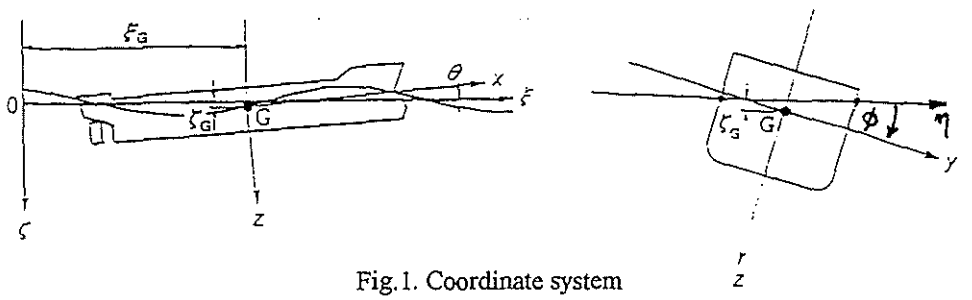

Fig.1. Coordinate system

And the displacement of submerged hull in waves must equals to the ship weight of the equilibrium condition in a still water and the pitching angle θ must be in the balance of pitching moment acting on the submerged hull. The Froude-Krylov moment $K(F.K)$ can be rewritten as:

$$K(F.K) = -\rho g \int_L dx \iint (y\cos\phi - z\sin\phi) dydz$$
$$- \rho g \overline{OG} \sin\phi \int_L dx \iint dydz$$
$$- \rho g a k \int_L e^{-k\sigma d} dx \iint (y\cos\phi - z\sin\phi)\cos k\Theta dydz \qquad (5)$$
$$- \rho g a k \sin\chi \int_L e^{-k\sigma d} dx \iint (y\cos\phi + z\sin\phi)\sin k\Theta dydz$$
$$- \rho g a k OG \sin\chi \int_L e^{-k\sigma d} dx \iint (\sin\phi\cos k\Theta - \sin\chi\cos\phi\sin k\Theta) dydz$$

In this equation, the first and the second terms are righting moments due to the hydrostatic force acting on the submerged volume of ship hull in waves. According to the strip method, the righting arm $\overline{GZ}$ is defined by these two terms as:

$$W\overline{GZ} = \rho g \int_L dx \iint (y\cos\phi - z\sin\phi)dydz + \rho g\overline{OG}\sin\phi \int_L dx \iint (y\cos\phi - z\sin\phi)dydz \qquad (6)$$

In studying the large amplitude rolling motion, the method of equivalent linearization has been utilized for describing a dynamic system in which large deviations from linear behavior are not anticipated. A reasonable approximation to the exact behavior of the real system, therefore, would be given by an equivalent linear system having linear coefficient approximately selected. The $\overline{GZ}(wave)$ of container carrier as shown in Fig.2 increases at the wave trough amidship and decreases at the wave crest amidship in comparison with the righting arm $\overline{GZ}(still)$ in still water as shown in Fig.3.

Items		Ship	Model
Length	L(m)	150	2.5
Breadth	B(m)	27.2	0.453
Depth	D(m)	13.5	0.225
Draught	d_f(m)	8.5	0.142
	d_a(m)	8.5	0.142
Block Coefficient	C_b	0.667	0.667
Metacentric Height	$\overline{GM}$(m)	0.3 0.6 0.9	0.051 0.077 0.112
Natural roll Period	T_ϕ	37.95 27.01 21.85	4.9 3.5 2.7
Model scale	---		1/60

Fig. 2. Principal particulars of container carrier

When the ship is rolling in astern seas, the rolling angle develops significantly large. Therefore, the equivalent metacentric height should be determined on the basis of the righting arm curve considered up to an appropriate angle of inclination as follows:

$$\int_0^{\phi_r} \overline{GM}(still)\phi\, d\phi = \int_0^{\phi_r} \overline{GZ}(still)\, d\phi$$

$$\int_0^{\phi_r} \overline{GM}(trough)\phi\, d\phi = \int_0^{\phi_r} \overline{GZ}(trough)\, d\phi \qquad (7)$$

$$\int_0^{\phi_r} \overline{GM}(crest)\phi\, d\phi = \int_0^{\phi_r} \overline{GZ}(crest)\, d\phi$$

where ϕ_r is the vanishing angle, $\overline{GM}(still)$, $\overline{GM}(trough)$ and $\overline{GM}(crest)$ the equivalent linearized metacentric heights in still water, wave trough and wave crest respectively.

A further consideration is required to specify a reasonable expression of $\overline{GM}(wave)$ leading to a really equivalent solution. For this problem, an assumption is made here that the variation of metacentric height $\overline{GM}(wave)$ is sinusoidal and finally it is given by the following form:

$$\overline{GM}(wave) = \overline{GM}(still)\left[1 + \frac{\Delta\overline{GM}}{\overline{GM}(still)}\cos(\omega_e t - k\xi_0)\right] \qquad (8)$$

where

$$\frac{\Delta\overline{GM}}{\overline{GM}(still)} = \frac{\overline{GM}(trough) - \overline{GM}(crest)}{2\overline{GM}(still)} \qquad (9)$$

The values of $\overline{GM}(still)$, $\overline{GM}(trough)$ and $\overline{GM}(crest)$ can be obtained by using the energy balance

concept, their values depend on the wave steepness H/λ, the wave to ship length ratio λ/L, the encounter angle of ship to waves χ and the metacentric height $\overline{GM}$ in still water. For λ/L=1, H/λ=1/20, $\overline{GM}$ =0.6m and χ =0 their values are shown in Fig.4, and the values of $\Delta\overline{GM}$ for several wave steepness, $\overline{GM}$ and encounter angle χ are given in Fig.5.

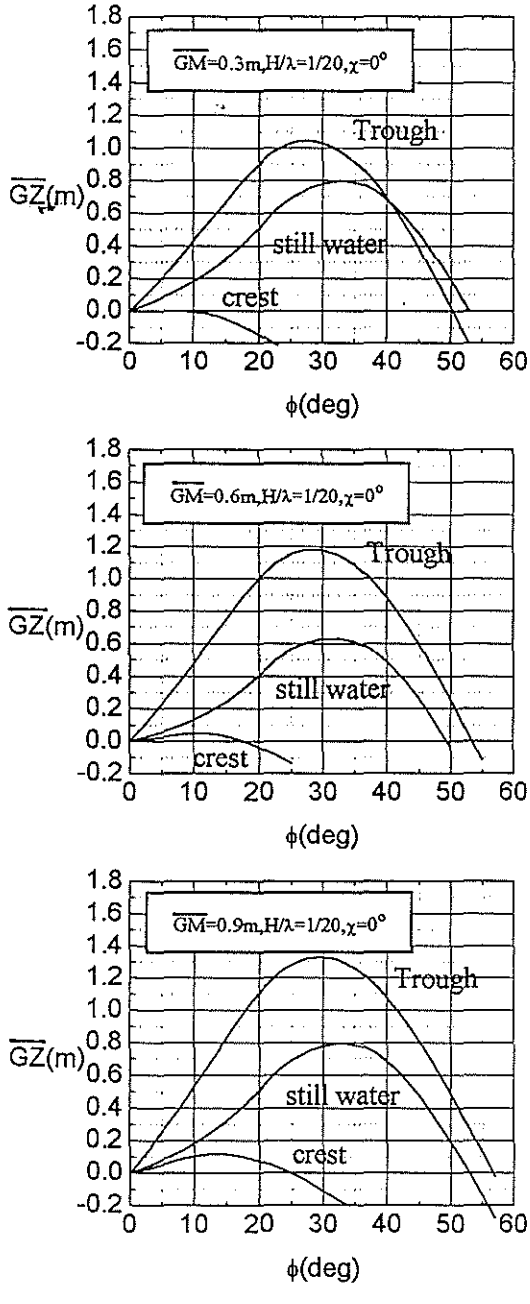

Fig. 3. The righting arm $\overline{GZ}$ curves of container carrier

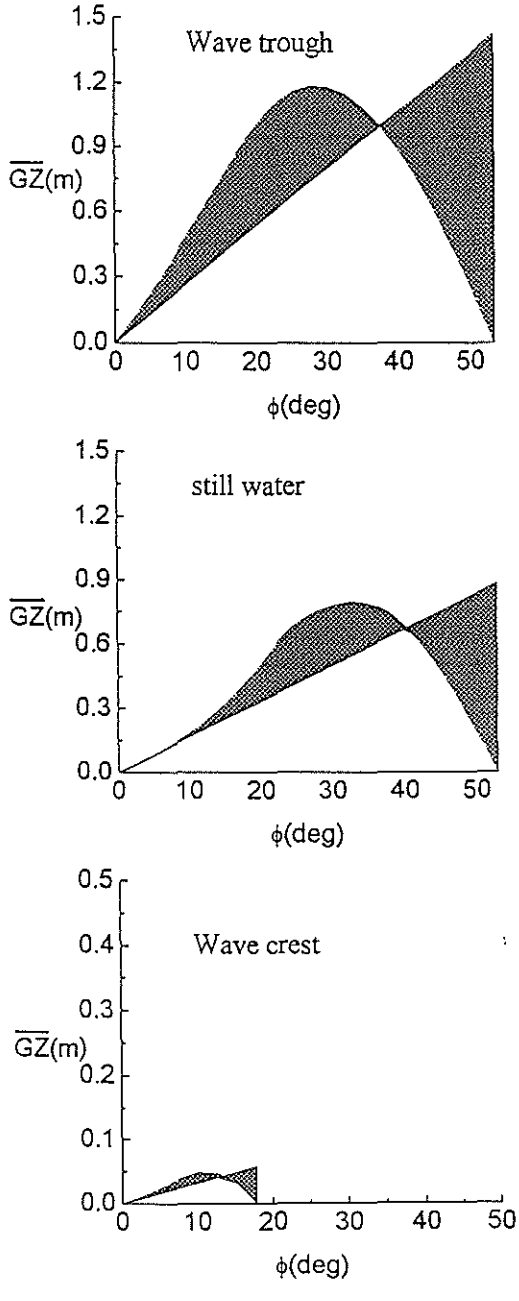

Fig.4. Equivalent linearized metacentric height for H/λ =1/20, $\overline{GM}$ =0.6m and χ =0

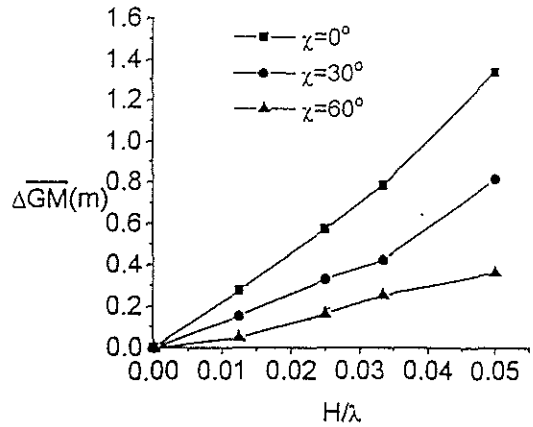

Fig.5. The variation of equivalent linearized metacentric height

3. MATHEMATICAL MODEL AND EXAMPLES OF NUMERICAL SIMULATION

According to the method mentioned in section 2, equivalent linearized equations can be described in the following form:

Combined motions of heave and pitch

$$\begin{aligned}&(m+m_z)\ddot{\zeta}_G + Z_{\dot{\zeta}_G}\dot{\zeta}_G + Z_{\zeta_G}\zeta_G + Z_{\ddot{\theta}}\ddot{\theta} + Z_{\dot{\theta}}\dot{\theta} + Z_{\theta}\theta = Z_C\cos\omega_e t + Z_S\sin\omega_e t\\ &(I_{yy}+J_{yy})\ddot{\theta} + M_{\dot{\theta}}\dot{\theta} + M_{\theta}\theta + M_{\ddot{\zeta}_G}\ddot{\zeta}_G + M_{\dot{\zeta}_G}\dot{\zeta}_G + M_{\zeta_G}\zeta_G\\ &\qquad = M_C\cos\omega_e t + M_S\sin\omega_e t\end{aligned} \tag{10}$$

Combined motions of sway, yaw and roll

$$\begin{aligned}&(m+m_y)\ddot{\eta}_G + Y_{\dot{\eta}_G}\dot{\eta}_G + Y_{\ddot{\phi}}\ddot{\phi} + Y_{\dot{\phi}}\dot{\phi} + Y_{\ddot{\psi}}\ddot{\psi} + Y_{\dot{\psi}}\dot{\psi} + Y_{\psi}\psi\\ &\qquad = Y_C\cos\omega_e t + Y_S\sin\omega_e t\\ &(I_{zz}+J_{zz})\ddot{\psi} + N_{\dot{\psi}}\dot{\psi} + N_{\psi}\psi + N_{\ddot{\eta}_G}\ddot{\eta}_G + N_{\dot{\eta}_G}\dot{\eta}_G + N_{\ddot{\phi}}\ddot{\phi} + N_{\dot{\phi}}\dot{\phi}\\ &\qquad = N_C\cos\omega_e t + N_S\sin\omega_e t\\ &(I_{xx}+J_{xx})\ddot{\phi} + K_{\dot{\phi}}\dot{\phi} + \overline{W}\overline{GM}\left[1+\frac{\Delta\overline{GM}}{\overline{GM}}\cos(\omega_e t - k\xi_0)\right]\phi\\ &+ K_{\ddot{\eta}_G}\ddot{\eta}_G + K_{\dot{\eta}_G}\dot{\eta}_G + K_{\ddot{\psi}}\ddot{\psi} + K_{\dot{\psi}}\dot{\psi} + K_{\psi}\psi = K_C\cos\omega_e t + K_S\sin\omega_e t\end{aligned} \tag{11}$$

where the hydrodynamic and hydrostatic coefficients are obtained from the ordinary strip method and the metacentric height taking into account the variation of righting moment in waves is given by the equivalent linearization mention in section 2. It should be noted that the last equation in Eq.(11) is a linear differential equation with respect to the rolling angle ϕ although the unique feature of the equation is the presence of time dependent coefficient of the rolling angle ϕ. Furthermore, this kind of equation has a property of considerable importance in ship rolling problem in that for certain values of the encounter frequency ω_e, the solution is unstable. Physically, this implies that if the roll motion described by Eq.(11) is taking place in unstable region, the amplitude of rolling grows up. The unstable encounter frequency may be found from unstable solution of Mathieu's equation, in which unstable roll occurs when encounter frequency ω_e is

equal to twice of the natural frequency ω_ϕ of roll. For this unstable condition $\omega_e = 2\omega_\phi$, the encounter frequency ω_e is given by:

$$\omega_e = \sqrt{\frac{g}{L}}\left|\sqrt{\frac{2\pi L}{\lambda}} - Fn\left(\frac{2\pi L}{\lambda}\right)\cos\chi\right| \tag{12}$$

and the natural frequency ω_ϕ is obtained from the natural rolling period T_ϕ defined by IMO resolution A 562 [8] as follows:

$$\omega_\phi = \frac{2\pi}{T_\phi}$$
$$T_\phi = \frac{2B}{\sqrt{GM}}[0.373 + 0.023(B/d) - 0.043(L/100)] \tag{13}$$

where L is the ship length, B the breadth, d the draft, Fn the Froude number and λ the wave length.
By using these relationship, it will be possible to specify the encounter frequency for the ship running with Fn and χ when the parametric resonance occurs.
In general, the parametric resonance keeps a critical rolling of the constant amplitude when the energy due to the roll damping is balanced with the energy due to the variation of metacentric height. The rolling angle grows up when the damping energy is smaller than energy due to the variation of metacentric height and it damps out when the damping energy is bigger than the energy due to the variation of metacentric height.
From the above physical point of view, several numerical simulations were carried out for the container carrier which is running with constant speed U and encounter angle χ in astern seas. Three kinds of metacentric heights, $\overline{GM}$ =0.3m, $\overline{GM}$ =0.6m and $\overline{GM}$ =0.9m of the container are selected to investigate the ship motion leading to capsize, the encounter angle is fixed at $\chi = 0^0, 15^0, 30^0, 45^0$ and 60^0. Figs.6, 7, 8, 9 and 10 are the time history of roll, pitch and yaw motions of the ship with metacentric height $\overline{GM}$ =0.6m in critical and unstable conditions. Finally, from the numerical simulations, it is possible to find out the critical roll of constant amplitude in parametric resonance. Fig.11 shows the waves steepness H/λ for encounter angle χ of the critical rolling motion leading to capsize.

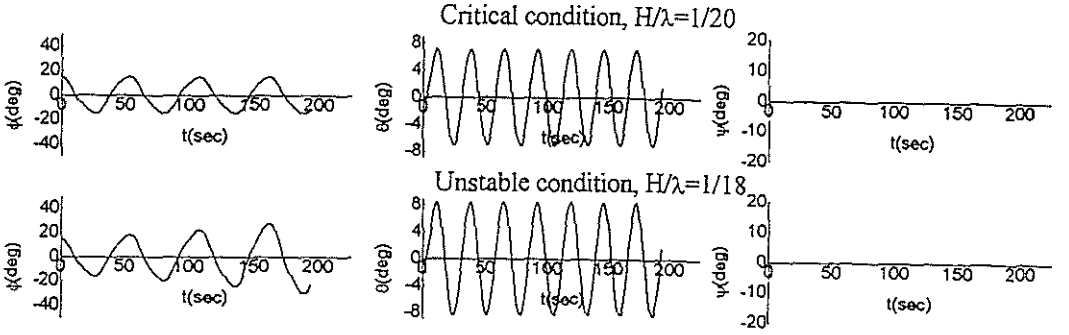

Fig.6. Time history of roll, pitch and yaw in critical and unstable motions $\overline{GM}$ =0.6m, Fn =0.10935 χ =0

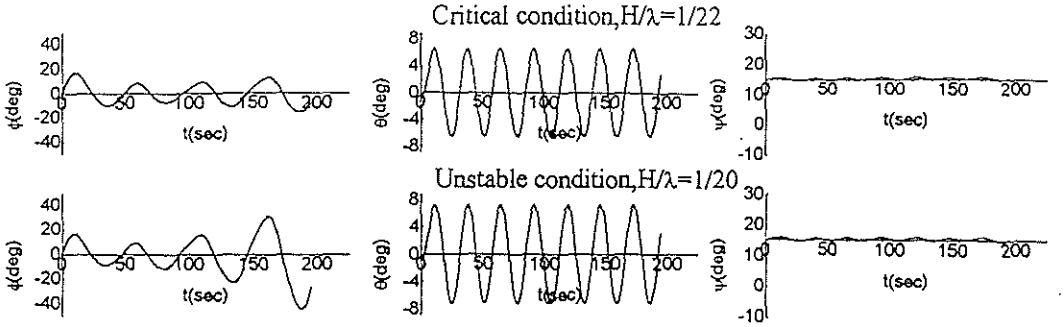

Fig.7. Time history of roll, pitch and yaw in critical and unstable motions $\overline{GM}$ =0.6m, Fn =0.11, χ =15

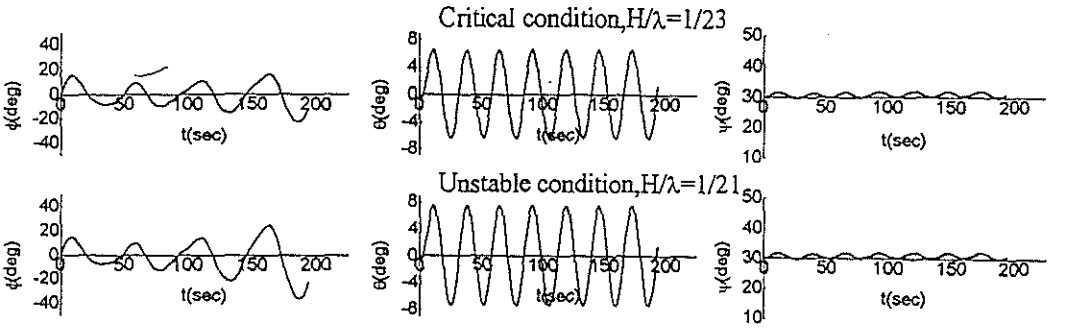

Fig.8. Time history of roll, pitch and yaw in critical and unstable motions $\overline{GM}$ =0.6m, Fn =0.1263, χ =30

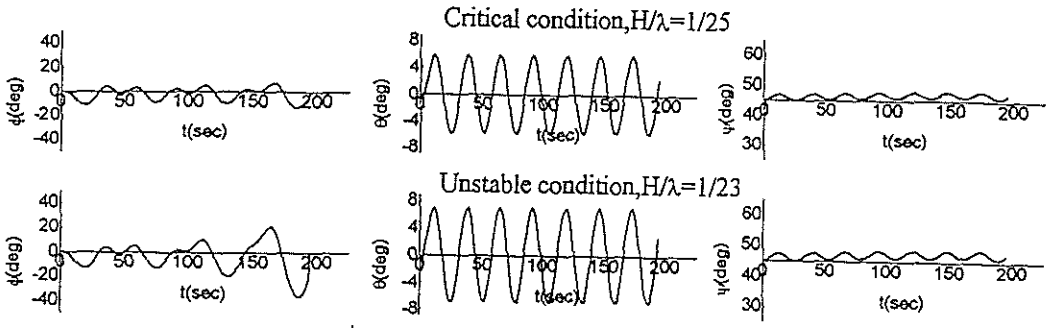

Fig.9. Time history of roll, pitch and yaw in critical and unstable motions $\overline{GM}$ =0.6m, Fn =0.15 χ =45

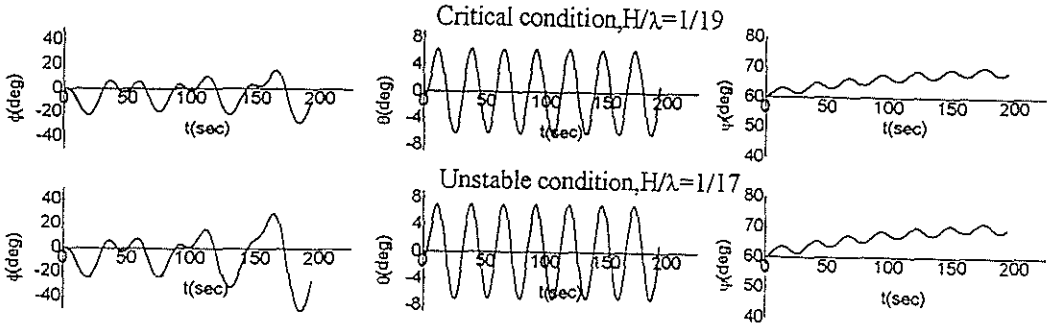

Fig.10. Time history of roll, pitch and yaw in critical and unstable motions $\overline{GM}$ =0.6m, Fn =0.22 χ =60

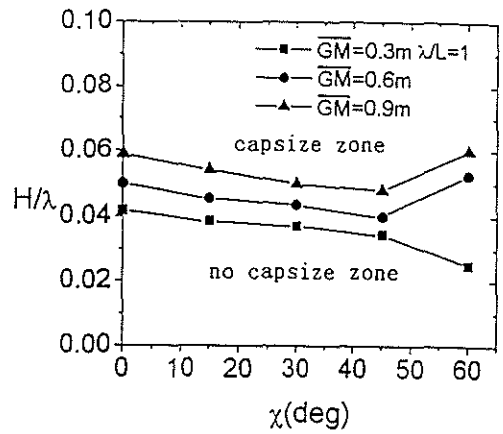

Fig.11. Critical line leading to capsize, H/λ vs χ

4. CONCLUDING REMARKS

An analytical study of ship capsize phenomenon due to parametric resonance is conducted to investigate the occurrence of the critical condition leading to capsize by making use of the ordinary strip method taking into account the variation of metacentric height with respect to relative position of ship to waves. The main conclusions are summarized as follows:

1. The ordinary strip method taking into account the variation of metacentric height in waves is usable for predicting the occurrence of parametric resonance
2. When the ship is running with large encounter angle such as $\chi = 45^0$, the rolling angle deforms due to the wave excitation as shown in Fig.9 although the ship usually rolls with the natural rolling period T_ϕ at the parametric resonance. This rolling motion comes from the combination of the wave induced stability varying with the natural rolling period and wave excitation varying with encounter period T_e
3. For the design $\overline{GM}$ =0.9m and operational $\overline{GM}$ =0.6m, the most dangerous condition leading to capsize is at encounter angle approximately 45^0, but for small metacentric height, $\overline{GM}$ =0.3m, the most dangerous condition is at encounter angle approximately to 60^0, because the Froude number becomes quite large to satisfy the condition of parametric resonance, then the ship is running with the velocity nearly equal to wave celerity. These computational results show a fairly good agreement with the experimental results[4) 5)]

This study was carried out under the scientific grant (No. 08305038) and RR 71 research panel of Shipbuilding Research Association of Japan. The authors would like to express their gratitude to the members of the RR 71, chaired by Prof. Fujino. The authors also wish to thank Prof. Saito at Hiroshima University for calculating the coefficients of radiation and diffraction.

REFRENCES

1. Kerwin, J.E., "Notes on Rolling in Longitudinal Waves", International Shipbuilding Progress, Vol.2, No.16, 1955,pp.597-614
2. Paulling, J.R., "The tranverse Stability of a Ship in a Longitudinal Seaway", Journal of Ship Research,

SNAME, Vol.4, No.4, 1961, pp.37-49
3. Hamamoto,M., Sera,W., Panjaitan,J.P, "Analysis on Low Cycle Resonance of Ship in Irregular Astern Seas", Journal of the Society of Naval Architects of Japan, Vol.178, 1995, pp.137-145
4. Umeda N.,Hamamoto,M., Takaishi,Y., Chiba, Y., Matsuda A., Sera,W., Suzuki, S., Spyrou, K., Watanabe, K., "Model Experiment of Ship Capsize in Astern Seas", Journal of the Society of Naval Architects of Japan, Vol.177, 1995, pp.207-217
5. Hamamoto,M., Enomoto, T., Sera,W., Panjaitan,J.P, Ito, H., Takaishi,Y., Kan, M., Haraguchi, T., Fujiwara, T., "Model Experiment of Ship Capsize in Astern Seas", second report, Journal of the Society of Naval Architects of Japan, Vol.179, 1996, pp.77-87
6. Hamamoto,M., Panjaitan,J.P, "Analysis on Parametric Resonance of Ships in Astern Seas", Proceeding of Second Workshop on Stability and Operational Safety of Ships, Osaka, November, 1996
7. Paulling,J.R., Oakley, O.H., Wood, P.D.,"Ship Capsizing in Heavy Seas: The Correlation of Theory and Experiments", Proceeding of the International Conference on Stability of Ships and Ocean Vehicles, Glasgow, 1975
8. A.R.J.M.Lloyd, "Seakeeping: Ship Behaviour in Rough Weather", Ellis Horwood Ltd., 1989
9. IMO,: The intact Stability Criteria, Resolution A, 562, 1985

Broaching and capsize model tests for validation of numerical ship motion predictions

J.O. de Kat (Maritime Research Institute Netherlands)

W.L. Thomas III (David Taylor Model Basin, NSWC, Carderock Division)

ABSTRACT

Model tests have been carried out with a frigate-type hull in waves leading to a variety of extreme motion events including capsizing. A specific requirement was the ability to perform tests in critical, stern quartering wave conditions at high speed and measure relevant parameters for validation of a large amplitude ship motion simulation program.

The paper describes model testing techniques, test data and some comparisons with numerical simulations related to large amplitude rolling, surfriding, broaching and capsizing in following to beam waves. Tests comprised maneuvering (zigzag) tests, roll decay in calm water, and regular waves of moderate to extreme steepness for a range of GM values.

INTRODUCTION

Since the cooperative research work presented by De Kat et al (1994), a second 4-year joint research effort on ship stability started in 1995 under sponsorship from the Cooperative Research Navies group. This CRNAV group, which comprises five navies (from Australia, Canada, Netherlands, United Kingdom and United States), U.S. Coast Guard and MARIN, focuses its current activities on the dynamic stability assessment of intact and damaged ships using numerical simulations.

The applied numerical tools should be subjected to proper verification and validation. An extensive database is available with seakeeping and manoeuvering data for intact ships. Suitable validation data concerning large amplitude ship motions of intact ships (including broaching and capsizing) are available to a very limited extent. To make the validation database more complete in terms of extreme conditions, tests were carried out in 1997 with a free-running frigate model.

This paper describes these model tests in detail, with the objective to provide insights into the physics of extreme motion events observed in the tests and discuss validation issues from a model testing perspective. The tests cover the most critical wave directions concerning dynamic stability during ship operations: following, stern quartering and beam seas were tested at different ship speeds with Froude number ranging from Fn = 0.1 to 0.4. Observed events include surfriding, broaching associated with surfriding, extreme rolling, and capsizing in a variety of modes.

EXPERIMENTAL SETUP

Fulfilment of the extreme motion objectives required a large basin capable of generating moderate and steep waves under arbitrary heading angles. A large test basin was required to maximize run length. The capability to generate steep waves allowed a test matrix to be developed, which would ensure the occurrence of extreme events. In addition to the tests in waves, the requirements included zigzag tests and roll decay tests at different speeds in calm water.

The test matrix for runs in waves required:

1. High speed runs in beam seas through following seas of suitable run lengths to allow capsizing, broaching, and surfriding.
2. Large amplitude regular waves having typical steepnesses (H/λ) of 1/20, 1/15, 1/10.

3. wave length to ship length ratios (λ /l) between .75 and 2.5

Basin

The capsize model tests and the calm water experiments were carried out in the Maneuvering and Seakeeping (MASK) Basin of the Carderock Division, Naval Surface Warfare Center.

The MASK is an indoor basin having an overall length of 110 m, a width of 73 m and a depth of 6.1 m, except for a 10.7 m wide trench parallel to the long side of the basin. The Basin is spanned by a 115 m long bridge supported on a rail system that permits the bridge to transverse half the width of the basin and to rotate up to 45 degrees from the longitudinal centerline. Models can be tested at all headings relative to the waves, with the wave makers located along two adjacent sides of the basin. A towing carriage is hung from the bridge. The carriage has a maximum speed of 7.7 m/s.

MODEL DESCRIPTION

The model chosen for this study has a conventional frigate hull form; a 1/36th scale was chosen for the fiberglass model. See Figure 1. The 3 meter model was large enough for accurate seakeeping measurements, yet was small enough to take advantage of the steeper waves produced in the MASK. The model was assigned the number 9096 by the Carderock Division, Naval Surface Warfare Center (CDNSWC).

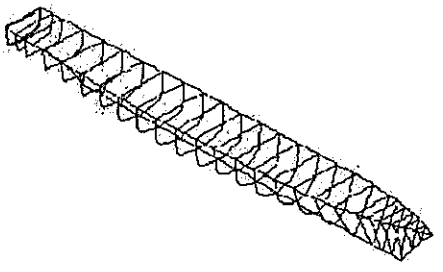

Figure 1. *Isometric sketch of frigate (Model 9096)*

The model was outfitted to be self-propelled using an autopilot for heading control. This autopilot uses a simple PID controller algorithm such that the desired rudder angle is:

$$\delta_{d\psi} = C_{1D}(\psi - \psi_d) + C_{2D}\dot{\psi}$$

where C_{1D} is the yaw gain and C_{2D} is the yaw rate gain.

The model was outfitted with bilge keels and twin rudders. Two four-bladed fixed pitch propellers (CDNSWC numbers 1991 and 1992) were installed on the model for inboard rotation.

A Plexiglas deck was installed to protect the instrumentation and machinery systems inside the hull from water damage during capsize events. The model was painted to enhance the display of the model during video recordings.

The outfitted model was tethered to the carriage by a cable bundle that contained control, power, and data signals. The cable was looped to minimize the effect of the cable tension on the model. The cable was connected to an overhead boom via a pulley that could be reeled in and out by a boom operator who stood on a platform mounted on the carriage. The boom could be yawed as desired by the boom operator. During the calm water and regular wave experiments, the carriage followed the model and the boom operator ensured that cable tension did not affect the model. The boom operator did this by pointing the boom so that it stayed above the model while reeling in or out the overhead pulley so that the cable remained slack. See Figure 2.

Before the start of a test in waves, the wave maker was turned on and the model held in position until a sufficient number of waves had passed. Subsequently the model would start slowly under its own power (at low RPM) and once it was on course properly, the propeller RPM was set to the required level associated with a calibrated speed in calm water. The boom and trolley system followed the model during the test.

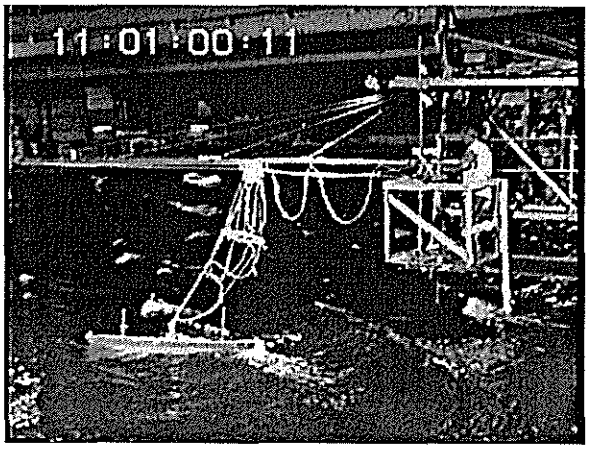

Figure 2. *Model tether arrangement*

Instrumentation

The carriage was equipped with a Ship Motion Recording (SMR) system developed by the CDNSWC Seakeeping Department. This system was connected to the sensors used in the model test as listed in Table 1 and described below.

Table 1. *Capsize model test data channels*

Measurement	Source
Basin Wave Height From Carriage (cm)	Sonic Transducer
Basin Wave Height on shore (cm)	Sonic Transducer
Carriage Speed (m/s)	Tachometer
Propeller RPM (rev/minute)	Tachometer
INS Hull Speed (m/s)	MILNAV™
INS Azimuth (°T)	MILNAV™
Pitch (deg)	MILNAV™
Pitch rate (deg/s)	MILNAV™
Roll (deg)	MILNAV™
Roll Rate (deg/s)	MILNAV™
Yaw Rate (deg/s)	MILNAV™
Rudder Angle (deg)	Autopilot
Rudder force, X direction (Newtons)	Block Gauge
Rudder Side force (Newton)	Block Gauge
Vertical Acceleration Forward (g)	Accelerometer
Longitudinal Acceleration Forward (g)	Accelerometer
Transverse Acceleration Forward (g)	Accelerometer
Vertical Acceleration Starboard (g)	Accelerometer
Longitudinal Acceleration Starboard (g)	Accelerometer
Transverse Acceleration Starboard (g)	Accelerometer
Relative Bow Motion, Port and Starboard (cm	Capacitance Probe
Relative Stern Motion, Port and Starboard (cm	Capacitance Probe

The primary sensor used in the model test was a KEARFOTT T16 *Miniature Integrated Land Navigation System* (MILNAV™). This inertial navigation system (INS) included a monolithic 3-axis Ring Laser Gyroscope and three, single axis linear accelerometers. The MILNAV had the capability to measure extreme pitch, roll, and yaw angles, rates and accelerations. It was also used to determine surge, sway, and heave displacements, velocities, and accelerations near the center of gravity of the model. These motions were translated to the ship's center of gravity reference for each load condition.

More details have been described by De Kat and Thomas (1998). Model speed was measured in three orthogonal directions using the MILNAV™ inertial navigation system. Propeller speed was measured using a tachometer which was mounted to the propeller shafting. Rudder angle was measured using the rudder feedback unit which as mechanically linked to the rudder tiller arm. Longitudinal and transverse rudder forces were measured using block gauges mounted on a free-floating plate that was attached to the rudder posts.

Model hydrostatics

The model was tested in three load configurations. These configurations comprised:

1. Full Load condition
2. Marginal GM condition
3. Failed GM condition

The load conditions were chosen with first priority given to the validation of the time domain simulation program FREDYN developed by the CRNAV group. Since the capsizing characteristics of this frigate were previously unknown, it was deemed necessary to choose a load condition to ensure that capsizing would occur. As an additional consideration, it was desired that one load condition resemble a realistic operating condition of the ship. Thus, the first and most conservative condition tested closely resembled the typical frigate Full Load operating condition. The two remaining load conditions were achieved by the raising of weights above the deck of the model to reduce transverse GM. This procedure ensured that displacement and freeboard remained constant for the three load conditions. Thus, the second load condition called "Marginal GM" represented a decrease in GM such that the model is in marginal compliance with the U. S. Navy Criteria (NAVSEA, 1976), which include a weather criterion. The third load condition called "Failed GM" represented a load configuration that is in violation of the U. S. Navy Stability Criteria; as such this is not a realistic operating condition.

A summary of the full scale load configurations tested is presented in Table 2. The GZ curve was measured for the full range from 0 to 180 degrees heel angle for the three loading conditions to provide comparison data as regards the computed hydrostatics.

Table 2. *Full Scale Load Conditions corresponding to model test*

Parameter	Load condition		
	Full load	Marginal GM	Failed GM
L_{PP} (m)	106.68	106.68	106.68
B (m)	12.78	12.78	12.78
T (m)	4.73	4.73	4.73
GM_T(m)	0.78	0.68	0.43
T_ϕ (sec)	12.3	13.3	17.1

The transverse metacentric height (GM_T) was checked prior to each run series in waves by conducting an inclining experiment. The roll, pitch and yaw gyradii (k_{44}, k_{55} and k_{66}) were determined using the pendulum method by swinging the model in the air. For each load condition, the model was suspended by a pivot located above the COG of the model and allowed to oscillate in e.g. pitch or roll. The gyradii were calculated from the respective oscillation periods.

Test conditions

The model test matrix was designed for runs in regular waves for the three load (GM) conditions for the purpose of identifying critical, extreme motion situations, including capsizing, broaching, harmonic resonance and surfriding. Regular waves were chosen instead of irregular waves to allow a better understanding of observed extreme events in terms of known wave length, steepness, and phase relation with respect to the model; an important factor was the ability to use the data for validating a time domain simulation model.

The critical wave length range involved waves with λ/L between 0.75 and 2.50 with associated wave steepness in the range of 1/20 and 1/10. Model speeds were chosen between Fn_0 = 0.1 and 0.35 in combination with the selected wave and heading conditions. The critical wave headings chosen included following seas and stern quartering seas predominantly. Some runs were performed in beam seas.

Runs were performed at selected critical headings and speeds, which were based on time domain simulations carried out *a priori*. In case of the "Failed GM" loading condition, the occurrence of a capsize event invoked procedures that isolated the capsize region at the particular wave length λ/L. In general this meant that follow-up runs were made in higher and lower wave steepnesses and at lower (or higher) speeds until no capsizes were found. Adjacent headings were also tested at the capsize steepness to identify the effects of heading variations.

Table 3 provides an overview of the test runs for the ship with the Failed GM condition; χ represents the nominal heading angle. Test conditions for the other two loading conditions were in principle similar.

λ/L	H/λ	Fn	χ (deg)						
			0	15	30	45	60	75	90
0.75	1/15	0.1							
		0.2			X				
		0.3							
		0.35		X	X				
	1/10	0.1		X					
		0.2			X				
		0.3		X					
		0.35		X	X	X			

λ/L	H/λ	Fn	χ (deg)						
			0	15	30	45	60	75	90
1.00	1/20	0.1							
		0.2			X				
		0.3			X				
		0.35		X	X				
	1/15	0.1			X				
		0.2				X			
		0.3		X	X	X			
		0.35	X	X	X	X			
	1/10	0.1							
		0.2							
		0.3		X	X				
		0.35		X	X	X			

λ/L	H/λ	Fn	χ (deg)						
			0	15	30	45	60	75	90
1.25	1/20	0.1							
		0.2			X				
		0.3			X				
		0.35	?	X	X				
	1/15	0.1				X			
		0.2				X	X		
		0.3			X	X			
		0.35	X	X	X	X	X		
	1/10	0.2							
		0.2		X	X				
		0.3		X	X				
		0.35			X				

λ/L	H/λ	Fn	χ (deg)						
			0	15	30	45	60	75	90
1.50	1/20	0.1							
		0.2							
		0.3							
		0.35			X				
	1/15	0.1				X			
		0.2				X			
		0.3		X	X		X		
		0.35		X	X	X	X		
	1/10	0.1							
		0.2							
		0.3		X	X				
		0.35		X	X	X	X		

λ/L	H/λ	Fn	χ (deg)						
			0	15	30	45	60	75	90
2.00	1/20	0.1							
		0.2							
		0.3		X					
		0.35		X					
	1/15	0.1							X
		0.2							
		0.3							
		0.35		X	X				

λ/L	H/λ	Fn	χ (deg)						
			0	15	30	45	60	75	90
2.50	1/20	0.1							
		0.2							
		0.3							
		0.35			X				
	1/15	0.1			X				X
		0.2							
		0.3			X				
		0.35		X	X				

Table 3. *Test matrix for Model 9096 in Failed GM condition (0 degrees is following seas)*

EXTREME MOTION EVENTS

The following provides a description of some extreme motion events, including:

- Surfriding (and periodic surging)
- Broaching
- Extreme rolling
- Capsizing

Surfriding

A ship in following seas can experience large speed fluctuations (at low encounter frequencies) about its mean forward speed. If the ship speed is sufficiently high, i.e. the speed that would be attained in calm water at a given propeller RPM and thrust, a wave may capture the ship and propel it at wave phase speed. The resulting speed can be significantly higher than the calm water speed.

The typical conjecture in surfriding research is that once captured by a wave, the ship attains a steady speed. An interesting result of the model tests presented here is that the ship can reach speeds well beyond the (steady) wave phase speed for an extended period before reaching a steady-state condition. To illustrate this, we consider the frigate running in following seas (zero degrees heading angle) of different periods and heights. The loading condition corresponds to the Full Load case discussed above. At a propeller RPM setting for calm water Froude number of $Fn\_0 = 0.3$, the ship experiences periodic oscillations in forward speed of significant amplitude, which increases with increasing wave amplitude (De Kat and Thomas, 1998).

The model tests show that for the speed range $Fn\_0 \leq 0.3$ wave capture (and hence surfriding) does not occur in the wave conditions tested. For $Fn\_0 = 0.35$ a drastic change in surge character occurs, for at this speed setting the frigate model does experience wave capture and surfriding events. In a number of tests where wave capture takes place in following waves, the ship is accelerated to a speed that lies well beyond the phase speed of the wave. Figure 3 provides an overview of measured maximum speeds for $Fn\_0 = 0.35$. The maximum ship speed increases with increasing wave steepness; for the conditions with $\lambda/L = 1$ the steepness tested is $H/\lambda = 0.077$ and 0.097, while for $\lambda/L = 1.25$ the steepness is $H/\lambda = 0.051$ and 0.092.

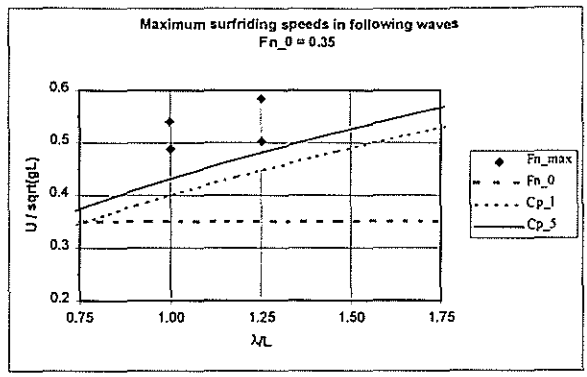

Figure 3. *Maximum attained ship speed (Fn_max) following wave capture in experiments. Cp_1 is the phase velocity based on linear wave theory; Cp_5 is the phase velocity for H/λ = 0.1*

For reference purposes in the figures presented in this paper, we use a definition for wavelength based on linear wave theory in deep water, i.e. $\lambda = gT^2/2\pi$, where T is the period. Cp_1 represents the phase speed according to linear wave theory, while Cp_5 is the phase speed determined according to Stokes 5th order theory (Fenton [5]); the phase speeds have been normalized by the square root of gL.

Figure 3 shows that especially for the steepest waves, the maximum ship speed reaches very high values. The time series describe the character of this behavior, as shown for run 231 in Figure 4, where $\lambda/L = 1.0$ and $H/\lambda = 0.1$.

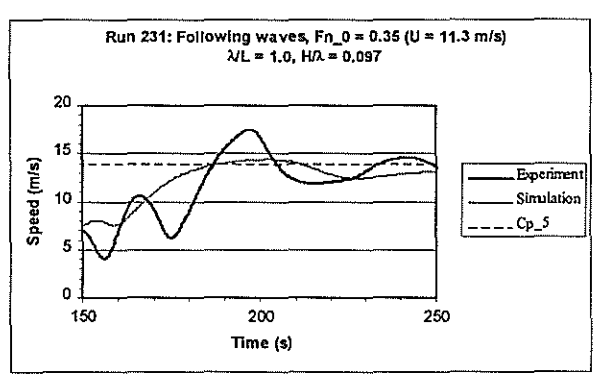

Figure 4. *Measured and predicted ship speed during surfriding events for run 231*

This figure shows that as the ship reaches a critical speed level in the model test, wave capture occurs and the ship accelerates to a speed well beyond its calm water speed. The observed mechanism is as follows: at approximately t = 180 s a wave crest reaches the stern of the ship and causes the ship to surge forward. At around t = 185 s the crest has reached the aft quarter (i.e. it has overtaken the ship slowly until the ship speed equals the celerity), at which stage the ship is subjected to a large surge force. This causes the ship to accelerate and overtake the wave crest, which by t = 200 s is situated at the stern again; the maximum speed is 17.5 m/s. While the ship accelerates and overtakes the wave crest, it buries the bow in the back slope of the preceding wave.

The (complete) submergence of the bow increases the resistance and eventually causes the ship to decelerate; between t = 205 s and 235 s the speed decreases to below the wave celerity. As the crest overtakes the ship, the ship speed increases again to the wave celerity level. As a consequence, the speed drops to 11.9 m/s before accelerating again to wave celerity level.

Numerical simulations (De Kat and Thomas, 1998) predict similar trends in forward speed fluctuations, but the maximum simulated speed of 14.4 m/s lies well below the measured maximum speed. As a consequence of the linear wave model in the simulation, the surfriding speed is equal to the linear wave celerity (Cp_1), which lies below the actual wave speed, Cp_5, by about 10%.

So far, the issue of transient forward speed above the wave phase speed has not been addressed in detail. The issue is of relevance especially for irregular following seas, where steep waves will be able to push the ship speed to high values for some time and cause bow submergence, with broaching as a possible consequence.

Broaching

The model tests show that the frigate investigated can experience broaching under certain conditions at high Froude number only (Fn_0 = 0.35). In general the ship proved to have good course keeping qualities in following and stern quartering waves, i.e. broaching did not occur frequently in the conditions tested at high Froude number. Two modes of broaching were observed:

1. High speed broach preceded by surfriding, with rapidly and monotonically increasing heading deviation in following and stern quartering waves
2. Large amplitude, low-frequency yaw (heading) oscillations in stern quartering waves

Figures 5a and 5b depict the occurrence of the first broaching mode for the ship in the Marginal GM Condition. The nominal (desired) heading is 15 degrees. Figure 5a shows both the longitudinal and transverse ship speeds, where Us is defined in the horizontal plane along the x-axis of the yawed ship, and Vs is perpendicular to Us in the horizontal plane. Figure 8 shows the steadily increasing heading angle once the ship has been captured by the wave afterv t = 70 s; the ship experiences moderately large heeling angles during the event. As a consequence of the test set-up, the broach ended when a tight tether line limited the motions.

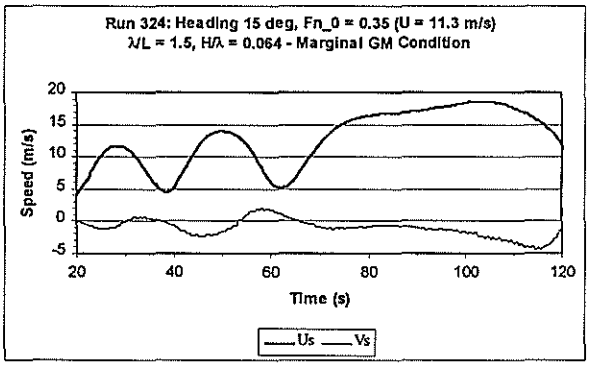

Figure 5a. *Mode 1 broach: Measured longitudinal and transverse ship speeds for run 324*

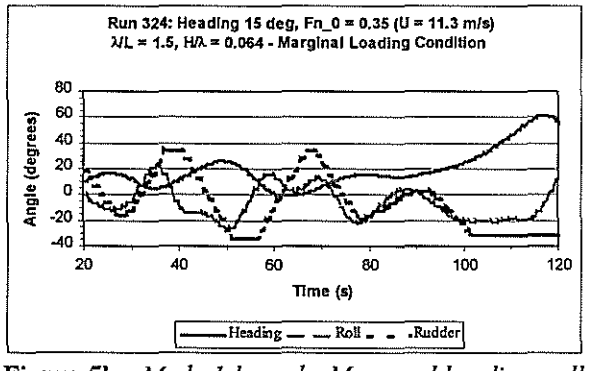

Figure 5b. *Mode 1 broach: Measured heading, roll and rudder angles for run 324*

Figures 6a and 6b depict the occurrence of the second broaching mode for the ship in the Full Load Condition, illustrating that the ship can experience large roll angles in this condition. Figure 8a shows that the ship has a significant mean negative drift velocity, i.e. it experiences a rather large drift speed to leeward while yawing. The highest transverse drift velocity occurs when the yaw angle (toward the wave) and forward speed increase while a wave crest is overtaking the ship (from aft to amidships). When the crest is in the midship area and the ship has reached its largest yaw deviation into the wave, the roll angle to leeward (negative sign) is largest; the reduction of the righting arm in the wave crest leads to asymmetric roll motions. In this case the ship experiences large roll angles, but it does not capsize.

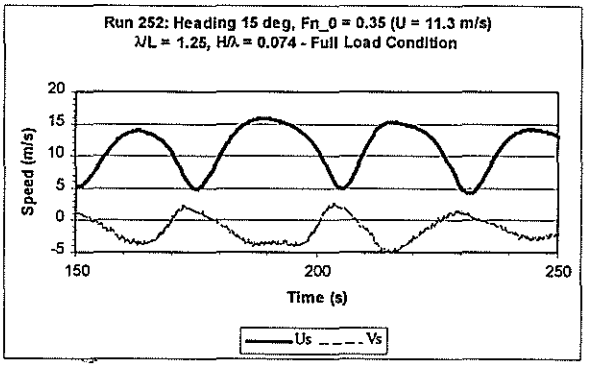

Figure 6a. *Mode 2 broach: Measured longitudinal and transverse ship speeds for run 252*

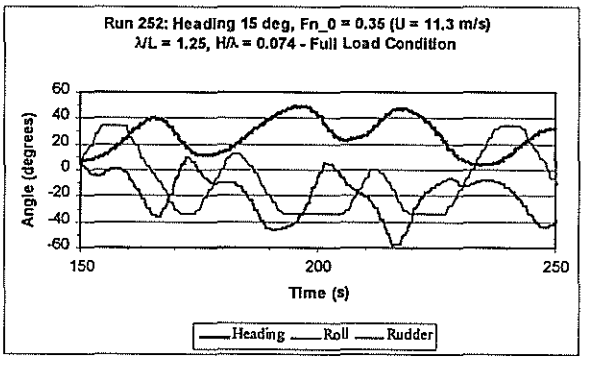

Figure 6b. *Mode 2 broach: Measured heading, roll and rudder angles for run 252*

The stable course keeping properties of the frigate in waves may be linked to its degree of directional stability in calm water. According to the simulations the ship is directionally very stable. The large skeg and twin rudders contribute to the frigate's directional stability.

Capsizing

The frigate did not capsize under any of the speed, heading and wave combinations tested in either the Full Load or Marginal Loading Condition. In the Failed Loading Condition, however, capsizes did occur frequently at the highest ship speeds (Fn_0 $\geq$ 0.3) in following and stern quartering waves; no

capsizes occurred at Fn_0 < 0.3, even though conditions included harmonic resonance in steep stern quartering and beam seas.

The following main modes of capsize could be distinguished from the experiments:

1. Loss of transverse stability in wave crest associated with surfriding or periodic surging
2. Dynamic loss of stability due to surge-sway-roll-yaw coupling
3. Broaching (mode 1 and 2)
4. Combinations of modes

The majority of observed capsizes were of mode 1 and 2. A mode 1 capsize is one where the ship capsizes while being overtaken slowly by a wave crest. For this capsize mode, typically the ship does not experience extreme roll motions before the final "half roll."

A mode 2 capsize involves significant rolling, and often the roll motion tends to build up in severity before capsizing occurs. We illustrate this mode for three experimental cases: run 414 with a short wavelength ratio ($\lambda/L = 0.8$), run 427 with $\lambda/L = 1.25$, and run 448 with a relatively long wave ($\lambda/L = 2.5$), as shown in Figures 7, 8 and 9, respectively.

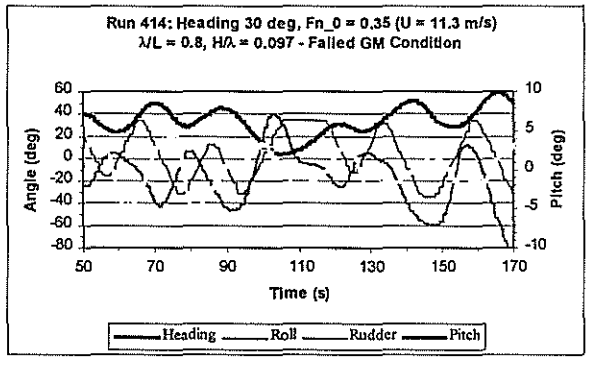

Figure 7a. *Mode 2 capsize: dynamic loss of stability (run 414) with measured heading, roll, pitch and rudder angles*

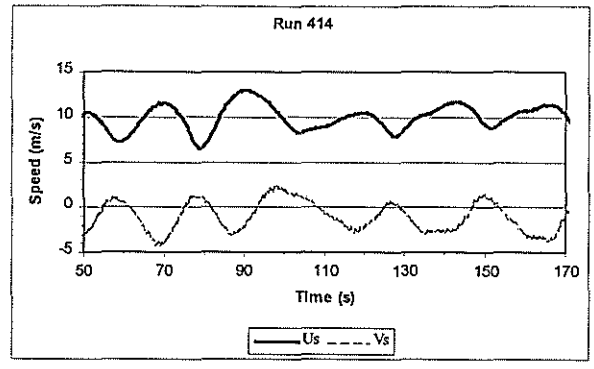

Figure 7b. *Measured ship velocities associated with mode 2 capsize (run 414)*

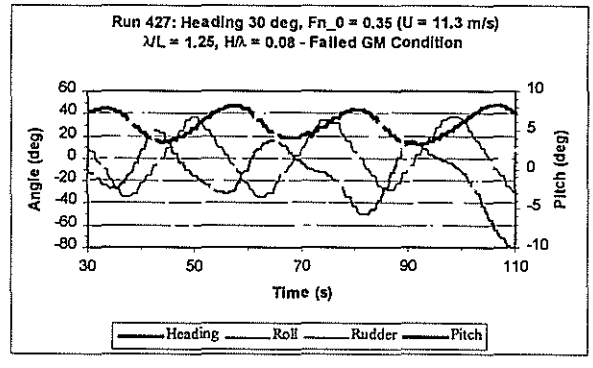

Figure 8. *Mode 2 capsize: dynamic loss of stability (run 427) with measured heading, roll, pitch and rudder angles*

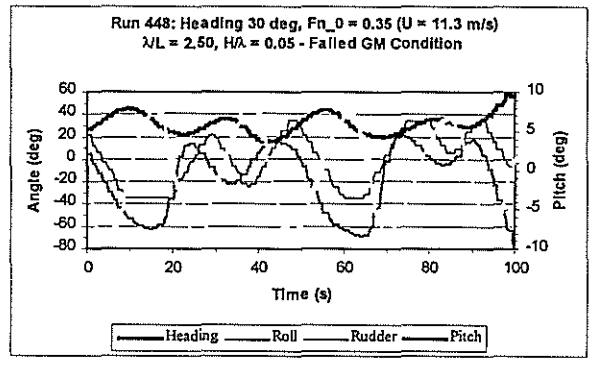

Figure 9a. *Mode 2 capsize: dynamic loss of stability (run 448)*

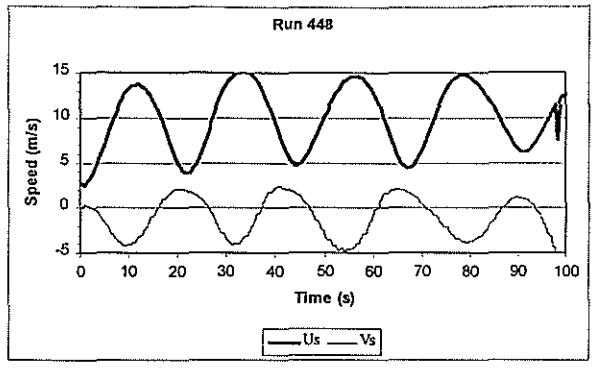

Figure 9b. *Ship velocities associated with mode 2 capsize (run 448)*

Although all three cases involve dynamically coupled rolling, the motion behavior differs significantly: for instance, the speed variations in run 414 are limited to relatively small fluctuations about the mean forward speed, the roll motion in run 427 shows increasing extreme roll angles to port (negative sign, to leeward), and the roll motion in run 448 has a double period. Concerning the latter, double period rolling ("period bifurcation") has been observed in some model tests with containerships in regular waves (Kan et al, 1994). In these dynamic (mode 2) capsize events the ship capsizes typically in the wave crest.

VALIDATION ASPECTS

This section discusses some model testing issues that bear relevance on validation of numerical simulations. In conjunction with the tests described above we will cover the following:

- Roll decay and influence of autopilot
- Measurement of ship velocities
- Measurement of ship position
- Wave height at ship-fixed reference point

Roll decay and inluence of autopilot

Roll decay tests in calm water provide information on roll period and damping as a funciton of ship speed. This type of testing is useful for validation against numerical predictions in the time domain.

Figure 10 provides an example of measured and predicted roll motion response in calm water at a Froude number Fn = 0.3 with an initial roll angle of 40 degrees. The two curves compare quite well for the frigate hull, but there is an offset in the model test data. The cause of the offset was found to be the autoilot: as the model heeled, a yaw moment was induced and the model started to veer off course. The ensuing rudder action demanded by the autopilot resulted in a (quasi-steady) heeling moment.

The recommendation for performing roll decay tests with large initial heel angles at forward speed is to switch off the autopilot.

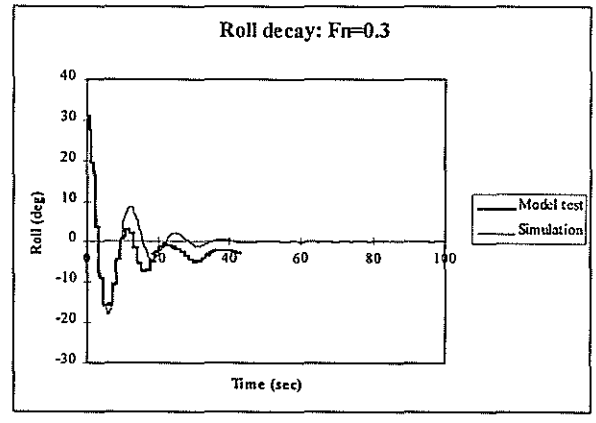

Figure 10. *Roll decay test at Fn = 0.3*

Measurement of ship velocities

It is not standard practice in seakeeping or capsize model tests to measure ship speed in longitudinal and transverse directions; even the direct measurement of instantaneous forward speed is not common. Typically one knows the calm water speed associated with the propeller RPM, which is assumed to be the mean speed.

As some of the tests discussed above show, a ship can experience significant velocity fluctuations periodically in both forward and transverse directions. Quantitative knowledge of these speed variations will contribute to a better understanding of the physics in the validation process.

Let us consider a typical stern quartering condition case: Figure 11a represents motion measurements for run 337. Waves overtake the ship (with Marginal GM) slowly from the starboard quarter. Each passing wave captures the ship briefly while the crest passes the amidships area. The stability reduction experienced by the ship induces the ship to heel to port at a large angle of roll. As the ship is released by the wave, the ship rolls back to starboard and uprights itself in the wave trough, resulting in asymmetrical roll behavior. This cycle repeats with the next overtaking wave.

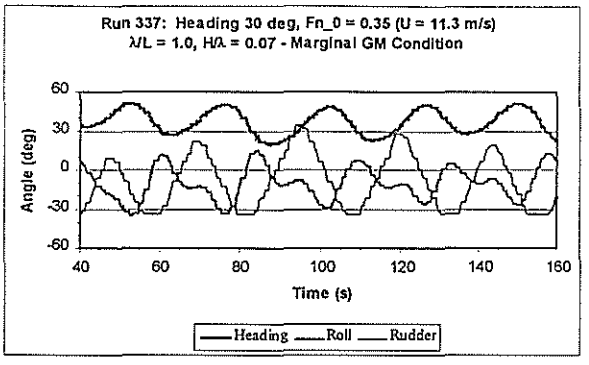

Figure 11a. *Run 337: motions in stern quartering waves (Marginal GM condition, Fn_0 = 0.35)*

As a consequence of the speed changes, the instantaneous drift angles can be substantial. To illustrate this aspect, we consider the velocity components Us and Vs associated with run 337 in Figure 13b. The instantaneous drift angle is given by

$$\beta(t) = \arctan\frac{Vs}{Us}$$

i.e., this is the drift angle with respect to the yawed x-axis of the ship in the horizontal plane.

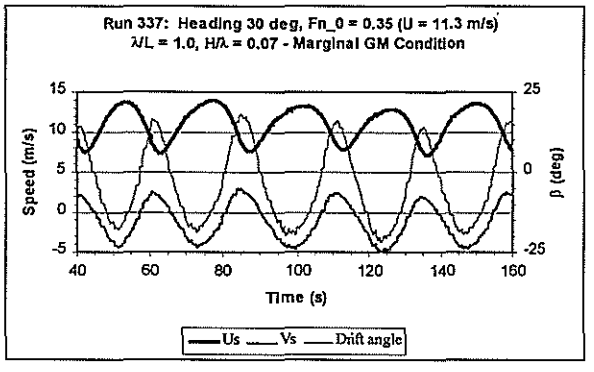

Figure 11b. *Ship velocities and drift angle associated with run 337*

Figure 11b shows the following:

- The transverse velocity can reach high values (up to -5 m/s to port) and it has a negative mean.
- The frigate undergoes large variations in instantaneous drift angle, with maxima of around 20 degrees to either side with respect to its longitudinal axis.
- The drift angle variations suggest a mean negative drift angle.

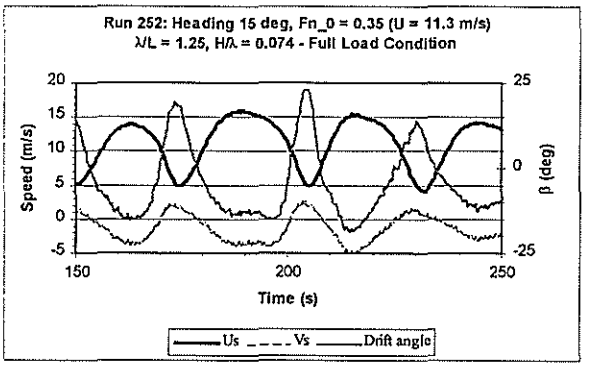

Figure 12. *Ship velocities and drift angle associated with run 252 (Broach shown in Fig. 6)*

Figure 12 shows the drift angle for run 252 (Mode 2 broach, see Fig. 6). It is noted for run 252 and 337 that while the ship is undergoing these velocity and drift angle variations, it is at the same time undergoing large yaw (heading) changes. The large drift angles and drift velocities will influence the ship motions and course keeping behavior, noting that seakeeping and maneuvering are intricately intertwined and should not be modeled independently to predict motions in these conditions.

Measurement of ship position

As is the case for ship velocities, ship position is typically not measured in seakeeping and capsize tests. Yet knowing the earth-fixed position of the ship's CoG at each time instant, allows the comparison between measured and simulated ship track in space for validation purposes.

The ship track provides an indication of the amount of drift a ship may experience in stern quartering waves, for example. Figure 13 shows the measured track for run 252, referenced against the "no drift" track, which is the track the ship would have followed along its average heading (around 30 degrees) in the absence of mean drift effects as of the point in time at t = 150 s. Also shown is the actual heading angle, which corresponds to the one shown in Figure 8b for the time period between t = 150 and 250 s.

Figure 14 shows similar information for run 337 between t = 50 and 150 s. Here the "No drift" track is based on a mean heading of 35 degrees. Figures 15 and 16 illustrate the amount of drift a ship can experience in steep stern quartering waves,

noting that the autopilot algorithm employed in the tests did not account for deviation from the desired path.

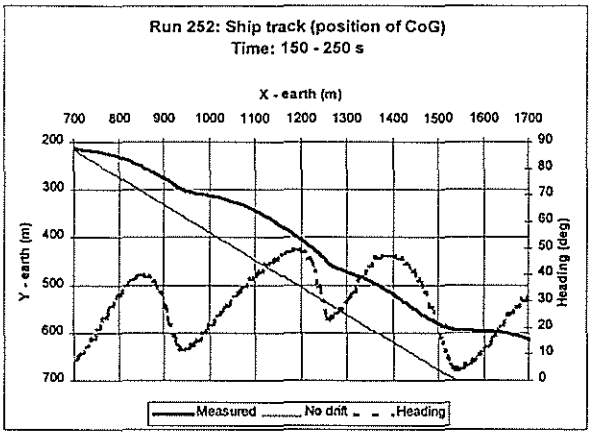

Figure 13. *Ship track and heading between associated with run 252 in stern quartering waves (waves travel along X-earth axis)*

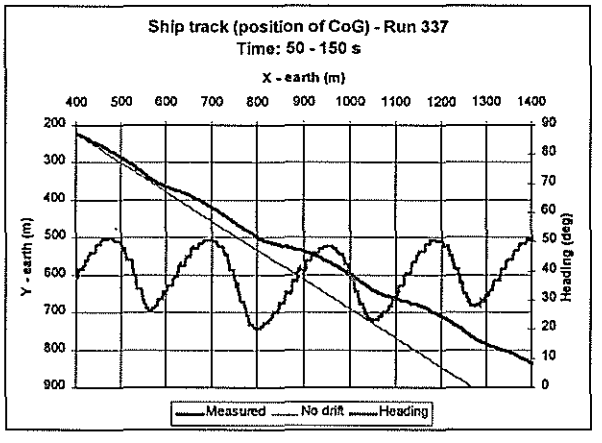

Figure 14. *Ship track and heading between associated with run 337 in stern quartering waves (waves travel along X-earth axis))*

In addition to defining the ship track, earth-fixed measurements will allow the determination of the ship with respect to the (presumably known) wave system.

Wave height at ship-fixed reference point

To achieve simulation conditions that are similar to the model test, it is necessary to know the position of the ship in the wave at any time instant. This allows e.g. to start the simulation with the correct initial conditions and phasing with respect to the wave crest.

In the tests discussed here the wave elevation was measured at a basin-fixed location and at two locations on the towing carriage. Using the latter data and the measured ship motions (including positions), the time series of the wave height at the center of gravity could be generated. Figure 15 provides an illustration of the estimated wave elevation for run 252.

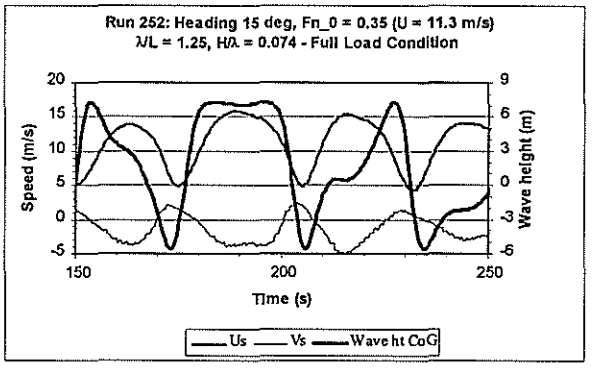

Figure 15. *Ship velocities and wave height at CoG for run 252 (Broach shown in Fig. 6)*

Figure 15 shows that while the ship experiences a significant transverse velocity to port (negative sign), it has a high forward speed and runs with the wave crest at the CoG (i.e., amidships) for an extended period of time between t = 175 and 200 s. Comparison with Figure 8b shows that the roll motions to port are in phase with the wave crest coinciding approximately with the CoG position, leading to reduced stability and hence large roll angles to the leeside during the passage of the wave.

CONCLUSIONS

Model tests with an intact frigate-type hull form were carried out to obtain data on extreme motions and capsizing in critical wave conditions. To control the conditions leading to these events, all tests comprised regular waves of moderate to extreme steepness. A primary objective of these tests was to generate data that would be suitable for the vallidation of a time domain, large amplitude ship motion simulation program.

The paper discusses details of the experimental setup and test procedures, as well as physics associated with some observed extreme motion events in astern wave conditions:

- Periodic surging and surfriding
- Broaching
- Extreme rolling
- Capsizing

Test conditions leading to surfriding show that a ship could attain transient speeds that exceed not only its calm water speed, but also the wave phase speed; bow submergence causes a significant increase in resistance and subsequent deceleration. A numerical model, which makes use of linear wave theory, underpredicts wave celerity and hence surfriding speeds for steep wave conditions.

KG was varied to simulate three load conditions in the model tests: (1) typical Full Load condition, (2) Marginal GM condition that just meets the navy stability criteria, and (3) a Failed GM condition. No capsizes occurred for the first two load conditions. Tthe most extreme rolling and capsizing occurred at high speed (Fn $\geq$ 0.3) in stern quartering waves.

An important observation is that a ship in steep stern quartering waves can experience large amplitude fluctuations in speed, both in longitudinal and transverse directions, and mean drift to leeward can be significant. Large variations in speed contribute to asymmetric rolling, as the ship spends more time (at higher speed and with reduced transverse stability) in a wave crest than in the wave trough.

From a validation perspective of a numerical simulation model, some of the conclusions for large amplitude motion tests in following and stern quartering waves are as follows.

- The autopilot should be switched off during roll decay tests at forward speed to avoid roll-yaw coupling.
- The measurement of ship velocity in longitudinal and transverse directions provides useful information on speed behavior and instantaneous drift angles.
- The measurement of earth-fixed ship position provides useful data on ship track and mean drift.
- Knowing the characteristics of the incoming wave system and earth-fixed ship position, enables one to determine the wave with respect to the ship model at any time instant.

ACKNOWLEDGEMENTS

The authors would like to express their gratitude to the Cooperative Research Navies Dynamic Stability group (navies from Australia, Canada, Netherlands, United Kingdom and United States, U.S. Coast Guard and MARIN) for their permission to publish this paper.

REFERENCES

De Kat, J.O., Brouwer, R., McTaggart, K. and Thomas, W.L., "Intact Ship Survivability in Extreme Waves: New Criteria from a research and Navy Perspective", *Proc. International Conference on Stability of Ships and Ocean vehicles STAB '94*, Melbourne, FL, Nov. 1994

De Kat, J.O. and Thomas, W.L., "Extreme Rolling, Broaching and Capsizing – Model Tests and Simulations of a Steered Ship in Waves", *Proc. Naval Hydrodynamics Symposium*, Washington, D.C, Aug. 1998

Kan , M., Saruta, T. and Taguchi, H., "Comparative Model Tests on Capsizing of Ships in Quartering Seas", *Proc. International Conference on Stability of Ships and Ocean vehicles STAB '94*, Melbourne, FL, Nov. 1994

NAVSEA Design Data Sheet 079-1. Department of the Navy, Naval Ship Engineering Center. June 1976

4th International Stability Workshop, St. John's, 27-29 September 1998

ONGOING WORK EXAMINING CAPSIZE RISK OF INTACT FRIGATES USING TIME DOMAIN SIMULATION

Kevin McTaggart, Defence Research Establishment Atlantic, Dartmouth, Nova Scotia

Abstract

This paper describes ongoing efforts to develop methods for predicting capsize risk of intact naval frigates. For a given ship condition, the risk of capsize is considered to be a function of ship speed, heading, significant wave height, and zero-crossing wave period. Implementation of the proposed procedure requires a numerical model for prediction of ship motions in severe seas. The program Fredyn, which uses a time domain strip theory approach, provides an appropriate combination of computational speed and accuracy for predicting capsize of slender naval frigates. When predicting capsize risk in irregular seas, the dependence of capsize occurrence on wave process realization must be considered. This dependence can be modelled by using Gumbel fits of maximum absolute roll angles obtained from several different realizations. The proposed risk analysis procedure can be extended to account for capsize avoidance procedures taken by ship operators.

NOMENCLATURE

B	ship breadth
D	seaway duration
H_C	capsize wave height
H_s	significant wave height
$H_{s,annual}$	annual max significant wave height
$\widetilde{H/\lambda}$	nominal wave steepness
L	ship length
N_C	number of capsizes
N_s	number of simulations
N_X	number of discretized values of X
$P(C_{annual})$	annual capsize risk
$P(C_D)$	capsize risk in seaway of duration D
$p_X(X)$	discretized probability of X
$Q_X(X)$	exceedence probability for X
T_p	peak wave period
T_z	zero-crossing wave period
V_s	ship speed
β	ship heading (180° for head seas)
$\phi_{max,D}$	max absolute roll angle in duration D
χ	wave phase seed number

INTRODUCTION

Risk analysis provides the most rational approach for designing safe ships. Kobylinski [1] gives an example of risk analysis applied to ship stability, while Mansour et al. [2] discuss application to structural design. The development of risk analysis approaches is relatively recent, and most ship design continues to be based on rules developed through experience. For stability of warships, the rules developed approximately 40 years ago by Sarchin and Goldberg [3] continue to be used by several navies.

Traditional design rules suffer from two primary problems. The resulting levels of safety for different ships can be highly variable, leading to insufficient safety in some cases and unreasonable restrictions in other cases. The second primary problem with traditional design rules is that they are not applicable to new designs that differ significantly from the ships upon which the rules were originally based. For example, Sarchin and Goldberg's rules were developed for warships with narrow sterns; however, modern warships have wide transom sterns, making them vulnerable to loss of stability during stern emergence, which can occur while riding on a wave crest. Consequently, modern warships may be more

vulnerable to capsize than originally intended by Sarchin and Goldberg.

This paper describes ongoing work to develop rational risk analysis procedures for the stability of intact naval frigates. The present research is being conducted in parallel with Canada's ongoing participation in the Cooperative Research Navies Dynamic Stability Project [4, 5].

THEORETICAL APPROACH

Initial work presented in References 6 and 7 assumed that if a ship were to capsize in a given year, it would capsize in the most severe annual storm as characterized by significant wave height. The developed capsize wave height approach was based on the following equation:

$$P(C_{annual}) = \sum_{i=1}^{N_{V_s}} \sum_{j=1}^{N_\beta} \sum_{k=1}^{N_{\widetilde{H/\lambda}}} \sum_{l=1}^{N_\chi} \frac{1}{N_\chi} p_{V_s}(V_{s-i}) \times p_\beta(\beta_j)\, p_{\widetilde{H/\lambda}}\left(\widetilde{H/\lambda}_k\right) \times \left[Q_{H_{s,annual}}\left(H_C \mid V_s, \beta, \widetilde{H/\lambda}, \chi\right)\right] \quad (1)$$

where $P(C_{annual})$ is annual capsize risk, N_X is the number of discretized values of random variable X, $p_X(X)$ is the probability mass function (PMF) for X, V_s is desired ship speed, β is desired ship heading relative to the waves, $\widetilde{H/\lambda}$ is nominal wave steepness, χ is a seed number for generating random waves, $H_{s,annual}$ is annual maximum significant wave height, $Q_{H_s,annual}(H_{s,annual})$ is the exceedence probability of significant wave height for the worst annual storm (typically three hour duration), and $H_C|V_s, \beta, \widetilde{H/\lambda}, \chi$ is the minimum significant wave height which causes capsize given $V_s, \beta, \widetilde{H/\lambda}$, and χ. Equation (1) assumes that if a capsize occurs at significant wave height H_C then capsize will occur all wave heights greater than H_C. The nominal steepness of the worst annual storm is given by:

$$\widetilde{H/\lambda} = H_s \frac{2\pi}{g T_p^2} \quad (2)$$

where T_p is peak wave period and g is gravitational acceleration. Storm data from the Canadian East Coast [8] indicate that a Gumbel distribution provides a good fit for $H_{s,annual}$ and a Weibull distribution provides a good fit for $\widetilde{H/\lambda}$.

A key assumption of Equation (1) is that capsize risk increases with significant wave height and that nominal wave steepness is of secondary importance. Subsequent work has shown that this assumption is too simplistic, and that the joint distribution of wave height and wave period must be considered; thus, it is inappropriate to consider only extreme annual storms based on significant wave height.

Present work is examining risk of capsize for all possible seaways. For a ship in a seaway of duration D (e.g. one hour), the probability of capsize is:

$$P(C_D) = \sum_{i=1}^{N_{V_s}} \sum_{j=1}^{N_\beta} \sum_{k=1}^{N_{H_s}} \sum_{l=1}^{N_{T_z}} p_{V_s}(V_{s-i})\, p_\beta(\beta_j) \times p_{H_s,T_z}(H_{s-k}, T_{z-l}) \times P(C_D|V_s, \beta, H_s, T_z) \quad (3)$$

where T_z is zero-crossing wave period, which is used for compatibility with wave data in Reference 9. Similar expressions have been presented by Kobylinski [1] and Dahle and Myrhaug [10, 11]. An important assumption of the above equation is that desired ship speed and heading are independent of wave conditions. This assumption is conservative because ship operators will alter speed and course to reduce capsize risk.

Once the probability of capsize for duration D has been computed using Equation (3), the associated annual probability of capsize can be computed as follows:

$$P(C_{annual}) = 1 - [1 - P(C_D)]^{1\ year/D} \quad (4)$$

NUMERICAL MODELLING OF SHIP CAPSIZE

A risk analysis approach such at that described above requires an accurate and efficient method for predicting ship capsize in a seaway. The present method uses the time domain program Fredyn, as described in References 4, 5, and 12. Fredyn considers forces from waves, wind, and ship maneuvering. Strip theory gives fast computation times and acceptable accuracy for naval frigates. It is uncertain whether Fredyn can provide acceptable accuracy for low L/B vessels such as small fishing boats. For a typical simulation in waves, the program runs approximately 15 times faster than real time on a 300 MHz Pentium II personal computer.

When the Cooperative Research Navies Dynamic Stability Project commenced in 1990, it was hoped that simplified numerical models could be developed for ship capsize. For example, a simplified numerical model would likely be adequate for predicting ship capsize at zero speed in beam seas. Subsequent research revealed that capsize modes for frigates typically require modelling of all six degrees

of freedom. Frigates appear to be vulnerable to capsize in following seas through loss of static stability while riding on a wave crest, parametric excitation, and broaching.

Validation and improvement of the Fredyn program is an ongoing process. For frigate motions in extreme conditions, a lack of useful experimental data for validation prompted a series of model tests described in References 13 and 14. Fredyn appears to give very good agreement with experiments for capsize of a frigate in waves.

SHIP CAPSIZE RISK FOR GIVEN CONDITIONS

The application of Equation (3) for prediction of capsize risk requires a suitable method to determine capsize risk for given conditions $P(C_D|V_s,\beta,H_s,T_z)$. For a Fredyn simulation of a ship in irregular waves, a random phase approach is used to generate a wave realization. The wave realization is dependent upon a seed number χ provided as input for generation of random wave phases. The occurrence of capsize can be highly dependent on the input seed number. Upon initial consideration, it would seem appropriate to determine $P(C_D|V_s,\beta,H_s,T_z)$ using N_s simulations with different seed numbers as follows:

$$P(C_D|V_s,\beta,H_s,T_z) = \frac{N_C}{N_s} \qquad (5)$$

where N_C is the number of simulations for which capsize occurs. The main disadvantage of this approach is that a large number of simulations can be required to obtain accurate estimates of $P(C_D|V_s,\beta,H_s,T_z)$. A much more efficient and useful approach is to apply a statistical fit to the maximum roll angles $\phi_{max,D}$ from N_s simulations of duration D. Figures 1 and 2 show fitted Gumbel distributions for a frigate in following seas with significant wave heights of 10 m and 12 m. The results indicate that a Gumbel distribution provides a very good fit to the conditional probability $Q_{\phi_{max,D}|V_s,\beta,H_s,T_z}(\phi_{max,D}|V_s,\beta,H_s,T_z)$. Work in progress suggests that only ten simulations are required to obtain good estimates for the conditional distribution $Q_{\phi_{max,D}|V_s,\beta,H_s,T_z}(\phi_{max,D}|V_s,\beta,H_s,T_z)$. An added benefit of using a fitted distribution for each seaway is that Equation (3) can be revised to give exceedence probabilities for all maximum roll angles in all seaways as follows:

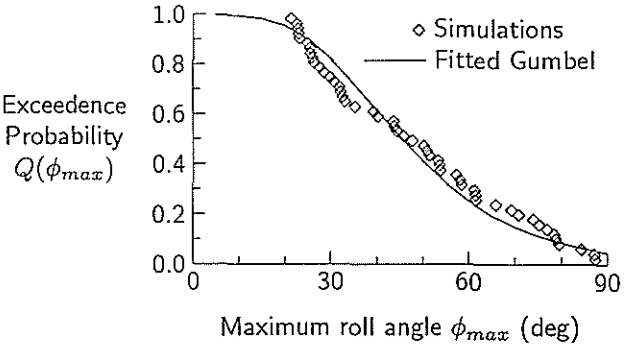

Figure 1: Roll Exceedence Probability for Frigate in One-Hour Seaway, $V_s = 10$ knots, $\beta = 30$ degrees, $H_s = 10$ m, $T_z = 10$ s

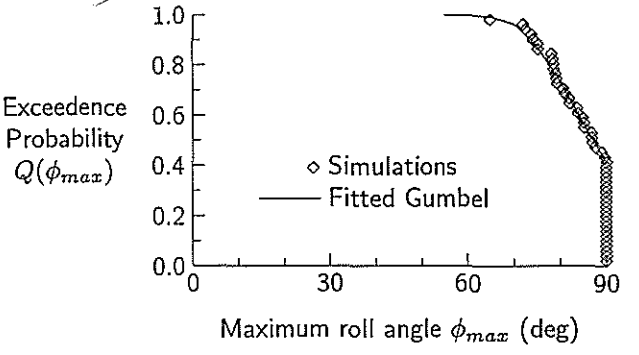

Figure 2: Roll Exceedence Probability for Frigate in One-Hour Seaway, $V_s = 10$ knots, $\beta = 30$ degrees, $H_s = 12$ m, $T_z = 10$ s

$$Q_{\phi_{max,D}}(\phi_{max,D}) = \sum_{i=1}^{N_{V_s}} \sum_{j=1}^{N_\beta} \sum_{k=1}^{N_{H_s}} \sum_{l=1}^{N_{T_z}} p_{V_s}(V_{s-i}) \times p_\beta(\beta_j)\, p_{H_s,T_z}(H_{s-k}, T_{z-l}) \times Q_{\phi_{max,D}|V_s,\beta,H_s,T_z}(\phi_{max,D}|V_s,\beta,H_s,T_z) \qquad (6)$$

INFLUENCE OF CAPSIZE AVOIDANCE BY OPERATOR

The risk analysis approach presented thus far does not consider efforts by the operator to reduce capsize risk. Weather routing and altering of course are two possible methods of reducing capsize risk. Faulkner and Williams [15] suggest that weather routing will not always reduce exposure to severe conditions. For a warship, mission requirements can provide a significant impediment to avoiding severe conditions.

Numerical simulations and experiments have shown that modern naval frigates are most suscep-

tible to capsize when travelling at high speed in high following seas. Figure 3 taken from Reference 7 shows the conditional probability of heading given capsize, and indicates that capsize risk can be greatly reduced by altering course. Fortunately, the quantitative results are consistent with operator practice of altering course to head seas in severe conditions.

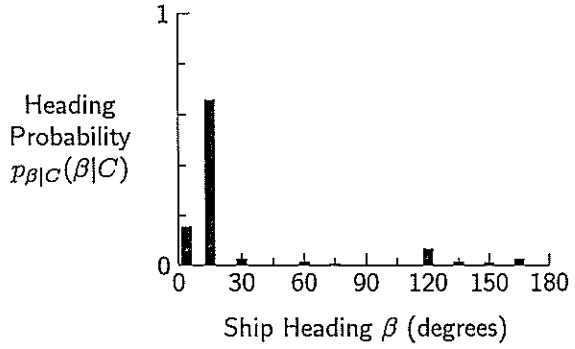

Figure 3: Conditional Probability of Ship Heading Given Capsize

Various researchers are examining ship operational records to determine operator actions in severe conditions. For example, Glen et al. [16] have recently completed a study for the Ship Structures Committee. Using operational profile data, it should be relatively simple to incorporate capsize avoidance behaviour into risk predictions by modifying Equation (3) to obtain:

$$P(C_D) = \sum_{i=1}^{N_{V_s}} \sum_{j=1}^{N_\beta} \sum_{k=1}^{N_{H_s}} \sum_{l=1}^{N_{T_z}} p_{V_s|H_s}(V_{s-i}|H_{s-k}) \times p_{\beta|H_s}(\beta_j|H_{s-k})\, p_{H_s,T_z}(H_{s-k},T_{z-l}) \times P(C_D|V_s,\beta,H_s,T_z) \quad (7)$$

The above equation neglects possible weather routing but considers altering of speed and course in response to significant wave height.

FUTURE PLANS

Work continues with the presented risk analysis procedure so that it can be used for routine engineering computations. Although the procedure has been implemented, there are several areas for refinement.

The properties of the Gumbel distribution suggest that simulation durations can be a fraction of the nominal seaway duration for which the capsize probability $P(C_D)$ is required. For example, it is possible that 10 simulations of 15 minute duration could be adequate to determine the statistical properties of maximum roll for a given seaway of 60 minute duration, thus permitting a significant reduction in computation time.

When applying the proposed risk analysis procedure, an acceptable level of capsize risk must be specified. Selection of an acceptable risk level is complicated by the fact that any risk analysis procedure gives risk predictions which are different from actual risk levels; thus, a risk analysis procedure usually has to be calibrated using past operational experience. The present proposed risk analysis method will likely be calibrated using operational data for naval ships which have had long service lives without any near capsizes.

As mentioned in the previous section, operator avoidance action will greatly reduce the risk of ship capsize. Equation (7) provides a promising approach for considering such avoidance action, and will likely be implemented as required operational profile data become available.

The ongoing validation and improvement of the Fredyn ship motion program will lead to improved capsize risk predictions. It is likely that Fredyn will eventually be superceded by another time domain code with a more sophisticated treatment of nonlinear and three-dimensional effects.

CONCLUSIONS

A rational method has been developed for predicting capsize risk of intact naval frigates. The method requires an accurate and efficient numerical model of ship motions in severe seas. The program Fredyn fulfills this role for naval frigates. For a ship in an irregular seaway, the occurrence of capsize can be highly dependent on the wave process realization. This effect can be effectively modelled by fitting a Gumbel distribution to maximum roll angles from several different seaway realizations. Future improvements to the risk model will include the effects of actions by ship operators to avoid ship capsize.

REFERENCES

[1] L.K. Kobylinski, "Rational Approach to Ship Safety Requirements," in *Second International Conference on Marine Technology* (Szczecin, Poland, 1997).

[2] A.E. Mansour, P.H. Wirsching, M.D. Lucket, A.M. Plumpton, and Y.H. Lin, "Structural

Safety of Ships," *Transactions, Society of Naval Architects and Marine Engineers* **105** (1997).

[3] T.H. Sarchin and L.L. Goldberg, "Stability and Buoyancy Criteria for U.S. Naval Surface Ships," *Transactions, Society of Naval Architects and Marine Engineers* **70**, 418–458 (1962).

[4] J.O. de Kat, "The Development of Survivability Criteria Using Numerical Simulations," in *United States Coast Guard Vessel Stability Symposium '93* (New London, Connecticut, March 1993).

[5] J.O. de Kat, R. Brouwer, K. McTaggart, and L. Thomas, "Intact Ship Survivability in Extreme Waves: Criteria from a Research and Navy Perspective," in *STAB '94, Fifth International Conference on Stability of Ships and Ocean Vehicles* (Melbourne, Florida, 1994).

[6] K.A. McTaggart, "Risk Analysis of Intact Ship Capsizing," in *United States Coast Guard Vessel Stability Symposium '93* (New London, Connecticut, March 1993).

[7] K.A. McTaggart, "Capsize Risk Prediction Including Wind Effects," in *Proceedings of the Third Canadian Marine Hydrodynamics and Structures Conference* (Dartmouth, Nova Scotia, August 1995), pp. 115–124.

[8] Canadian Climate Centre, "Wind/Wave Hindcast Extremes for the East Coast of Canada, Volume 1," Technical Report, Prepared under contract by MacLaren Plansearch Ltd. and Oceanweather Inc., 1991.

[9] British Maritime Technology Limited, *Global Wave Statistics*, Unwin Brothers, London, 1986.

[10] E. A. Dahle and D. Myrhaug, "Risk Analysis Applied to Capsize of Smaller Vessels in Breaking Waves," *Transactions, Royal Institution of Naval Architects* **136**, 237–252 (1994).

[11] E. A. Dahle and D. Myrhaug, "Capsize Risk of Fishing Vessels," *Schiffstechnik (Ship Technology Research)* **43**, 164–171 (1996).

[12] J.P. Hooft and J.B.M. Pieffers, "Maneuverability of Frigates in Waves," *Marine Technology* **25**(4), 262–271 (1988).

[13] J.O. de Kat and W.L. Thomas III, "Extreme Rolling, Broaching, and Capsizing-Model Tests and Simulations of a Steered Ship in Waves," in *22nd Symposium on Naval Hydrodynamics* (Washington, August 1998).

[14] J.O. de Kat and W.L. Thomas III, "Broaching and Capsize Model Tests for Validation of Numerical Ship Motion Predictions," in *Fourth International Stability Workshop* (St. John's, Newfoundland, September 1998).

[15] D. Faulkner and R.A. Williams, "Design for Abnormal Ocean Waves," *Transactions, Royal Institution of Naval Architects* **139** (1997).

[16] I.F. Glen, R.B. Paterson, and L. Luznik, "Sea Operational Profiles for Strucutural Reliability Assessments," Report 4737C.FR, Fleet Technology Limited, 1998. Prepared for Defence Research Establishment Atlantic and Ship Structures Committee.

A Standard Method For Presentation of Capsize Data

M Renilson, Australian Maritime College, and **M Hamamoto**, Osaka University

ABSTRACT

One of the major difficulties involved in investigating vessel capsizing in following and quartering seas is in presenting the results in a systematic manner. The difficulty is in how to show the results of the variation of the five critical variables (λ/L; h/λ; χ; KG; and Fn) in a simple presentation. A method is proposed which allows straightforward comparison between different vessels, and with the existing IMO regulations which are based on statical stability concepts only.The capsize boundaries obtained in regular waves are distilled into a single plot of maximum permissible KG' (=KG/B) to avoid capsize in waves as a function of Froude Number.It is shown that the maximum KG' which will allow the vessel to meet the existing IMO regulations applicable to the vessel type can also be included on this plot.

NOTATION

B	Vessel beam
Fn	Froude number
G_FM	Metacentric height
G_FZ	Righting lever
h	Wave height
KG	Vertical centre of gravity position
KG'	Non-dimensional vertical centre of gravity position (=KG/B)
L	Vessel length
θ	Heel angle
θ_f	Angle of downflooding
λ	Wavelength
χ	Vessel heading to waves (χ = 0° represents following seas)

INTRODUCTION

Existing IMO regulations for the intact stability of vessels are based purely on statical concepts utilizing the G_FZ curve and the G_FM value as follows:

Criterion	IMO minimum
Area under the G_FZ curve between 0° and 30°	3.15m-deg
Area under the G_FZ curve between 0° and 40° (or 0° and θf, whichever is less)	5.16m-deg
Area under the G_FZ curve between	

30° and 40° (or 30° and θ_f, whichever is less)	1.72m-deg
G_FZ at 30° or greater	0.20m
Angle for maximum G_FZ	25degrees
G_FM	0.15m (0.35m for fishing boats)

Although these criteria do take the non-linear restoring moment into account they are based on statical stability alone and do not consider the dynamics of the behaviour of the vessel in the waves. IMO has adopted criteria to take into account the effect of the wind etc, however all existing criteria are still based on statical rather than dynamical concepts. (IMO 1995)

With the recent advances in knowledge of the behaviour of ships in rough seas and the advent of modern computing the time has come to develop new criteria based fully on dynamical concepts.

BACKGROUND

Studies of capsizing in following and quartering seas have been conducted over a number of years by a range of investigators. In each case they have had to cope with the following variables for every vessel type investigated: λ/L; h/λ; χ; KG; and Fn. The difficulty is in conducting experiments or time domain simulations with a systematic variation of each of these variables, and in presenting the results in a standard manner that enables ready comparison with other investigations.

In addition, the results are often not of use to designers who need to assess the safety of their proposed designs.

PROPOSED METHOD

A method is proposed for analysing and displaying capsize data in a manner which allows ready comparison with other vessels and with the existing IMO regulations. It is suggested that once experience with this method has been gained, criteria based on it could be developed and used for future stability regulations.

Results in regular waves are used, as being 'deterministic' they are easier to obtain than those in irregular waves, allowing for ready comparison between different vessels. It has often been demonstrated that in following and quartering seas the results are very similar for regular and irregular waves. (Takaishi, 1982)

To simplify the process it is desirable to conduct all the investigations at a constant wave steepness. In order to investigate the relative safety of a vessel it is reasonable to investigate its behaviour in steep waves. A number of existing investigations have utilised different wave steepnesses, making it impossible to compare the results. To overcome this it is proposed that a standard wave steepness of $h/\lambda = 1/15$ be used for all studies of capsizability in future. If this value is adopted as a standard by all investigators in the field then it will be possible to compare different designs on an equal basis. This is necessary to be able to develop standard stability regulations based on rational dynamical concepts.

The first step in the proposed method is to determine the maximum KG value that the vessel can have without capsizing for a fixed λ/L value and Froude Number at the wave steepness of $h/\lambda = 1/15$. This process is repeated for a range of heading angles and the resulting capsize boundary can be represented on a plot of heading angle, χ, against KG as shown for a fictitious vessel in figure 1.

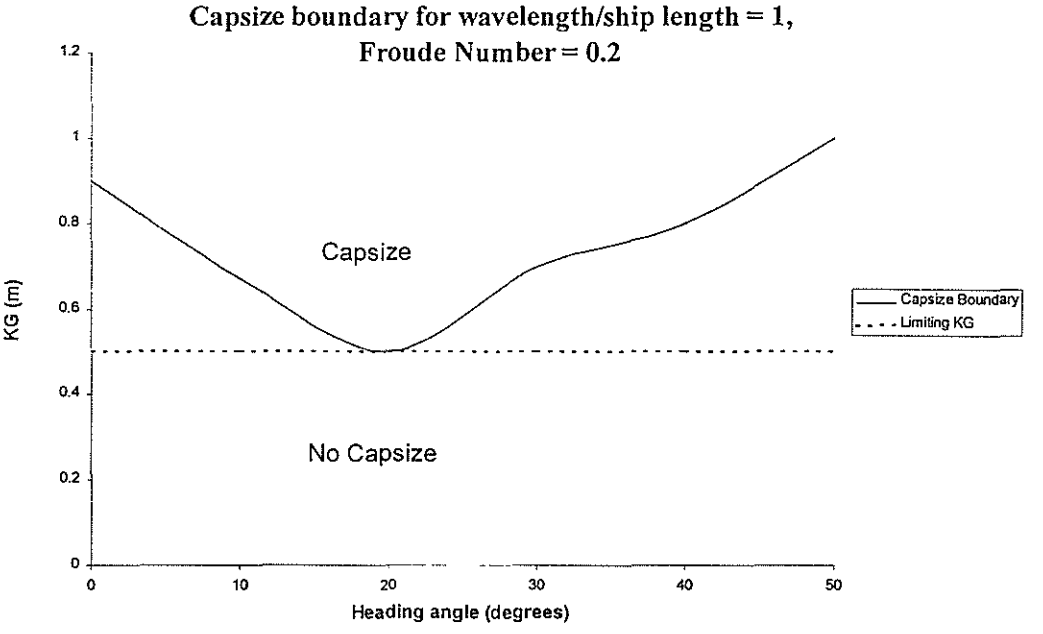

Figure 1: Example of capsize boundary for single λ/L and Fn

For a given heading angle, if the vessel is loaded with a KG value higher than the boundary shown in figure 1 it will capsize in waves of steepness $h/\lambda = 1/15$ or above, whereas if it has a KG value lower than the boundary it is safe in waves with this steepness.

As it is clearly necessary to load the vessel in such a way that it does not capsize at any heading, the important aspect of this boundary is its minimum value, and this can be considered the limiting KG value for the vessel in this λ/L and at this Froude Number.

As can be seen from figure 1, the limiting value of KG for this case is 0.5m. If the vessel has a greater KG value than this it will capsize at headings other than 20°.

Of course, as it is possible to encounter waves with different lengths this exercise must be repeated for a range of wavelengths and in each case the limiting KG value can be obtained as before. These limiting KG values can then be plotted against λ/L as shown in figure 2.

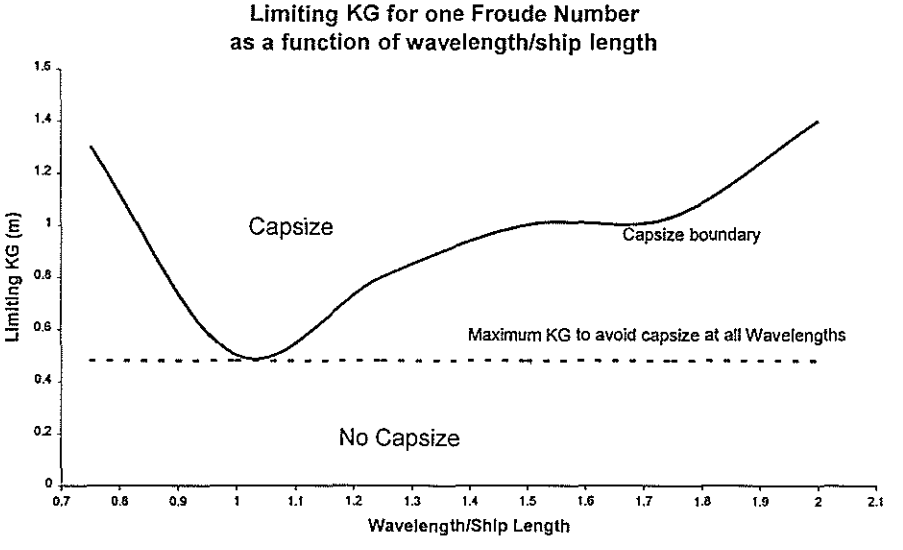

Figure 2: Example of limiting KG for one Froude Number

In figure 2 the capsize boundary indicates the maximum KG which the vessel can be loaded to without capsizing in waves of steepness $h/\lambda = 1/15$ at any heading at that one Froude number. The wavelength/ship length ratio most likely to cause a capsize in waves of steepness $h/\lambda = 1/15$ can easily be determined from this figure. In the case of this fictitious vessel this is 1.03, and at that wavelength/ship length ratio the maximum KG value that the vessel can have without capsizing is 0.48m.

As the ship may encounter waves of any length this means that it is necessary for the KG to be less than 0.48m to guarantee against capsize. This then is the maximum permissible KG for this vessel to travel in following and quartering seas at a Froude number of 0.2.

This can be non-dimensionalised by dividing by the vessel's beam, B, to give KG′ (= KG/B).

This process can then be repeated for the range of speeds, as shown in figure 3. Here the curve is the boundary of the maximum KG′ that the vessel can sustain without capsizing at any heading and any wavelength combination in waves of steepness $h/\lambda = 1/15$. What this means is that if the KG′ value is greater than this for a particular Froude number then there will be at least one combination of heading and wavelength which will cause the vessel to capsize in waves of steepness $h/\lambda = 1/15$. Conversely, if the KG′ value is less than this for a particular Froude number then it will not capsize at any heading in any wavelength in waves of steepness $h/\lambda = 1/15$. This value of KG′ can then be termed the limiting KG′ to prevent capsize at that Froude number.

The maximum KG′ permitted for this fictitious vessel to meet the IMO stability regulations is also shown on figure 3, and it can be seen that at the lower Froude numbers the IMO regulations may be considered too conservative, whereas at the higher Froude numbers they allow a higher KG′ than that permitted by the dynamic approach.

As the dynamic approach is based on the behaviour of the vessel in a wave steepness of $h/\lambda = 1/15$, which was chosen relatively arbitrarily as a 'typical' steep wave, considerable experience will be required with this comparison before it will be possible to discard the statical approach which has been built up over many years. However, if the proposed approach is adopted as uniform by researchers in this field, and the results regularly compared with those from the statical approach then it will be possible to develop the correlation between the approaches. Once this has been done, the dynamical approach can be adopted in favour of the statical approach, and the assessment of vessel stability will be greatly improved.

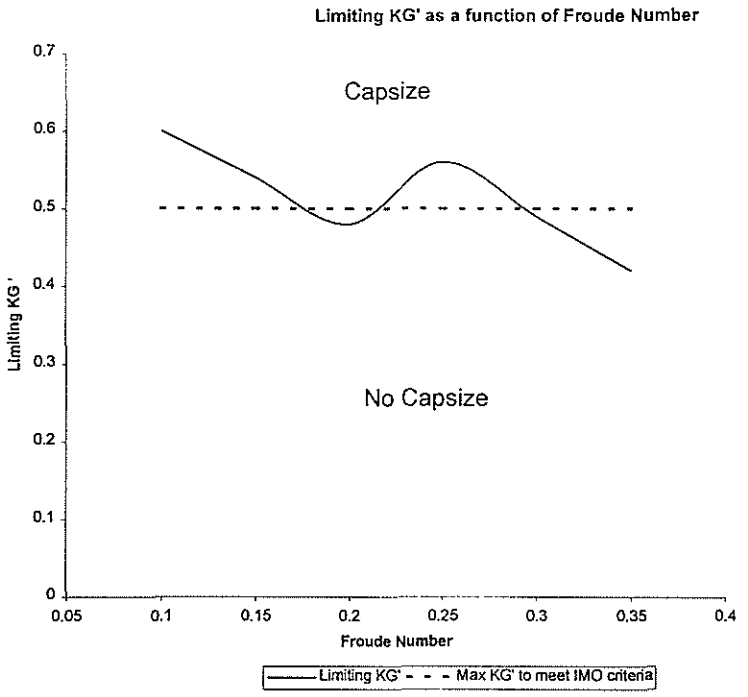

Figure 3: Limiting KG′ as a function of Froude Number

The final plot, shown in figure 3, is therefore a very good guide to the likelihood of a given vessel capsizing in following and quartering seas, and can reasonably be used to compare the stability of different vessels in a standard manner.

CONCLUDING REMARKS

A simple but comprehensive method for analysing capsize data has been demonstrated.

With this method a vast array of data is distilled into a single plot of limiting KG′ as a function of Froude Number, allowing for straightforward comparison between different vessels, and enabling the designer and operator to easily assess the likelihood of capsize for a given vessel. It is also possible to include the maximum KG′ that will allow the vessel to meet the IMO criteria on this plot for reference.

It is suggested that this method now be used as standard to compare the likelihood of capsize for different vessel types, and that the results be compared with the maximum KG′ obtained from the existing IMO regulations in each case. Once experience with this approach has been developed it will be possible to use it rather than the existing statical methods to assess vessel stability in future.

REFERENCES

IMO, 1995, "Code on intact stability for all types of ships covered by IMO instruments' Published by the International Maritime Organisation.

Takaishi, Y, 1982, "Consideration on the Dangerous Situations Leading to Capsize of Ships in Waves" STAB'92, Tokyo, Japan, October 1982.

ACKNOWLEDGMENTS

The work reported was conducted during the first author's stay in Japan, which was made possible by Osaka University and the authors are grateful to the University for this support.

4th International Stability Workshop in St John's, Canada
Session 1 Numerical and Physical Modelling of Intact Stability
28 September 1998

New Remarks on Methodologies for Intact Stability Assessment

by
N. Umeda
National Research Institute of Fisheries Engineering (NRIFE), Japan

Abstract

This paper provides new ideas on methodologies for intact stability assessment. An proposal of standard plan of physical model experiments based on a regule fâlsi method is presented with an example recently carried out at the seakeeping and manoeuvring basin of NRIFE. For the assessment with a numerical model, it is reported that the sudden change concept proposed at the first ship stability workshop was successfully applied to solve the initial-value dependence problem in intact stability. Moreover, it is numerically confirmed that an invariant manifolds analysis of a fixed point near a wave crest can be used for a stability assessment as an alternative to conventional numerical experiments for capsizing due to broaching.

Introduction

Rapid progress in ship design and heightening acceptable risk level of public make empirical criteria based on casualty statistics rather out-of-date. As a result, stability assessment with rational methods, namely, physical or numerical experiments, is highly expected. However, the methods of assessment for this purpose have not yet been fully established, while those for seakeeping or manoeuvring have almost been done. Thus, each research organisation is attempting stability assessment by trial and error.

Ship capsizing is a transition from a stable and nearly upright equilibrium to a stable and nearly upside-down one under external random excitation. Thus, a ship motion relating to ship stability is nonlinear and transient with undeterministic excitation. Therefore, the methodology for seakeeping, which deals with stationary ship motions with undeterministic excitation, or manoeuvring, which deals with transient motions mainly with deterministic excitation, cannot be directly applied to ship stability. For example, an initial condition can be easily specified for manoeuvring tests in calm water but it cannot be done in waves. While a steady motion dealt in seakeeping does not depend on initial conditions very much, ship stability crucially depends on the initial conditions. Although an actual ship meets short-crested irregular waves, its wave height and other particulars cannot be specified in advance. If a ship motion is almost linear like that relating in seakeeping, the value of wave height used in experiments is not very important. However, as capsizing is completely nonlinear, some philosophy to determine a wave height for stability assessment is essential.

NRIFE has engaged in intact stability assessment for various fishing vessels since

70's.[1] Among its activities the author found a possibility for standardisation of stability assessment with some new ideas. In this paper, he presents these new ideas for stimulating discussion among experts. More comprehensive report of the investigation based on these ideas will be published in separate publications.

Physical Model Experiments

So far capsizing model experiments have been carried out mainly in irregular waves. This is because there is a possibility that some nonlinear phenomena may occur only in irregular waves. Experiments in irregular waves should be repeated with so many different realisations to obtain statistically meaningful results. Number of realisation increases significantly when capsizing probability is reasonably small. And majority of actual ships are so. Thus, this kind of experiment is not appropriate for practical purpose. To avoid this difficulty, Takaishi [2] proposed the use of encounter group wave, which can be found when the ship velocity component is nearly equal to group velocity of principal wave energy, for capsizing experiments in irregular waves as worst scenario in irregular seas. In this situation, since the encounter wave profile tends to sinusoidal in time, capsizing experiments in irregular waves can be carried out in a rather deterministic way.

On the other hand, experimental results accumulated until now have not yet shown a clear evidence of a unique mode of capsizing in irregular waves. In the most of cases, if the maximum amplitude of the wavemaker is limited to be a certain value, capsizing in long-crested irregular waves occurs much more easily than that in short-crested waves and capsizing in regular waves occurs much more easily than that in irregular waves. [3] Takaishi's proposal is also based on the fact that capsizing due to regular excitation is more dangerous than that due to random excitation. Thus, the use of regular wave is not simply conservative and we should pay more attention to experiments in regular waves.

Considering the above, the author proposes an experiment plan as follows. First, we carry out capsizing model experiments in extremely steep regular waves. If the model does not capsize, we can presume that the possibility of capsize of this ship in any irregular waves is negligibly small. If the model capsizes, the possibility of capsize of this ship in certain irregular waves is unknown. Then, if necessary, we should carry out capsizing model experiments in irregular waves [4] or assessment based on stochastic theory [5-6]. As you see, the experiment in regular waves has an important role to minimise the size of whole assessment program. In case of relative assessment, critical wave steepness for capsizing can be used as an index, and can be determined with a set of capsizing model experiments in regular waves. Another problem is how to determine ship speed or heading angle. As widely accepted, the most dangerous operational condition is a run in quartering seas. Thus, it is obvious to test a model in quartering seas with lower wave steepness than in beam seas.

Details of our standard test plan is shown in Table 1. First, a model is adjusted to have a specified metacentric height, GM, as well as a specified freeboard and gyro radius in pitch or yaw. Then a natural roll period and damping coefficients are measured with roll decay tests. (I&II) Next, the relationship between the propeller revolution and ship speed is obtained by model runs in still water. Or it can be obtained by standard pro-

pulsion tests. (III) The turning test in still water with the maximum rudder angle and maximum speed is recommended. If the model capsized, the rudder angle or ship speed should be limited not to capsize only due to a turning motion. (IV) Next step is experiments in regular waves. Wave period is equal to or slightly longer than the natural roll period and wave steepness, H/λ, is specified to be 1/7 as critical one. Because of wave breaking, measured wave steepness can be smaller than 1/7 but should be larger than 1/10. The model drifts in these waves with an idling propeller. If the hull form is longitudinally symmetric or nearly so, the model meets waves from side. If the model capsizes, experiment is repeated with sufficiently small wave steepness to find a periodic attractor. It is obvious that a capsizing boundary exists between these two wave steepness. Thus, the critical wave steepness for capsizing can be determined within a required accuracy by repeating experiments with a regule falsi method, which is often used in the numerical analysis. (V) If the natural roll period is twice as long as the natural heave or pitch period, it is recommended that a similar procedure should be applied for the wave period corresponding to the natural heave or pitch period. Then we conduct model runs in regular head waves, whose steepness is slightly smaller than the critical one for capsizing with an idling propeller. The wave length to ship length ratio, λ/L, is set to be about 1.5 because ship motions become significant in this wave condition. Since wave steepness is extremely large, the ship speed cannot be so large even with the maximum propeller revolution, and not so crucial for capsizing. If we observe capsizing, the critical wave steepness for capsizing in head seas can be determined again with the regule falsi method. (VI) Finally model runs in quartering seas should be commanded. The wave steepness is set to be slightly lower than the critical one for capsizing with an idling propeller. The wave length to ship length ratio should cover the range between 1.0 and 1.5. Before a generated water wave train propagates enough, the model is kept near the wavemaker without propeller revolution. Then at a certain moment we command to immediately increase the propeller revolution up to the specified one and to make the auto pilot active for the specified course. Repeating these model runs, the critical combination of the nominal Froude number, Fn, and auto pilot course, χ_c, or the critical wave steepness for capsizing in quartering seas can be identified. (VII)

Table 1 Standard programme of capsizing model experiment at NRIFE

(I)	Preparing Model (Weighting, Ballasting, Measuring Gyro Radius)
(II)	Inclining Test & Roll Decay Test
(III)	Speed Trial in Calm Water
(IV)	Turning Test in Calm Water
(V)	Capsizing Test without Forward Velocity in Regular Waves
(VI)	Capsizing Test with Forward Velocity in Regular Head Waves
(VII)	Capsizing Test with Forward Velocity in Regular Following/ Quartering Waves

As an example of experimental assessment based on the above scheme, this paper presents the conclusions of intact stability assessment for a 34.5 m-long Japanese purse seiner, as follows.

1) Under the condition, (GM=0.75m in full scale) , that does not satisfy the IMO Intact Stability Code, the model capsized in beam, head and quartering seas. The critical wave steepness for capsizing in quartering seas is the lowest among them.

2) Under the condition, (GM=1.00m), that critically satisfies the IMO Code, no capsizing was observed in beam and head seas but capsizing occurred in quartering seas with the wave steepness 1/9.2 and the nominal Froude number 0.43. The capsizing modes were either the loss of stability on wave crest or broaching. The time series for capsizing due to broaching are presented in Fig. 1. The coordinate systems used throughout this paper are shown in Fig. 2.

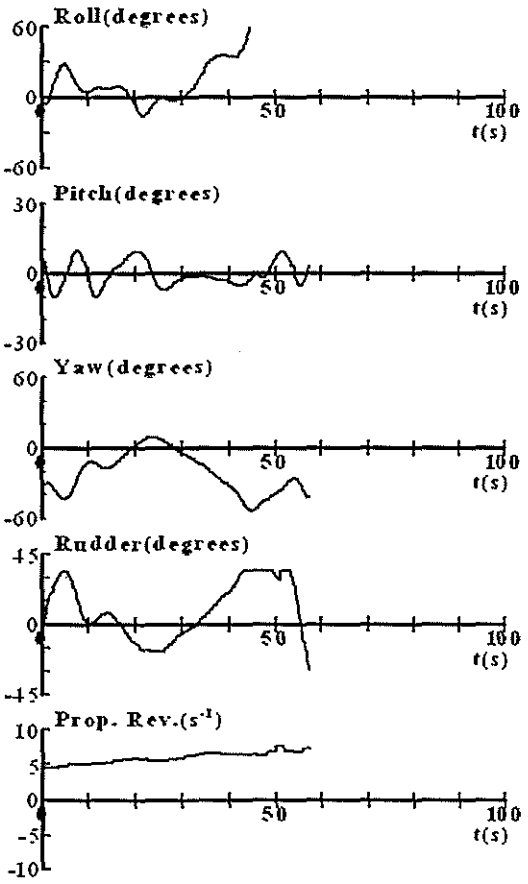

Fig. 1 Capsizing due to broaching observed in physical model experiments. (H/λ=1/9.2, λ/L=1.5, χ_c=-10 degrees, Fn=0.43, GM=1.0m, rudder again K_P=1; in full scale.)

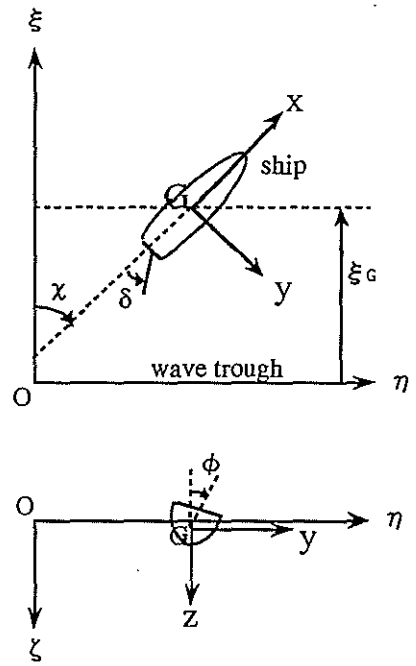

Fig. 2 Coordinate systems.

ξ_G: londitudinal position of centre of gravity from a wave trough. It can be nondimensionalised with a wave length.

u: surge velocity. v: sway velocity. These can be nondimensionalised with a wave celerity,c. χ: heading (or yaw) angle from a wave direction. r: yaw rate. It can be nondimensionalised with the surge velocity and ship length. ϕ: roll angle. p: roll rate. It can be nondimensionalised with the surge velocity and ship length. δ: rudder angle.

3) In case of GM=1.25m, only capsizing due to broaching was observed. When we further increased GM up to 1.46m, no capsizing occurred but broaching without capsizing was still observed.

To obtain the above conclusions, about 300 model runs were made in the seakeeping and manoeuvring basin. The details of these experiments will be published with comparisons with nonlinear dynamics.

Numerical Experiments

Since capsizing is nonlinear, whether capsizing occurs or not depends on the initial condition. Therefore, it is essential in physical or numerical experiment to properly choose the initial condition. In particular, we can input any initial conditions for numerical models but stability assessment only for a certain initial condition is not useful. Although numerical experiments for all possible initial condition sets can be carried out for an uncoupled roll model [7], it is practically impossible to do so for capsizing in quartering seas. Because, the initial value space of the surge-sway-yaw-roll-auto pilot model is at least eight dimensional. As a result, numerical experiments have often been carried out for the "worst initial condition" for capsizing. For example, Vassalos [8] or Munif and Hamamoto [9] proposed that the wave crest at the midship is the "worst initial condition" as a result of some pilot runs. However, since a complete search for the worst initial condition cannot be done, these proposals must be limited in their applicability.

Considering the above and reminding that all initial conditions do not have same practical meanings, the author proposed the "sudden change concept" at the first ship stability workshop.[10] In this concept, first the ship is assumed to be in a certain stable steady state under a certain set of control variables, such as propeller revolution and auto pilot course, and then we suddenly change these control variables, in a way of the step function, as shown in Fig. 3. By a numerical model in time domain we observe how the ship tends to new steady state. These sudden change of the control variables corresponds to actual operational practice at sea. If the preceding state is periodic, the phase lag of the operational command to a wave is not unique. Thus we have to repeat numerical integration from 0 to 2π as the phase lag of the operational command to a wave. However, since the initial value set of phase space is limited to be one dimensional and the set of the initial control valuable is two dimensional, the procedure is still applicable for practical purpose . Later on Spyrou made a similar proposal to this "sudden change concept".[11]

In this paper, to provide a way to terminate the "worst initial condition" problem, numerical results based on the "sudden change concept" with the purse seiner used in the physical experiments are presented. The preceding steady state is a harmonic periodic motion for the nominal Froude number, Fn, 0.1 and the auto pilot course, χ_c, 10 degrees, shown in Fig. 4. Because of symmetry, all lateral motions are zero. With a certain phase lag of the operational command to a wave, in other words, a certain initial longitudinal condition of the ship centre to a wave trough, $(\xi_G/\lambda)_0$, the nominal Froude number and the auto pilot course are suddenly changed to the specified value and 10 degrees, respectively. Fig. 5 shows the results of this numerical experiments; the ab-

scissa is the initial longitudinal position and the ordinate is the new nominal Froude number. In case of the nominal Froude number is smaller than 0.3247, the ship tends to new periodic attractor as a result of change in control variables. In case of the nominal Froude number is larger than 0.3248, the ship experiences unstable surf-riding, broaching and capsizing. Here it is noteworthy that the boundary between the two does not depend on initial longitudinal condition at all. As far as initial condition is set to be a steady state under the previous control variables, the results of change in the control variables do not depend on the initial conditions of the state variables. This suggests that the "sudden change concept" is much more efficient for numerical experiment than the "worst initial condition" approach. Furthermore, this fact justifies the procedure of physical model experiments that described in the previous section because a sudden change method is also used in the physical experiments . For operational practice, it is important that commands for auto pilot course or engine telegraph may be given anytime under a periodic motion.

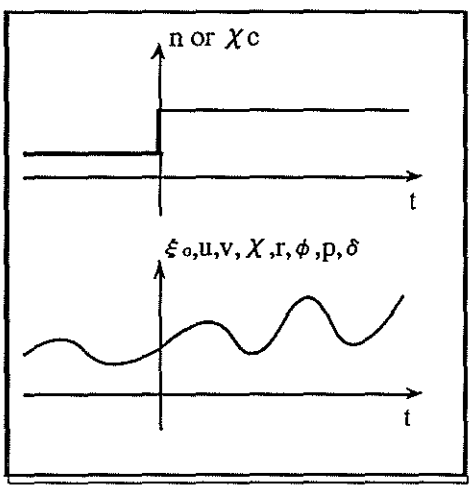

Fig. 3 Sudden change concept

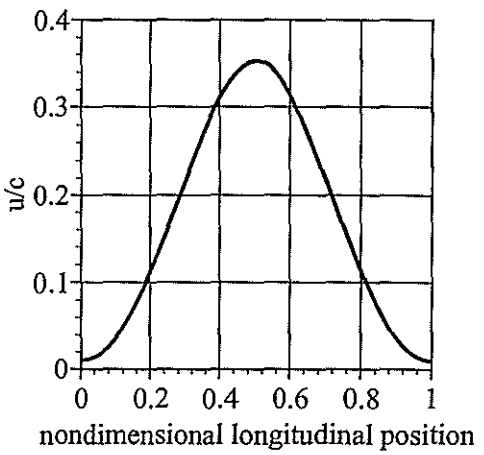

Fig. 4 Periodic motion (H/λ=1/9.2, λ/L=1.5, Fn=0.1, χ_c=0 degrees)

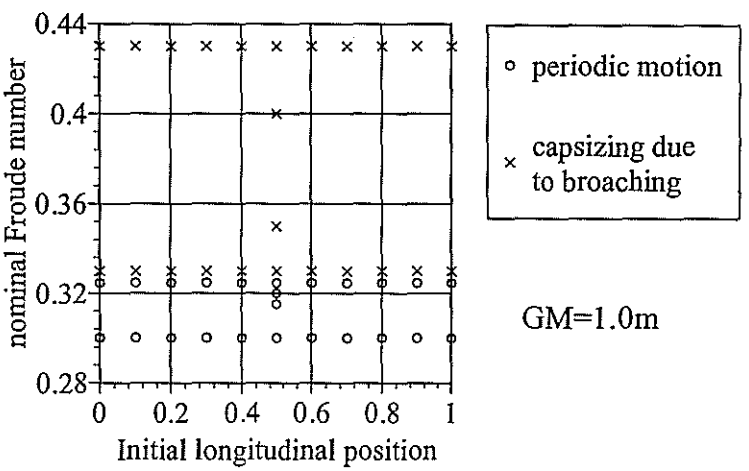

Fig. 5 Results of numerical experiments based on sudden change concept (H/λ=1/9.2, λ/L=1.5, K_P=1; from Fn=0.1, χ_c=0 degrees to χ_c=10 degrees)

The periodic attractor for the new nominal Froude number 0.3247, shown in Figs. 6-8, is not sinusoidal, although the periodic attractor for the nominal Froude number 0.1 is. When the ship centre situates on downslope near wave crest, $\xi_G/\lambda \sim -0.59$ or -0.41, the trajectory behaves like a saddle. Here the relative velocity of the ship to a wave is almost zero and the ship spends on a wave crest for longer time duration than a wave trough. This phenomenon is known as "riding on crest"[12], and is completely different from surf-riding, which occurs on downslope near a wave trough.[13] It is interesting that superharmonic roll motion, in which three cycles of motion are found within one cycle of excitation, exists here.

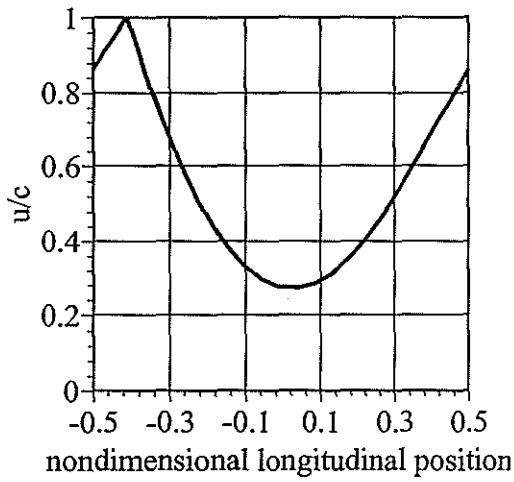

Fig. 6 Periodic attractor in surge (Fn=0.3247 and χ_c=10 degrees)

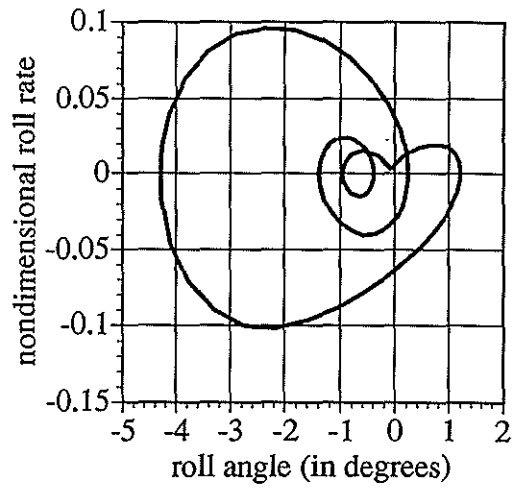

Fig. 8 Periodic attractor in roll (Fn=0.3247 and χ_c=10 degrees)

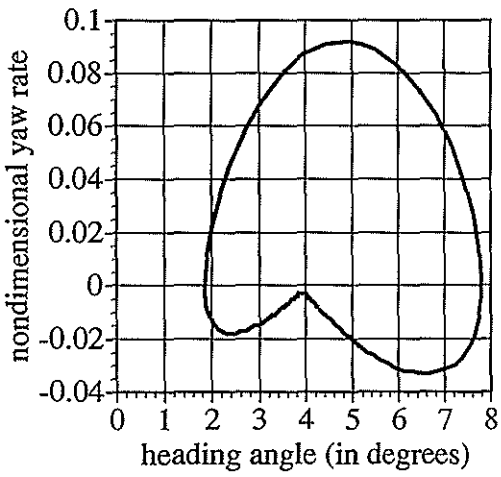

Fig. 7 Periodic attractor in yaw (Fn=0.3247 and χ_c=10 degrees)

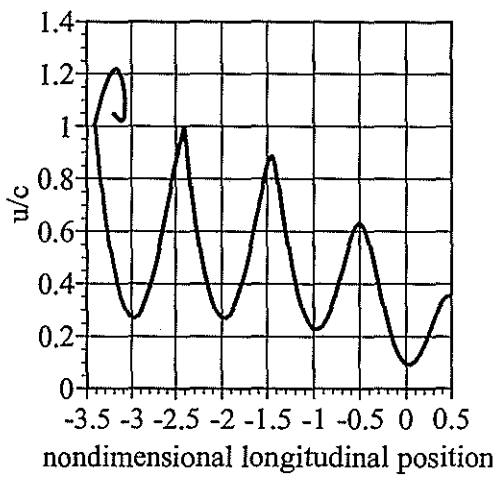

Fig. 9 Transient behaviour in surge (Fn=0.3248 and χ_c=10 degrees)

The transient behaviour leading to capsizing for the new nominal Froude number 0.3248 is shown in Figs. 9-11. At the final stage, the ship centre situates on downslope

and the ship violently turns to starboard despite of the maximum opposite rudder action. And then she capsized to port side. This is capsizing due to broaching. Here capsizing has a role as a kind of attractor.

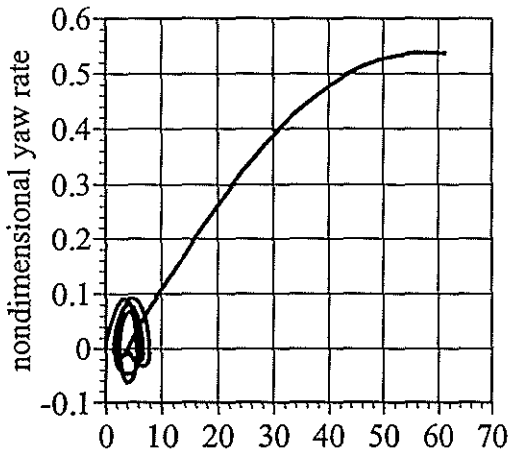

Fig. 10 Transient behaviour in yaw (Fn=0.3248 and χ_c=10 degrees)

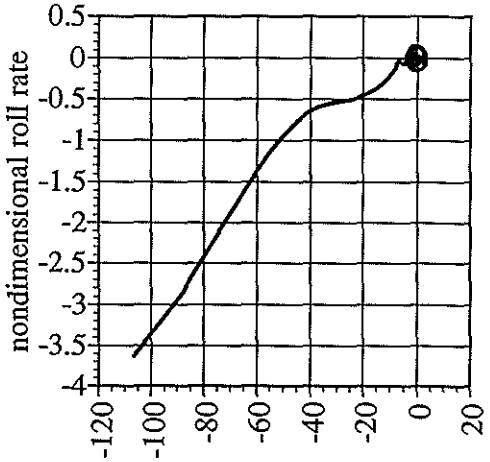

Fig. 11 Transient behaviour in roll (Fn=0.3248 and χ_c=10 degrees)

Nonlinear Dynamics

It is desirable to apply nonlinear dynamics for more rigorously identifying the initial-condition dependence for capsizing. Besides capsizing in beam seas, the author [14-15] and Spyrou [11, 16] have applied nonlinear dynamics to broaching and capsizing in quartering seas since 1992. As steady states, the surf-riding equilibria and periodic motions were identified and their local stability were discussed with a mathematical model. If a stable periodic motion cannot exist and a stable equilibrium can exist, stable surf-riding can occur. If the equilibrium becomes unstable, the ship can suffer broaching. Since surf-riding, broaching and capsizing are transitions between different steady states, the analysis focused on steady states may explain the occurrence of these phenomena to some extent. However, to more precisely identify the critical conditions for these phenomena, it is necessary to investigate transient states. In other words, the invariant manifold analysis is essential.

For uncoupled surf-riding, the global structure of initial-condition dependence has been identified by an invariant manifold analysis of a unstable surf-riding equilibrium. [17] For surf-riding in quartering seas, which is coupled with lateral motions, it is shown that an unstable invariant manifold of a surf-riding equilibrium point with the maximum opposite rudder angle corresponds to a typical behaviour of broaching. [14] In this investigation, an invariant manifold analysis of a surf-riding equilibrium point with a proportional auto pilot, whose gain K_P=1.0, is carried out and compared with the numerical experiments based on "sudden change concept".

Since the mathematical model used here [10,15] has four degrees of freedom, the state vector is eight dimensional. The eigenvalues of surf-riding equilibrium point near wave crest for Fn=0.3248 and χ_c=10 degrees are shown in Fig. 12. Since one eigenvalue

has a positive real part and seven eigenvalues have negative real parts, this equilibrium point is a saddle of index one in eight dimensional phase space. An invariant manifold, or an outset, is obtained by numerically integrating the state equation from the equilibrium point with a small perturbation for the positive or negative direction of eigenvector of the eigenvalue having a positive real part. Since the index of the saddle is one, the manifold, or hyper surface, is one dimensional, namely, a trajectory. All points on this manifold situate on this manifold for $-\infty<t<\infty$. This is the reason why this manifold is invariant.

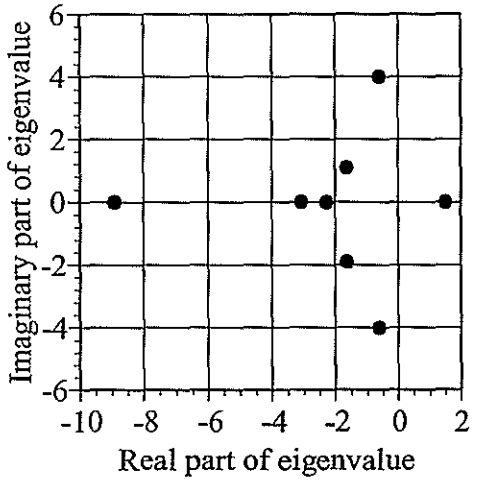

Fig. 12 Eigenvalues of a surf-riding equilibrium point near wave crest (Fn=0.3248 and χ_c=10 degrees)

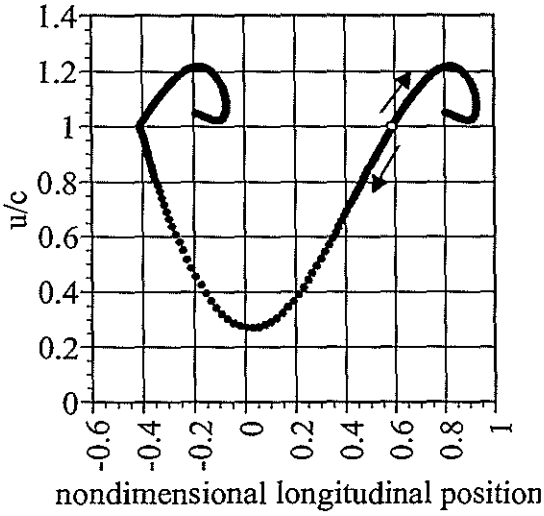

Fig. 13 Unstable invariant manifolds of a surf-riding equilibrium point (Fn=0.3248 and χ_c=10 degrees)

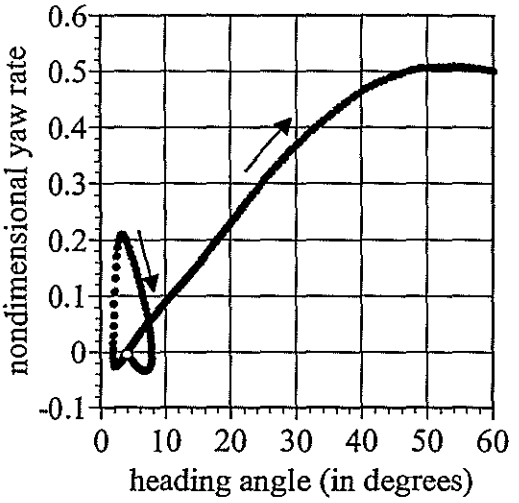

Fig. 14 Unstable invariant manifolds of a surf-riding equilibrium point (Fn=0.3248 and χ_c=10 degrees)

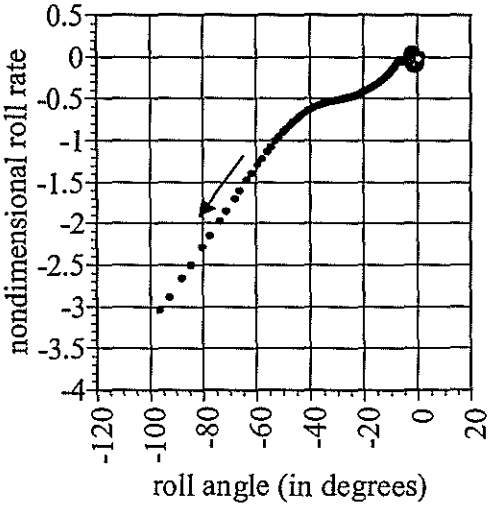

Fig. 15 Unstable invariant manifolds of a surf-riding equilibrium point (Fn=0.3248 and χ_c=10 degrees)

Figs. 13-15 show the unstable invariant manifolds of surf-riding equilibrium point near wave crest for Fn=0.3248 and χ_c=10 degrees. The trajectory towards downslope shows that the heading angle rapidly increases to starboard despite of the maximum opposite rudder angle and then the ship capsizes to the port side. During these behaviour the ship centre remains on wave downslope and at the final stage the ship centre situates on downslope near wave trough. This is a typical example of capsizing due to broaching. The trajectory towards upslope approaches a saddle next to the original saddle and then realises capsizing due to broaching. The unstable invariant manifolds towards both directions tend to capsizing due to broaching.

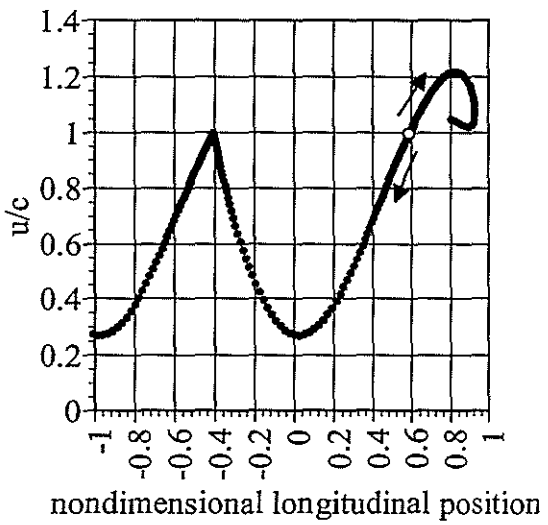

Fig. 16 Unstable invariant manifolds of a surf-riding equilibrium point (Fn=0.3247 and χ_c=10 degrees)

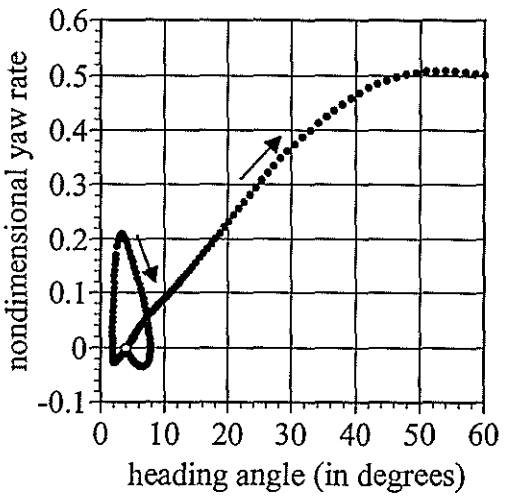

Fig. 17 Unstable invariant manifolds of a surf-riding equilibrium point (Fn=0.3247 and χ_c=10 degrees)

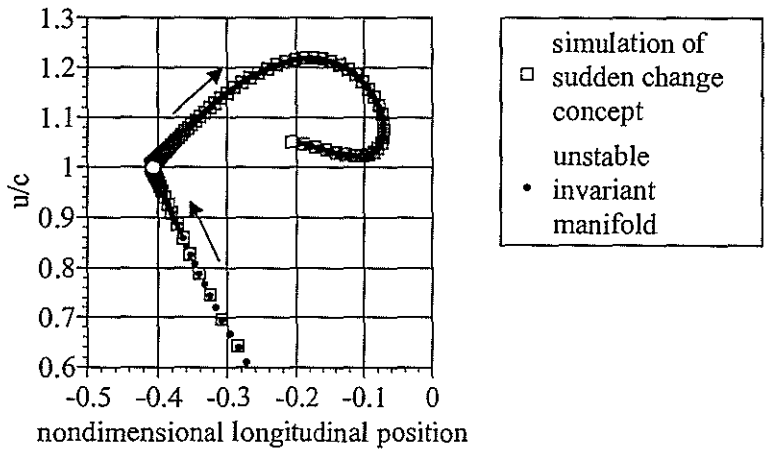

Fig. 18 Comparison between the numerical experiment based on sudden change concept and the unstable invariant manifold (Fn=0.3248 and χ_c=10 degrees)

Figs. 16-17 show the unstable invariant manifolds for Fn=0.3247. Here the trajectory towards downslope tends to capsizing due to broaching like the previous example. However, the trajectory towards upslope approaches the saddle next to the original one and then tends to a periodic attractor. Thus we can presume that between Fn=0.3247 and Fn=0.3248 there is a nominal Froude number whose unstable invariant manifold of a saddle tends to a different saddle. This is the "heteroclinic connection". Thus, if the ship situates below this heteroclinic trajectory, capsizing due to broaching is not likely to occur. That is to say, the nominal Froude number for the heteroclinic bifurcation is the critical condition for capsizing due to broaching. In the numerical experiment described before, the initial value was a periodic orbit for Fn=0.1 and χ_c=0 degrees and the critical condition for capsizing exists in 0.3247<Fn<0.3248. Thus, the results of this numerical experiment completely agree with the conclusion from the present invariant manifold analysis. Moreover, Fig. 18 shows that the invariant manifold towards upslope well corresponds to the trajectory obtained by the numerical experiment based on the "sudden change concept". The further investigation in this direction is now under way. As you see, the nonlinear dynamics has a possibility to be substituted for a numerical experiment.

Acknowledgements

This research was partly supported by the Grant-in Aid for Scientific Research of the Ministry of Education, Science and Culture of Japan, and the author would like to acknowledge the support from its project leader, Professor Hamamoto from Osaka University.

References

[1] Tsuchiya, T., R. Kawashima, Y. Takaishi and Y. Yamakoshi : Capsizing Experiments of Fishing Vessels in Heavy Seas, Proc. of the Int. Symp. on Practical Design in Shipbuilding, Tokyo, 1977, pp.287-294.

[2] Takaishi, Y. : Consideration on the Dangerous Situations Leading to Capsize of Ships in Waves, Proc. of the 2nd Int. Conf. on Stability of Ships and Ocean Vehicles, Tokyo, 1982, pp.243-253.

[3] Umeda, N., M. Hamamoto, Y. Takaishi et al.: Model Experiments of Ship Capsize in Astern Seas, J. of Soc. of Nav. Arch. of Japan, Vol.177, 1995, pp.207-217.

[4] Umeda, N., T. Fujiwara and Y. Ikeda : A Validation of Stability Standard Applied to Hard-Chine Craft Using the Risk Analysis on Capsizing, J. of the Kansai Soc. of Nav. Arch., Japan, No.219, 1993, pp.65-74, in Japanese.

[5] Umeda, N. and Y. Yamakoshi: Probability of Ship Capsizing due to Pure Loss of Stability in Quartering Seas, Naval Architecture and Ocean Engineering, Vol.30, 1993, pp.73-85.

[6] Belenky, V.L.: Analysis of Probabilistic Balance of IMO Stability Regulation by Piece-Wise Linear Method, Marine Technology Transactions, Polish Academy of Science, Vol.6, 1995, pp.5-55.

[7] Thompson, J.M.T.: Transient Basins -A New Tool for Designing Ships against

Capsize, *Dynamics of Marine Vehicles and Structures in Waves*, (W.G. Price et al. Editors), Elsevier Science Publishers (Oxford), 1991, pp. 325-331.

[8] Vassalos, D., N. Umeda, M. Hamamoto and M. Tsangaris: Modelling Extreme Ship Behaviour in Astern Seas, Trans. of the Roy. Inst. of Nav. Arch., (to be appeared).

[9] Munif A. and M. Hamamoto: Manoeuvring Motion of a Ship in Waves, Marine Dynamics Committee, MC45-6, 1998.

[10] Umeda, N.: Application of Nonlinear Dynamical System Approach to Ship Capsize in Regular Following and Quartering Seas, Proc. of the Workshop of Numerical and Physical Simulation of Ship Capsize in Heavy Seas, Strathclyde, 1995, (to be appeared.)

[11] Spyrou, K.: A New Method to Analyse Escape Phenomena in Multi-Degree Ship Dynamics Applied to the Broaching Problem, Pro. of the 6th Int. Conf. on Stability of Ships and Ocean Vehicles, Varna, Vol.1, 1997, pp.83-91.

[12] Grochowalski, S., J.B. Archibald, F.J. Connolly and C.K. Lee: Operational Factors in Stability Safety of Ships in Heavy Seas, Proc. of 5th Int. Conf. on Stability of Ships and Ocean Vehicles, Melbourne, Vol.4, 1994.

[13] Umeda. N.: written discussion to [12], Proc. of 5th Int. Conf. on Stability of Ships and Ocean Vehicles, Melbourne, Vol.6, 1994.

[14] Umeda, N. and Renilson, M.R. : Broaching - A Dynamic Analysis of Yaw Behaviour of a Vessel in a Following Sea, *Manoeuvring and Control of Marine Craft* (Wilson, P.A. editor), Computational Mechanics Publications (Southampton), 1992, pp.533-543.

[15] Umeda, N., D. Vassalos and M. Hamamoto: Prediction of Ship Capsize due to Broaching in Following/ Quartering Seas, Proc. of the 6th Int. Conf. on Stability of Ships and Ocean Vehicles, Varna, Vol.1, 1997, pp.45-54.

[16] Spyrou, K.: Surf-Riding, Yaw Stability and Large Heeling of Ships in Following / Quartering Waves, Sciffstechnik, Bd.42, 1995, S.103-112.

[17] Umeda, N. : Probabilistic Study on Surf-Riding of a Ship in Irregular Following Seas, Proc. of the 4th Int. Conf. on Stability of Ships and Ocean Vehicle, Naples, 1990, pp.336-343.

Ship Capsize Assessment and Nonlinear Dynamics

K.J. Spyrou[1]

Certain aspects of ship stability assessment in beam and in following seas are discussed. It is argued that the use of detailed numerical codes of ship motions cannot solve alone the assessment problem. On the other hand, whilst simplified models can be very useful for acquiring a fundamental understanding of the dynamics of capsize, still a good number of theoretical obstacles need to be overcome. In respect to beam sea capsize, firstly we discuss the structure of the mathematical model and the types of excitation. Then we consider the mechanism of roll damping very near to capsize angles and we point out a very interesting connection that exists with the specification of predictors of capsize based on Melnikov's method. Finally we sketch out a constrained design optimization procedure which can be used for finding those ship parameters' values where resistance to capsize is maximized. In respect to the following sea, we show that if capsize is examined in a transient sense, it should be possible to have a unified treatment of pure-loss and parametric instability. We also show what is the qualitative effect on the stability transition curves from bi-chromatic waves.

INTRODUCTION

Whilst one might think of many different methods for assessing the behaviour of a system, there is little doubt that the most reliable are those which are based on sufficient understanding of the system's key properties. For ship stability assessment however the application of this principle has been, so far at least, less than straightforward; because the behaviour of a ship in an extreme wave environment, where stability problems mostly arise, is often determined by very complex, hydrodynamic or ship dynamic, processes.

Ideally one would wish of course to have a full, meticulously developed and validated mathematical model of ship motions on which to carry out detailed analysis of dynamic behaviour and instability. Unfortunately this seems still to be well beyond our reach. But even if such a model were available, we would hardly know how to carry out in depth analysis for the nonlinear dynamical system in hand[2]. As a result, one can see two lines of research evolving, and it is essential that interaction between the two is encouraged: the first dealing with detailed mathematical modelling of the motion; whereas the second aiming to provide a better understanding of dynamic behaviour on the basis of simpler models that can capture however key features of the system's response. Areas of concern can be identified however in either of these directions: As the mathematical model of ship motion becomes larger, there is a cumulative effect from the uncertainties that often underlie the various assumptions and the unavoidable empiricism which lurks behind model development. On the other hand, when a simple model is used it is sometimes uncertain to what extent the observed behaviour corresponds to that of the real system.

The first direction represents essentially the extension of the traditional seakeeping approach

[1] Centre for Nonlinear Dynamics and its Applications,
University College London,
Gower Street, London WC1E 6BT, UK
email: k.spyrou@ucl.ac.uk

[2] As is well known, the motion of a body on the surface of the sea entails partial differential equations (PDEs) for its description. As evidenced from approximations of PDEs from systems of ordinary differential equations (ODEs), an infinite number of ODEs is required for absolute equivalence. This corresponds to the well known fact that memory effects (or frequency dependence of hydrodynamic coefficients) render the system's state-space infinite dimensional.

from small towards larger amplitude motions. However the second is quite novel in naval architecture. Its importance is owed to the fact that nonlinearity can make large amplitude responses follow completely different patterns that their smaller-amplitude counterparts. As is nowadays increasingly realized, a ship, like many other dynamical systems, can exhibit a very rich envelope of large-amplitude behaviour which is sometimes very difficult to unravel. In order to understand the underlying principles of safety-critical behaviour one needs to have an effective methodology which will guide his search and here is where the techniques of nonlinear dynamics' can provide truly valuable inputs.

These techniques enable, at first instance, better focus during physical model testing. This is essential because in extreme seas comparisons between theory and experiment are non-trivial due to the fact that the number of unknowns involved is very large. But perhaps the more far-reaching implication is that they offer a potential for developing effective methods of stability assessment that can combine scientific rigour with practicality for better design and safer operation. This potential allows us to start thinking also about intregrated assessment methods of intact stability which will cover mechanisms of capsize associated with different environments and ship-wave encounters.

In the previous Workshop in Crete we have outlined some of our recent work along the above lines: We proposed a method of interfacing the findings of the nonlinear dynamics approach of ship capsize with design, in respect to the mechanism of capsize in resonant beam seas [1]. Also we continued our investigations of the instabilities of the following/quartering sea, discussing the interesting parallel that exists between yaw (related with broaching) and roll instabilities (related with pure-loss and parametric instability) [2].

The present paper consists of two parts: Firsly we discuss, very much in the spirit of this Workshop, some of the problems that exist in developing an effective stability assessment in beam-seas. Then we explain a practical assessment method for pure-loss and parametric instability in following seas.

BEAM-SEA CAPSIZE

A number of issues are currently under debate, such as the suitability of single roll or coupled models, the use of deterministic or stochastic-type of excitation; and the quantitative prediction of damping especially up to very large angles.

The suitability of the mathematical model

It is quite common, especially after Wright and Marshfield [3] to model roll motion in regular beam waves by expressing the roll angle relatively to the local wave slope. A single-degree roll equation is then used to describe roll dynamics with nonlinearities in damping and in restoring. For ships with small beam compared to the wave length, it is often reasonable to assume that, in sinusoidal beam waves they experience a fluctuating "effective gravitational field" $\mathbf{g}_e$ where the centrifugal acceleration of the water particle is combined with the acceleration of gravity $\mathbf{g}$ [4]. This says essentially that a small boat beam to long waves tends to follow the motion of the water particles and it allows direct use of the calm-sea restoring of the ship in the equation of relative roll. From an axes system tracking the motion of a water particle and having one axis always tangent to the wave surface the single roll model is then perfectly adequate.

But if it is intended to carry out model experiments, the physical model should rather not be constrained rigidly in sway because then the model cannot follow the motion of the water particles and direct comparison between theory and experiment becomes difficult. On the other hand, if the model is not constrained at all, it is likely to yaw and to have also a mean drift which also hinders comparisons with theory.

There is of course the possibility also that the ship "cannot" follow the motion of the water particles. Then the coupled roll sway and heave need to be considered along with the type of wave excitation as the above single roll model has encountered its limits. This is even more evident if the effect of non-regular waves is under consideration. However, one must bear in mind here that, unlike some seakeeping studies where we examine performance degradation during a voyage, in intact-ship capsize we are only concerned about an almost momentary event which is usually the result of encountering a small number of steep, often quite similar, waves with which the ship cannot cope.

The nature of the excitation deserves however some further attention: In our capsize studies we are usually restricting our analysis, one might think unjustifiably, in excitations produced by steep but non-breaking waves. This is an idealization which can result in unsafe predictions; because in the extreme environments where we investigate capsize, wave breaking is quite common. The nature of such excitations, a combination of smooth

and impacting, and their magnitude can be very conducive for capsize.

But even if we assume that the structure of the conventional mathematical model is satisfactory, at least two further tasks need to be tackled: (a) To derive roll damping coefficients that can be applicable for near-capsize-angle motions; and (b) to identify capsize thresholds in terms of combinations of wave amplitude and frequency. Interestingly, the two tasks are, as shown below, in fact intrinsically connected.

Derivation of damping coefficients

Currently it is quite common to derive the damping coefficients from free roll decrement data under the assumption that the undamped roll would be basically harmonic. However, near capsize the nonlinearity of restoring is very strong rendering the response of a rather different type. This means that energy dissipation near capsize angles is not taken into account accurately when the coefficients are derived, although the values of these coefficients are critical in the theoretical investigation of capsize.

To explain these, let us consider a scaled equation of free roll with a quite general, quintic-type restoring curve:

$$\ddot{x}+D(\dot{x})+x+\delta x^3-(\delta+1)x^5=0 \qquad (1)$$

where $x=\dfrac{\varphi}{\varphi_v}$ with φ the real roll angle and φ_v the vanishing angle. Differentiation is carried out in respect to scaled time $\tau=\omega_0 t$ where ω_0 is the 'undamped' natural frequency and t is the real time. $D(\dot{x})$ is the damping function that normally includes a linear plus an absolute quadratic or cubic component of roll velocity; and δ parametrizes the whole family of quintic restoring curves and therefore through δ we can establish a correspondence with the real (GZ) of our ship.

As has been shown in [5], if damping is neglected we can obtain the following exact "Hamiltonian" solution for large amplitude relative free roll (assuming that the "ship" was released with zero intial velocity):

$$x=x_0\frac{\mathrm{cn}(u,\,k)}{\sqrt{1-\lambda^2\,\mathrm{sn}^2(u,\,k)}} \qquad (2)$$

where x_0 is the initial angle at $\tau=0$; λ is a function of x_0 and δ; cn, sn are the so called jacobian elliptic functions (respectively elliptic cosine and elliptic sine) with argument $u=w t$, and modulus k; w is also a function of x_0 and δ. We note that when $k\to 0$ we have the linear, case and the solution (2) becomes harmonic; whereas for $k\to 1$ we obtain the hyperbolic solution that defines the boundary of the 'undamped' safe basin.

In order to find damping coefficients appropriate for extreme roll angles we need to know how energy is dissipated at these angles which requires to know the trajectory in $(x,\,\dot{x})$ from one peak (that is, one crossing of the zero velocity line) to the next, see Fig. 1.

For a linear roll equation such a solution is rather straightforward:

$$x=x_0e^{-\zeta\tau}\sin\left(\sqrt{1-\zeta^2}\,\tau-\theta\right) \qquad (3)$$

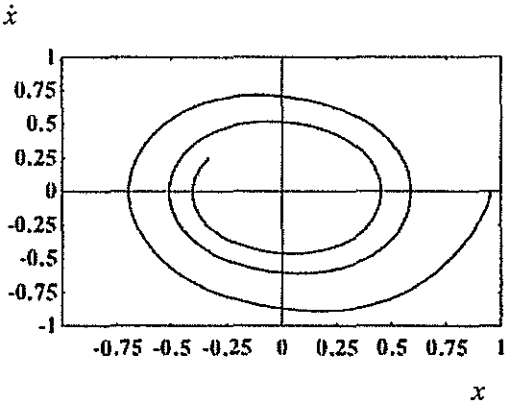

Fig. 1: Numerically derived roll decay for a quintic polynomial when $x_0=0.95$. By c_1 and c_3 are indicated respectively the linear and the cubic damping coefficients (nondimensional).

Expressions for "mildly" nonlinear (GZ) can also be derived through a perturbation approach. But for the strongly nonlinear case, if damping is present, exact analytical solution cannot be obtained; and a perturbation-like approach (with damping's nonlinearity as small quantity) involving elliptic functions is extremely complex whilst the accuracy achieved may be doubtful.

In [5] we have shown that it is possible to identify fully analytically the roll decrement per half-cycle for roll angles arbitrarily close to the vanishing angle if we assume the roll trajectory to constitute a perturbation of the Hamiltonian solution. As will be shown next this fits nicely with the Melnikov method of capsize assessment which is based on the same principle.

Predictors of capsize

Such predictors can be derived from an analysis either of steady-state or from transient roll responses [1]. To resolve an issue which was raised

in last year's Workshop, by "steady-state capsize" we mean the absence of stable steady-state solution in the vessel's response. If such a state does not exist at a certain level of wave forcing and damping, the ship simply cannot stay upright. On the other hand, by "transient capsize" we mean that. although a stable state might exist, at the initial transient stage the response is such that capsize occurs. As is obvious, the threshold wave slope of transient capsize should be lower than that of steady-state capsize. For this reason it is more sensible to predict capsize on the basis of transients [6].

A good criterion of incipient transient capsize can be derived from the so-called Melnikov's method through which we can find an analytical approximation of the critical wave slope, given the frequency ratio, where manifold tangencies arise and the domain of bounded roll motion starts becoming fractal, triggering rapid loss of the safe area of state space. Melnikov's method has been applied both in a deterministic and in a stochastic context.

It is remarkable that the critical condition derived from Melnikov's method can be interpreted also as an energy balance: Essentially, Melnikov's method "says" that to identify the critical wave slope given the damping, one should balance the work done by the forcing with the energy dissipated through damping *around the remotest orbit of bounded roll* (heteroclinic or homoclinic orbit depending on whether a symmetric or a biased in roll ship is studied). What makes such an interpretation particularly interesting is that it provides a connection with the widely debated in the early eighties method of energy balance for capsize assessment. That method however relied on harmonic or nearly harmonic responses.

Another observation on Melnikov is that it makes use of the perturbed Hamiltonian dynamics approach. This is the same fundamental assumption that has allowed, as discussed in the previous subsection, to find analytically the roll decrement during decay experiments for arbitrarily large initial roll.

From the above observations the conclusion may be drawn that the tasks of deriving damping coefficients and of predicting capsize are intrinsically connected and that, consistency in the followed approaches should be ensured.

Stability of symmetric and of biased ship

As has been pointed out by Thompson [6], the presence of even small bias, can reduce very considerably the critical wave slope where capsize occurs. It seems logical that a dynamic stability criterion should take into account this fact; but how much bias in needed in the assessment is very hard to define in a rational manner.

As is well known, a ship can become biased as the result of wind loading or cargo imbalance; but what is further notable is that a ship shows a "preference" to capsize towards the wave; and that in large waves an initially symmetric ship may develop also some "dynamic" list towards the wave. This would possibly require consideration of sway and higher order wave effects to explain but whether these matters should be taken into account in a capsize assessment is a rather open question at this stage.

About the design problem

It is of course highly desirable the information produced from the analysis of dynamics to be linked with the design process. Unfortunately, until recently this problem had not even been addressed, [1]. Generally, there are two main problems that need to be solved: Firstly, how to maximize the critical wave slope where manifold tangencies arise, over a range of wave frequencies; and secondly how to generate practical hull shapes given some desirable form of the restoring curve identified from the first task [essentially the inverse of the conventional task of deriving the (GZ) curve given a hull]. Here we shall discuss in further detail the first task.

Let's take the rather generic equation of roll with linearized damping and cubic-type (GZ) which has been thoroughly studied in the past:

$$\ddot{x}+2\zeta\dot{x}+x-x^3=F\sin(\Omega\tau) \qquad (4)$$

$$F=\frac{I}{I+\Delta I}\frac{Ak\Omega^2}{\varphi_v},\quad \zeta=\frac{B}{2\sqrt{Mg(GM)(I+\Delta I)}}$$

with B the dimensional equivalent damping, M the ship mass; and I, ΔI, respectively the roll moment of inertia and the added moment.

It can be noticed that in the expression of the equivalent damping ratio ζ, (GM) appears in the denominator which means that for our scaled equation increase of (GM) reduces ζ! However, at the same time the forcing is reduced even more since $F\propto\Omega^2=\dfrac{\omega^2}{\dfrac{Mg(GM)}{I+\Delta I}}$.

From Melnikov we find the critical forcing F_M to be:

$$F_M = \frac{4\zeta \sinh\left(\frac{\pi\Omega}{\sqrt{2}}\right)}{3\pi\Omega} \qquad (5)$$

In order to understand the meaning of this we should go back to dimensional quantities in which case we can obtain the following expression of critical wave slope $(Ak)_M$:

$$(Ak)_M = \frac{2B}{3\pi}\frac{Mg}{I(I+\Delta I)}\varphi_v(GM)\frac{\sinh\left(\frac{\pi\sqrt{I+\Delta I}}{\sqrt{2Mg(GM)}}\omega\right)}{\omega^3} \qquad (6)$$

where ω is the wave frequency.

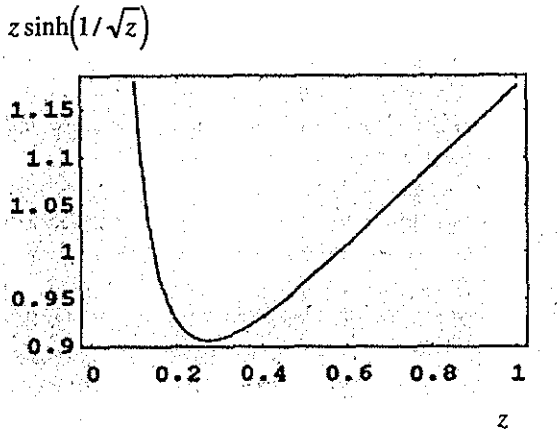

Fig.2: Basic trend of the dependence on (GM) on the critical wave slope

Increase of damping or of the vanishing angle are the typical ways to improve the resistance to capsize according to this mechanism [6]. However some more intriguing observations are possible also on the basis of Fig. 2: Expression (6) allows for having a situation where very low (GM) can, under certain circumstances, be beneficial! It is essential therefore that the findings are not applied blindly but an understanding about the physical mechanisms involved is developed, and areas of practical validity are established.

As for any resonance mechanism, it can be dealt with by increasing damping and/or by detuning our system from the excitation. As the natural frequency of the ship depends on (GM), such detuning can be achieved not only by increasing but also by reducing (GM). In fact, it is possible that if the phase of rolling response is nearly opposite to the phase of the wave, then the "absolute" roll motion (the wave slope plus the relative to it roll angle) can be very little, giving the impression that ship is "insensitive" to the excitation. Of course, under no circumstances could be advised to set low (GM) for the ship because then capsize can easily happen from other reasons.

In a practical context it is sensible, rather than trying to establish the capsize limits of the ship, to set threshold absolute roll angles beyond which the ship is in grave danger of capsize due for example to cargo shift. In such a case however, we must be very careful in the interpretation of the output of a roll motion equation like (2). Because a small relative angle could mean a quite substantial one in absolute terms given the wave slope; and on the other hand, as hinded earlier, the phase between the roll response and the wave can make absolute rolling to be very large or very small.

As has been outlined in [1] it should be possible to combine an expression like (6) with an optimisation process, given certain ship parameter constraints obtained from existing stability standards. For example, for the considered simplest possible case of cubic restoring, the Naval Engineering Standard 109 would produce as far as (GM) and φ_v are concerned, the following constraints:

The area criteria for (GZ) up to 30deg, 40deg and between 30 and 40deg give:

$$\text{(a) } (GM)\left(0.137 - \frac{0.019}{\varphi_v{}^2}\right) \geq 0.08 \qquad (7)$$

$$\text{(b) } (GM)\left(0.244 - \frac{0.059}{\varphi_v{}^2}\right) \geq 0.133 \qquad (8)$$

$$\text{(c) } (GM)\left(0.107 - \frac{0.04}{\varphi_v{}^2}\right) \geq 0.048 \qquad (9)$$

Further constraints:

$$\max(GZ) \geq 0.3 \Rightarrow \text{ (d) } 0.385(GM)\varphi_v \geq 0.3 \qquad (10)$$

$$\text{(e) } (GM) \geq 0.3 \qquad (11)$$

$$\varphi_{(GZ)_{\max}} \geq 30\,\text{deg} \Rightarrow \text{ (f) } \varphi_v \geq 0.9064\,\text{rad} \qquad (12)$$

(this is less than the recommended range of at least 70 deg).

The above lines are essentially sketching out an optimization process where Ak, expressed on the basis of (6), or preferably with a more detailed expression of the criterion taking better account of the hull, is sought to be maximized while making

sure that realistic constraints like the above, are being satisfied.

It is very interesting that our concerns about the bias effects, expressed earlier, can be incorporated also into such a procedure. Let us consider the a - parametrized family of restoring curves with bias, where $a=1$ means a symmetric system and $a=0$ means a system allowing only one-sided escape [6]:

$$\ddot{x}+2\zeta\dot{x}+x(1-x)(1+ax)=f\sin(\Omega\tau) \qquad (13)$$

In [7] it has been shown that it is possible to find analytically an expression for the critical (Ak) for small and for large bias, respectively as following[3]:
Perturbation of symmetric system (small bias):

$$F_M=\frac{\sqrt{2}\sinh\left(\frac{\Omega\pi}{\sqrt{2}}\right)\left(2\sqrt{2}\zeta-1+a\right)}{3\Omega\pi} \qquad (14)$$

Strongly "one-sided" escape (large bias):

$$F_M=2\zeta\sqrt{a}\,\frac{\left[3\alpha\beta^2\cosh^{-1}\left(\frac{\alpha}{\beta}\right)-\sqrt{\alpha^2-\beta^2}\left(\alpha^2+2\beta^2\right)\right]}{6\sqrt{2}\pi\mu\sqrt{\alpha^2-\beta^2}\sin\left[\mu\cosh^{-1}\frac{\alpha}{\beta}\right]} \qquad (15)$$

$$\alpha=\frac{2(2a+1)}{3a},\ \beta=\sqrt{\frac{2(1-a)(2+a)}{3a}},\ \mu=\frac{\Omega}{\sqrt{1+a}} \qquad (16)$$

Again, the quantities will have to be expressed in dimensional form in order to be able to find the true critical relationship of ship parameters.

CAPSIZE IN A FOLLOWING SEA

As is well known, in a following sea a ship may capsize due to severe fluctuations of its righting arm. Capsize can occur either from a sudden divergent roll ("pure-loss") or from a more dynamic process ("parametric"), where roll is built-up in an oscillatory and gradual manner. Traditionally, the two mechanisms are considered independently. However, as they are both the result of time-dependence of the roll righting arm (in fact dependence on the position of the ship on the wave), the propensity for capsize could be assessed more effectively if the two were treated in a unified manner.

Commonly, the parametric mechanism is examined on the basis of the principal and the fundamental resonance regions on the stability chart of a Mathieu-like equation. However, such a chart corresponds in fact to long term asymptotic behaviour which is rather unrealistic for a ship. This has created some controversy about the true relevance of the parametric scenario; because, although at realistic levels of ship roll damping the domain of the principal, and often of the fundamental resonance extend sometimes to feasible levels of restoring variation amplitude, this picture is correct if the considered number of wave cycles goes to infinity. Practically however, it is more important to know whether the instability becomes noticeable within a small number of wave cycles. But if the "allowed" number of wave cycles is small, the building-up of large roll requires very intensive variation of restoring which may, and one would indeed hope to, be unrealistic.

Another matter that needs to be taken also into account, more in respect to the pure-loss scenario, is the physical time required for capsize: At lower frequencies of encounter the ship may capsize more easily because it stays for longer time at unfavourable for stability regions of the wave. But because the ship is advancing very slowly relatively to the wave, the time for capsize can be excessively high. It is quite obvious in this case that for capsize assessment it becomes important where the ship was at $t=0$. One possible way to deal with this dependence on the initial phase is to assume that the ship, at $t=0$ is just entering the negative restoring region of the wave. For sinusoidal variation of (GM) this phase, say χ, is given from $\chi=-\arccos\left(\frac{1}{h}\right)$ where h is the amplitude of variation of (GM).

The major effect that the number of cycles has on the first resonances is shown clearly in Fig. 3 for a typical linear Mathieu-type roll equation which, on the basis of scaled quantities, takes the form:

$$\frac{d^2x}{d\tau^2}+\frac{2k\sqrt{a}}{\omega_0}\frac{dx}{d\tau}+a(1-h\cos 2\tau)x=0 \qquad (17)$$

where $a=\frac{4\omega_0^2}{\omega_e^2}$, $x=\frac{\varphi}{\varphi_v}$ but this time $2\tau=\omega_e t$ (time nondimensionalized in respect to the

[3] These analytical results are of importance also for [8] and [9] where Melnikov's critical wave slope had been identified only numerically.

encounter frequency ω_e). Also, ω_0 is the (dimensional) natural frequency and k is the equivalent damping factor ($2k = \frac{B}{I+\Delta I}$).

In Fig. 3 we examined whether the roll angle reaches the level of the vanishing angle within a prescribed number of wave cycles.

It is noted that if only four cycles are considered the h required is very high ($h = 2.1$, not shown in the graph). As the order of the resonance increases the required amplitude becomes less dependent on the number of wave cycles; but the practical relevance of these resonances for a ship is rather minimal. It is also noted that, the lower the number of cycles the more influential becomes the initial position of the ship on the wave.

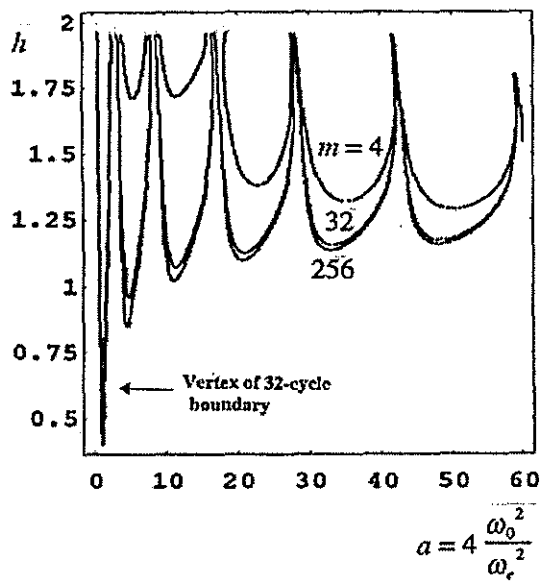

Fig. 3: Capsize regions in respect to the first six resonances, with parameter the considered number of encounter-wave cycles m. The initial heel was $x_0 = 0.01$ and as capsize was considered its 100-fold increase; $2k/\omega_0 = 0.025/0.144$.

Fig. 4 provides a unique combined view of regions of pure-loss and parametric instability on the basis of cubic-type restoring where the nonlinear term is time independent. This is allowed by the fact that behaviour is examined in a transient sense. Capsize occurrences are recorded if they happen in a small number of cycles and within limited physical time.

Of course, different hull forms will result in different restoring variation laws which, in turn, will give different arrangements of the capsize boundaries. At the moment, we are still lacking a systematic procedure for dealing with this fact. This is an area of research currently considered.

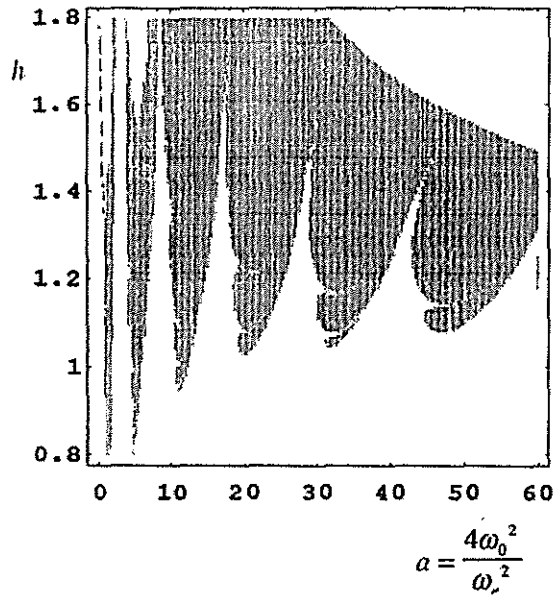

Fig. 4: Capsize regions for cubic-type restoring in less than 8 wave cycles and requiring less than 300 sec (natural frequency in calm sea 0.381sec^{-1}). The dark regions correspond to capsize according to the parametric scenario. The white upper-right region is capsize in less than 50 sec and is according to the to pure-loss mechanism. Quick capsizes ($t < 50$ sec) occur also in the first two resonances and it is notable that the required amplitude h is comparable with that of pure loss. The graph is drawn with $2k = 0.025$ and $x_0 = 0.1$.

Behaviour in bi-chromatic seas

A possible extension of the traditional examination of parametric instability on the basis of sinusoidal variation of (GM), is to study the behaviour of a ship under the effect of a wave group containing at least two independent frequencies . We shall assume that, in a qualitative sense, this could bring about a quasiperiodically varying restoring which, for two frequencies present, results in the following roll equation:

$$\frac{d^2x}{d\tau^2} + \frac{2k\sqrt{a}}{\omega_0}\frac{dx}{d\tau} + a\left[1 - rh\cos 2\tau - (1-r)h\cos 2\nu\tau\right]x = 0 \qquad (18)$$

In (18) the parameters r and ν represent respectively the relative strength of the basic frequency and the ratio of the second frequency to the basic.

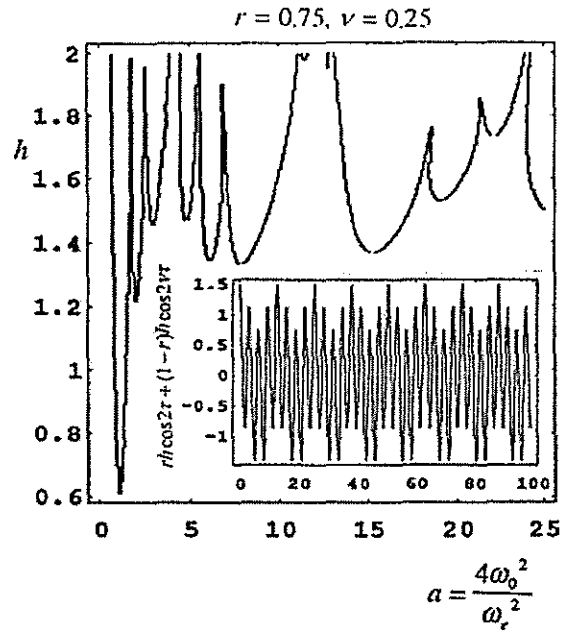

Fig. 5: Parametric instability in bi-chromatic waves for 32 wave cycles.

A general characteristic of the response is that a number of new "spikes" are growing on each primary resonant. However the effect of the extra frequency is not very influential on the principal resonance which extends at relatively low levels of required (GM) variation amplitude h.

REFERENCES

[1] SPYROU, K.J., COTTON, B., THOMPSON, J.M.T. (1997) Developing an interface between the nonlinear dynamics of ship rolling in beam seas and ship design, *Proceedings*, 3rd International Workshop on Theoretical Advances in Ship Stability and Practical Impact, Hersonissos, Crete, October, 9 pages.

[2] SPYROU, K.J. (1997) The role of Mathieu's equation in the horizontal and transverse motions of ships in waves: Inspiring analogies and new perspectives, *Proceedings*, 3rd International Workshop on Theoretical Advances in Ship Stability and Practical Impact, Hersonissos, Crete, October, 14 pages.

[3] WRIGHT, J.H.G. & MARSFIELD,W.B.(1980) Ship roll response and capsize behaviour in beam seas, RINA *Trans.*, **122**, 129-148.

[4] THOMPSON, J.M.T., RAINEY, R.C.T. & SOLIMAN, M.S. (1992) Mechanics of ship capsize under direct and parametric wave excitation, *Phil. Trans. R. Soc. Lond. A* **338**, 471-490.

[5] SPYROU, K.J. & THOMPSON, J.M.T.(1998) A consistent analytical framework for the study of ship capsize and the problem of damping at extreme angles, *to be published*

[6] THOMPSON, J.M.T.(1996) Designing against capsize in beam seas: Recent advances and new insights, *Applied Mechanics Reviews*, **50**, 5, 307-325.

[7] GURD, B.A. (1997): A Melnikov analysis of the Helmoltz-Thompson equation, *MSc Thesis*, Centre for Nonlinear Dynamics and its Applications, University College London, September.

[8] JIANG, C., TROESCH, A.W. & SHAW, S.W. (1996) Highly nonlinear rolling motion of biased ships in random beam seas, *Journal of Ship Research*, **40**, 2, 125-135.

[9] KAN, M. (1992) Chaotic capsizing, *Proceedings*, The 20th ITTC Seakeeping Committee, Osaka, September 10-11.

The Modeling of the Excitation of Large Amplitude Rolling in Beam Waves

Alberto Francescutto & Giorgio Contento [1]

ABSTRACT

In this paper the effect of the excitation modeling on the fitting capability of the nonlinear roll motion equation to experimental data is studied. Several frequency dependent and constant effective wave slope coefficients are derived for five different scale models corresponding to different ship typologies by a Parameter Identification Technique. The frequency domain behavior of the obtained coefficients is discussed and compared with linear diffraction (strip theory) results and I.M.O. suggested values. It appears that a mathematical modeling with constant damping parameters and frequency dependent excitation could give very good results. As regards the excitation parameters, a common trend for slender bodies is evidenced.

Key words: *Nonlinear Dynamics, Roll Motion, Simulation, Parameter Identification.*

MATHEMATICAL MODELLING OF SHIP ROLLING

In this paper some results regarding a simplified mathematical modeling of ship rolling, possibly using as much as possible constant coefficients, are reported in synthesis. More details can be found in [1-3].

The incident wave is assumed long enough to be described by the local slope $\alpha(t)$ where

a) Absolute angle description

$$(I_G + \delta I)\ddot{\varphi} + N\dot{\varphi} + D_1|\dot{\varphi}|\dot{\varphi} + D_2\dot{\varphi}^3 + \ldots + \Delta\overline{GZ}(\varphi) = E(t)$$

The excitation E(t) following Blagoveshchensky [4]:

$$E(t) = \chi_\varphi{}^I \Delta\overline{GM}\alpha + \chi_\varphi{}^{II} I_\nabla \ddot{\alpha} + \chi_\varphi{}^{III} N\dot{\alpha} + \chi_\varphi{}^{IV} \delta I \ddot{\alpha}$$

I_∇ is the inertia of the 'liquid hull';

$\chi_\varphi{}^j$ $(0 \le \chi_\varphi{}^j \le 1)$terms included to account for the hull shape/coefficients and for the ratio between wave parameters and hull breadth and draught.

In normalized form as follows:

$$\ddot{\varphi} + 2\mu\dot{\varphi} + \delta_1|\dot{\varphi}|\dot{\varphi} + \delta_2\dot{\varphi}^3 + \ldots + \omega_0{}^2\varphi + a_3\varphi^3 + a_5\varphi^5 + \ldots = e(t)$$

with

$$e(t) = \pi s_w\left[\left(\alpha_1\omega_0{}^2 - \alpha_2\omega^2\right)\cos(\omega t) - 2\mu\alpha_3\omega sin(\omega t)\right]$$

where α_2 accounts for both terms $\chi_\varphi{}^{II} I_\nabla$ and $\chi_\varphi{}^{IV}\delta I$

The last contribution in e(t), proportional to the linear damping, is of order O(1/ω) with respect to the former and can be neglected:

$$e(t) = \pi s_w\omega_0{}^2\left[\alpha_1 - \alpha_2\left(\frac{\omega}{\omega_0}\right)^2\right]\cos(\omega t)$$

The roll excitation reminds the Morison's approach to wave loads. Here the incident flow characteristics are represented by the local wave slope $\alpha(t)$ and by its derivatives $\dot{\alpha}(t), \ddot{\alpha}(t)$ instead of the traditional velocity and acceleration in a representative point. Each term in

[1] DINMA - University of Trieste, via A. Valerio, 10 - 34127 Trieste, Italy
e-mail: francesc@univ.trieste.it

e(t) has been derived under the *Froude-Krilov hypotheses* and *long wave approximation*. The presence of the hull on the incident flow is accounted for only in some so called 'effective wave coefficients' $\chi_\varphi{}^j$. In this way an important feature of wave load is lost when the wave length becomes comparable with the transversal dimension of the body, i.e. in the diffraction regime. A tentative formulation is here proposed as follows:

$$e(t) = \pi s_w \omega_0{}^2 e^{-\left[\omega/\alpha_1\right]^{\alpha_2{}^2}} \cos(\omega t)$$

Often, no explicit dependence of the amplitude of the excitation on the wave frequency appears. In this case e(t) reads as follows:

$$e(t) = \pi s_w \omega_0{}^2 \alpha_1 \cos(\omega t)$$

Summarizing:

$$\ddot{\varphi} + 2\mu\dot{\varphi} + \delta_1|\dot{\varphi}|\dot{\varphi} + \delta_2\dot{\varphi}^3 + \ldots + \omega_0{}^2\varphi + \sum_{i=1}^{M} a_{2i+1}\varphi^{2i+1} =$$

$$\pi s_w \omega_0{}^2 \alpha_0{}^* \cos(\omega t)$$

$$\alpha_0{}^*(\omega) = \begin{cases} \alpha_1 - \alpha_2\left(\dfrac{\omega}{\omega_0}\right)^2 \\ \alpha_1 \\ e^{-\left[\omega/\alpha_1\right]^{\alpha_2{}^2}} \end{cases}$$

b) Relative angle description

Assuming the same hydrodynamic model for the damping and the same notations as in the previous section, the equation of roll motion in the relative angle approach can be written following Wright-Marshfield [5]:

$$I_G\ddot{\varphi} = -\delta I(\ddot{\varphi} - \ddot{\alpha}) - N(\dot{\varphi} - \dot{\alpha}) - M_R(\varphi - \alpha)$$

where $M_R(\varphi - \alpha)$ is the restoring moment. Introducing the relative angle $\vartheta = \varphi - \alpha$ and dividing by $I_G + \delta I$, we obtain

$$\ddot{\vartheta} + 2\mu'\dot{\vartheta} + \delta'_1|\dot{\vartheta}|\dot{\vartheta} + \delta'_2\dot{\vartheta}^3 + \ldots + \omega_0{}^2\vartheta + \sum_{i=1}^{M} a_{2i+1}\vartheta^{2i+1} =$$

$$-\frac{I_G}{I_G + \delta I}\pi s_w \omega^2 \cos(\omega t)$$

The two approaches are equivalent since they correspond only to a different grouping of the terms. Some differences are due to the fact that:

- in the absolute angle approach only the first term in the development of $\overline{GZ}(\varphi - \alpha) - \overline{GZ}(\varphi)$ is retained corresponding to the fact that the nonlinear dependency on the wave slope is neglected;
- because of the relative angle approach, the inertia loads are accounted for only by the term δI

Moreover, in the assumed relative angle approach only one "unknown" coefficient

$$\alpha_0{}^* = \frac{I_G}{I_G + \delta I}$$

is left to account for the "reduction" of the wave slope effectiveness. In this sense the relative angle model is equivalent to the "constant" wave slope reduction.

DISCUSSION AND CONCLUSIONS

The application of an efficient Parameter Identification Technique, developed on the basis of an idea from Haddara and Bennet [6], to a large series of experiments conducted at the University of Trieste allowed to obtain the following results:

a) Overall capability of the proposed excitation models

Absolute angle: As far as the form of the excitation is concerned, it can be seen from the graphs and from the residual χ^2 in Table 2 that frequency dependent effective wave slope coefficients work better than the constant. This becomes particularly evident outside the peak zone where the difference between estimated and measured values can exceed 100% even if at these frequencies the absolute roll amplitudes are quite small (few degrees). In Fig. 1 and Fig. 2 the results obtained from a highly non-linear restoring, giving rise to bifurcation, and from a mildly non-linear one respectively are reported.

Relative angle: quite similar results with some shortcoming in the mathematical modeling. The $\alpha_0{}^*$ are indeed quite small, so that the introduction of a double factor could be more adapt.

b) Dependency on the righting arm modeling

In some cases the Parameter Identification Technique exhibited an "hyper-sensitivity" to the GZ description mostly in the presence of a strongly nonlinear behavior.

c) Identification of a common trend

An evident frequency dependence of α_0^* is observed (Fig. 3,5). A common trend is evidenced that could be used as a default, at least for slender bodies.

d) Identified damping

The identified values of the damping coefficients, while different for the different ship typologies, show great stability with respect to the excitation modeling.

If the relative angle approach is adopted, then the values of the identified damping coefficients differ from those in the absolute angle.

Several mathematical models were tried. Basically the linear-plus-quadratic and linear-plus-cubic showed almost the same fitting capability, so that using one or the other is a matter of preference.

e) Use of perturbative solution in the PIT

This method was attempted and in some cases gave quite good results, in comparison with the numerical exact solution, at the cost of much less computing time. On the other hand, the results were not so reliable in the cases where high non-linearity was present in the righting arm.

f) Comparison with diffraction theory and I.M.O. suggestions

The frequency dependence of α_0^* is still observed when this parameter is obtained through a linear diffraction-strip theory based code (Fig. 6). However the forecasts of $\alpha_0^*(\omega)$ from the strip theory are usually quite higher than the results from the Parameter Identification method here used with the notable exception of the fishing vessel.

Finally, for sake of completeness, the I.M.O. suggested value of α_0^*, typically indicated with "r", for the roll amplitude computation in the Weather Criterion is compared with experimental results (Fig. 4,7). Here again, with the exception of the fishing vessel, the "r" values are sensibly higher than the observed ones. The deviation of course is on the right side, leading to an overestimation of the rolling amplitude when applying the Weather Criterion. High values of "r" are probably due to the fact that usually this coefficient is obtained by measuring the heeling moment due to waves at fixed model.

REFERENCES

1. Contento, G., Francescutto, A., Piciullo, M., 1996, On the effectiveness of constant coefficients roll motion equations. *Ocean Engineering*, Vol. 23, pp. 597-618.

2. Francescutto, A., Contento, G., 1997, An Investigation on the Applicability of Simplified Mathematical Models to the Roll-Sloshing Problem. *Proc. 7th International Conference on Offshore and Polar Engineering - ISOPE'97*, Honolulu, The Int. Society of Offshore and Polar Engineering, Vol. 3, pp. 507-514.

3. Francescutto, A., Contento, G., Biot, M., Schiffrer. L., Caprino, G., 1998, The Effect of Excitation Modeling in the Parameter Estimation of Nonlinear Rolling. *Proc. 8th International Conference on Offshore and Polar Engineering - ISOPE'98*, Montreal, The Int. Society of Offshore and Polar Engineering, Vol. 3, pp. 490-498.

4. Blagoveshchensky, S.N., 1962, *Theory of Ship Motions*. Dover Publications, Inc., New York, Vol. 2.

5. Wright, J. H. G., Marshfield, B. W., 1980, Ship Roll Response and Capsize Behavior in Beam Seas. *Trans. RINA*, Vol. 122, pp. 129-148.

6. Haddara, M.R., Bennett, P., 1989, A Study of the Angle Dependence of Roll Damping Moment. *Ocean Engineering*, Vol. 16, pp. 411-427.

AKNOWLEDGMENTS

This Research has been developed with the financial support of the Italian National Research Council under Contract 97.03187.CT07.

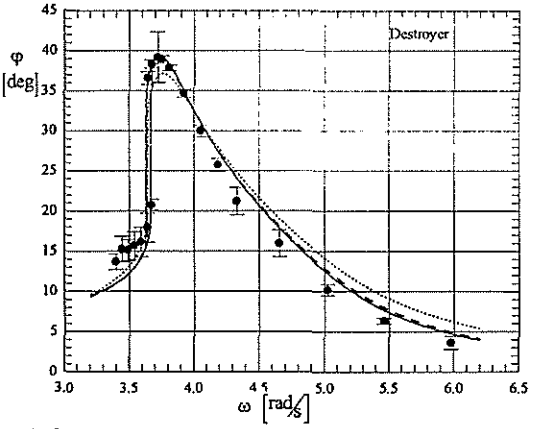

Figure 1. Steady roll amplitudes of a scale model of a destroyer in a regular beam sea. [● experimental data; ——— (eqns 9, 8.1); ····· (eqns 9, 8.2); – – – – (eqns 9, 8.3)].

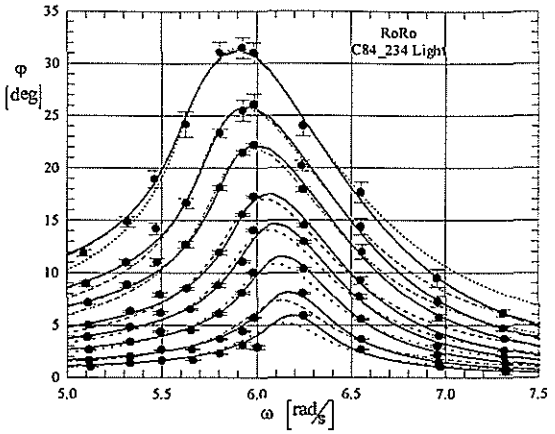

Figure 2. Steady roll amplitudes of a scale model of a RoRo (C84_234 Light) in regular beam sea. [● experimental data; ——— (eqns 9, 8.1); ····· (eqns 9, 8.2); — — — (eqns 9, 8.3)

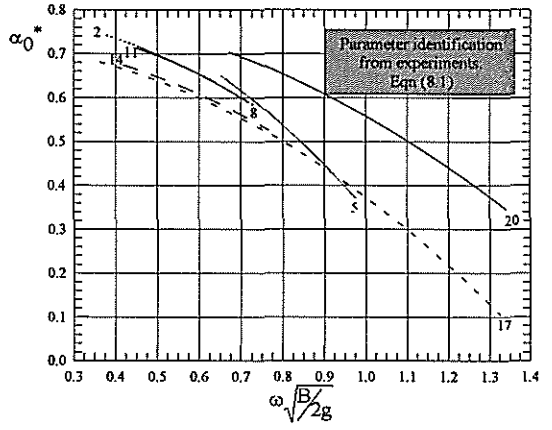

Figure 3. Effective wave slope coefficient α_0^* derived by PIT from eqn (8.1) versus the non-dimensional wave frequency for the different ship models (see Table 2 for curve labels).

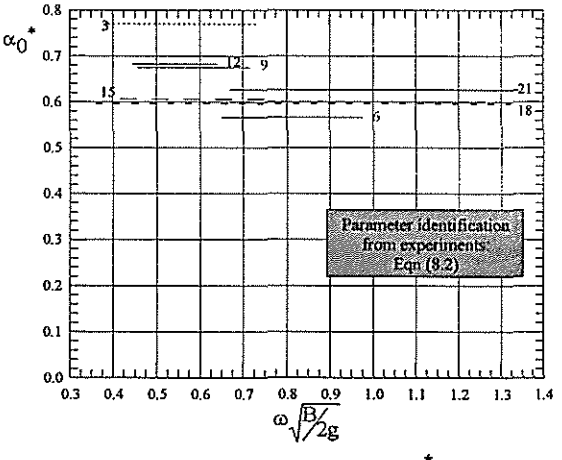

Figure 4. Effective wave slope coefficient α_0^* derived by PIT from eqn (8.2) versus the non-dimensional wave frequency for the different ship models (see Table 2 for curve labels).

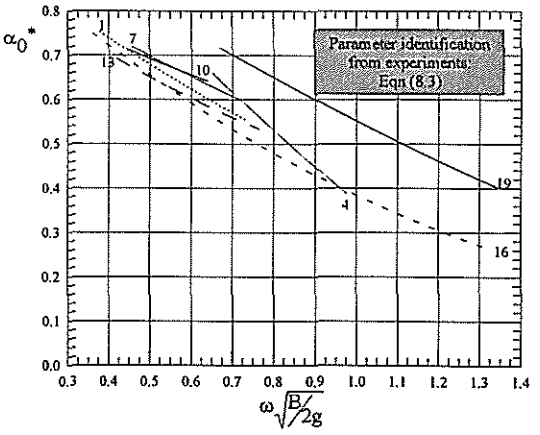

Figure 5. Effective wave slope coefficient α_0^* derived by PIT from eqn (8.31) versus the non-dimensional wave frequency for the different ship models (see Table 2 for curve labels).

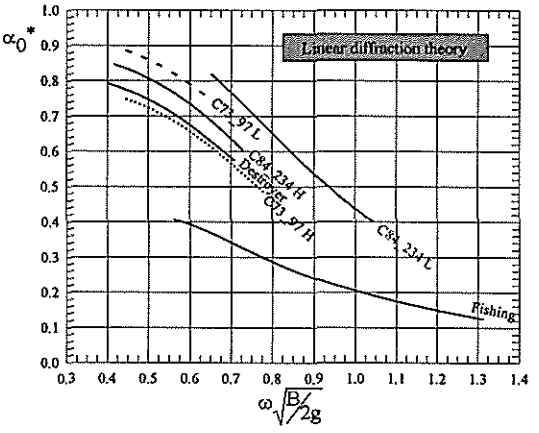

Figure 6. Effective wave slope coefficient α_0^* from a linear diffraction code (strip theory) versus the non-dimensional wave frequency for the different ship models.

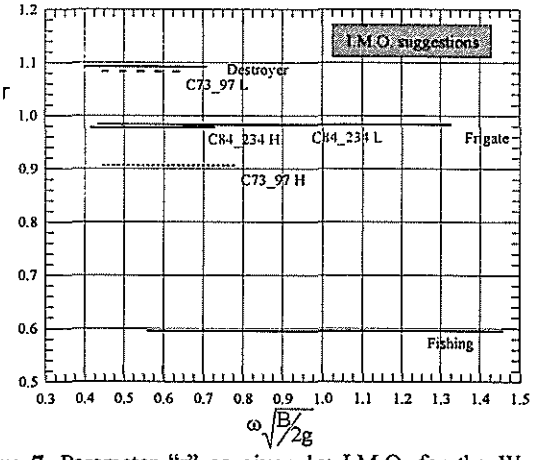

Figure 7. Parameter "r" as given by I.M.O. for the Weather Criterium versus the non-dimensional wave frequency for the different ship models.

Table 1.

	Destroyer C83_227	Frigate C84_236	Fishing C86_253	RORO (A) C73_97		RORO (B) C84-234	
Lpp [m]	2.532 ± 0.001	2.400 ± 0.001	2.000 ± 0.001	2.464 ± 0.001		1.752 ± 0.001	
B [m]	0.273 ± 0.0005	0.285 ± 0.0005	0.552 ± 0.0005	0.380 ± 0.0005		0.333 ± 0.0005	
Scale	1:50	1:50	1:12.5	1:50		1:30	
LOADING CONDITION				LIGHT	HEAVY	LIGHT	HEAVY
Displacement Δ [N]	262.4 ± 0.2	253.0 ± 0.2	1243.5 ± 0.2	464.3 ± 0.2	605.2 ± 0.2	251.3 ± 0.2	316.06 ± 0.2
T [m]	0.0800 ± 0.0005	0.0810 ± 0.0005	0.2450 ± 0.0005	0.0970 ± 0.0005	0.1175 ± 0.0005	0.0800 ± 0.0005	0.0950 ± 0.0005
Trim [m]	0.0000 ± 0.0005	0.0000 ± 0.0005	0.0000 ± 0.0005	0.0000 ± 0.0005	0.0000 ± 0.0005	0.0000 ± 0.0005	0.0000 ± 0.0005
$\overline{KG}$ [m]	0.1083 ± 0.0005	0.1155 ± 0.0005	0.1900 ± 0.0005	0.1541 ± 0.0005	0.1521 ± 0.0005	0.1130 ± 0.0005	0.1350 ± 0.0005
$\overline{GM}$ [m]	0.0217 ± 0.0005	0.0289 ± 0.0005	0.1020 ± 0.0005	0.0320 ± 0.0005	0.0384 ± 0.0005	0.0660 ± 0.0005	0.0330 ± 0.0005
Natural frequency ω_0 [rad / s]	4.6045 ± 0.005	5.020 ± 0.005	5.240 ± 0.005	3.696 ± 0.005	4.217 ± 0.005	6.296 ± 0.005	4.379 ± 0.005
Wave frequency. range ω [rad / s]	3.30 ≤ ≤ 6.00	3.79 ≤ ≤ 10.80	4.22 ≤ ≤ 7.82	3.27 ≤ ≤ 4.42	3.49 ≤ ≤ 5.24	5.10 ≤ ≤ 7.31	3.62 ≤ ≤ 5.29
Nondim. frequency range $\omega\sqrt{B/2g}$	0.39 ≤ ≤ 0.71	0.46 ≤ ≤ 1.30	0.71 ≤ ≤ 1.31	0.46 ≤ ≤ 0.62	0.49 ≤ ≤ 0.73	0.66 ≤ ≤ 0.95	0.47 ≤ ≤ 0.69
Wave steepness Sw	1/30	1/20	1/125, 1/50	1/90, 1/50, 1/30	1/30, 1/20	1/300, 1/200, 1/125, 1/90, 1/70, 1/50, 1/40, 1/30	1/300, 1/200, 1/125, 1/90, 1/70, 1/50, 1/40, 1/30

Table 2.

Ship model	Load cond.	Resid.	Damping model			Excitation model				Restoring					
		χ^2	μ	δ_1 quad.	δ_2 cubic		α_1	α_2	r (IMO)	GZ	ω_o	a3	a5	a7	a9
Destroyer		0.03239	0.3050	0	0	expo	10.011	1.051	**1.092**	FRT	**4.6045**	**-56.498**	**182.04**	-305.52	213.508
		0.03532	0.3131	0	0	quad	0.800	0.120	**1.092**	FRT	**4.6045**	**-56.498**	**182.04**	-305.52	213.508
		0.07123	0.3464	0	0	const.	0.7701	0	**1.092**	FRT	**4.6045**	**-56.498**	**182.04**	-305.52	213.508
RoRo C84_234	Light	0.0070	0.1216	0.1630	0	expo	7.688	1.426	**0.9826**	PIT	6.216	-26.104	48.770	0	0
		0.0070	0.1251	0.1649	0	quad	0.8759	0.3478	**0.9826**	PIT	6.218	-27.00	52.167	0	0
		0.0122	0.1728	0.1249	0	const.	0.5662	0	**0.9826**	PIT	6.1599	-23.87	46.61	0	0
	Heavy	0.01104	0.0746	0	0.0613	expo	10.9736	0.9870	**0.9775**	FRT	**4.379**	**3.799**	**-15.248**	**0**	**0**
		0.01096	0.0752	0	0.0614	quad	0.8001	0.1331	**0.9775**	FRT	**4.379**	**3.799**	**-15.248**	**0**	**0**
		0.01274	0.0775	0	0.0616	const.	0.6750	0	**0.9775**	FRT	**4.379**	**3.799**	**-15.248**	**0**	**0**
RoRo C73_97	Light	0.0112	0.0812	0	0.2039	expo	13.422	0.8707	**1.083**	linear	**3.696**	**0**	**0**	**0.**	**0.**
		0.0111	0.0820	0	0.2043	quad	0.7878	0.0986	**1.083**	linear	**3.696**	**0**	**0**	**0.**	**0.**
		0.0121	0.0798	0	0.2031	const.	0.6818	0	**1.083**	linear	**3.696**	**0**	**0**	**0.**	**0.**
	Heavy	0.0032	0.0552	0	0.1740	expo	9.2662	0.9429	**0.9066**	PIT	**4.217**	-16.97	69.76	-48.01	0
		0.0035	0.0576	0	0.1744	quad	0.7365	0.1230	**0.9066**	PIT	**4.217**	-18.28	83.13	-81.27	0
		0.0063	0.0274	0	0.1896	const.	0.6059	0	**0.9066**	PIT	**4.217**	-28.45	188.15	-346.35	0
Frigate		0.00851	0.3918	0	0	expo	8.603	1.086	**0.9834**	PIT	**5.02**	-19.19	-67.80	309.46	-309.50
		0.01027	0.3857	0	0	quad	0.7272	0.1298	**0.9834**	PIT	**5.02**	-25.52	-13.54	156.69	-172.59
		0.01625	0.3620	0	0	const.	0.5961	0	**0.9834**	PIT	**5.02**	-40.02	113.13	-209.07	168.91
Fishing		0.00451	0.1632	0.2514	0	expo	8.5376	1.202	**0.5953**	linear	**5.24**	**0.**	**0.**	**0.**	**0.**
		0.00425	0.1668	0.2517	0	quad	0.8240	0.2058	**0.5953**	linear	**5.24**	**0.**	**0.**	**0.**	**0.**
		0.00807	0.1683	0.2553	0	const.	0.6260	0	**0.5953**	linear	**5.24**	**0.**	**0.**	**0.**	**0.**

PIECEWISE LINEAR APPROACH TO NONLINEAR SHIP DYNAMICS

Vadim L. Belenky[1]

ABSTRACT

The paper considers piecewise linear dynamical system as a model of ship nonlinear rolling and capsizing. Main advantage of the model is a possibility to describe capsizing directly: as a transition to oscillations near upside down stable equilibrium. Such a transition can be expressed in analytical functions that allows to derive symbolic solutions for both regular and irregular seas. Practical application of the model concerned estimation of beam seas ship capsizing probability per unit of time.

The proposed paper, however, does not deal with stochastic matters. The following consequence was reproduced. Free undamped roll motions were studied, a dependence of free period vs. amplitude was derived. This figure was used as a backbone curve to obtain approximate solution for steady state forced roll motion by equivalent linearization. Then, using previous result as the first expansion an exact steady state solution was derived. The last figure allows to analyze motion stability; it was and found that the system is capable for both fold and flip bifurcations. Deterministic chaos was observed as a result of period doubling sequence. Also it was found that safe basin of the piecewise linear system experiences erosion as conventional nonlinear system. So, general behavior of piecewise linear system was found identical to conventional nonlinear one: even two ranges of piecewise linear term (triangle GZ curve in positive stability range) was enough for observe above nonlinear phenomena and all the solutions were expressed in analytical form without any simulation procedures.

INTRODUCTION

There is a dual purpose for ship capsizing study: developing rational stability regulation and physical knowledge of phenomenon. The second one is necessary to be ready for new types of ship and ocean vehicles.

It seems that probabilistic approach might be the most important for future regulation development, having in mind stochastic character of wind / wave environment. Physical nature of capsizing as «a transition to motion near another stable (upside down) equilibrium» is a nonlinear phenomenon and can be studied by means of nonlinear dynamics.

A capsizing model is an outcome of this study. Adequacy is the main requirement. Another requirement is a usability for regulation purposes, including possibility of application of probabilistic approach.

MODELS OF CAPSIZING

Mathematical models of capsizing can be classified as follows:

- Energetic approach that is the background of weather criteria;
- Motion stability of steady-state rolling (Wellicom,1975), (Ananiev, 1981), (Nayfeh, 1986), Virgin (1987)
- Classical ship stability definition or separatrix crossing model, (Sevastianov,1979), (Umeda 1990)
- Safe basin or transient behavior approach (Rainey, 1990), (Falzarano, 1990)
- Piecewise linear approach, (Belenky, 1989)

The recent development of the last one is a subject of our consideration. We will be concentrated mainly on adequacy, advantages and drawbacks of this model.

[1] National Research Institute of Fisheries Engineering, Japan

BACKGROUND OF PIECWISE LINEAR MODEL

We consider the simplest model that contains capsizing as «...a transition to stable equilibrium, dangerous from practical point of view» (Sevastianov 1982), so we should have at least two stable equilibria: upright and upside down, see fig.1:

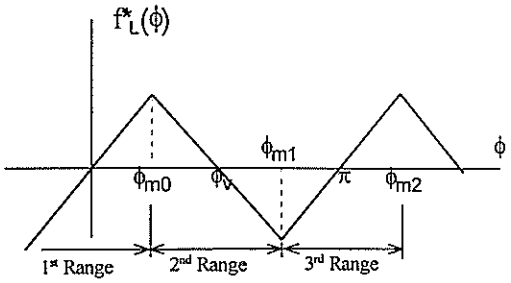

Figure 1 - Piecewise linear model of GZ curve

A differential equation of ship rolling, corresponding to this model:

$$\ddot{\phi} + 2\delta\dot{\phi} + \omega_\phi^2 f_L^*(\phi) = \alpha_E \omega^2 \sin(\omega t + \varphi_E) \qquad (1)$$

Here: ϕ-roll angle, δ-damping coefficient, ω_ϕ-natural frequency, ω-excitation frequency, α_E-effective excitation amplitude, φ_E-initial phase angle. The motion is described by two linear solution linked by initial conditions at junction points:

$$\phi = \begin{cases} \phi_{0a} e^{-\delta t} \sin(\omega_0 t + \varepsilon) + q_a \sin(\omega t + \beta_q) \\ A e^{\lambda_1 t} + B e^{\lambda_2 t} + p_a \sin(\omega t + \beta_p) \end{cases} \qquad (2)$$

where A, B, ϕ_{0a}, ε - arbitrary constants depending on initial conditions at junction points, λ_1, λ_2 - eigenvalues, ω_0 - frequency of initial free damped roll motions.

There is no way to simplify this model further, otherwise we shall get rid of capsizing as we defined it above.

What is good about this model, besides its simplicity?

ADVANTEGES AND DRAWBACKS

Capsizing Description

Early study of piecewise linear model of capsizing (Belenky 89) and (Belenky 93) showed that capsizing will happen if the value of arbitrary constant A (if λ_1 is positive) becomes positive. The solution at the 2nd linear range becomes unbounded and reaches the 3rd linear range that describes oscillation near upside down position of equilibrium. If this value is negative, then the solution will be back to the 1st range, and capsizing will not happen at leas at this semi-period of rolling. So the piecewise linear model offers clear criteria for immediate capsizing - sign of arbitrary constant A that is determined by formula:

$$A = \frac{(\dot{\phi}_1 - \dot{p}_1) - \lambda_2(\phi_1 - p_1)}{\lambda_1 - \lambda_2} \quad , \qquad (3)$$

where $\phi_1, \dot{\phi}_1$ - are initial condition at junction point ϕ_{m0} and $p_1, \dot{p}_1$ are values of partial solution at the moment of crossing level ϕ_{m0}.

Probabilistic Approach

Another important advantage of the model is a very easy way to apply probabilistic approach: probability of capsizing is just a probability of upcrossing (that is very well studied in stochastic processes) with positive value of the arbitrary constant:

$$P_T(X) = P_T(\phi > \phi_{m0}) P(A > 0) . \qquad (4)$$

The probability of upcrossing is connected with time (since upcrossings are Poisson flow), which makes entire probability of capsizing dependent on time of exposure. The last figure is essential for correct probabilistic approach to ship stability regulation see (Sevastianov, 1982) or (Sevastianov ,1994)

Accuracy Control

Piecewise linear model can be used not for analytical study but as simulation tool as well. Algorithm contains the following steps:

1. Find the range where given point is;
2. Calculate next point with the given time step.
3. If the next point is within the same range, repeat step 2 until changing range or end of simulation.
4. If the next point in within the next range, find crossing time and crossing initial conditions. Then calculate the next point using the solution on the next range.
5. Repeat step 2 until changing range or end of simulation.

The algorithm has only one iteration procedure - crossing time search. It is numerical solution of nonlinear algebraic equation. Its accuracy can be checked easily - we just substitute crossing time into solution (2). All other steps involve calculation of elementary trigonomentric and exponential functions that can be done really accurate nowdays (at least error is known in advance).

So, even working with high amplitudes, we are still able to control accuracy and error accumulation.

Practical Applicability

Practical using of the piecewise linear model for calculation of capsizing probability in beam seas and wind was found to be possible as well, see details in (Belenky 94) and (Belenky 95). Practical applicability was reached by using of «combine» model of the GZ curve, see fig2.

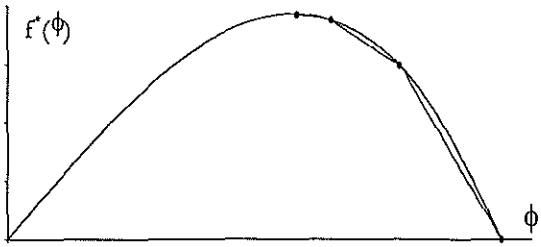

Figure 2 - «Combined» model

Known Problems

Stability in beam seas is just a part of the problem In order to obtain a real practical solution it is necessary to take into account changing GZ curve in following and quartering seas. «Brute force» attempt is senseless: if linear coefficients of piecewise linear term are dependent on time harmonically (the simplest case of regular following seas), the expression (1) becomes Mathew equation range wise, that does not have general solution expressed in elementary functions. So fully analytical solution will be not available, and all other advantages of piecewise linear model would vanish.

The problem can be solved in pure stochastic manner, using whole probability formula, see (Belenky 1997). However, this solution cannot satisfy, because of difficulties of inclusion of other degrees of freedom. In author's opinion, the most perspective way is to consider two- and multy- dimensional piecewise linear term.

Another problem is general adequacy. It is clear, that behavior of «combined system» (fig. 2) approximates real ship rolling. However it is not clear if the system (1) is capable for the same nonlinear phenomena that conventional rolling equation. So far only capsizing behavior was similar.

So we cannot proceed with the simplest piecewise linear model (that only makes a sense because of simplicity) unless we make sure that all nonlinear phenomena, rolling has been known for, could be found in the piecewise linear one too.

NONLINEAR STUDY OF PIECEWISE LINEAR SYSTEM

To prove adequacy of piecewise linear model, we should show, that it is capable for the *same nonlinear phenomena that are known for mathematical model of nonlinear rolling: It would be good if we could reproduce the same sequence of study that was applied to nonlinear rolling since early 1950ies:

- Free rolling is not isohronic: period of free undamped roll motion depends on initial amplitude;
- Response curve of nonlinear forced rolling contains non-functionality: there is an area with several amplitudes corresponding to the same excitation frequency;
- Stability analysis of steady state nonlinear roll motion shows that some regimes are unstable (Wellicome 1975), (Ananiev, 1981);
- This instability leads either to fold (escape through positive real direction) or flip bifurcation (escape through negative real direction) and consecutive period doubling may lead to chaotic response(Nayfeh 1986) (Virgin 1987).
- Dangerous combination of parameters of external excitation looks like erosion of safety basin area (Rainey 1990)

FREE OSCILLATION OF PIECWISE LINEAR SYSTEM

Let's consider first the most simple case of free motion: if there is no bias. If initial amplitude lies within the first range (see fig.1), we have pure linear oscillations: period does not depend on initial conditions - system is isohronic. If the initial amplitude is located within the second range, the period is described by formula from (Belenky 95-a):

$$T(\phi_a)=\frac{4}{\omega_\phi}\left\{\frac{1}{\sqrt{k_2}}\operatorname{arccosh}\frac{\phi_V-\phi_{m0}}{\phi_V-\phi_a}+\right.$$

$$\left.+\frac{1}{\sqrt{k_1}}\arctan\frac{\phi_{m0}\sqrt{k_1}}{\sqrt{k_2}\sqrt{(\phi_V-\phi_{m0})^2-(\phi_V-\phi_a)^2}}\right\} \quad (5)$$

here k_1 and k_2 are angle coefficients of the first and the second range correspondingly, ϕ_V is angle of vanishing stability. As it could be clearly seen, from (5), the period depends on initial amplitude, so the system is not isohronic, if initial amplitude equals to angle of vanishing stability, the period becomes infinite.

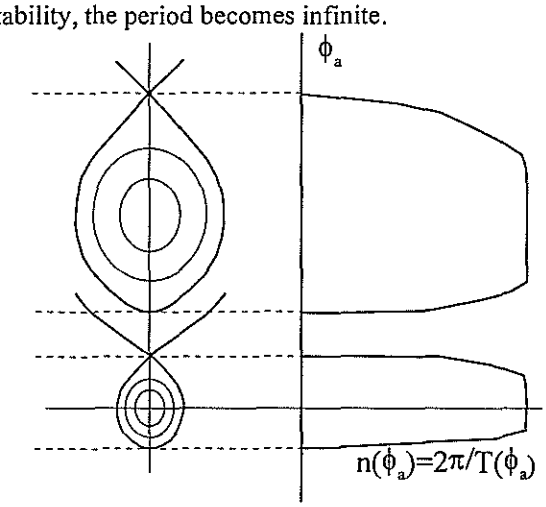

Figure 3 - backbone curve: undamped frequency dependence on initial amplitude and phase plane of free motion of piecewise linear system with bias

If there is bias, the period is expressed by a formulae that are simple but rather bulky see (Belenky 98). Here we show only image of the backbone curve, along with phase plane (build for another equilibrium as well) see fig 3. All phase trajectories can be expressed analytically, however, formulae are rather bulky as well and could be found in (Belenky 98).

The system is definitely not isohronic.

STEADY STATE FORSED MOTION

Equivalent Linearization

Since we have the backbone curve, the next step is evident, we can get approximate solution for steady state force motion using equivalent linearization. It means that we substitute real system by linear one that has the same period of free oscillation. We can do the same procedure with piecewise linear system (Belenky 95-a)

$$\phi_a = \frac{\alpha_E}{\sqrt{\left[\left(\omega_\phi(\phi_a)\right)^2 - \omega^2\right]^2 + 4\delta^2\omega^2}} \qquad (6)$$

Appearance of the approximate response curve is show in fig 4. Phase curve can be calculated analogously.

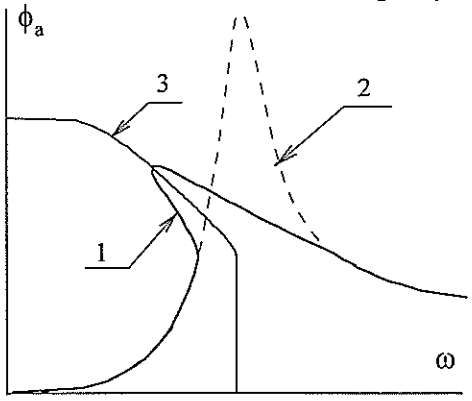

Figure 4- Response curve of piecewise linear system by equivalent linearization (1), response curve of linear system at the first range (2) and backbone curve (3) α_E=0.2, ϕ_{m0}=0.5, δ=0.1 s^{-1}, k_1= k_2=1 s^{-2}, ϕ_v=1, bias 0.05

Exact Steady State Solution

Steady state piecewise linear solution consists form fragments of linear solutions (2) as well as transition one. The only difference between transition and steady state solutions are crossing velocities and periods of time spent in different ranges of piecewise linear term. So if we find such figures that provide periodic solution with excitation frequency, steady state problem will be solved, (Belenky 97-a). These conditions can be formalized as a system of simultaneous algebraic equations, if we look at unbiased case first, it is enough to consider just half of period:

$$\begin{cases} f_0(T_0, \dot\phi_0, \varphi_0) = \phi_{m0} \\ \dot f_0(T_0, \dot\phi_0, \varphi_0) = \dot\phi_1 \\ f_1(T_1, \dot\phi_1, \varphi_0 + \omega T_0) = \phi_{m0} \\ \dot f_1(T_1, \dot\phi_1, \varphi_0 + \omega T_0) = -\dot\phi_0 \\ T_0 + T_1 = \pi \cdot \omega^{-1} \end{cases} \qquad (7)$$

Here functions f_0 and f_1 are solutions (2) at the first and second ranges of the piecewise linear term correspondingly, see also fig.5.

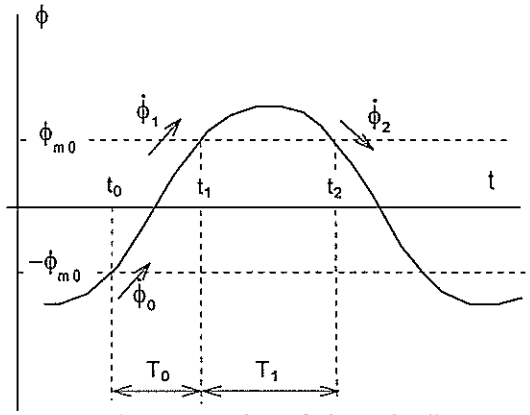

Figure 5-Steady state motion of piecewise linear system

The system (7) can be solved relative to unknown values T_0, T_1, $\dot\phi_0, \dot\phi_1$, and φ_0 using any appropriate numerical method. Results of equivalent linearization can be used for calculation of initial values of the unknown values, that makes calculations more fast and simple.

Biased case is more complicated. Main difficulty here is not only to consider entire period of motion, here we meet so-called «cross mode problem» Asymmetry caused by bias may affect on number of crossings per period: it is not necessary four as fig. 5 shows; period can contain two crossings as well. So considering biased steady state motions (that is especially important for further bifurcation analysis), we need to know in advance how much crossing will be hosted by one period. It can be done by searching frequency that provides «two crosses and one touch»; we use the system analogous to (7), that has excitation frequency as unknown value as well, see details in (Belenky 98). Resulting response curve is shown in fig. 6

As it could be seen from figure 6, response curve has quite conventional form, including hysteresis area, where three amplitudes corresponds to one excitation frequency.

We call this steady state solution exact despite numerical method was used to calculate crossing characteristics; accuracy is still controllable: we always can substitute these figures into system (7) and check how solution turns equations into equalities.

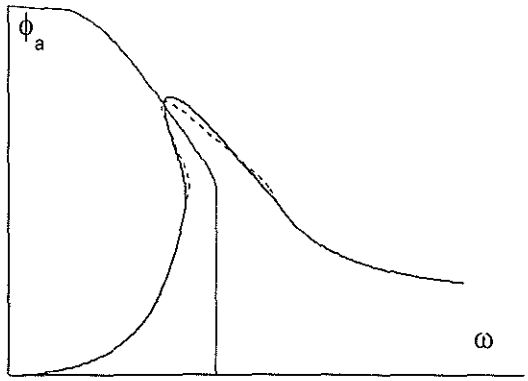

Figure 6- Exact response curve of piecewise linear system. (dotted line shows response of linearized solution) α_E=0.2, ϕ_{m0}=0.5, δ=0.1 s^{-1}, k_1= k_2=1 s^{-2}, ϕ_v=1, bias 0.05

We can call this steady state solution analytical (or, at least semi-analytical), despite the numerical method was used; solution still defined by formulae (2), so we still can manipulate it analytically.

MOTION STABILITY AND BIFURCATION ANALYSIS

The next conventional step is the motion stability determination. Analogous problem was considered in (Murashige 1998) for piecewise nonlinear system. We also will search stability indicators as characteristics of Jacobian matrix (eigenvalues and trace-determinant)

So we calculate Jacobian matrix for each range. The resulting Jacobian can be calculated as a product of the above, with regard on cross mode:

$$J_{4cross} = J_3 \cdot J_2 \cdot J_1 \cdot J_0 \quad (8)$$

$$J_{2cross} = J_1 \cdot J_0 \quad (9)$$

Partial derivatives of Jacobian matrix should be calculated numerically. Analytical expression for these figures are not available, because formulae (2) cannot be inverted in elementary functions.

Results of motion stability calculation are shown in figures 7 and 8.

Figures 7 and 8 indicates presence of unstable steady state regimes, fold and flip bifurcations. Let's examine them more close.

We get three responses in the hysteresis area, one of them is pure linear or trivial, so it is definitely stable. Two piecewise linear response were obtained from the same system of equation (like (7) depending on cross mode) using two different initial points. One of these initial points corresponds to high amplitude response of equivalently linearized solution; another one is from the middle one. The middle solution is unstable, the high one - stable see fig 9.

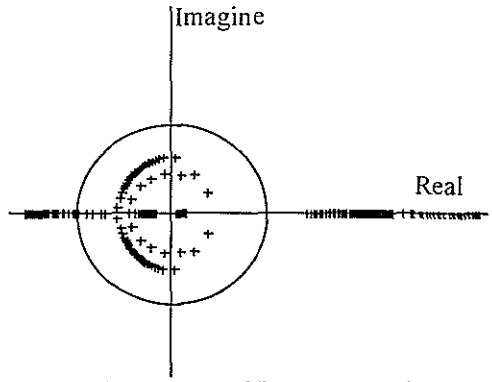

Figure 7. - Eigenvalues of Jacobian matrix of biased piecewise linear system

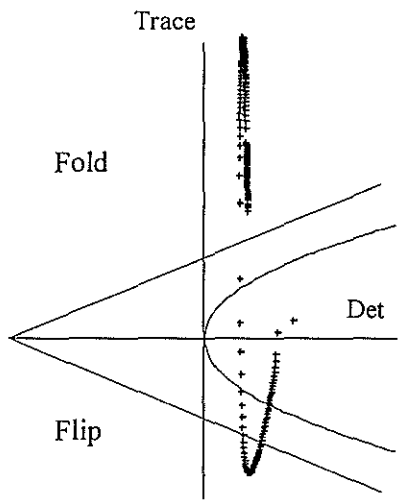

Figure 8 - Trace -determinant plane of Jacobian matrix of biased piecewise linear system

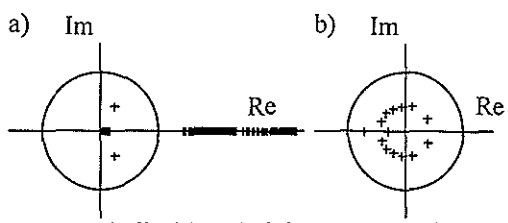

Figure 9 - Middle (a) and high (b) amplitude response stability indexes

Eigen values escape unit circle through positive direction, what is an indication of fold bifurcation. To see it of phase plane, we should reproduce unstable steady state regime and then disturb it in eigen vectors direction: the system will «jump» towards to stable mode, see figure 10. Such type of behavior exactly the same in piecewise linear and nonlinear systems.

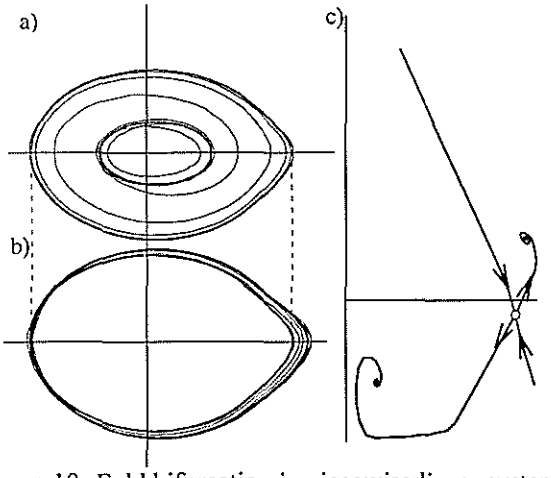

Figure 10- Fold bifurcation in piecewise linear system: «jump down» (a), «jump up» (b), invariant manifold (c), ω=0.77

Another possible type of nonlinear behavior is flip bifurcation: sequence of period doubling, see fig.11 leading to deterministic chaos, fig 12.

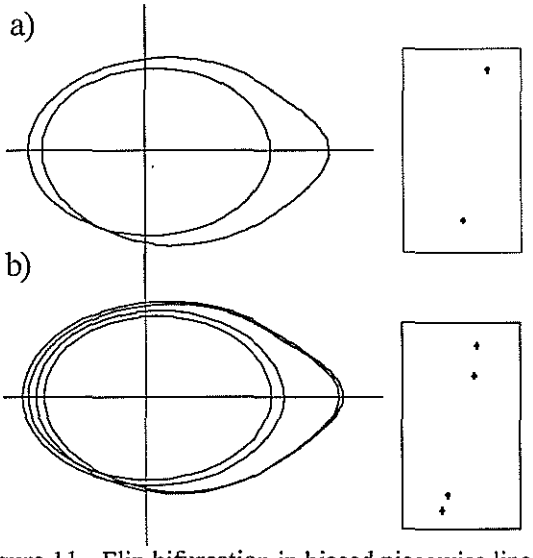

Figure 11 - Flip bifurcation in biased piecewise linear system: phase trajectories and Poincare maps, (a) ω=0.99 (b) ω=0.97.

Form of phase trajectories of piecewise linear system is very similar to conventional nonlinear ones: nothing indicates piecewise linear origin of figures 10-12.

Concluding motion stability and bifurcation analysis we can state that piecewise linear system is capable for such nonlinear type of behavior as motion instability leading to bifurcations; moreover, it is possible to use conventional tools for nonlinear analysis of piecewise linear system.

Flip bifurcation was also found for unbiased piecewise linear system (Belenky 98).

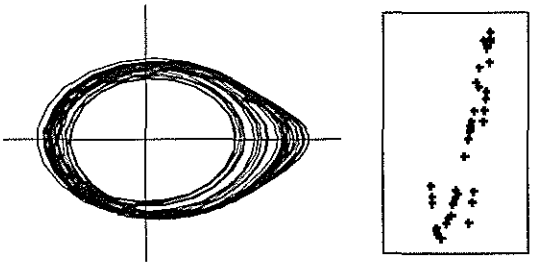

Figure 12 Deterministic chaos in piecewise linear system. ω=0.92439

SAFE BASIN ERROSION

Another important nonlinear quality of severe ship rolling is erosion of safe basin (Rainey ,1990), (Falzarano, 1990). Relative area of the safe basin was considered as stability criteria in (Rainey 1990).

We check if the piecewise linear system is capable for this type of behavior. Calculation were carried with the resolution 90x90 for a square: $\pm 1.5 \cdot \phi_V \times \pm 1.5 \cdot \phi_V \cdot \omega_\phi$.

Excitation frequency was used as a control parameter. All other parameters were the same as for above samples. Some of the results are shown on fig.12.

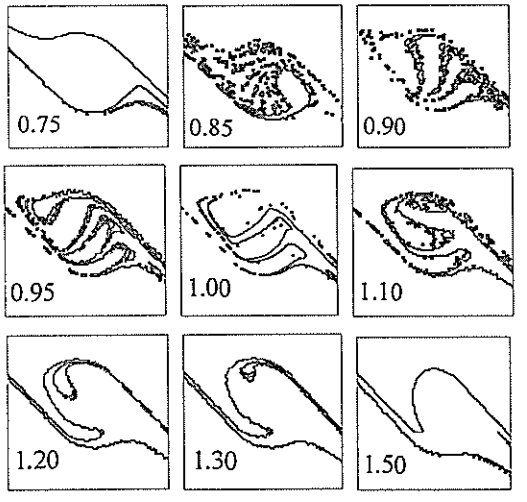

Figure 12 - Erosion of safe basin of piecewise linear system

The results are summarized in a form of dependence of the safe basin relative area on excitation frequency:

$$S_R(\omega) = \frac{A_{SB}(\omega)}{A_{SB}|_{\alpha_E=0}} \qquad (10)$$

Here: $A_{SB}(\omega)$ - area of the safe basin at given frequency, $A_{SB}|_{\alpha_E=0}$ - area of safe basin of free damped motion; see fig.13.

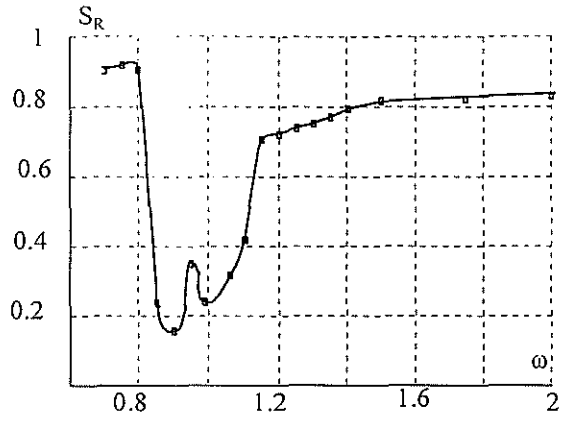

Figure 13- Relative safe basin area vs. excitation frequency.

As it could be clearly seen from figures 12 and 13, the safe basin of piecewise linear system experiences erosion, that leads to decreasing of its area. This behavior is similar to conventional nonlinear one.

FINAL COMMENTS: ADEQUACY OF PIECWISE LINEAR MODEL

The above study has shown that:

- Free motion of piecewise linear system is not isohronic; period of undamped free oscillations depends on initial amplitude (initial heel angle);
- Equivalent linearization can be applied to approximate characteristics of steady state motion of the piecewise linear system;
- Exact characteristics of steady state motion can be calculated using the only assumption that this motion is periodic; exact steady state motion can be expressed by elementary functions, however, some of parameters are results of numerical solution of a system of simultaneous algebraic equations
- Response curve of a piecewise linear system (both approximate and exact) contains non-functionality (or hysteresis): an area where three amplitudes correspond to one frequency;
- Conventional stability analysis can be applied to a piecewise linear system.
- Piecewise linear system is capable for fold and flip bifurcations, consecutive flip bifurcation leads to deterministic chaos in piecewise linear system.
- Safe basin of piecewise linear system experiences erosion, when waves become dangerous.

Since a piecewise linear system is capable for conventional nonlinear behavior it is adequate tool for qualitative analysis of nonlinear ship dynamics.

ACKNOWLEDGMENT

Contents of this work is partially based on research funded by Science and Technology Agency of Japan, STA fellowship Id No 269115 and carried out at National Research Institute of Fisheries Engineering (NRIFE). Help of Dr. Naoya Umeda (NRIFE) was very fruitful and highly appreciated.

REFERENCES

Ananiev, D. On stability of forced rolling motion with given stability diagram, Trans. of Kaliningrad Technical Institute "Seakeeping of Ships", Kaliningrad, 1981, Vol. 93, pp. 17-25 (in Russian).

Belenky, V.L. A new method of statistical linearization in severe rolling and capsizing problem, Proc. of 18th SMSSH, Varna 1989

Belenky, V.L. A capsizing probability computation method, Journal of Ship Research, Vol. 37, No. 3, Sept. 1993

Belenky, V.L. Piece-wise linear methods for the probabilistic stability assessment for ship in a seaway, Proc. of 5th STAB Conference, vol. 5, Melbourne, Florida, 1994

Belenky, V.L. Analysis of probabilistic balance of IMO stability regulation by piece-wise linear method, Marine Technology Trans. of Academy of Science, Gdansk, 1995.

Belenky, V.L. 1995-a On the dynamics of piecewise linear system Proc. of Int. Symp. on Ship Safety in a Seaway: Stability, Manoeuvrability, Nonlinear Approach (SEVASTIANOV SYMPOSIUM), vol.1, Kaliningrad, 1995

Belenky, V.L. On capsizing risk function estimation due to pure loss stability in quartering seas, Proc. of 6th International Conference on Stability of Ships and Ocean Vehicles (STAB'97), Vol.1,Varna 1997

Belenky, V.L., 1997-a Some problems of Stochastic Dynamics of Piecewise Linear and Nonlinear Systems, Seminar at Naval Architecture Department., University of Michigan, Ann Arbor, Mich.13 March

Belenky, V.L Dynamics of Multiple Equilibria Piecewise Linear System, Dynamical Brainics Seminar, Aihara Laboratory, Department of Mathematical Engineering and Information Physics, University of Tokyo, 18 June 1998

Falzarano J.M. Predicting complicated dynamics leading to vessel capsizing. Ph.D. Dissertation, Naval Architecture Department, The University of Michigan, Ann Arbor, Mich., June 1990

Murashige, S., Komura, M, and Aihara,K. Nonlinear roll motion and bifurcation of a ro-ro ship with flooded water in regular beam seas. R. Soc., 1998, in press

Nayfeh, A.H., Khdeir, A.A. Nonlinear rolling of biased ships in regular beam waves, International Shipbuilding Progress, Vol. 33, 1986, p. 84.

Rainey, R.C.T, Thompson, J.M.T., Tam, G.W. and Noble, P.G. The transient capsize diagram - a route to soundly-based new stability regulations, Proc. of 4th STAB Conference, Naples, 1990

Sevastianov N.B. and Fam Ngock Hoeh Boundary between the domains of stable and unstable free ship motion in drift-rolling regime, Trans. of Kaliningrad Technical Institute "Seakeeping of Fishing Vessels", Kalininrgad, 1979, Vol. 81, pp. 17-25 (in Russian)

Sevastianov N.B. Probabilistic stability regulation as a problem of reliability theory, *Trans. of Register of the USSR,* Vol.12, Leningrad, 1982, PP. 94-100, (in Russian).

Sevastianov N.B. An algorithm of probabilistic stability assessment and standards, Proc. 5th STAB Conference, Melbourne, Florida, 1994

Umeda, N., Yamakoshi, Y., Tsichiya T. Probabilistic study on ship capsizing due to pure loss of stability in irregular quartering seas. Proc. 4th STAB Conference, Naples, 1990.

Virgin, L.N., The nonlinear rolling response of a vessel including chaotic motions leading to capsize in regular seas, Applied Ocean Research Vol.9, No.2, PP.89-95, 1987

Wellicome, J. An analytical study of the mechanism of capsizing, Proc. 1st STAB conference, Glasgow, 1975

4TH INTERNATIONAL STABILITY WORKSHOP
STABILITY AND OPERATIONAL SAFETY OF SHIPS
St, John´s, Canada, September 1998

Full Scale Trials - An Important Element in the Research on High Speed Ship Performance in Following Seas.

Olle Rutgersson
Dept. of Naval Architecture, KTH
Stockholm, Sweden
Royal Institut of Technology

Summary

Studies of stability problems in following waves for high speed monohulls will be carried out as a joint Finnish and Swedish research program sponsored by the Navies in the two countries. The program will be started by extensive full scale studies where the behaviour in following waves will be characterised by oscillation tests.
It is proposed to use some test procedures originally used to characterise calm water manoeuvring performance of ships. The procedures will be slightly modified and it is anticipated that the results might be used as the measure of the ability of the ships to stay on course in following waves and thereby avoiding the risk for broaching.
The test results will also be used for validation of mathematical models being developed for theoretical studies of the behaviour described.

Introduction

Work on research and development on broaching and other undesired behaviour of ships in following seas are often focused towards the risk for capsize. However ship behaviour in following seas can be dangerously detoriated without having a direct risk for capsize. Especially the reduced maneouvring performance for a ship entering a harbor or a narrow passage into an archipilago when approaching from the open sea in following waves is of great concern to many operators.

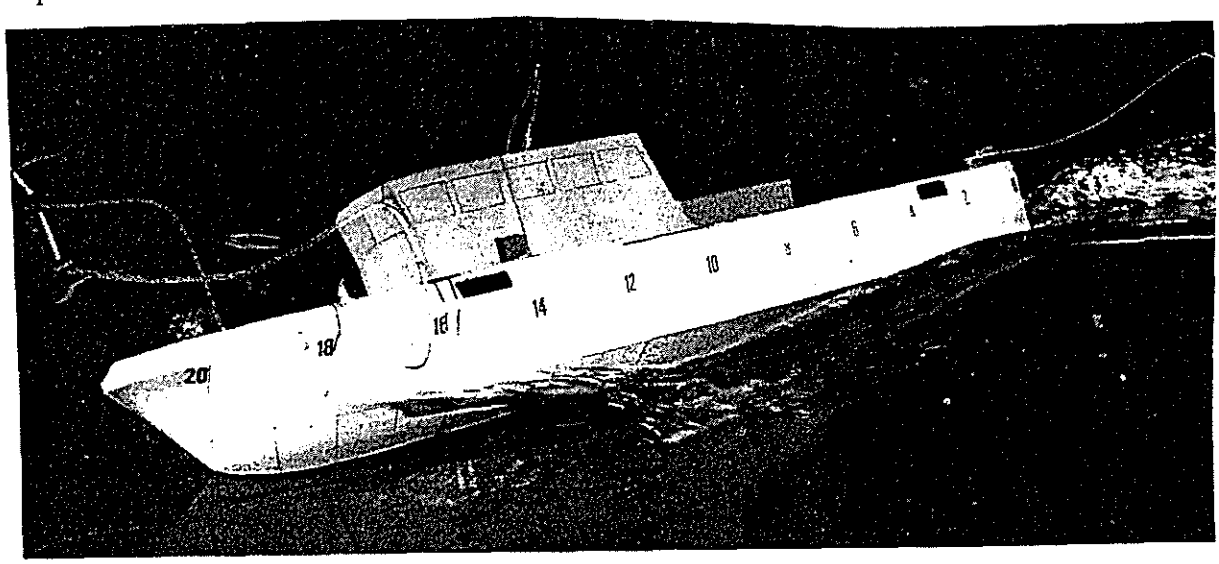

Figure 1. Model of patrol craft broaching in stern quartering waves.
(From Rutgersson and Ottosson 1987)

In the Baltic Sea, high-speed monohulls with planing and semiplaning hulls are frequently used by the Coast Guards and the Navies in the area. The major seakeeping problems experienced with these vessels are broaching to or resonant rolling phenomena in stern quartering seas. Usually the behaviour is developed as a combined rolling-yawing oscillation which is very unpleasant and which can turn into a situation where the vessel is out of control.

Attempts to develop mathematical tools and experimental techniques to study the risk for broaching is an ongoing international process reported in earlier Stability Workshops and Conferences (Renilson 1982, Umeda 1996 and Vassolos 1997). In the Nordic countries earlier work have been carried out by SSPA in cooperation with the Swedish Navy (Rutgersson and Ottosson 1987).

A new research project is now initiated in Finland and Sweden. The aim is to develop practical operational and design oriented criteria and tools for studies of high-speed monohulls in following sea conditions. The work will be joinly sponsored by the Finnish and the Swedish Navies and carried out by SSPA and KTH in Sweden and VTT in Finland. The project will start with an extensive fullscale trials program. The reasons for this are threefold:

* the practical experience of the operators when handling these vessels in following sea conditions can then be included in the study.
* attempts will be made to develop a trial technique in fullscale where the margin against resonant rolling and broaching to phenomena, may be determined by oscillation tests in fullscale.
* the test results will be used to define problems to be studied in the more theoretical part of the project. Access to test results for validation of the developed tools is of course also important.

An interesting part in the present project is that two major types of vessels will be studied. The first vessel is the somewhat larger "coastal corvette" type where the major problem is the classical broaching to phenomenon in open sea. The other and smaller type of vessels more often experience the resonant rolling phenomenon in stern quartering seas (Hua 1997).

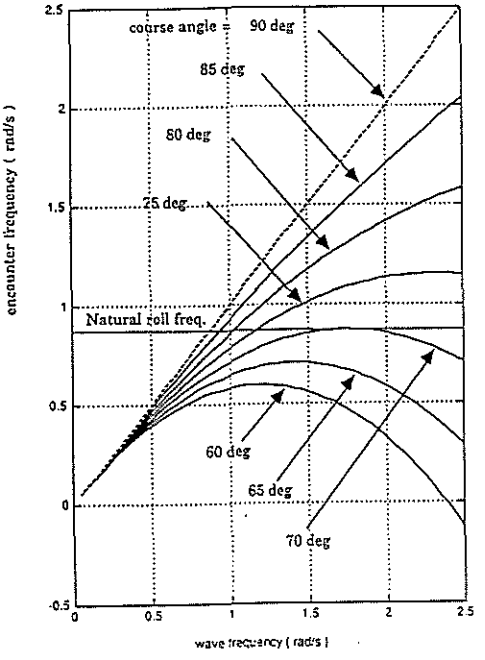

Figure 2. Focusing effect exciting resonant rolling on ships in quartering waves. (Hua 1997)

At the full scale tests it is intended to use procedures to actively oscillate the ships in waves and thereby having the possibility to receive more information than is usually done from normal straight course tests. The test procedures will be presented and discussed.

Proposed Tests.

In the test program ships with potentially good and bad behaviour in following waves will be used. Portable measduring systems using a Saetex MRU-6 sensor giving motions in all six degrees of freedom will be used together with a GPS registration of the track, a measurement of the rudder angle and probably a wave bouy registration of the wave environment.

Test procedures for three different "broaching tests" have been worked out:

* straight course test
* zigzag test
* reversed spiral test

Straight course test.

The test is a simulation of realistic conditions where the helmsman (or autopilot) tries to keep the ship on course at a desired speed and heading in following waves. From the time signals the variations in heading angle, roll angle and speed can be recorded at different wave -heights, -lengths, ship speeds and heading for the typical rudder action used on board. From practical point of view condensation of these data will form valuable information for the master of expected behaviour of the ship in following seas.

It is not anticipated that real broaching situations where the ship cannot be brought back on course will occur during the limited time span for these tests. These tests therefore probably cannot give very reliable information on the real risk for broaching.

Zigzag test.

The zigzag tests represents a popular calass of tets where the ships manouevring characteristics are determined on free running models or in full scale in oscillation manoeuvres simulating the behaviour of a ship trying to stay on course inspite of external disturbancies. It is thertefore believed to be a suitable test for characterising the risk for broaching on ships in following waves. The procedure of the test is: from a steady course and speed condition starboard rudder to a predetermined angle is given, when the course change up to an also predetermined angle is reached a counteraction with port rudder is given. An oscillatory motion is then going on as long as counteracting rudder motions are given. A typical view of a zigzag test and the measured parameters are given in Fig 3 from Brix 1993. Overshoot angle and timelag are two parameters representative of the manoeuvring capacity of the ship.

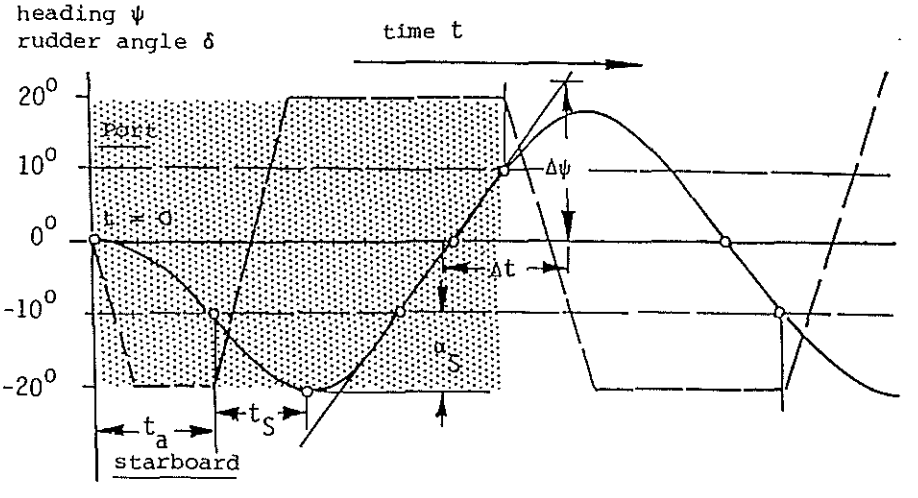

Figure 3. Zigzag test and typical parameters. (Brix 1993)

Carrying out zigzag tests in calm water the period of the oscillations will be determined by the period of the ship in yawing motion. When carrying out the same tests in following waves the ship based period will be influenced by the encounter period of the waves and in conditions close to broaching the wave encountering period will be driving the motions.

In conditions in following waves the helmsman will probably use fairly large rudder angles. It is therefore suggested to use large rudder angles also for the zig zag tests. On the other hand it might be dangerous to use large angles of course changes before giving counter active rudder angles. A typical suggested zigzag test therefore would be a 20 / 10 degrees test.

The phase lag between the ship motions and the waves will be imporatant for the exact ship response to the exiting rudder action. It is therefore proposed to run these tests for as many wave encounters as possible. The tests will be run in different shipspeeds and wave conditions from calm water up to waves where the proposed rudder angle is no longer enough to keep the ship on course.

The results can be given as overshoot angles and time lags for different wave conditions and operating conditions for the ship. The combination of conditions where the used rudder angle are not enough to stay on course is one indication where the risk for broaching might be large. It is also anticipated that analysis of the over shoot angles and time lags can be used to determine some kind of margin against broaching for different operational conditions.

Reversed spiral test.

As the zigzag test is believed to simulate the initial conditions in a broach, another test is also needed where the ability to stop a broach is better simulatied. It is suggested that a type of reversed spiral test might simulate this. In a reversed spiral test in calm water the helmsman (or autopilot) tries to keep the ship at a steady turning rate by actively work with the rudder. The results are then prsented as a graph of turning rate as a function of the mean rudder angles. A typical result for an unstable ship is given in Figure 4 from Brix 1993. The width of the unstable area is then a measure of the course keeping ability of the ship in the conditions tested.

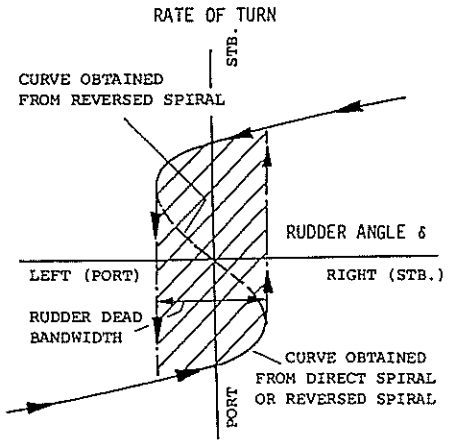

Figure 4. Results from spiral tests for an unstable ship. (Brix 1993)

The proposed spiral tests in following waves will be carried out always starting with zero degrees heading. Starting for instans on a wave crest a starboard turn with constant radius will be initiated and proceeded until 90 degrees heading angle is reached (beam seas). After reaching steady turning conditions in beam seas a port turn at the same turning rate will be carried through until the heading angle zero degrees is reached again. These tests will be repeated with initial turn using starboard and port rudder for as many wave encounters as possible and for different wave and speed conditions covering calm water to waves where dagerous respons is anticipated.

It is believed that the spiral tests will simulate the rolling bahaviour of a broching ship in a more realistic way than the zigzag test and therefore also gives a more realistic view of the possibilities to interupt an initiated broach tha the zigzag test. Comparison of the width of the unsteady rudder area for different wave- and speed conditions probably also will give information about the margin against broaching. With a width close to the maximum possible rudder angle the risk for a real broach must be very large.

Concluding remarks.

As a Nordic continuation of studies of stability problems in following waves for high speed monohulls of the planing and semi planing type an extensive program for full scale tests will be carried out.

It is proposed to use some test procedures originally used to characterise calm water manoeuvring performance of ships. The procedures will be slightly modified and it is anticipated that the results might be used as the measure of the ability of the ships to stay on course in following waves and thereby avoiding the risk for broaching.

The test results will also be used for validation of mathematiocal models being developed for theoretical studies of the bahaviour described.

References

Renilson, M.R.:"An Investigation into the Factors Affectingthe Likelyhood of Broaching-to in Following Seas." STAB 82, Tokyo 1982.

Umeda N. :"Some Remarks on Broaching Phenomena". Second Workshop on Stability and Operational Safety of Ships, Osaka, Japan, 1996.

Vassolos D. et al :"Numerical and Physical Modelling of Ship Capsize in Heavy Seas: State of the Art." STAB 97, Varna 1997.

Rutgersson O., Ottosson P.:"Model Tests and Computer Simulations- An Effective Combination for Investigation of Broaching Phenomena". Trans. SNAME 1987.

Hua J.:"Explanation to a Large Roll Motion Phenomenon in Irregular Waves." STAB 97, Varna 1997.

Brix J.: Manoeuvring Technical Manual". Seehafen Verlag Gmbh, Hamburg, 1993.

Some Effects of Dynamics on Damage Stability

by Dr. Ian W. Dand, BMT SeaTech Ltd, UK.

ABSTRACT

The concept of dynamic stability is introduced in relation to damaged vessel survivability. After comparing dynamic and static stability, some forms of dynamic instability, generally related to vessels with forward speed, are discussed. There then follows a discussion of two relevant series of experiments for damaged ro-ro vessels. The paper concludes with the view that the concept of stability in relation to the survivability of a damaged vessel should not be restricted to transverse stability alone.

INTRODUCTION

One of the most significant advances in recent years in the study of damage stability has been the introduction of dynamics into the analysis. This has been done using physical models to explore and illuminate the problem with the result that computer simulations, (which incorporate our understanding of the physics gained from physical models) are now becoming available.

This recognition of the important role dynamics can play in damage stability heralds a major advance in the study of ship stability. However, like all advances into new fields of endeavour, it brings with it a number of unanswered questions which indicate fruitful areas of further research.

The purpose of this paper is to mention some of these areas, illustrated by the result of recent work carried out at BMT. First, however, the general notion of dynamic, as distinct from static, stability must be mentioned

DYNAMIC AND STATIC STABILITY

The terms dynamic and static stability are used throughout this paper.

By **static stability** is meant the tendency of a body to return to its original condition after being perturbed.

By **dynamic stability** is meant the tendency of the body to return to its original motion after a perturbation.

A vessel which is statically stable could be, for example, an intact vessel which, when heeled to an angle returns to the upright because of the hydrostatic restoring moment due to buoyancy. Static stability is a well-known concept and forms the basis of most calculations of ship stability at the design stage. Note that no motion is considered in static stability; once the motion of the vessel, as it rolls back to the upright, is introduced, dynamic stability comes into play.

Many restoring forces and moments exist in the world of dynamic stability, but that which limits roll motion (as distinct from the main driving force of buoyancy) is primarily that of damping. This may be of viscous origin and, when present, allows the roll motion to die away gradually until the equilibrium, upright, position is regained.

The theme of this paper therefore, is to look at the effects of motion – dynamics – in connection with damage stability and to see how such effects can modify conclusions drawn from a slavish adherence to information obtained solely from statics.

This is therefore broadening the concept of stability from the narrow idea of static transverse stability, related to capsize, to stability of the vessel in general, with particular reference to the damaged case.

DYNAMIC INSTABILITIES

The advent of high speed passenger-carrying vessels in the waters of the world brings with it the spectre of dynamic instability. If such a vessel is damaged at speed, any ingress of water so caused could result in a catastrophic dynamic instability leading to capsize, sudden stops or "pitch poling". In other words, the speed and motions of the vessel make any sudden change in statics – mass, inertia and attitude – potentially lethal.

The capsize of the "Herald of Free Enterprise" is a frightening testament to this. The amount of water

initially taken on board through the bow doors would almost certainly not have capsized the intact vessel at rest; with the added ingredients of speed and turn a catastrophic capsize resulted.

Various forms of dynamic instability have been identified, many for high speed craft. The ITTC High Speed Marine Vehicle Committee identified some of these and listed them in its report to the 21st ITTC in 1996. The following list gives these, with some additions:

1. **Loss of GM due to Wave System**

If a displacement vessel moves fast enough, its wave system can be characterised by crests at bow and stern combined with a trough amidships. If the hull form is fine enough, the loss of buoyancy and waterplane area caused by the wave trough can cause an apparent loss of transverse GM. The vessel may then loll over to one side or the other.

In some cases this heel may couple into yaw and the vessel begin to turn. The turn may induce further heel, which induces further yaw and so on. Taken to extremes the vessel may suffer a catastrophic heel and turn, leading to capsize.

2. **Course Keeping**

Poor dynamic stability about the vertical axis gives rise at best to poor course-keeping and at worse to loss of control. Although problematic in themselves, these tendencies become more serious from a safety perspective as speed increases. In extreme cases a "calm water broach" can occur if the yaw instability couples into heel.

3. **Bow Diving and Plough-In**

Bow diving and plough-in at wave speed occur when a vessel, moving into or with a wave system, comes off one wave and ploughs into the next. For a high speed passenger ferry carrying vehicles, the need for adequate buoyancy forward (possibly a problem for catamarans with fine forebodies) together with adequate bow door arrangements is essential if the vessel is not to be engulfed.

4. **Porpoising**

Porpoising is a well-known pitch instability which affects high speed planing craft. It is now amenable to elimination by design, but was the cause of catastrophic accidents to some early high speed vessels.

5. **Chine Tripping**

Chine tripping is experienced on planing hard chine monohulls when turning. The chine may dig in and cause a powerful and sudden heeling moment. In extreme cases the vessel could roll over at high speed.

6. **Take Off**

High speed catamarans may experienced large aerodynamic lift forces and pitch moments at speed or in waves. This is caused by air flow over and under the bridge deck which, in extreme cases, could cause the vessel to lift from the water and rotate in pitch. At present such behaviour is confined to high speed, light weight, vessels.

7. **Spray Rail Engulfing**

A high speed vessel receives a not inconsiderable amount of lift forward from the spray rails, which, on some designs, may double as fenders. Tank tests have shown that, once a certain speed is exceeded, these may cease to deflect the bow wave or spray and become engulfed. When this happens the bow may drop, to the accompaniment of large sheets of green water thrown into the air at the bow. Speed may reduce at the same time. In extreme cases bow dive may occur.

8. **Effect of Critical Speed**

Recent tank tests and full scale trials on a high speed passenger catamaran in shallow water have identified loss of directional stability when moving at or near the critical speed. This speed is defined as

$$\sqrt{gh}$$

Equation 1

where h is the water depth and is about the speed at which solitary waves or solitons may be shed and hydraulic jumps created. Whether or not solitons are shed, it is common for the vessel's own wave system to be characterised at such speeds by a high, steep, and often breaking, following wave similar in form to a hydraulic jump. This is situated just astern of the vessel and its upstream influence gives a tendency to broach. This is perhaps analogous to the loss of directional stability experienced by aircraft flying through the transonic speed range and has been felt not only by the present-day vessels in shallow water, but also by high speed torpedo boats passing through a narrow, shallow, harbour entrance at speed in World War 2.

Outstanding Issues with Dynamic Instabilities

Some of the dynamic instabilities identified above have resonances with "conventional" as well as high speed ferries. Instabilities 1 to 3 fall into this category; the added problems caused by damage leading to water ingress at speed are so obvious that they do not need emphasising here.

The remaining instabilities may be dismissed as only pertaining to high speed specialist vessels. Such a dismissal would ignore the trend in modern high speed passenger vessels to push speeds ever higher in both deep and, increasingly, shallow waters.

It would seem therefore that the following issues are outstanding, all of which would benefit from focussed research:

- continue to identify, by means of tank tests and experience, further forms of dynamic instability.

- explore, by means of physical model testing and, later, numerical models, the effect of water ingress through damage openings on such instabilities.
- identify design methods and test techniques which identify and eliminate potential dynamic instabilities at the design stage.
- include linear and angular velocities in numerical capsize prediction models.
- investigate in more detail the physics of the instabilities listed above with a view to eliminating them by design and/or rules of operation.

EFFECT OF FORWARD SPEED ON CAPSIZE

As a gesture towards the thesis of this paper that dynamic effects on damage instability can be of importance, a short series of model experiments was carried out as part of BMT's internally-funded research. The aim was to investigate whether the introduction of a steady forward speed to a damaged model, in stable equilibrium at rest in calm water, could induce instability.

The model used for this was that of the "Pride of Bruges" with a tapered damage opening amidships. The model was run at a range of steady forward speeds in calm water and head waves with two damaged freeboards (each with its corresponding GM) and a note was made of the heel angle.

CALM WATER EXPERIMENTS

Figure 1 shows the results obtained at the small residual freeboard equivalent to 0.25 metres with a corresponding GM of 2.7 metres. Although there was some measurable effect on heel as speed increased, heel angles were extremely small, no water came aboard and transverse stability was not compromised. Observation of the flow showed that the damage opening caused virtually no disturbance to the free stream and there was no evidence of flow transfer between the free stream and the flooded compartment below the subdivision deck.

This experiment indicated that hydrodynamic effects from a "clean" damage opening, fundamental to the usual drifting type of damage stability model tests, were negligible. Clearly in such a situation, where the damage is located amidships, dynamic instabilities will not arise.

But is the clean cut damage opening typical of what actually happens? In a real situation the damage will generally occur when one or both ships are moving, causing the plating of both to tear and buckle. If the ships subsequently break away from each other, especially if both are still moving, further tearing of the hull structure is likely. It is therefore more likely that damage openings in real accidents will be anything but clean and could have flaps of metal hanging in or out of the opening. Furthermore, the vessel will almost certainly not be stopped in the water after break-away and will in all probability be moving, turning and heeling.

This scenario paints a quite different picture to that of the vessel moving at zero drift angle, with a clean damage opening. In order to explore this, a further series of experiments was carried out. In these, the damage opening was modified to incorporate a flap to represent the possible after-effects of torn metal as the ships break apart (Figure 2). The experiment was then repeated, and Figure 3 shows the result.

Over a threshold speed the flow impinging on the flap rose up to enter the subdivision deck, even though the model had a residual freeboard equivalent to 1.0 metre and a GM equivalent to 1.01 metre. Once water had entered the subdivision deck, it gathered on the damage side due to an initial heel angle of 0.1° in that direction. Increasing speed caused more water to come aboard, the heel to increase and the residual freeboard to reduce. Ultimately as speed increased further the subdivision deck became engulfed and the model capsized.

When the experiment was re-run with a 2° drift angle which opened the damage to the on-coming flow, events were even more dramatic and capsize occurred rather more rapidly (Figure 4). The implications of this result were:

- if the damage had been forward at a point where the curve of the hull was equivalent to a 2° (or more) tangent angle, then water would have been taken aboard at zero drift angle.
- if the vessel had been turning after break-away with a drift angle of 2° or more, water would have been induced to flow on to the subdivision deck over a give speed.

EXPERIMENTS IN WAVES

When head seas, equivalent to a height of about 2.1 metres, were introduced into the experiment, water was taken aboard at a speed some 3 knots less than that for calm water and a capsize resulted (Figure 5). Reducing the residual freeboard to 0.25 metres resulted in water coming aboard at all speeds – due to the waves themselves at low speeds and due to the flap and waves at the higher speeds.

CONCLUSIONS

What conclusions, if any, can be drawn from such a brief study? Some do suggest themselves and these are:

1. A clean damage amidships induces no loss of stability due to forward speed in calm water at speeds up to 20 knots.
2. A flap representing torn shell plating which extended beyond the side shell had a major effect in calm water

by causing water to enter the subdivision deck at forward speeds above 10 knots.
3. Head seas increase the chance of water entry and capsize.
4. Drift angles which open the damage to the oncoming flow increase the chance of water entering the subdivision deck with a "flapped" type of damage.

It may be argued that some of these conclusions apply only to forward speeds well in excess of those likely to be experienced by a conventional ro-ro ferry, such as the Pride of Bruges, after breakaway following collision. While this may be true, it may be remarked that high speed ferries, whether monohull or multihull, may well have such high residual speeds after collision.

Outstanding Issues

This work has been of a preliminary, exploratory nature and could be followed up with more detailed studies. These could include:

1. Increase the degrees of freedom to incorporate sway, yaw and heel.
2. Vary the position of the damage opening.
3. Explore the effect of a "scoop" type of damage opening.
4. Determine limiting intact GM values with forward speed.

DYNAMICS OF WATER INGRESS

Dynamic effects are relevant not only to whole body motions, but also to details of the fluid flow at or near the damage location. Details of water ingress or egress have been studied by others elsewhere, but coupling it with the effects of ingress and egress on body motions has received little attention.

Because of this, the UK Marine Safety Agency (now the Marine and Coastguard Agency) funded a research study into the topic to be carried out by BMT under the auspices of the Ship Stability Research Centre at the University of Strathclyde. This provided a valuable opportunity to focus on the details of water ingress and egress at a damage opening confined to the case of a damaged, drifting, vessel.

It was decided at the outset that this study would be driven by a series of specially-designed model experiments, the results of which would both identify, and provide data for, a model of motion damping due to water ingress and egress.

Methodology

In order to measure damping, the use of captive models was necessary. Conventional techniques had to be modified to allow for the fact that the mass, and hence draught, of the model could change throughout a run as floodwater accumulated on the subdivision deck.

This implied that model state would change with time and hence vary throughout a run. This called for an analysis technique which would, if necessary, cater for such variation. One was developed, based on parameter identification and using an assumed regression model, for both intact and damaged cases.

Both heave and roll motion was required because observation of freely-drifting model tests had suggested that heave played as important a part as roll in the physics of water ingress and egress on a damaged model. A system was therefore devised, using computer-controlled hydraulic actuators, which could apply both heave and roll in any desired combination. An advantage of this system was its ability to provide any type of motion rather than be restricted to the purely sinusoidal.

In addition to studying the forces and responses of the captive model, it was felt to be of value to compare water ingress and egress with the same model, but with it free to move when excited by beam waves. Disconnecting the hydraulic actuators achieved this goal.

Damping was measured using the force and moment response of the captive model to a known input motion, while water on deck was measured in the usual way by a series of strategically-placed wave probes. All experiments were recorded by two video-cameras showing water movement on the deck and through the damage opening.

Simple models representing the mid-body only were used, one having a conventional midship section while that of the other was semi-circular. The latter was chosen so that its form damping in roll would be as small as possible.

Results Obtained

Results were obtained for a number of cases involving pure roll, pure heave and coupled heel/roll with the captive model. A range of regular waves was used with the model when free to move.

Damping was found to be best represented by a "linear plus quadratic" model. Figure 6 shows the deduced coefficients for linear form damping of the intact model with a ship-shaped body section, while Figure 7 shows the deduced coefficients for the quadratic component. Figures 8 and 9 show the equivalent coefficients for the damaged case, also indicating the effects of halving the size of the damage opening.

Figure 10 shows a comparison of the deduced quantities of water on deck for similar forced and free motions; it may be noted that the pure roll motion resulted in the least quantity of water build-up.

CONCLUSIONS

The main conclusions of the study were as follows:

1. Side and deck damage do in fact have an effect on the stiffness and damping terms in the equations of motion.
2. Length of side damage has a negligible effect on stiffness, although the shortest length tested appeared to have an effect on quadratic damping terms.
3. Of the motions of roll and heave, the latter appears to be dominant in getting water on the subdivision deck, while the former is helpful in drain-off or trapping on the side remote from the damage if there are no deck obstructions.
4. The motion of the floodwater on deck seemed to have little effect on body motions, other than inducing a mean heel and bodily settlement in the water as the mass of water on deck increased.
5. Wave or motion frequency (as well as amplitude) is important in determining the amount of water which gains access to the subdivision deck.
6. Phasing between heave and roll is important in determining the amount of water on deck.
7. Floodwater egress through the damage opening is similar to weir flow; floodwater ingress is not.

OUTSTANDING ISSUES

The study was revealing, but some issues remained outstanding. Among these were:

1. A full hull damaged model on the motion rig should be used to explore the effect of hull shape.
2. The effect of freeboard, damage position and GM on the stiffness and damping terms, should be explored.
3. Integrate the additional stiffness and damping model into numerical flooding/capsize models.

CONCLUDING REMARKS

This paper has promoted the thesis that dynamic stability, in its many forms, should be the foundation upon which questions of damage and survivability should be built. This implies that considerations of the survivability of ro-ro vessels (for example) should not be confined solely to consideration of transverse stability. The advent of lightly-built high speed passenger-carrying vessels to the waters of the world demands that our horizons for their safety be broadened. No longer will traditional design methods, rooted in statics, be satisfactory for such vessels, especially if they are damaged. The behaviour of the vessel in the immediate post-collision phase may be crucial to their survivability.

The time is right for a new approach.

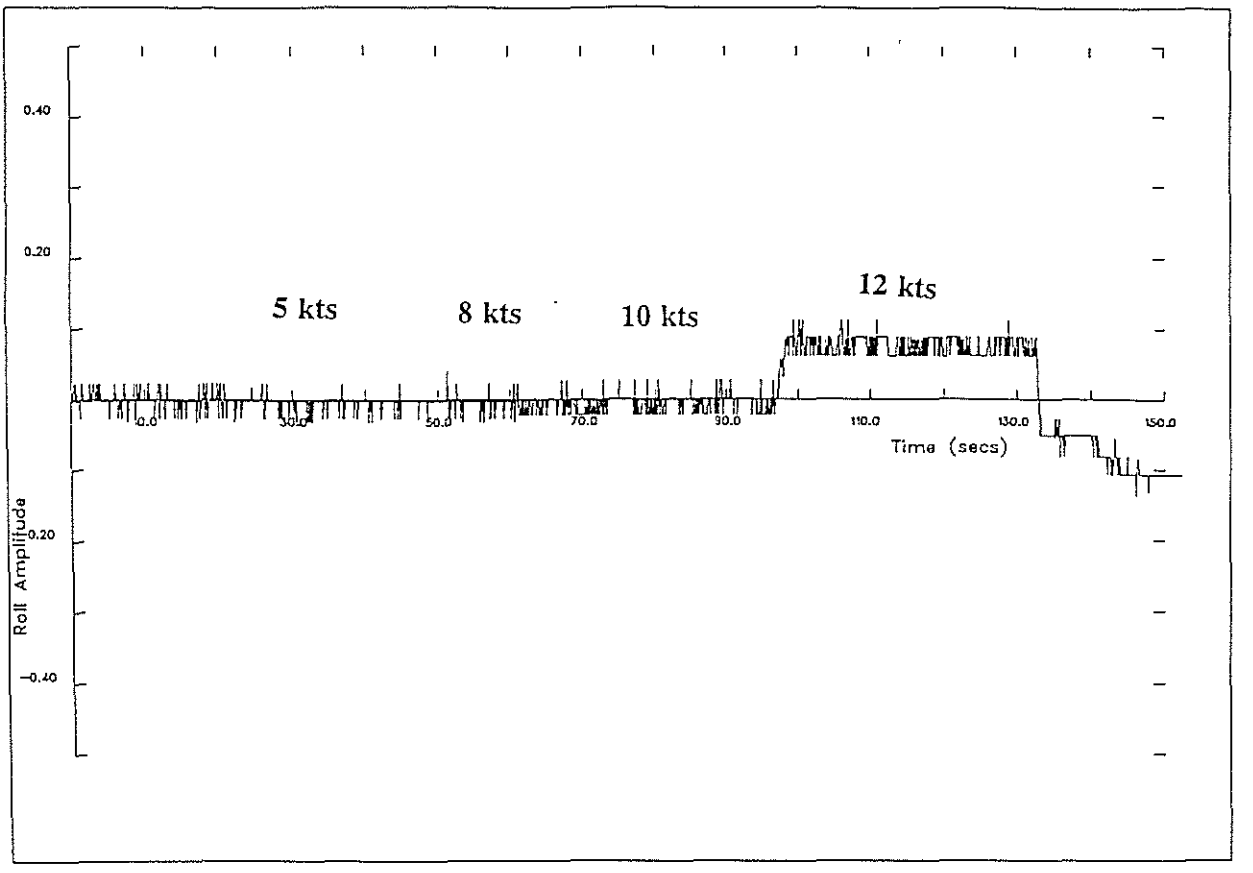

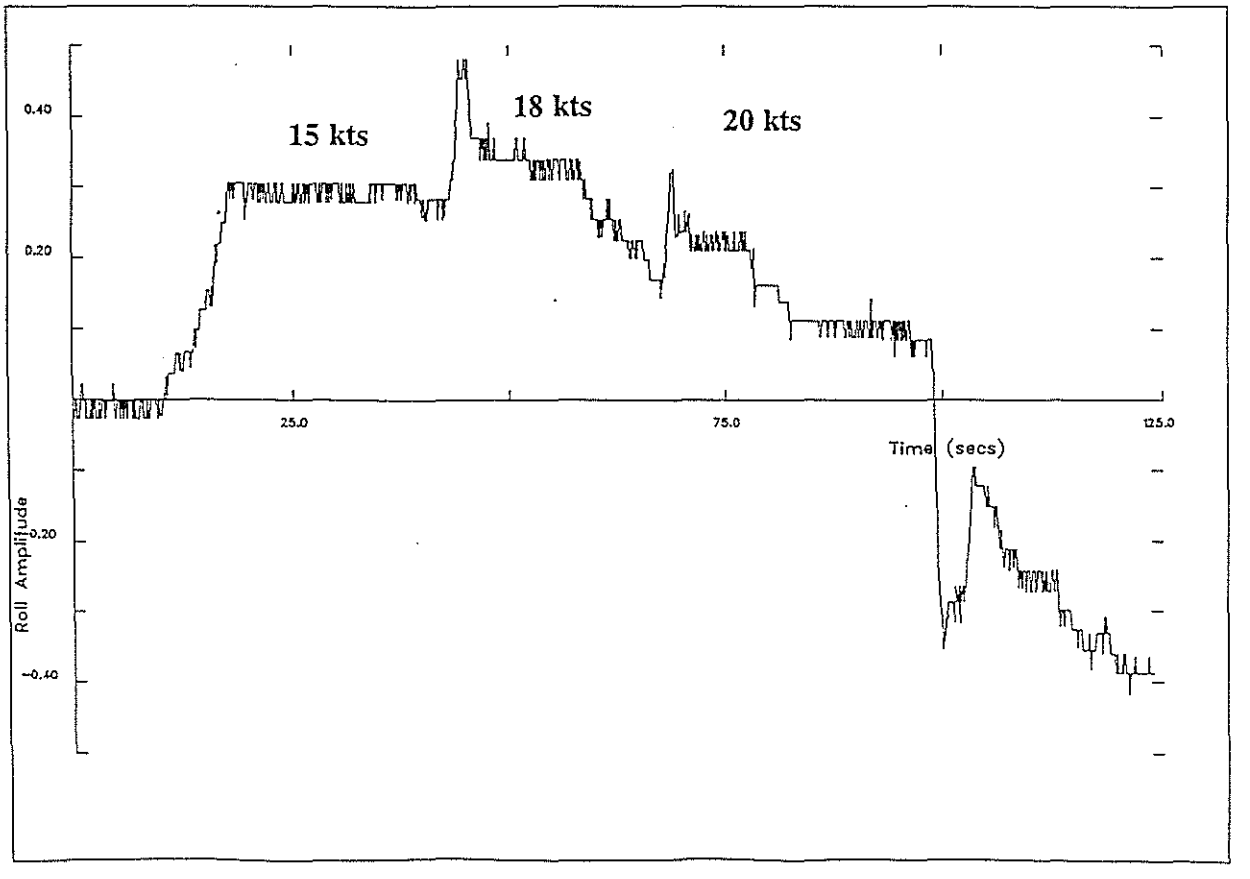

Figure 1. Measured Heel Induced by Forward Speed - Clean Damage Opening

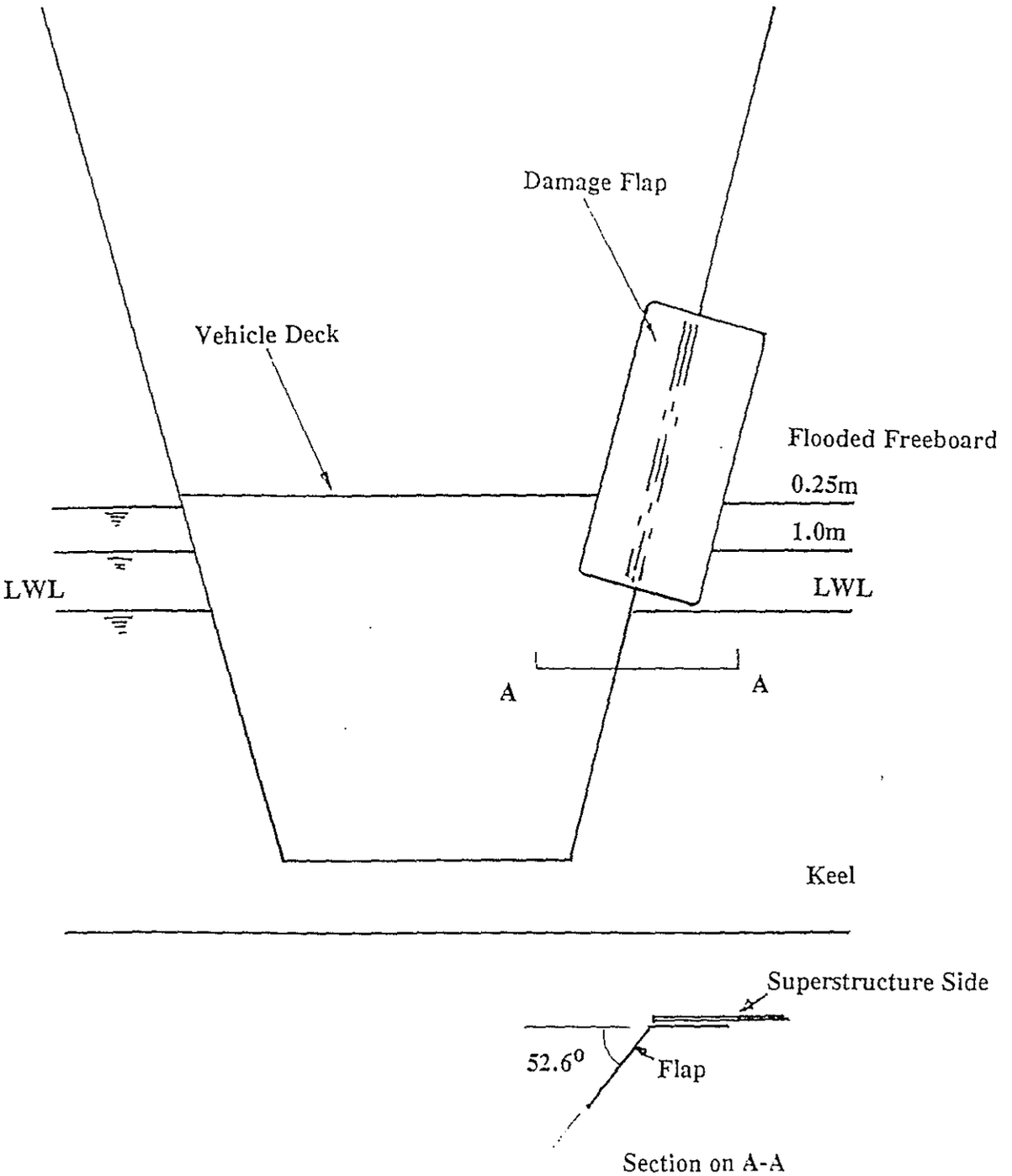

Figure 2. Damage Flap Configuration

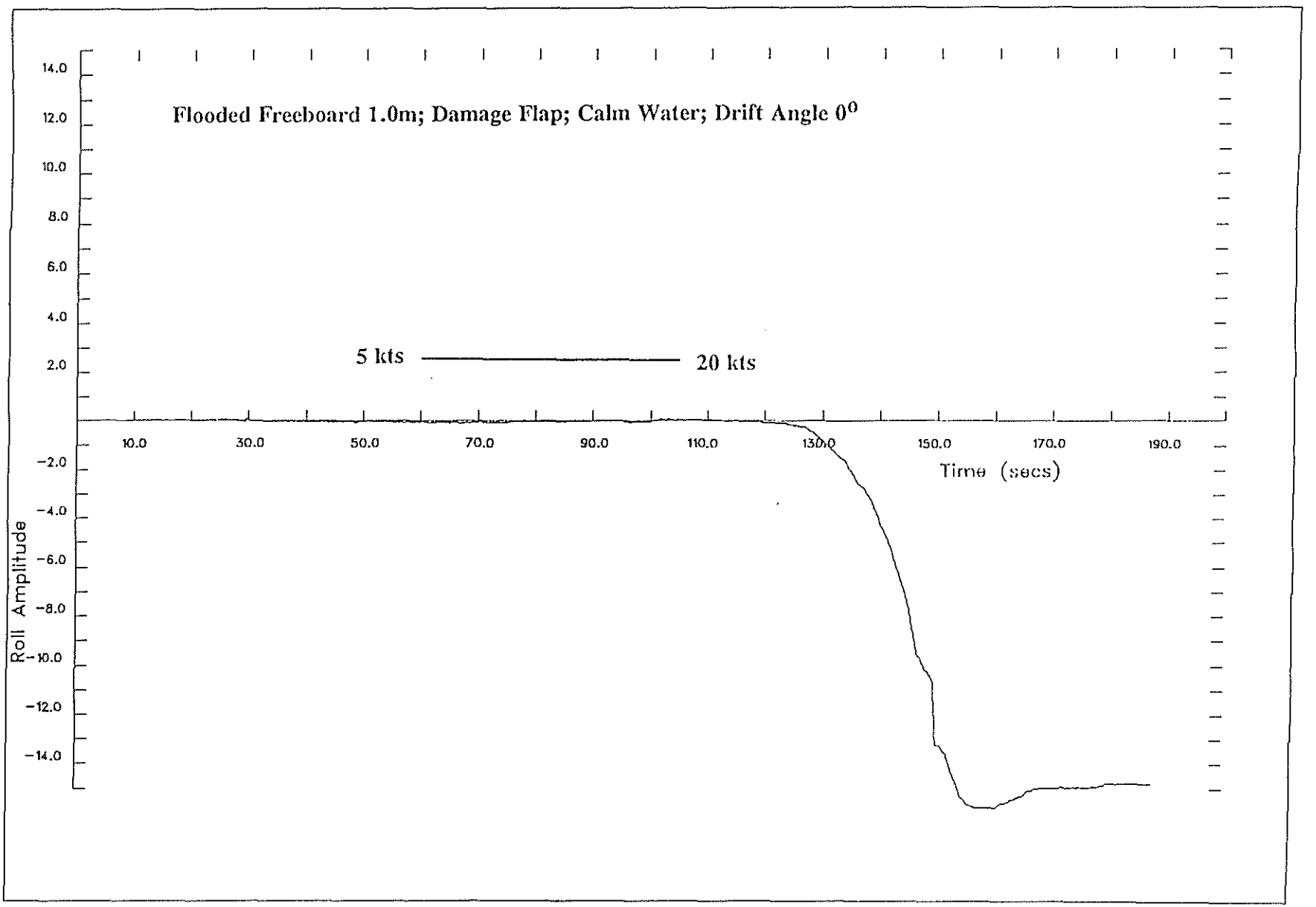

Figure 3. Measured Heel Induced by Forward Speed - Effect of Flap

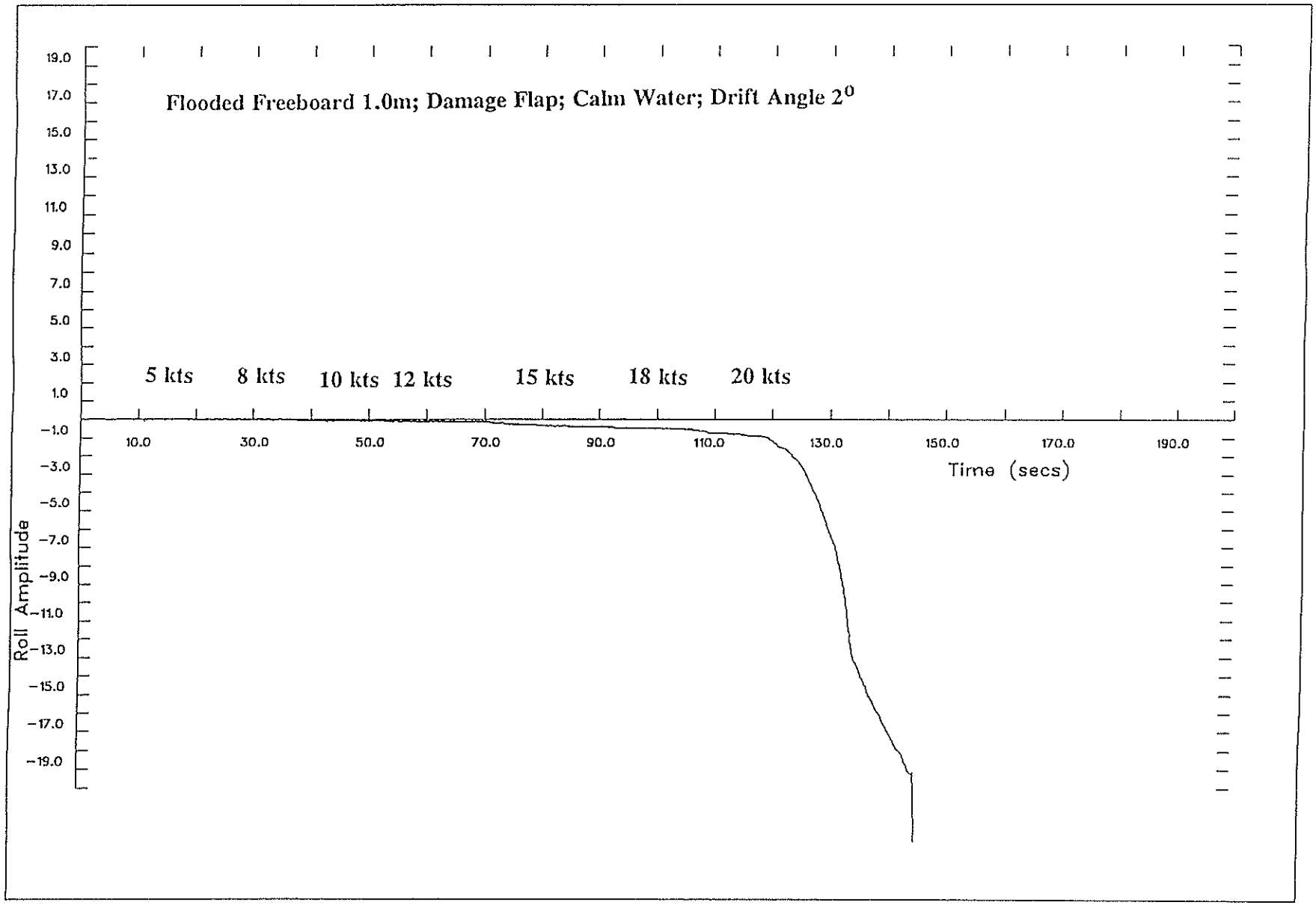

Figure 4. Measured Heel Induced by Forward Speed

- Effect of Flap and Drift Angle

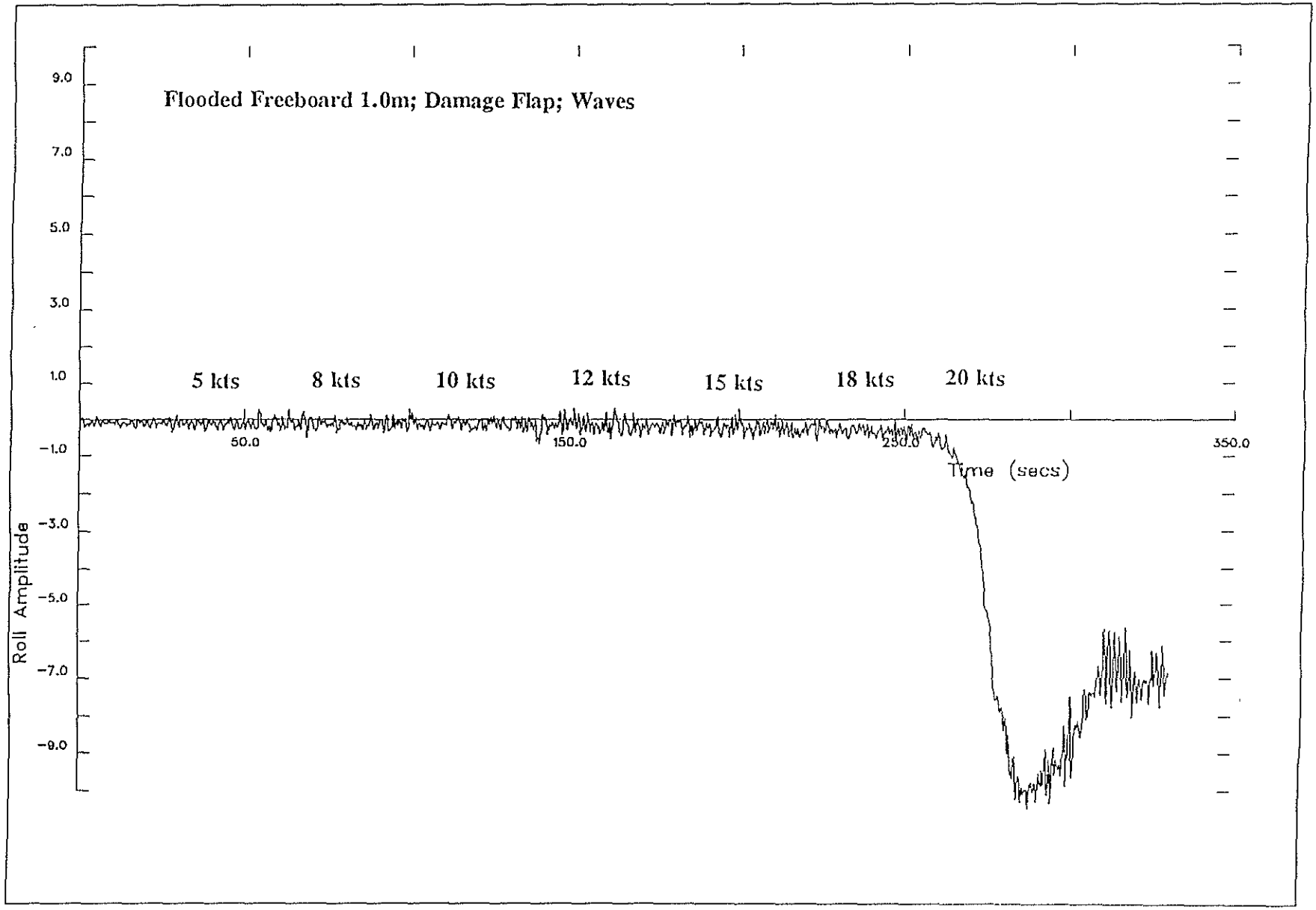

Figure 5. Measured Heel Induced by Forward Speed - Effect of Head Waves

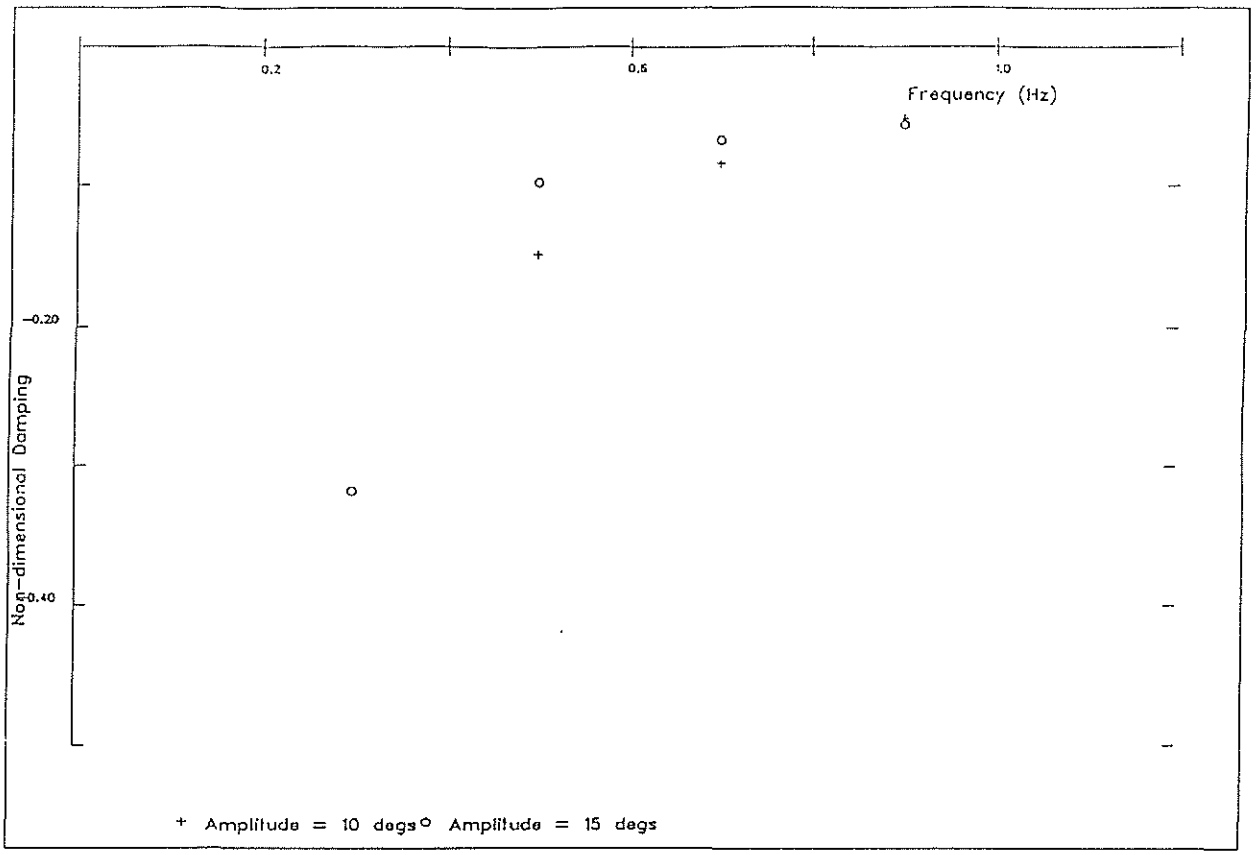

Figure 6. Deduced Linear Damping Coefficient in Forced Roll - Intact, Ship Section

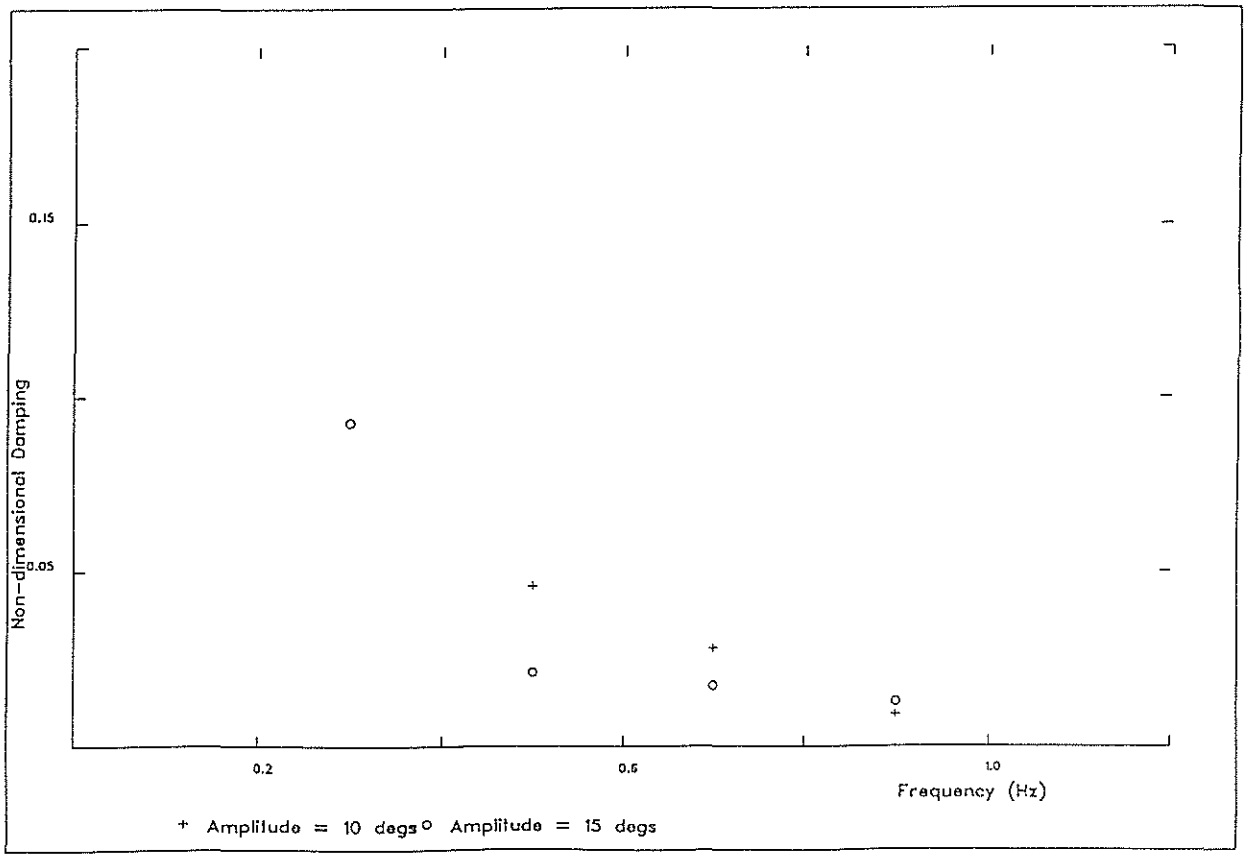

Figure 7. Deduced Quadratic Damping Coefficient in Forced Roll - Intact, Ship Section

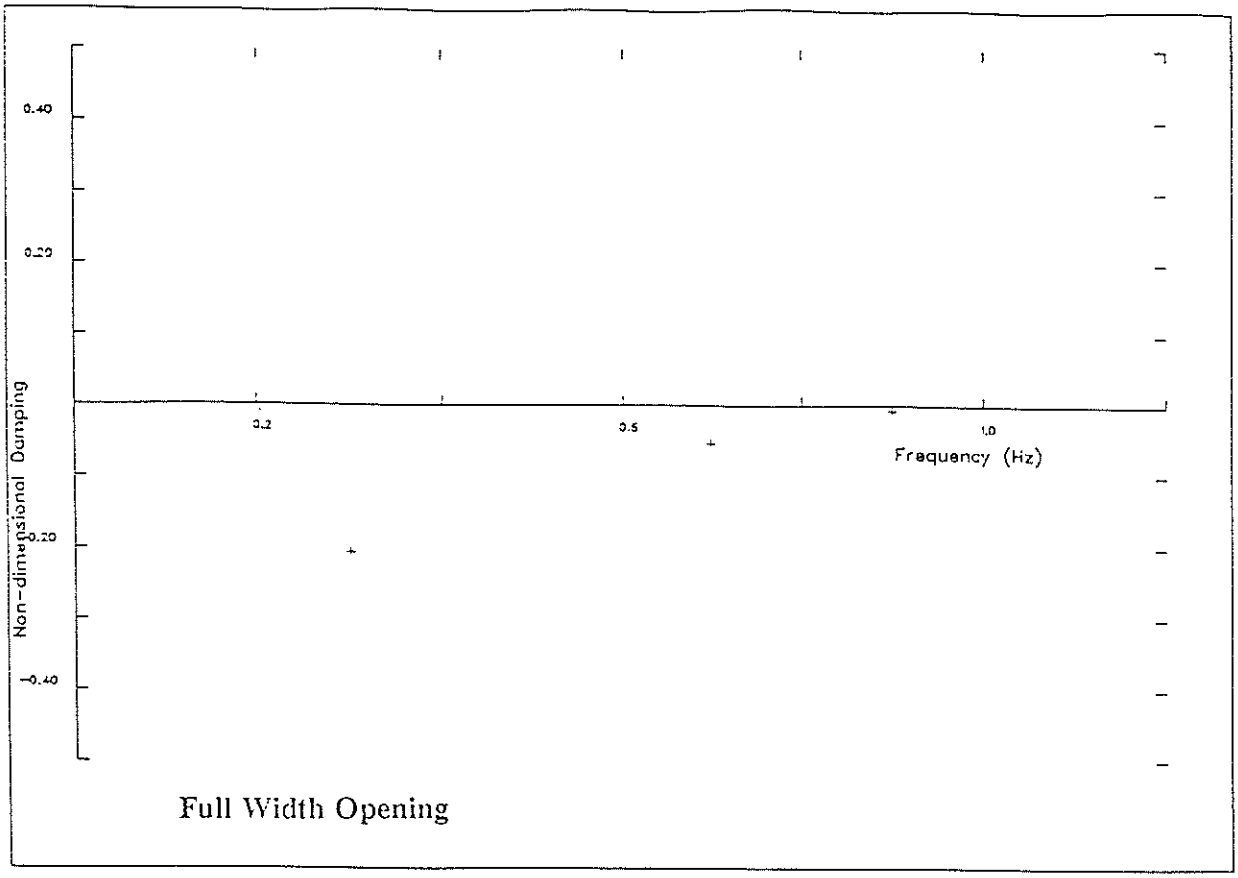

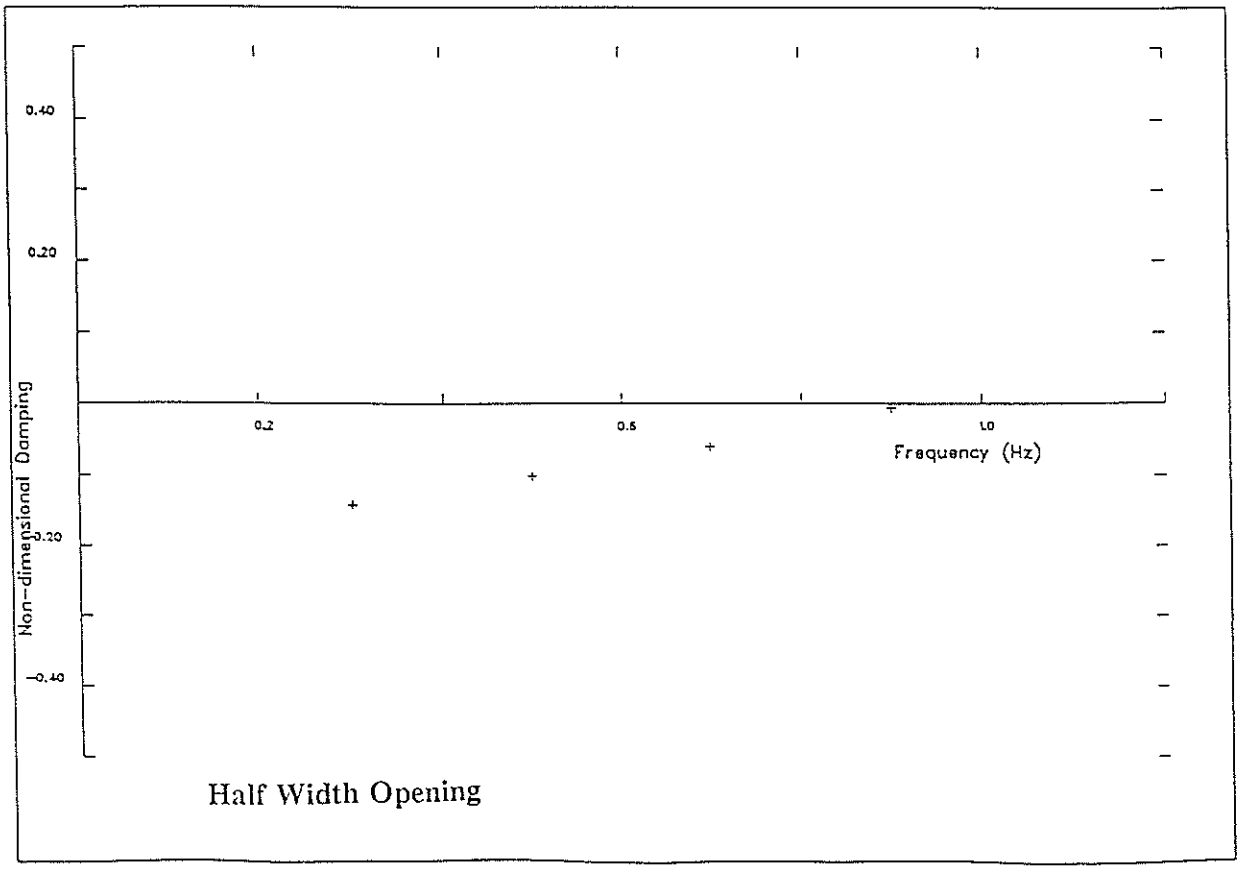

Figure 8. Deduced Linear Damping Coefficients in Forced Roll - Effect of Damage Opening Size

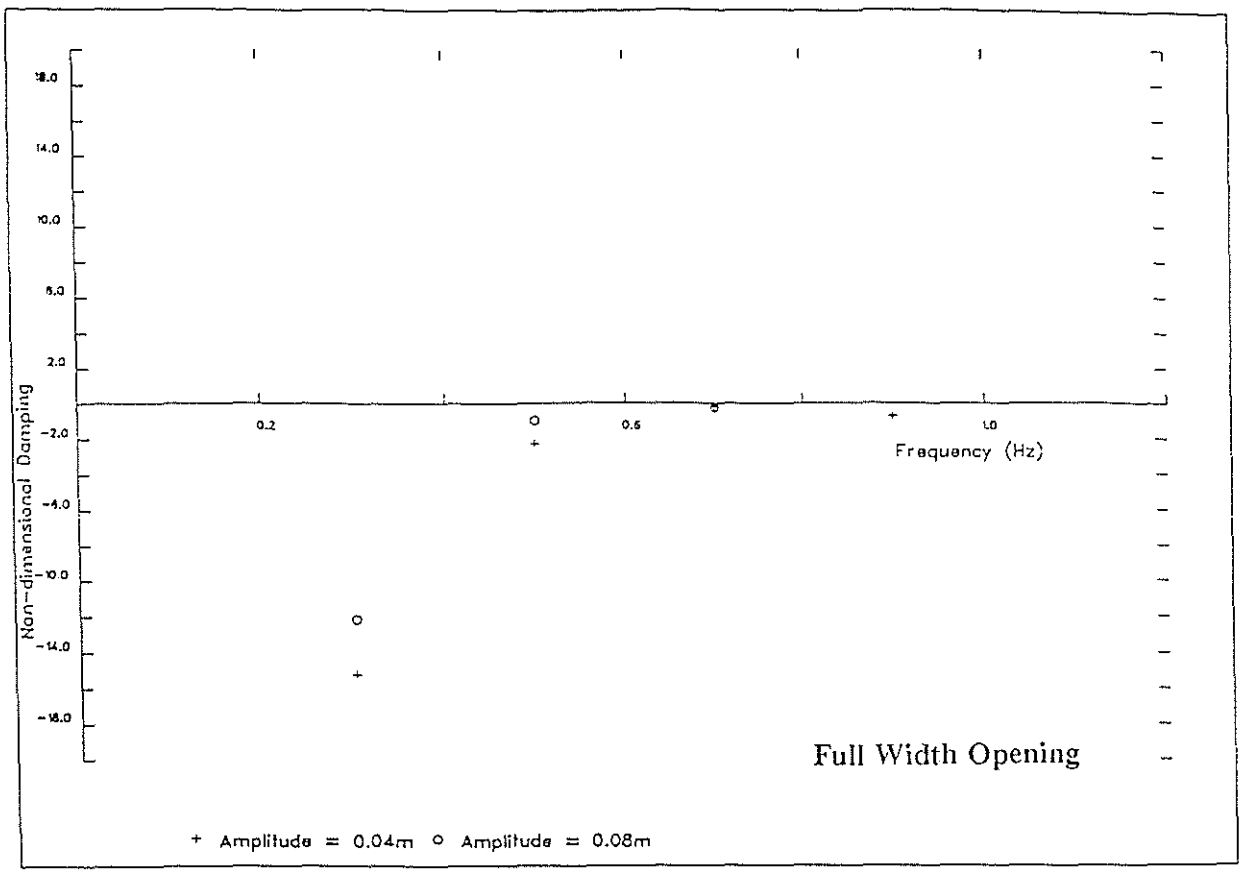

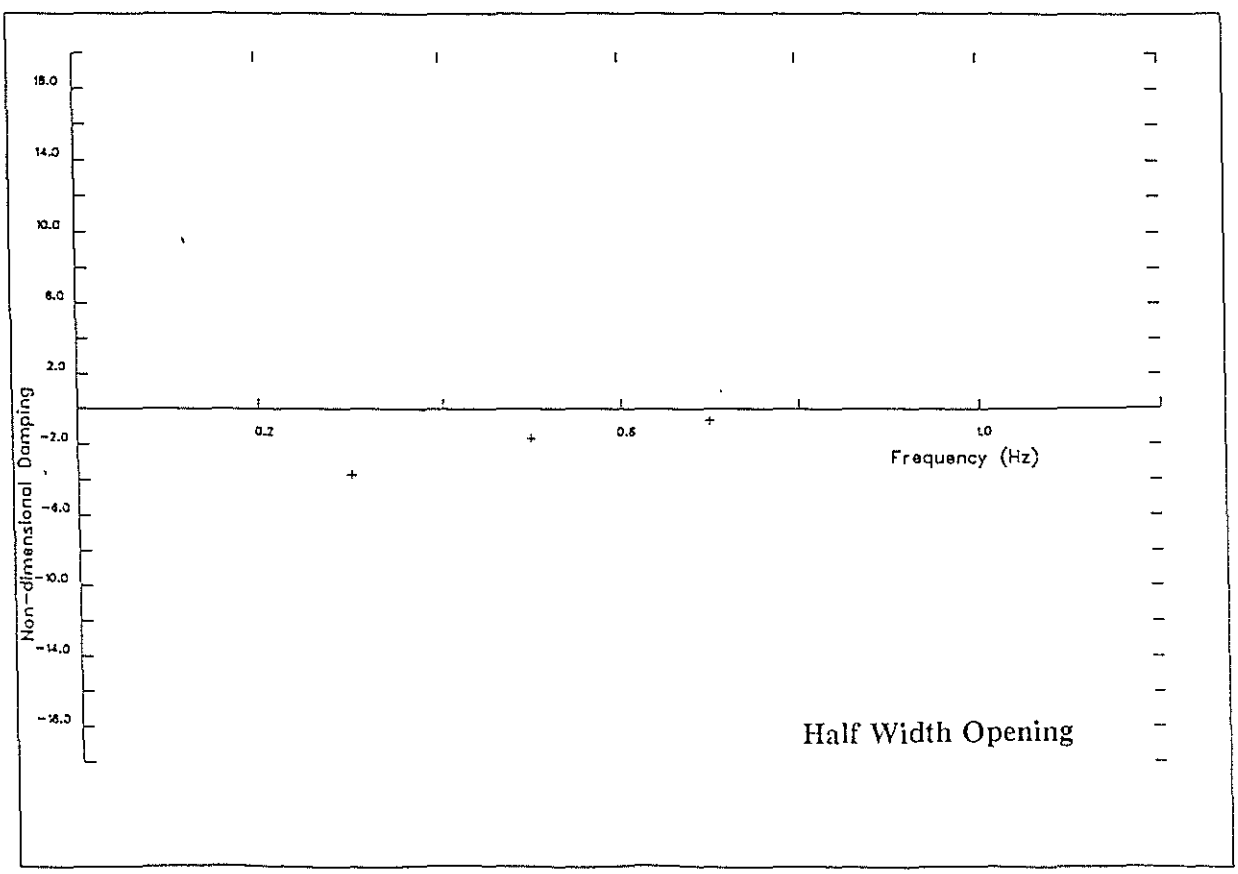

Figure 9. Deduced Linear Damping Coefficients in forced Heave - Effect of Damage Opening Size

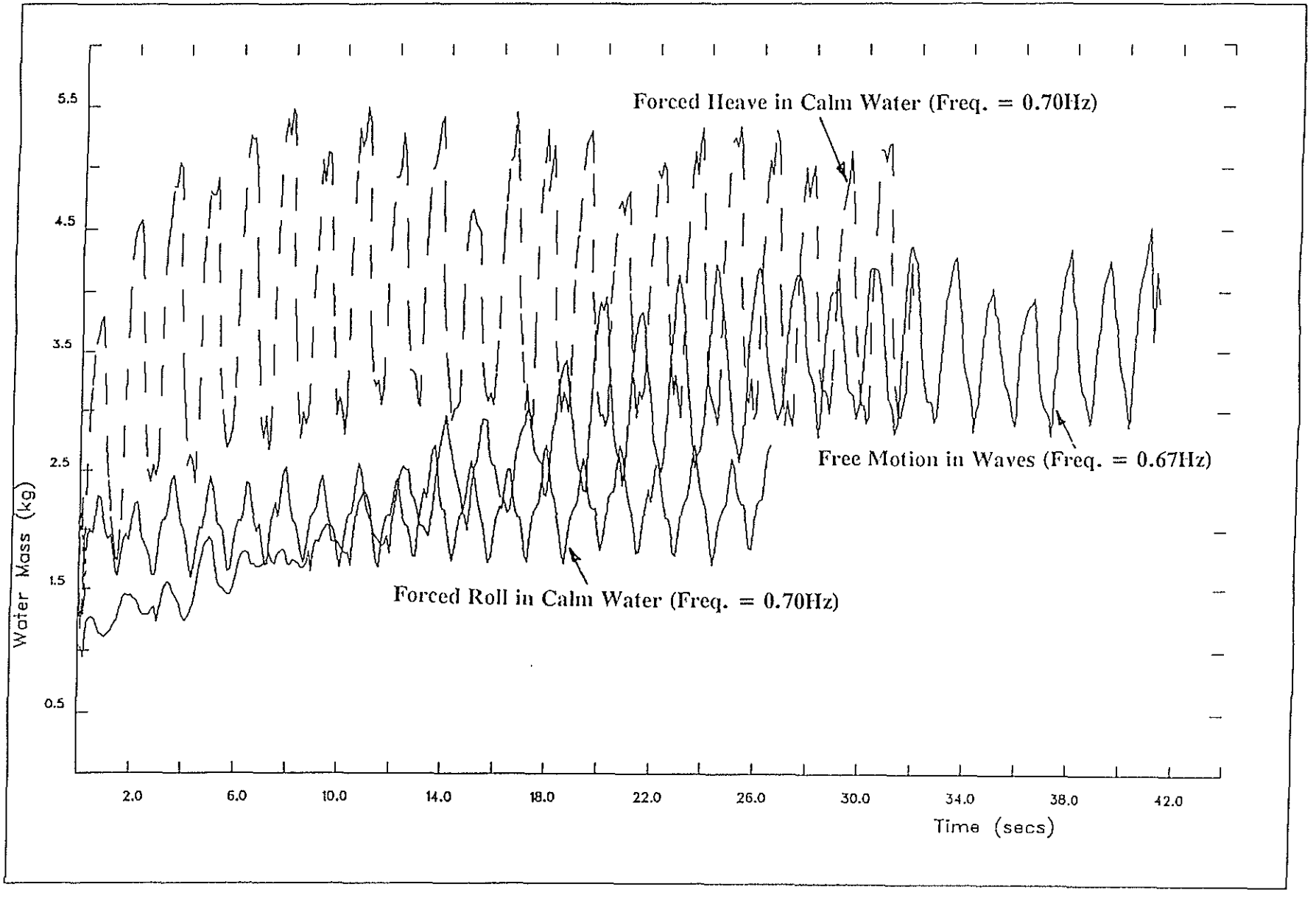

Figure 10. Comparison of Water on Deck

STABILITY OF A PLANING CRAFT IN TURNING MOTION

Yoshiho IKEDA[1], Hideaki OKUMURA[1] and Toru KATAYAMA[1]
[1]Depertment of Marine System Engineering, Osaka Prefecture University

1. Introduction

For a planing craft in turning at high speed, the stability quality is a very important factor for its safety. However, the characteristics of hydrodynamic forces acting on a planing craft in turning condition have not been clarified yet.

In the present study, six component hydrodynamic forces acting on a model obliquely towed at constant high speed are measured for various attitudes, rise, heel and trim, in the towing tank of Osaka Prefecture University.

The measured data shows that the hydrodynamic forces significantly depends on the running attitude, that the restoring roll moment becomes negative for moderate heel angle, and that it decreases with increasing yaw angle, or angle of attack rapidly.

2. Experimental Setup

The model used in the experiment is a 1/4-scale model of a personal watercraft with waterjet propulsion. The principal particulars of the model are shown in Table 1. The hull is harchine type, and has a duct without any impeller.

The experimental setup is shown in Fig.1. The model is captured by a 6-component load cell, and towed by an unmanned carriage the maximum speed of which is 15m/s. The rise H (mm), heel angle ϕ (deg), trim angle τ (deg) and yaw angle β (deg) are systematically changed as shown in Table 2. The rise here is defined by vertical displacement of the center point of rotation to change trim angle, which is located at 0.178m from the keel line at midship. The zero levels of all measured forces are set at rest just before starting of the carriage. The measured roll, pitch and yaw moments around the load cell are converted into the values about the standard location of the center of gravity of the craft.

Table 1. Principal particulars of model

length(m)	L	0.630
breadth(m)	B	0.223
depth(m)	D	0.100
draft(m)	d	0.055
Ship weight(kgf)	W	5.796
KG(m)		0.107
LCG from transom(m)		0.255
Deadrise angle(degree)		22

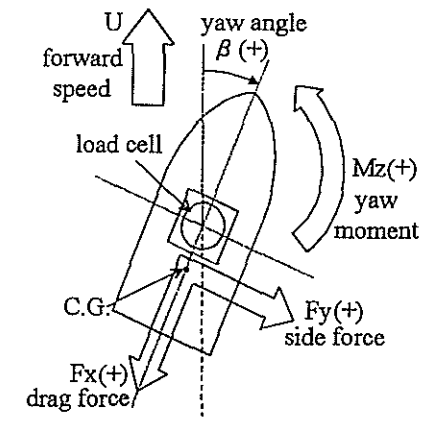

Top view

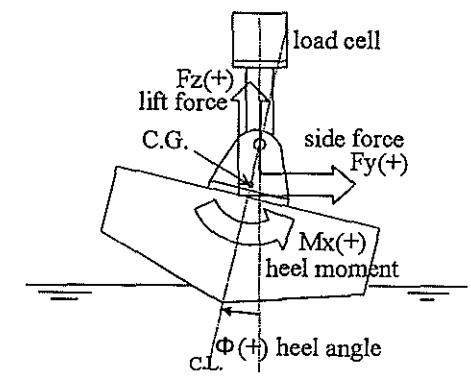

Posterior view

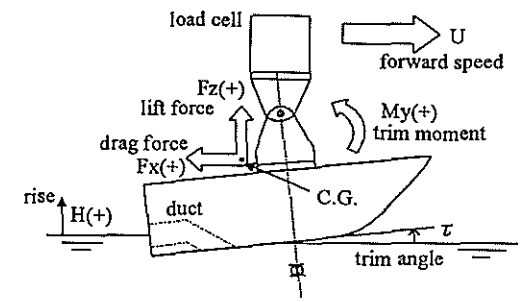

Side view

Fig.1 Schematic views of experimental setup and coordinate system

Table 2. Experimental conditions

Condition	A	B	C
rise H(mm)	20	30	40
heel ϕ (degree)	20	30	10
trim τ (degree)	2	4	4
yaw β (degree)	10	10	10

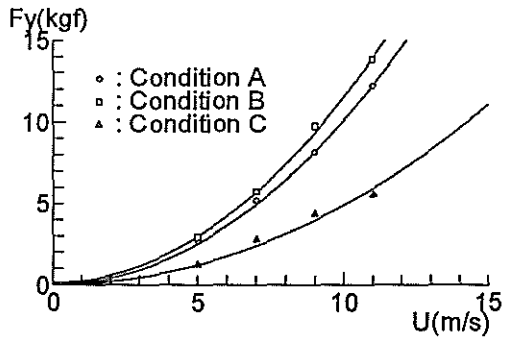

Side Force

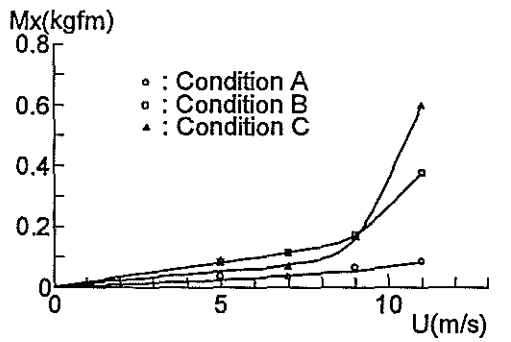

Roll Moment

Fig.2 Effects of advance speeds on forces acting on fully captive model

The measured forces are nondimensionalized as follows,

$$C_{Fx} = \frac{Fx}{0.5\rho SyU^2} \quad (1)$$

$$C_{Fy} = \frac{Fy}{0.5\rho SyU^2} \quad (2)$$

$$C_{Mx} = \frac{Mx}{W \cdot B} \quad (3)$$

$$C_{My} = \frac{My}{0.5\rho SxLU^2} \quad (4)$$

$$C_{Mz} = \frac{Mz}{0.5\rho SyLU^2} \quad (5)$$

$$C_{Fz} = \frac{Fz}{0.5\rho SzU^2} \quad (6)$$

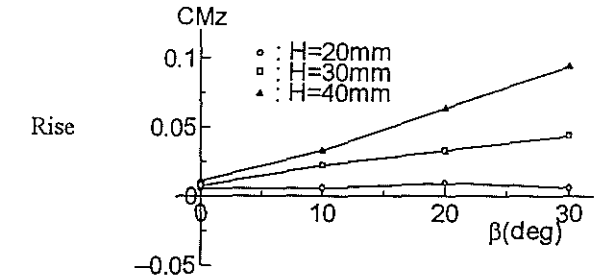

at heel ϕ =20deg, trim τ =4deg

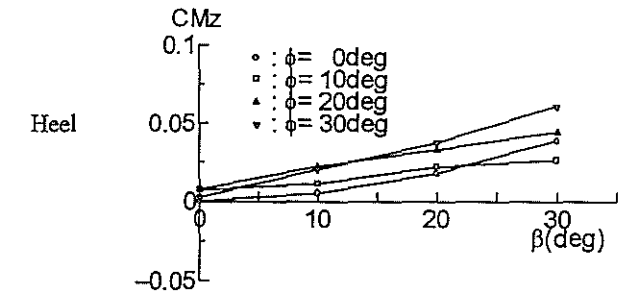

at rise H=30mm, trim τ =4deg

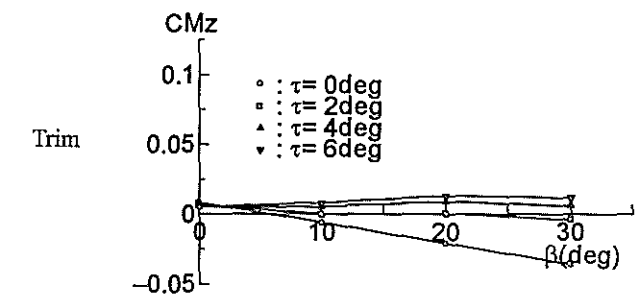

at rise H=20mm, heel ϕ =20deg

Fig .3 Effect of running attitude on yaw moment coefficient

where, Fx: resistance, Fy: transverse force, Fx: vertical lift, Mx: roll moment, My: trim moment, Mz: yaw moment, Sy: projected area of wetted body from side, Sz: waterplane area, L: overall length of a craft, B: breadth, W: displacement and ρ : density of water. In them, Sy and Sz are calculated for each attitude without any disturbance on free surface.

3. Experimental Results

Effect of advanced speed

Measurements of hydrodynamic forces acting on the hull are carried out for various advanced speeds in the range of Froude number between 2.0 and 4.4. Measured transverse force and roll moment are shown in Fig.2. The results of transverse force are in proportional to square of advanced speed as shown in this figure. It was confirmed that the results of resistance, vertical lift, trim moment and yaw moment show the same tendency too. Measured roll moment, however, is not in proportional to square of speed at high advanced speed.

Rise

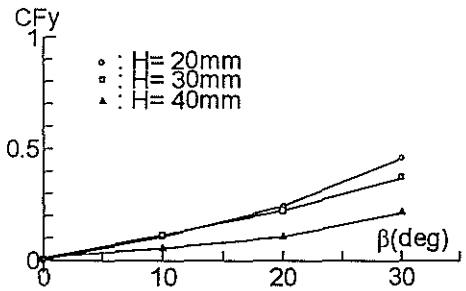

at heel ϕ =10deg, trim τ =0deg

Heel

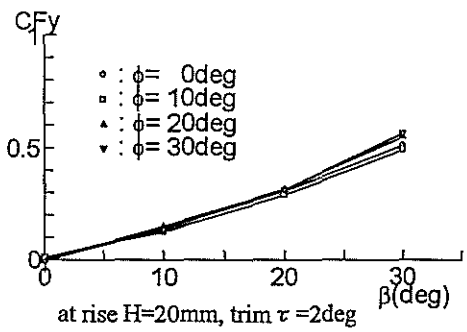

at rise H=20mm, trim τ =2deg

Trim

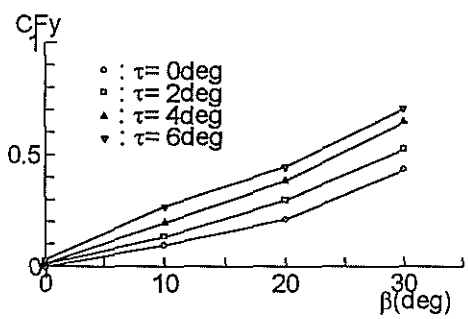

at rise H=30mm, heel ϕ =20 deg

Fig.4 Effect of running attitude on side force coefficient

Rise

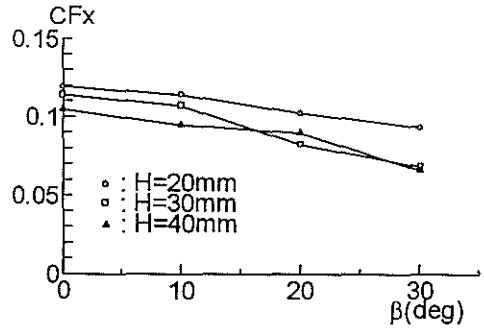

at heel ϕ =20deg, trim τ =4deg

Heel

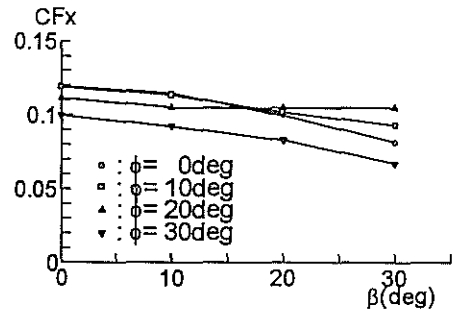

at rise H=20mm, trim τ =4deg

Trim

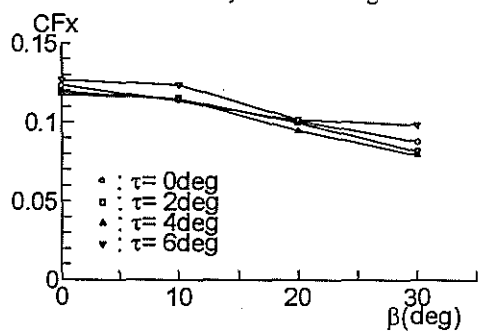

at rise H=30mm, heel ϕ =20 deg

Fig.5 Effect of running attitude on drag coefficient

Experimental results

Some typical results of measured hydrodynamic forces are shown in Figs.3-8.

4. Discussions

Yaw moment

Yaw moment significantly affects the maneuverability of a craft. The measured results are shown in Fig.3, in which the value is positive when the restoring moment is acted. The results shown in Fig.3 show that the yaw moment is usually positive, and the positive value increases as a craft rises. This suggests that a planing craft has a good course keeping ability in planing condition. This fact is in good agreement with the conclusion by Kobayashi et.al.(1995). The experimental results show that for attitude with zero trim and small rise yaw moment becomes negative. This suggests that turning ability of such a craft becomes good for such attitude.

The experimental results at zero yaw angles demonstrate that yaw moment is generated by heel angle.

Transverse force

Measured transverse force is shown in Fig.4. The force is in proportional to yaw angle, or angle of attack. The effect of rise on transverse force is not significant except when trim angle is zero. The effect of trim angle on it is significant as shown in this figure.

Resistance

Resistance may affect speed reduction in maneuvering motion. Measured force is shown in Fig.5. The results show that resistance in oblique towing condition gradually decreases with increasing yaw angle.

Vertical lift force

Vertical lift may affect planing condition in turning motion. Measured results are shown in Fig.6. The results show that

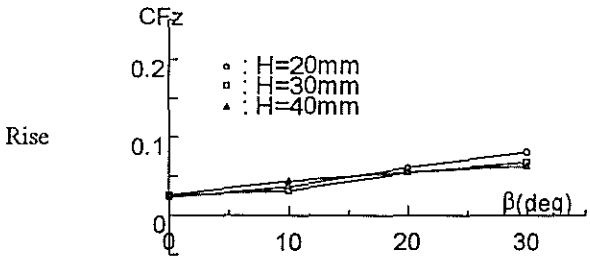

at heel ϕ =20deg, trim τ =4deg

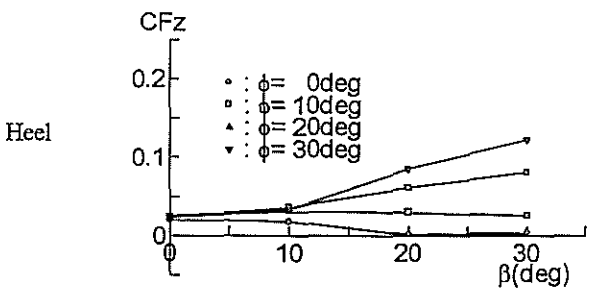

at rise H=20mm, trim τ =4deg

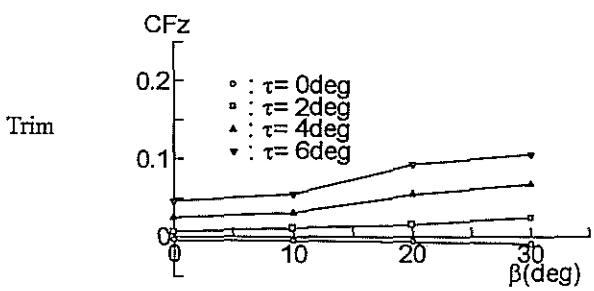

at rise H=30mm, heel ϕ =20 deg

Fig.6 Effect of running attitude on vertical lift coefficient

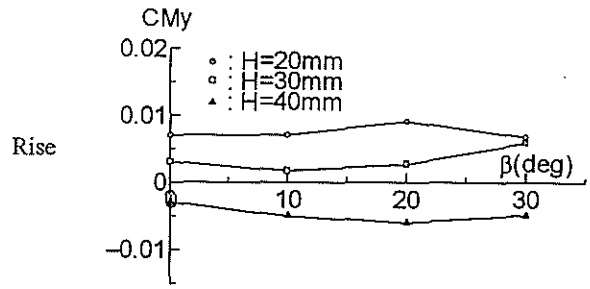

at heel ϕ =10deg, trim τ =4deg

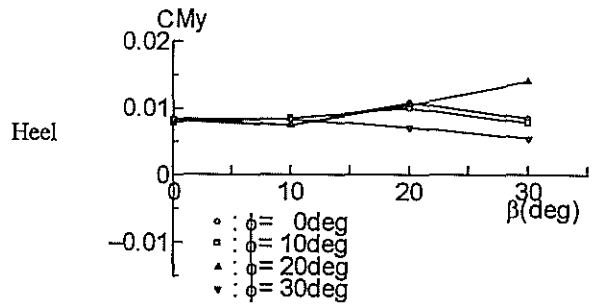

at rise H=20mm, trim τ =6deg

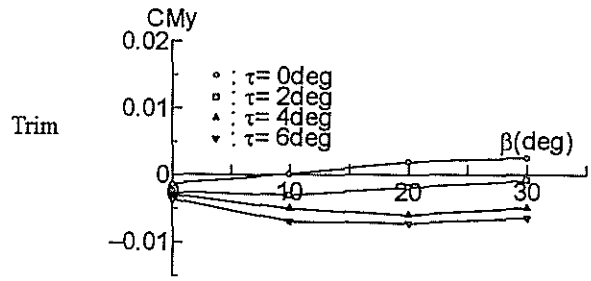

at rise H=40mm, heel ϕ =10 deg

Fig.7 Effect of running attitude on trim moment coefficient

vertical lift force mainly depends on trim angle, and the effect of rise on it is small. When yaw angle is small (β <10deg.), the lift is independent of heel angle. When yaw angle is large, however, the lift force increases with increasing heel angle. At large yaw angle, the lift force decreases with yaw angle when heel angle is small, and increases up to several times of the value at β =0. This may be because the increase of heel angle works as increasing angle of attack.

Trim moment

Trim moment is one of most important factor for planing because vertical lift force depends on it. Measured trim moment is shown in Fig.7. The trim moment is almost constant without any effect of yaw angle when heel angle is moderate (ϕ <20deg). The moment significantly depends on rise. At small rise, bowup moment is acted on the hull. As rise increases, the bowup moment decreases, and when rise is large bowdown moment becomes to be acted on it. At large heel condition, the trim moment is significantly affected by trim and yaw angles.

Heel moment

Measured heel, or roll moment is shown in Fig.8. The values in this figure show dynamic component of roll restoring moment, which does not include static component at Fn=0. The results demonstrate the roll moment decreases with increasing yaw angle, and becomes negative at large yaw angle.

5. Stability at High Speed Turning

GZ curves are calculated from the measured heel moment shown in previous chapter and calculated static restoring moment as shown in Figs.9-11. The results demonstrate that large negative moment is acted on the hull at large yaw angle. Certain amount of the negative moment may be cancelled by drift force and horizontal component of thrust force of waterjet as shown in Fig.12. However, large negative moment may cause large heel in high speed turning.

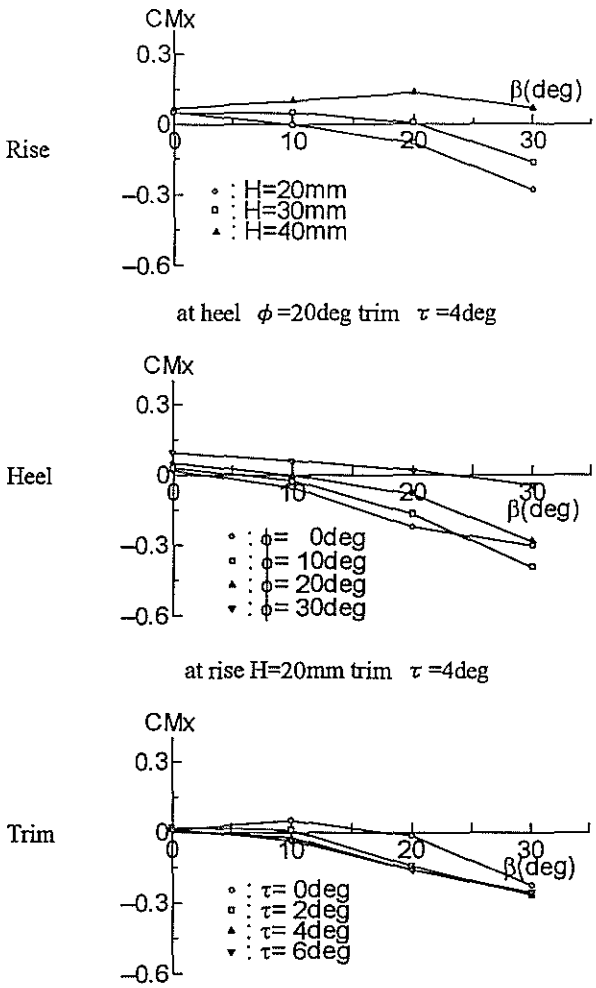

Fig.8 Effect of running attitude on heel moment coefficient

6. Conclusions

Measurements of 6-component hydrodynamic forces acting on a planing hull obliquely towed in constant speed are carried out for various attitudes in a towing tank, and following conclusions are obtained.

(1) Hydrodynamic forces acting on a planing hull obliquely towed significantly depend on running attitudes. Therefore, in maneuvering of such planing craft it should be needed to take into account the effects of attitude on hydrodynamic derivatives.

(2) At planing condition, strong restoring moment in yaw is acted on the hull. Therefore, the craft have good course keeping performance at high speed.

(3) Dynamic forces decreases roll restoring moment at large yaw angle. Therefore large heel can occur in high speed turning for a planing craft.

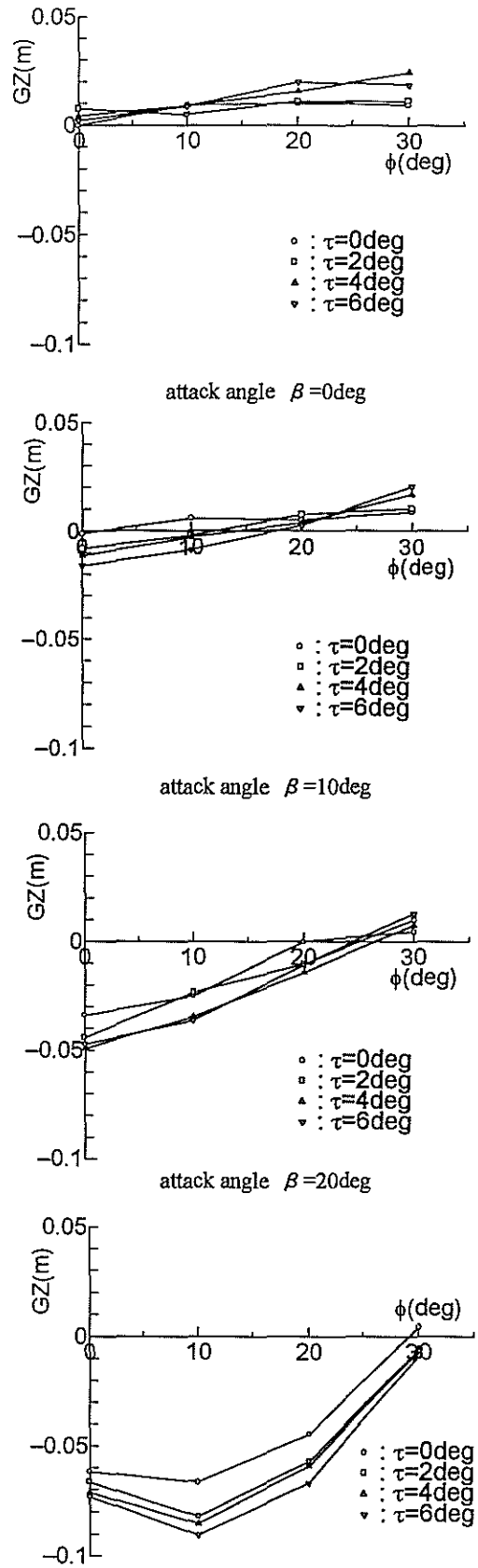

Fig.9 GZ curve at H=20mm

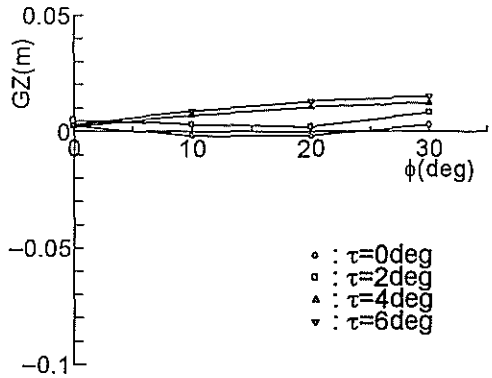

attack angle β =0deg

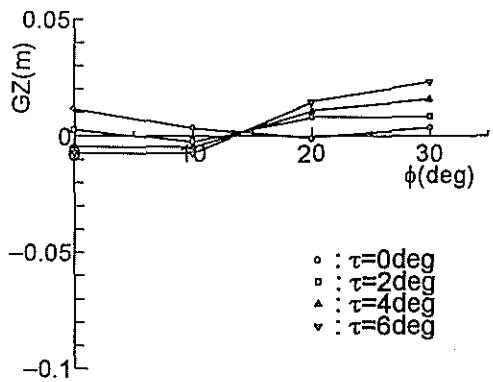

attack angle β =10deg

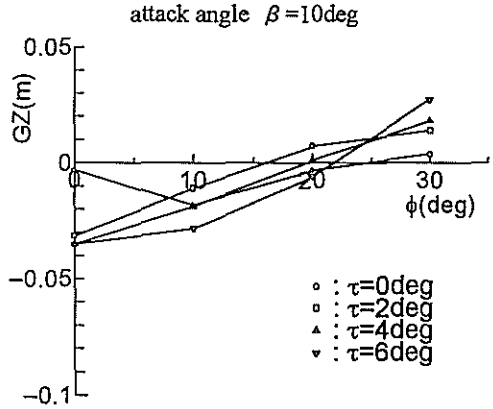

attack angle β =20deg

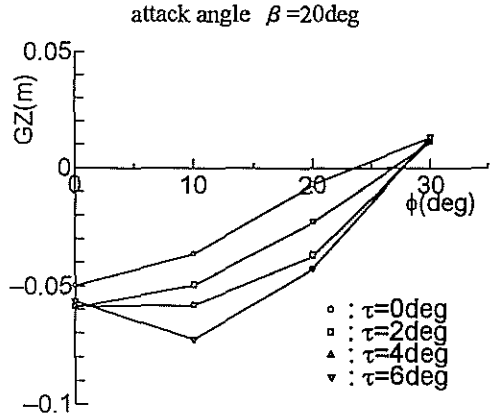

attack angle β =30deg

Fig.10 GZ curve at H=30mm

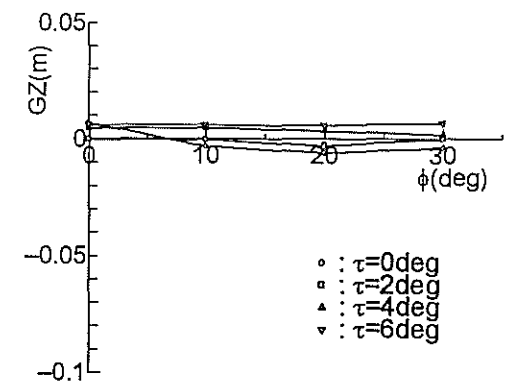

attack angle β =0deg

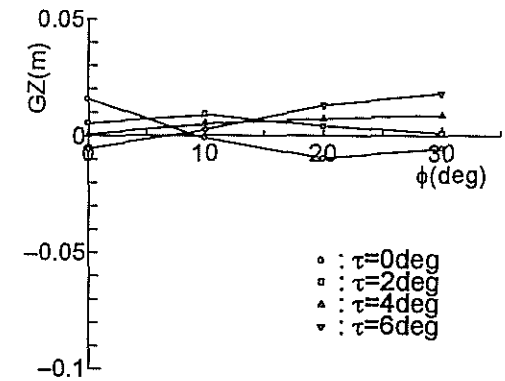

attack angle β =10deg

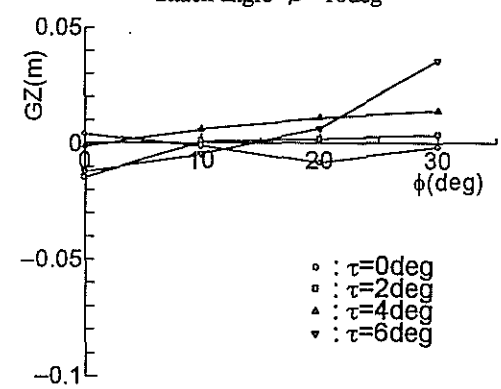

attack angle β =20deg

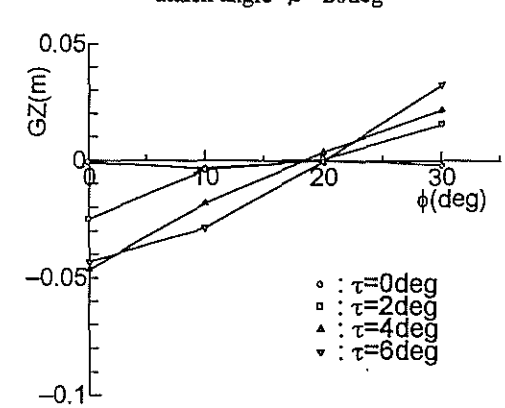

attack angle β =30deg

Fig.11 GZ curve at H=40mm

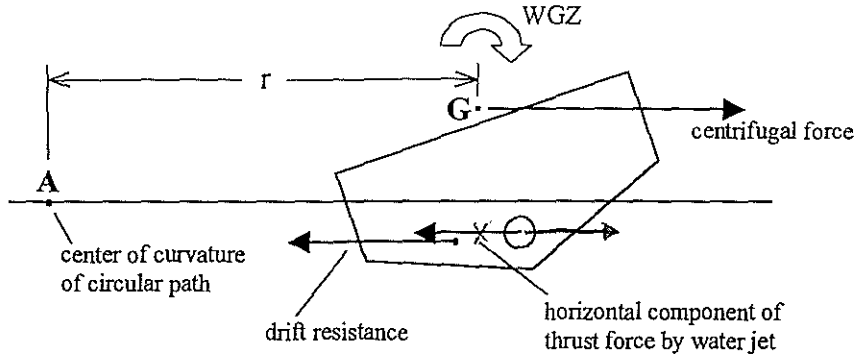

Fig.12 Forces acting on a planing hull during steady turning motion

References

Hiroaki Kobayashi, Yasuo Arai, Atsushi Ishibashi, Shigeyuki Okuda, Yasuhiro Okamoto and Akifumi Takeuchi (1995), A Study on the Maneuverability of High-Speed Boat. Journal of the Kansai Society of Naval Architects, Japan, 223, 81–90, (in Japanese)

An Experimental Study on the Improvement of Transverse Stability at Running for High-Speed Craft

Yushu Washio[1], **Katsuro Kijima**[2], and **Tetsuo Nagamatsu**[3]

ABSTRACT

It is well known for high-speed crafts that transverse instability might occur at running higher than a certain speed. In this study model experiments in the towing tank were carried out to examine the transverse instability at various speeds and $\overline{GM}$ values with the hard chine hull form and to develop a device for improvement of transverse stability. The captive model tests were carried out to search for the range of instability, and were done at various speeds in three different conditions of $\overline{GM}$ values to examine hydrodynamic forces such as heel moments and sway forces acting on the hull in specified instability conditions. As a result, it is confirmed this ship model loses transverse stability at higher speed and smaller $\overline{GM}$ as expected. For the improvement of transverse stability, three types of effective spray strip including ordinary one were added to the hull as appendages respectively and its effect were examined. As a result, so-called "Reaction Flap" on the fore part of the hull which is one of three types, showed remarkable improvement. The existence of "Reaction Flap" results in being almost negligible for the resistance. This "Reaction Flap" makes conventional mono-hull form possible to be more stable at relatively higher speed without specific design.

1. INTRODUCTION

It is known for high-speed crafts that transverse instability might occur at running higher than a certain speed even though they posses adequate static stability applied relevant criteria (Marwood et al., 1968), (Millward, 1979), (Schwanecke et al., 1992), (Suhrbier, 1978).

Generally a hard chine hull is relatively more stable than a round bilge hull at the same conditions at running. However even for a hard chine hull, a effective device for improvement of transverse stability is required because there is a possibility of instability at higher speed at running.

In this study model experiments in the towing tank

[1] Mitsubishi Heavy Industries, Ltd., Japan
[2] Kyushu University, Japan
[3] Kagoshima University, Japan

were carried out to examine the transverse instability at various speeds and $\overline{GM}$ values for a high-speed craft with conventional hard-chine. Then, for the improvement of transverse stability, three types of spray strip including ordinary one were added to the hull as appendages respectively and were also examined to be effective for the transverse stability.

The resistance test with the most effective appendages chosen among them was also carried out in order to grasp the influence upon the propulsive performance.

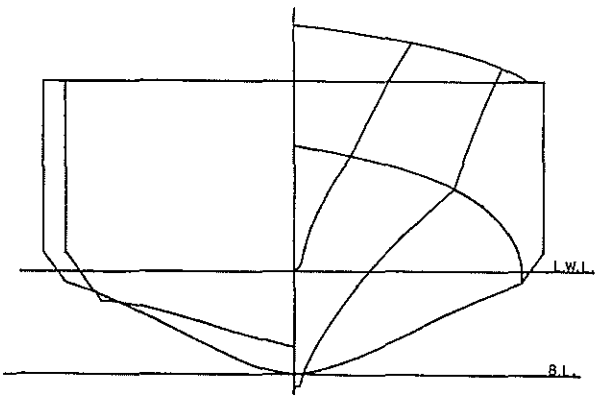

Fig.1 Hard-chine type hull form used in the present experiment

2. EXPERIMENTS

2.1 Ship Model

A typical example of a hard chine hull form is shown in Photo. 1, which one of the authors applied to the large high-speed passenger craft.

In this study model experiments in the towing tank were carried out to examine the transverse instability at various speeds and $\overline{GM}$ values. The ship model was used the typical type of a hard chine hull form shown in Fig.1 in order to search the range and limit of instability for higher speed or smaller $\overline{GM}$ in comparison with the original planned values.

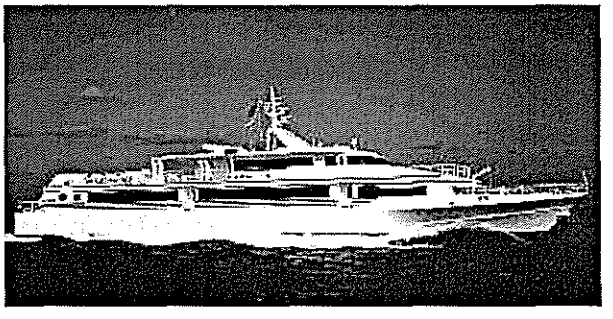

Photo. 1 Conventional Hard-Chine type High-Speed Craft at running

The principal dimensions of the ship model are 3.8m in length, 0.63m in breadth, 0.14m in draft, and the scale ratio is 1/12.3 to the full scale ship.

In order to improve the transverse stability, it seems easy to increase the breadth of ship. Because it is known by the results of recent research that wider breadth is so effective as larger $\overline{GM}$ value, or lower center of gravity.

However, too much wide breadth might give bad effects upon other characteristics such as propulsive performance and seakeeping quality etc. So generally it is easier way for designers to change the type of ships from mono-hull to twin hull, so-called catamaran to improve transverse stability with keeping the other performance as it is.

It must be important for naval architects how to improve the hull form and optimize total performance of ships at a practical design stage.

It will be preferable to improve the transverse stability without changing to other types from mono-hull because mono-hull has many advantages in comparison with other types of hull forms. In this point of view, some ideas for a mono-hull are already proposed such as special types of stabilized fins and outriggers added to the outside of hull, but most of them do not always give better results to keep a same performance of original hull.

In this study the methods of improvement which keep advantages of a mono-hull are proposed and the experiments by using a towing tank were carried out to examine the effects as expected.

As it is known by the recent research (Suhrbier, 1978), spray strips are effective for the improvement of transverse

stability, three types of spray strip including ordinary one were added to the hull as appendages individually as shown in Fig.2 and Fig.3.

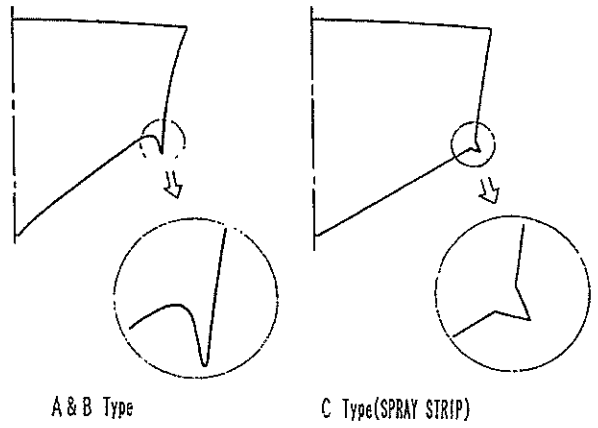

Fig.2 Section of "Reaction Flap" and spray strip

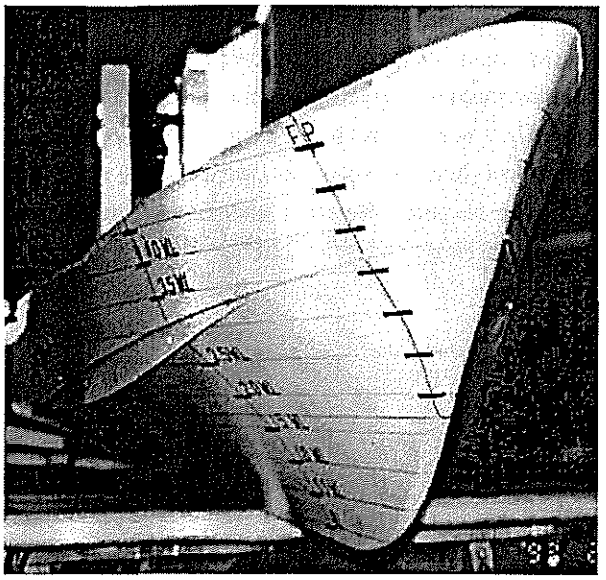

Photo. 2 Ship model with "Reaction Flap"

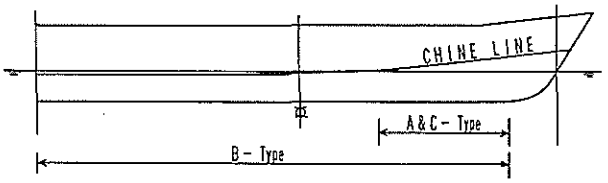

Fig.3 Applied zone of "Reaction Flap" and spray strip

These appendages are intended to make use of the restoring force against transverse instability which is produced by bow waves creeping up above the still waterline at high-speed and colliding against these appendages as shown in Photo. 1.

A-type and B-Type are given as name of "Reaction Flap" which form an upset-U-shaped cross section by themselves and the side hull platings so as to produce a restoring force against bow waves.

A-Type is provided at the fore parts of the hull alongside the chines above still waterline, and B-Type is the extension of A-Type to the aft end of the hull alongside the chines which submerge below still waterline at after part of the hull. The Photo. 2 shows the model with "Reaction Flap" of A-type.

C-Type is ordinary spray strip which form wedge shaped cross section only at the fore parts of the hull alongside the chines above still waterline as A-Type.

2.2 Method of Measurement

For high-speed crafts the transverse instability might occur at running higher than a certain speed.

This phenomenon is observed as the ship will begins to heel firstly by instability at running, and then to turn not to keep the course and finally capsizes in the worst case. Therefore it is very difficult to simulate thus phenomenon perfectly by using a towing tank for the restriction of measurements, so many experiments were carried out by using a ship model restricted motion (Baba et al., 1982), (Millward, 1979).

In this study firstly the experiments were carried out under the fixed condition of sway and yaw motion, and finally done for various speeds in three different $\overline{GM}$ chosen under the fixed condition of all motion.

In the experiments under the fixed condition of sway and yaw motion, the degree of change of running trim and heel, and the range of instability were measured as a change of $\overline{GM}$ value and speed.

The experiments under the fixed condition of all motion were carried out to examine hydrodynamic forces such as heel moments and sway forces acting on the hull for specified instability conditions. The heel moments and the side forces were measured at various heeling angles under the same conditions such as running trim and dipping gained from the results of experiments under fixed condition of sway and yaw motion.

For the experiments of the ship model fixed all motion, the schematic diagram of measurement is shown in Fig.4, and the coordinate system and symbols in Fig.5.

The model has twin hanging rudders, but not propellers. And all experiments were done at the Towing Tank of Nagasaki Research and Development Center, Mitsubishi Heavy Industries, Ltd.

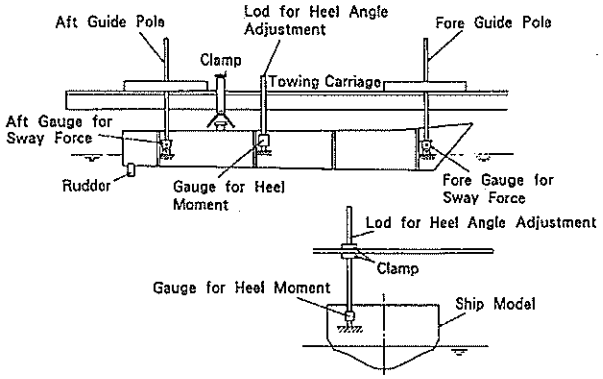

Fig.4 Schematic diagram of measurement

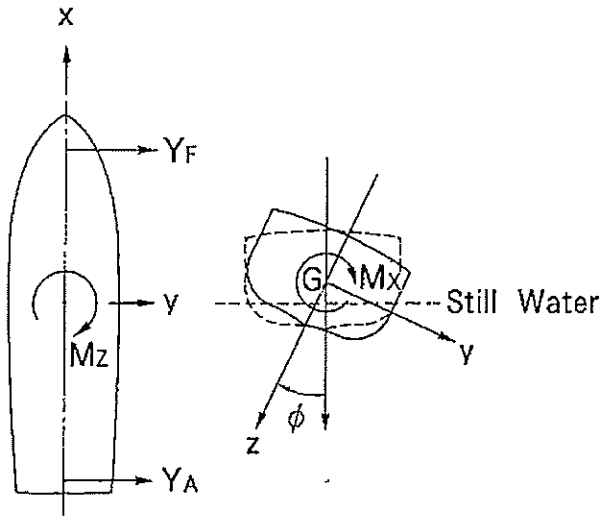

Fig.5 Coordinate system and symbols

3. RESULTS OF EXPERIMENTS

3.1 Results of Experiments for Transverse Stability

At first, experimental results for the ship model without appendages for improvement of instability are described. This model is called by "the original hull" hereinafter.

By the experiments of using the original hull fixed sway and yaw motion, it was observed to be stable by maintaining certain heel angle at relatively lower speed, but not to be stable at higher speed and to result in capsizing finally at further high speed.

The tests were started from searching for such limits of $\overline{GM}$ value and speed which might cause a transverse instability resulting in capsizing finally, and then tests were done at various speeds for three different conditions of $\overline{GM}$ values chosen.

The results of experiments, measured heel angles : ϕ which were saturated values finally for individual speed are shown in Fig.6(a). (The values of figures hereinafter correspond to the model scale.)

As shown in Fig.6(a), the heel angle : ϕ increases in larger value as increasing speed and finally the model capsize for all $\overline{GM}$ chosen.

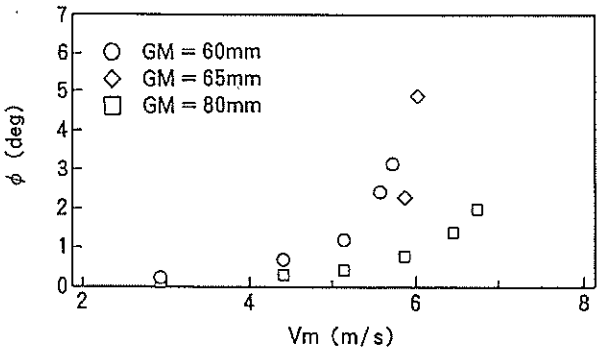

Fig.6(a) Measured heel angle

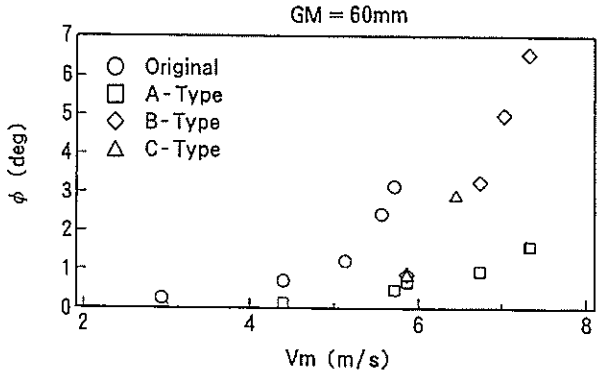

Fig.6(b) Measured heel angle

Also the time histories of heel, heave and pitch

measured at running in the case of $\overline{GM}$=60mm are shown as Fig.7(a) and Fig.7(b) for reference.

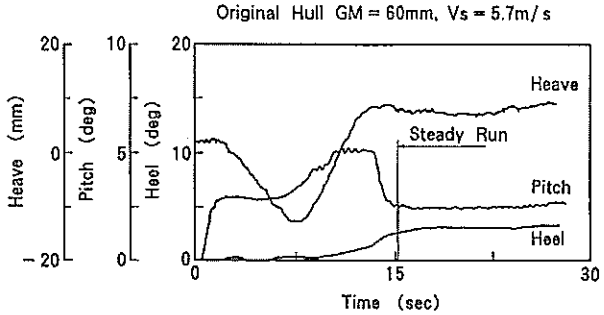

Fig.7(a) Time history of heel, heave and pitch measured at running

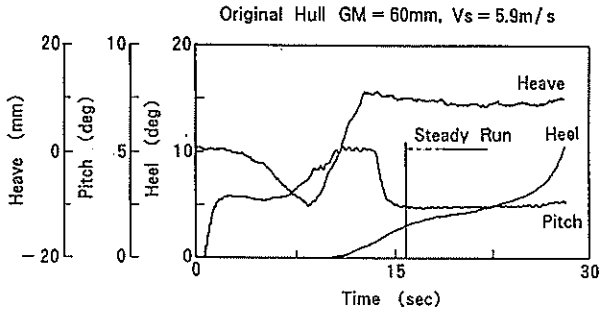

Fig.7(b) Time history of heel, heave and pitch measured at running

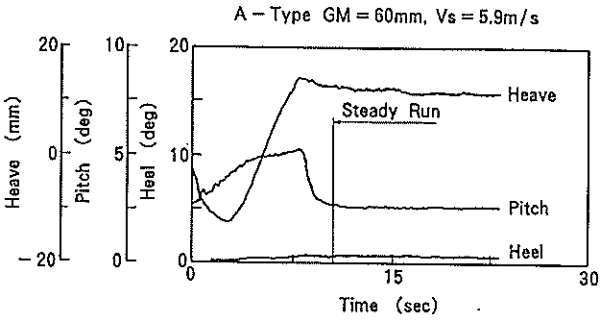

Fig.7(c) Time history of heel, heave and pitch measured at running

Fig.7(a) is a time history in the case of the model speed of Vs=5.7m/s which shows heave and pitch motion vary with a large amplitude in the range of transient acceleration before the model reaches to run steady, and reaches to be stable and a saturated certain levels.

Fig.7(b) is also a time history in the case of the model speed of Vs=5.9m/s which shows heave and pitch motion are reached to be steady state and a saturated certain value when the model reaches to run steady as in the case of Vs=5.7m/s, but the heel angle does not reach to be stable and grows rapidly until resulting in capsizing at last.

The speed of the model at capsizing was Vs>5.9m/s in the case of $\overline{GM}$=60mm, Vs>6.1m/s in the case of $\overline{GM}$=65mm and Vs>7.0m/s in the case of $\overline{GM}$=80mm.

Thus it is found by the experiments the hull form used in this study is so unstable as the speed is higher and $\overline{GM}$ value is smaller.

Fig.6(b) shows the measured results under the conditions of models with appendages such as "Reaction Flap" and spray strips with $\overline{GM}$=60mm.

Comparing with the results of the original hull at the same speed, heel angles are reduced by adding the above all appendages of A-Type, B-Type and C-Type. In particular, A-Type, so-called "Reaction Flap", extending along both side platings nearly from a bow in a direction towards a stern shows remarkable improvement in comparison with other appendages, in which heeling angle : ϕ is very small even at the speed of Vs=7.3m/s.

Fig.7(c) shows a time history of heel, heave and pitch measured at running of Vs=5.9m/s in the case of "Reaction Flap", A-Type. The heel angle : ϕ of the model with A-Type keeps as a constant small value at steady running in comparison with the original hull as shown in Fig.7(b) which heel angle is still increasing after steady running.

Side views of the original hull and that with "Reaction Flap", A-Type at running are as shown in Photo. 3.

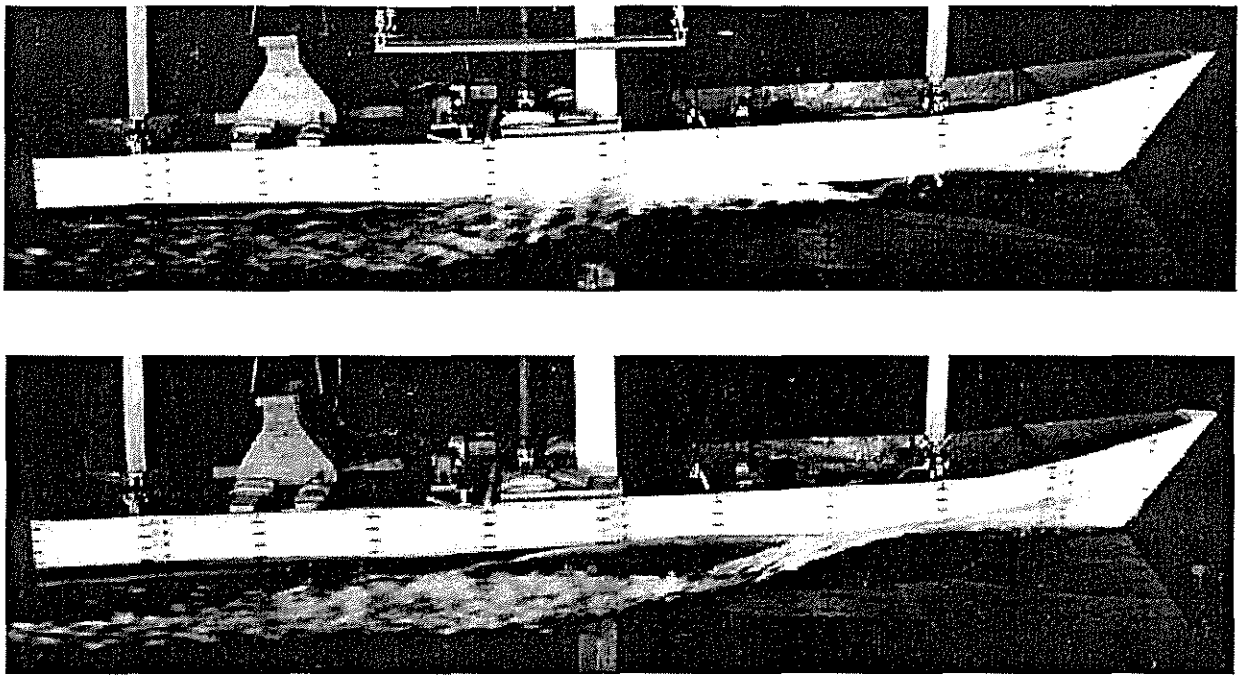

Photo. 3 Side view of original hull and that with "Reaction Flap" at running

By considering the results of above, the experiments under the fixed condition of all motions were carried out only for the original hull with and without "Reaction Flap", A-Type. Also the tests were done for a constant value of $\overline{GM}$=60mm at two cases of speed, one is at Vm=4.4m/s and at Vm=5.9m/s, which are stable and heavy unstable respectively for the original hull.

Measured heel moments : Mx for the above are shown in Fig.8(a) and Fig.8(b).

For the original hull heel moment : Mx against heel angle : ϕ is relatively very small at the speed of Vm=4.4m/s which means to become unstable when the model is forced to heel by some disturbance. And at Vm=5.9m/s, the heel angle : ϕ increases more and more by some disturbance and finally capsizes because heel moment : Mx has a positive slope against heel angle : ϕ as shown in Fig8(a).

On the contrary in the case of the hull with A-Type, the model is stable at both speed of Vm=4.4m/s and 5.9m/s even when heeling because heel moment : Mx has a negative slope against heel angle : ϕ as shown in Fig8(b).

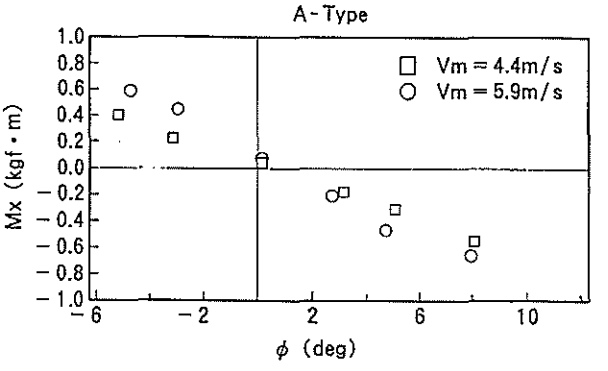

Fig.8(a) Measured heel moment

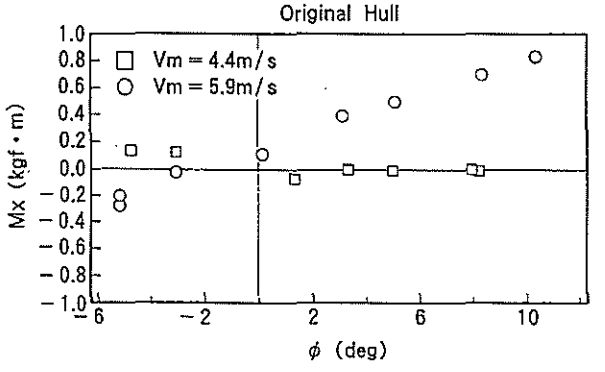

Fig.8(b) Measured heel moment

Then Fig.9(a) and Fig.9(b). show measured sway forces at the positions of fore and aft perpendiculars of the model at the speed of Vm=5.9m/s.

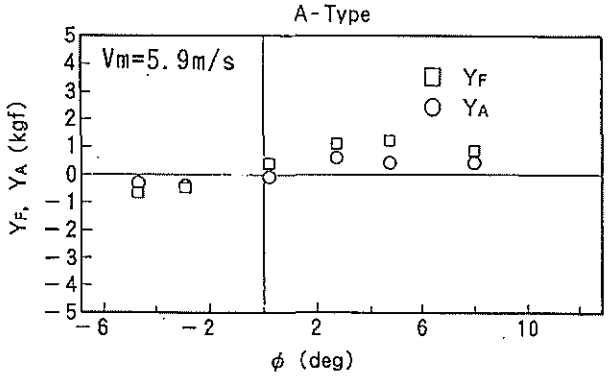

Fig.9(a) Measured sway forces

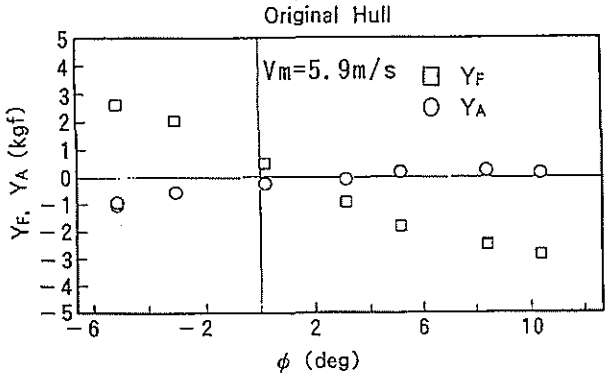

Fig.9(b) Measured sway forces

For the original hull when the model heels starboard side (ϕ >0), the value of sway force at the fore perpendicular : Y_F is negative (direction of the force is from starboard side to port side) and the value of sway force at the aft perpendicular : Y_A is zero. Then the hydrodynamic force acts to turn the model to the port side. When ϕ <0, vice versa.

Yaw moment increases as increase of sway force $|Y_F|$ by growing heel angle : ϕ , therefore a turning circle decreases. And then heel angle : ϕ increases more and more because centrifugal force to the hull becomes larger.

However for the hull with A-Type, both of absolute values of Y_F and Y_A are small and have a positive slope against heel angle : ϕ. This means the model results in being stable at running because yaw moment is small and turning direction is opposite to the original hull which makes heel angle : ϕ decrease even if the model might slightly sway to the heeling side.

Concluding the results of experiment, it is found "Reaction Flap", A-Type shows remarkable improvement of transverse stability at high-speed running.

3.2 Result of Resistance Test

The resistance test with "Reaction Flap" of A-Type was carried out in order to examine the influence upon the propulsive performance. The test were done under the fixed condition of sway, yaw, and roll motion.

The result of resistance test is shown as compared to that of the original hull in Fig.10. The existence of "Reaction Flap" on the fore part of the hull, A-Type results in being almost negligible for the resistance.

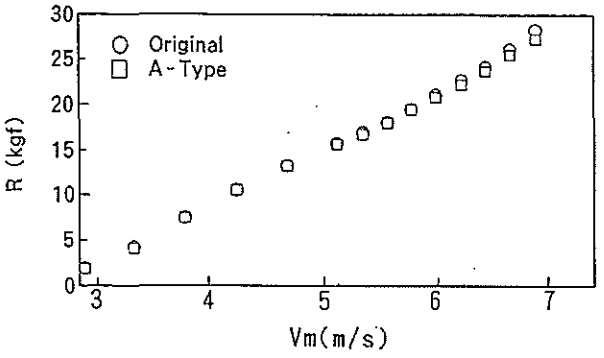

Fig.10 Resistance test result

4. CONCLUDING REMARKS

It is well known for high-speed crafts that transverse instability might occur at running higher than a certain speed.

Taking the above characteristics into consideration, in this study a research of the method to improve transverse stability at running are carried out through experiments without loosing advantageous characteristics of mono-hull as possible such as propulsive performance and seakeeping quality etc.

At first the range or limits of instability for various speeds and different $\overline{GM}$ values were experimentally examined for the ship model of a hard chine high-speed craft.

Then three types of effective spray strip including ordinary one were added to the original hull as appendages respectively and were also examined transverse stability.

As a result, so-called "Reaction Flap", one of three types, extending along both side hull platings nearly from a bow in a direction towards a stern shows remarkable improvement in comparison with other appendages although other types of strip are found to be also effective to improve the transverse stability.

And the existence of "Reaction Flap" on the fore part of the hull is also found to be negligible for the resistance.

This "Reaction Flap" shows one of possibilities for conventional mono-hull form to develop more stable at relatively higher speed without changing hull form or principal dimensions. Also it is useful to keep transverse stability by adding the "Reaction Flap" in the case of demands for raising the center of gravity or increasing speed when planning conversion of the ship.

References

Baba, E., Asai, S. and Toki, N., "A Simulation Study in Sway-Roll-Yaw Coupled Instability of Semi-Displacement Type High Speed Craft", Proceedings of the 2nd International Conference on Stability of Ships and Ocean Vehicles, Part IV, The Society of Naval Architects of Japan, Tokyo Japan, 1982.

Ibaragi, H., Kijima, K. and Washio, Y., "Study on the Transverse Instability of a High-Speed Craft", Transactions of The West Japan Society of Naval Architects, No.91, Mar. 1996.

Kijima, K., Ibaragi, H. and Washio, Y., "Study On the Transverse Instability of a High-Speed Craft", 2nd Workshop on Stability and Operational Safety of Ships,1996.11.

Marwood, W. J. and Bailey D., "Transverse Stability of Round-Bottomed High Speed Craft Underway", NPL report 98, Oct.1968.

Millward, A. ; Preliminary Measurements of Pressure Distribution to Determine the Transverse Stability of a Fast Round Bilge Hull, ISP, Vol.26, No.297, 1979.

Schwanecke, H. and Muller-Graf, B., "Die Dynamische Querstabilitat Schneller Rundspantund Knickspantboote", Bericht Nr.1201/92, Versuchsanstalt fur Wasserbau und Schiffbau, 02, 1992, Berlin.

Suhrbier, K.R., "An Experimental Investigation on the Roll Stability of a Semi-Displacement Craft at Forward Speed", Symposium on Small Fast Warship and Security Vessels, RINA(1978).

Washio, Y. and Doi, A., "A study on the Dynamical Stability of High-Speed Craft", Transactions of The West Japan Society of Naval Architects, No.82, Aug. 1991.

Washio, Y, Ibaragi, H. and Kijima, K., "Study on the Transverse Instability of a High-Speed Craft (Continued)", Transactions of The West Japan Society of Naval Architects, No.94, Aug. 1997.

The Stability Assessment of Small Working Craft Without Reference to Hydrostatic Data

Richard Birmingham[1]

ABSTRACT

The initial stability of a vessel can be evaluated by the established procedure of the inclining experiment, provided that the vessel's lines or hydrostatics are available. For many small working craft however no record exists of these particulars, and therefore the inclining experiment can only be undertaken if it is accepted that the lines will also have to be taken from the vessel in order to generate the necessary data. This paper explores the relationship between the roll period and the metacentric height and demonstrates that in theory it is possible to evaluate the initial stability from the change in roll period as a pair of weights are moved vertically and horizontally above the deck, without requiring reference to any hydrostatic data. A procedure requiring only five observations is described, and the necessary calculations detailed, however the difficulties in implementing such a procedure are also discussed. Further work to identify extensions to this procedure which could be of practical use to a surveyor are outlined.

INTRODUCTION

The conventional procedure for evaluating a vessel's initial stability is the inclining experiment, in which weights are moved across the deck and the angle of heel measured. By reference to the hydrostatic particulars of the vessel in the trial condition the metacentric height and position of the centre of gravity can be found. However for many small craft, such as fishing and other work boats, neither the hull lines nor the hydrostatic data are available. The results of an inclining experiment can only be interpreted, therefore, if the lines are also taken off the vessel and the necessary data derived. Clearly this adds considerably to the cost and practicality of the inclining experiment as a way of assessing the initial stability for such craft.

Methods for obtaining an estimate of initial stability for such vessels, based on the natural period of roll, have long been recognised. These rely on the use of a stop watch to measure the roll period, and assumptions concerning the transverse mass moment of inertia of the vessel. In the first part of this paper it will demonstrated however, that in theory it is possible to derive the vessel's initial stability (together with the vertical centre of gravity and displacement) by a direct calculation which uses as its only input the periods of roll as a pair of weights are positioned in pre-defined

Table 1: Nomenclature

B	breadth of vessel
d	vertical distance weights moved
Δ	displacement of vessel
f	a correlation factor
g	acceleration due to gravity
$\overline{GM}$	metacentric height (initial stability)
h	x offset of ellipse centre
I'	effective mass moment of inertia
k	y offset of ellipse centre
m	combined mass of weights
T	vessel's natural period of roll
u	minor demi-axis of ellipse
v	major demi-axis of ellipse
x	horizontal co-ordinate
y	vertical co-ordinate

[1] Department of Marine Technology, The University of Newcastle upon Tyne, England NE1 7RU

locations on and above the deck. The success of such a procedure depends on the ability to measure the period of roll to a high degree of accuracy, and while modern computer technology provides more than adequate precision, interference from hydrodynamic factors associated with the vessel reduce the accuracy achievable. These difficulties are described in the latter part of this paper, which culminates with a discussion of how such a procedure may be practically implemented to provide stability data for a small craft without reference to its lines or hydrostatics.

THE RELATIONSHIP BETWEEN INITIAL STABILITY AND THE PERIOD OF ROLL

The link between stability and a vessel's natural period of roll has been acknowledged for several centuries, indeed it was reported that in 1628 a roll experiment aboard the *Vasa* was halted due to the alarming results [1]. Unfortunately this did not prevent the vessel's loss due to capsize on her maiden voyage.

The period of roll is still used today to assess the stability of fishing vessels. For example the Marine Safety Agency suggests that by obtaining an average time for the period of roll (T) by stop watch, the metacentric height of a vessel ($\overline{GM}$) can be estimated from the following formula [2]:

$$T = \frac{fB}{\sqrt{\overline{GM}}} \qquad (1)$$

This expression uses the breadth of the vessel (B), and a correlation factor (f). The value of the correlation factor is dependent on the vessel type. In metric units it varies form 0.95 for double boomed beam trawlers, to 0.60 for vessel's with a live fish well. If an appropriate value of the correlation factor can be identified, then the initial stability $\overline{GM}$ can be estimated from the results of a basic roll test. While this may be satisfactory in many cases, it can be envisaged that on occasion there could be considerable error, especially where the vessel does not conform to a recognised class of craft, or where it has been substantially modified.

It is possible however to define the precise relationship between stability and the period of roll which can be defined by considering the righting moment at small angles of heel, and assuming simple harmonic motion. It can then be shown [3] that the period of roll, T, is given by:

$$T = \frac{2\pi\sqrt{I'}}{\sqrt{g\Delta\overline{GM}}} \qquad (2)$$

In this expression there are three vessel related variables: the displacement (Δ), the effective transverse mass moment of inertia which includes the effects of added mass (I'), and the metacentric height ($\overline{GM}$). The last of these is considered the measure of initial stability, and it is the relationship of this with the period of roll, T, which is of interest. However it is the presence of the other two variables which complicates the direct assessment of stability from the period of roll. (It is worth noting that equations 1 and 2 are of the same form if it is accepted that the radius of gyration is a function of the vessel's beam).

GEOMETRY AND THE PERIOD OF ROLL

In the inclining experiment weights are moved across a vessel's deck and the induced angle of heel noted. The movement of weights also impacts on the period of roll, but as an angle of heel is not desired for a roll based experiment pairs of weights must be moved symmetrically about the centre plane of the vessel. The period of roll will be affected by moving such pairs of weights horizontally away or toward the centre plane, or by moving them vertically, as both actions affect either the position of the vertical centre of gravity (and hence $\overline{GM}$), or the mass moment of inertia, or both. By considering how changes in the geometric position of a pair of such weights influences the period of roll, it is possible to devise a procedure in which both the metacentric height and the mass moment of inertia can be changed in a systematic way. In theory the observed changes in the period of roll can then be used with equation 2 to find the initial stability of the vessel, without recourse to correlation factors.

Moving the weights only horizontally has no impact on the vertical centre of gravity (and therefore does not alter $\overline{GM}$), but it does alter the mass moment of inertia. By using Pythagoras's theorem it can be shown that regardless of where the vertical centre of gravity is located this change in the mass moment of inertia (I') is given by equation 3, where the mass of the combined weights are m, and the dimensions x_a and x_b are as defined in Figure 1. Moving the weights away from the centre plane increases the mass moment of inertia, and vice versa.

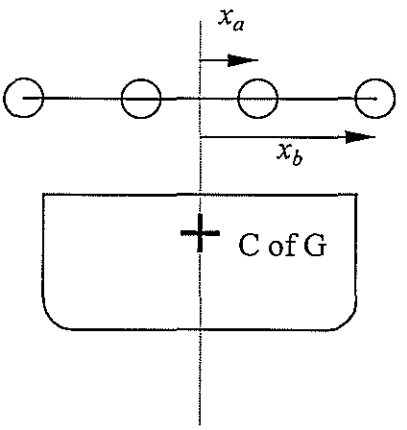

Figure 1: Horizontal definition for two positions of a pair of weights placed symmetrically about the centre plane.

$$\delta I' = m\left(x_b^2 - x_a^2\right) \qquad (3)$$

Vertical movement of the weights clearly changes the vertical centre of gravity, and hence the metacentric height. This effect is given by equation 4, where d is the vertical distance that the weights are moved:

$$\delta \overline{GM} = \frac{md}{\Delta} \qquad (4)$$

A purely vertical movement of the weights also alters the mass moment of inertia, but it is impossible to establish the magnitude of this change without knowing the position of the vertical centre of gravity. It is evident however that a downward movement of the weights will reduce the mass moment of inertia, provided that the weights remain above the vessel's centre of gravity. As a movement of the weights outboard increases the mass moment of inertia it is possible to both lower the weights and simultaneously move them horizontally such that the net change in the mass moment of inertia is zero. For this to be the case as the weights are lowered they must follow an elliptical path, which starts on the centre plane, and is furthest form the centre plane when the weights are at the same height as the vessel's own centre of gravity, as shown in Figure 2.

The fact that the locus of the weight positions for constant I' follows an elliptical path can be used to derive another equation. If the centre of gravity did not change as the weights were moved, then the locus for constant I' would describe a circle. The distortion of the circle into an ellipse is due to the downward drift of the centre of gravity as the weights are lowered. The difference between the major and minor demi-axes of the ellipse, v and u, is a measure of the change in the vertical position of the centre of gravity:

$$\delta \overline{GM} = v - u \qquad (5)$$

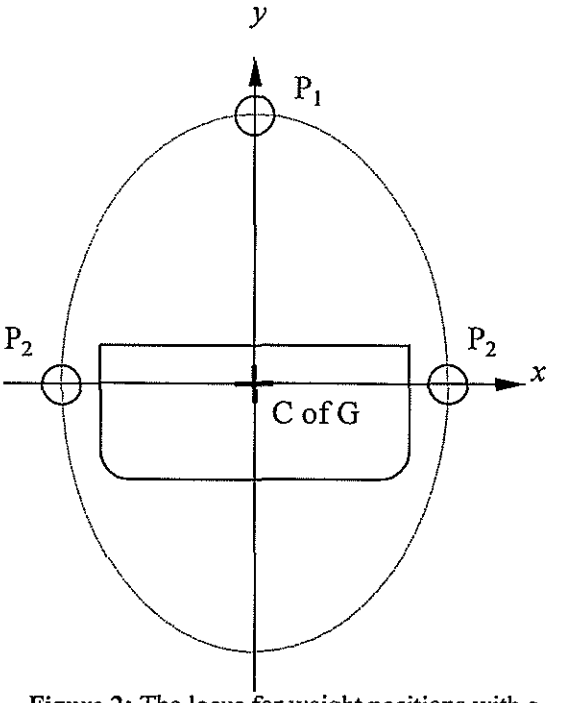

Figure 2: The locus for weight positions with a constant mass moment of inertia.

THE BASIS OF DIRECT ASSESSMENT OF STABILITY

It is the existence of this locus for weight positions which will maintain a constant mass moment of inertia which enables a direct evaluation of initial stability. If the period of roll is measured when the weights are on the centre line and high above the deck, and then the position is identified which corresponds to the maximum outboard location of weights with the same mass moment of inertia, and the roll period is again measured, sufficient data will have been gathered to calculate the metacentric height.

The theory can be easily summarised as follows. For the two cases observed (with the weights in positions 1 and 2 as shown in Figure 2) both the vessel's displacement (Δ) and mass moment of inertia (I') are unknown, although they have the same value in each case. The metacentric height ($\overline{GM}$) however, is

different in each case. There are therefore four unknowns: Δ, I', $\overline{GM}_1$ and $\overline{GM}_2$. To solve this problem four equations are needed. The basic equation for the period of roll, equation 2, can be used twice with the appropriate values T_1 and T_2 being used with $\overline{GM}_1$ and $\overline{GM}_2$ respectively. In addition the difference between $\overline{GM}_1$ and $\overline{GM}_2$ is defined in two independent ways in equations 4 and 5. These can be used to provide the third and fourth equations which can be re-stated as in equations 6 and 7 below:

$$\overline{GM_2} - \overline{GM_1} = \frac{m(y_1 - y_2)}{\Delta} \qquad (6)$$

$$\overline{GM_2} - \overline{GM_1} = y_1 - y_2 - x_2 \qquad (7)$$

With four equations for four unknowns the problem is solvable, however this theory presupposes that the ellipse describing weight positions with a constant value of I' can be found. To demonstrate how this can be achieved it is necessary to consider again how the geometry of the weight positions effects the relevant variables. As already discussed the weights can be moved horizontally only, so keeping $\overline{GM}$ constant, or they can be moved along an elliptical path which maintains I' constant. There is however a third path which will alter both $\overline{GM}$ and I' in such a way that the period of roll, T, is kept constant, as shown in Figure 3.

This third locus, where T is constant, has a property which can be used to find the locus for constant I'.

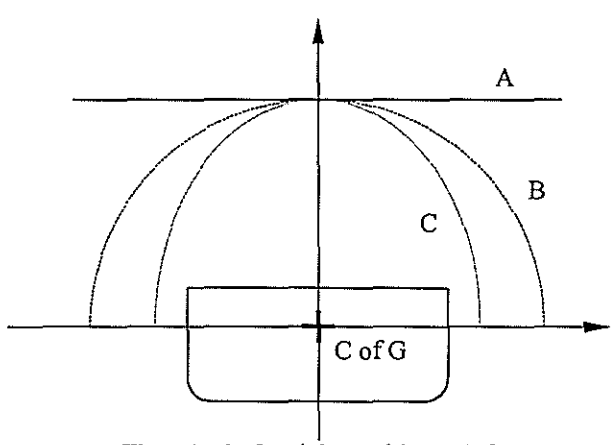

Figure 3: Three loci of weight positions: A for constant metacentric height; B for constant period of roll; C for constant mass moment of inertia.

This can be shown by first manipulating equation 2 to obtain a general expression for the partial derivative of I' with respect to $\overline{GM}$:

$$\frac{\partial I'}{\partial \overline{GM}} = \frac{T^2 g \Delta}{4\pi^2} \qquad (8)$$

Evidently when the weights are moved along the locus that maintains the period of roll, T, constant, then this partial derivative is also a constant. If weights positioned on the centre plane are taken as a first case, and a second position is found below this, where the weights are positioned outboard such that the two periods of roll are the same, then the change in I' from the first case to the second can be found from the product of the partial differential of I' with respect to $\overline{GM}$ and the actual change in $\overline{GM}$:

$$\delta I' = \frac{\partial I'}{\partial \overline{GM}} \delta \overline{GM} \qquad (9)$$

which, by substituting from equations 8 and 4, yields:

$$\delta I' = \frac{T^2 g m d}{4\pi^2} \qquad (10)$$

From this expression the change in the mass moment of inertia between the first position (high on the centre plane) and the second position (with weights lower and outboard as shown in Figure 4) can be calculated. As it is possible to calculate the change in the mass moment

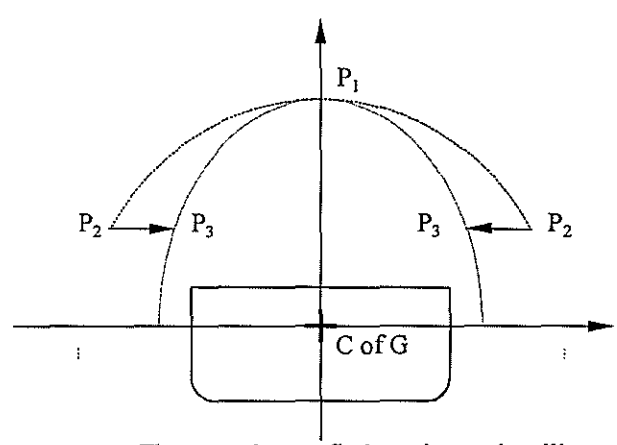

Figure 4: The procedure to find a point on the ellipse with constant mass moment of inertia: by experiment P_2 is found where the period of roll is as for P_1, then P_3 is calculated such that δI from P_2 to P_3 is the same as δI from P_1 to P_2.

of inertia when the weights are moved purely horizontally, from equation 3, so the distance toward the centre plane that the weights should be transferred in order to restore the mass moment of inertia to the same value as for the first position can be calculated.

Identifying points on the ellipse which defines the locus of constant mass moment of inertia can therefore be achieved. Having shown that this is possible it follows that the direct evaluation of initial stability on the basis outlined above is theoretically valid.

A CALCULATION REQUIRING THE MINIMUM NUMBER OF OBSERVATIONS

The direct evaluation of initial stability is based on the identification of two positions which are on the major and minor axes of an ellipse which is centred on the centre of gravity of the vessel. The period of roll when the weights are located at these positions must be established in order to provide the four equations necessary to proceed with the theoretical calculation. In this section a calculation will be described which uses five observations, the theoretical minimum number, however in the next section the practical difficulties of implementing this simplest of procedures will be discussed.

In this procedure the pair of weights are first positioned together on the centre plane well above the deck. This position is taken to be the extreme vertical point of an ellipse around which the weights can be moved without altering the mass moment of inertia. By positioning the weights in four more locations, and recording the period of roll, it is theoretically possible to find all the desired results, including the initial stability, by using the nine stage calculation summarised below.

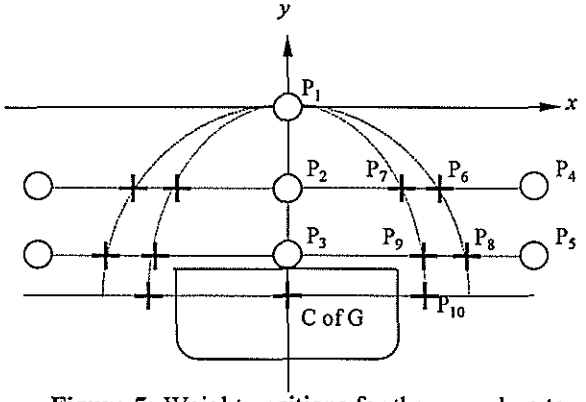

Figure 5: Weight positions for the procedure to calculate initial stability: Positions P_1 to P_5 are observed experimentally, positions P_6 to P_{10} are derived and the period of roll calculated.

The five weight positions necessary are as follows: the first is with both weights together on the centre plane, as high as is practicable above the deck, the second at about half the height of the first (again on the centre plane), and the third on or near the deck (also on the centre plane). The fourth and fifth positions have the weights located at the same heights as the second and third respectively, but at some distance from the centre plane. These positions are shown in Figure 5, as are all the additional positions described below for which data is derived. The calculation uses the first position to define the ellipse of interest, as it is taken to be the extreme point of the ellipse's major axis. This point is also taken as the origin in defining the x and y co-ordinates of the other positions. The calculation to find the extreme point of the minor axis then proceeds in stages 1 to 5 below. The vertical position of this point is the same as the vessel's centre of gravity. Stages 6 to 9 below demonstrate how the mass moment of inertia, the displacement and the metacentric height are also derived.

1. Positions 2 and 4 are used to find position 6 (which is at the same height as position 2). This will have the same period of roll as position 1. This is achieved by reducing equation 2 to a simple form which defines the relationship between the period of roll and the distance of the weights from the centre line, given that the weights can only be moved horizontally, and therefore that $\overline{GM}$ will not change.

If the constants c_1, c_2 and c_3 represent $\left(2\pi/\sqrt{g\Delta\overline{GM}}\right)$, $\left(I' + my^2\right)$ and (m) respectively, then equation 2 can be written as:

$$T = c_1\sqrt{c_2 + c_3x^2} \qquad (11)$$

By further combining the constants this relationship reduces to an expression with only two unknown constants, a, and b:

$$T = ax^2 + b \qquad (12)$$

By substituting for T_2, x_2 and T_4, x_4 it is possible to find a and b.

Setting $T_6 = T_1$ it is possible to find x_6 from the same equation.

2. Position 7 (also at the same height as 2) which will have the same mass moment of inertia as position 1 is then found from equations 10 and 3 as discussed above, and the period of roll at this position again interpolated form the observed periods for positions 2 and 4.

From equation 10:

$$\delta I'_{(1\text{ to }6)} = \frac{T_1^2 gm(y_1 - y_6)}{4\pi^2} \qquad (13)$$

(an increase in I')

And from equation 3:

$$\delta I'_{(6\text{ to }7)} = -m(x_6^2 - x_7^2) \qquad (14)$$

(a decrease in I')

As $\delta I'_{(1\text{ to }6)} = -\delta I'_{(6\text{ to }7)}$ it is possible to find x_7. Interpolate to find T_7.

3. Positions 3 and 5 are used in a similar way to establish the position and period of roll for positions 8 and 9. Position 9 has the same mass moment of inertia as positions 1 and 7.

4. Positions 1, 7 and 9 are three points on the required ellipse and can be used in the standard equation for such a curve to calculate the major and minor demi-axes, v and u.

The standard equation for an ellipse, centred at (h,k), and with the minor and major demi-axes defined as u and v, is given by:

$$\frac{(x-h)^2}{u^2} + \frac{(y-k)^2}{v^2} = 1 \qquad (15)$$

If position 1 is defined as (0,0) and is on the major axes with the ellipse below it, it can be shown that $h = 0$ and $k = -v$.

In this case the equation for the ellipse simplifies to:

$$\frac{x^2}{u^2} + \frac{(y+v)^2}{v^2} = 1 \qquad (16)$$

Use (x_7, y_7) and (x_9, y_9) to find u and v.

5. The dimensions of the demi-axes fully define the ellipse. They therefore give the position of the vessel's centre of gravity in relation to position 1, and the extreme horizontal position possible for the weights such that the mass moment of inertia is the same as in position 1, i.e. position 10.

The vessel's centre of gravity is given by: $(0,-v)$.

Position 10 is given by $(u,-v)$.

6. The mass moment of inertia for all points on the ellipse is found from any two points on the ellipse at which the period of roll is known, such as positions 1 and 9. This is achieved by using equation 2 for both positions, and then subtracting one from the other to obtain an expression for the change in metacentric height. Equation 4 provides an alternative expression for this, and if the two are equated it is found that displacement (the other unknown variable) is cancelled from the equation, and so the mass moment of inertia can be found.

From equation 2:

$$\delta \overline{GM}_{(1\text{ to }9)} = \frac{4\pi^2 I'}{g\Delta T_9^2} - \frac{4\pi^2 I'}{g\Delta T_1^2} \qquad (17)$$

From equation 4:

$$\delta \overline{GM}_{(1\text{ to }9)} = \frac{m(y_9 - y_1)}{\Delta} \qquad (18)$$

From which I' can be found:

$$I' = \frac{mg(y_9 - y_1)}{4\pi^2}\left(\frac{T_9^2 T_1^2}{T_1^2 - T_9^2}\right) \qquad (19)$$

7. The change in the metacentric height between positions 1 and 10 can be expressed in terms of moments, equation 4, or in terms of the geometry of the ellipse, equation 5. As position 10 is now defined, as are the demi-axes of the ellipse, equations 4 and 5 can be used to find the displacement of the vessel.

From equation 4:

$$\delta \overline{GM}_{(10\text{ to }1)} = \frac{m(y_{10} - y_1)}{\Delta} \qquad (20)$$

From equation 5:

$$\delta \overline{GM}_{(10\text{ to }1)} = v - u \qquad (21)$$

From which Δ can be found:

$$\Delta = \frac{m(y_{10} - y_1)}{v - u} \qquad (22)$$

8. In stages 6 and 7 above the mass moment of inertia and the displacement have been found. Therefore

equation 2 can be used to find the metacentric height for any point on the ellipse for which the roll period is known, such as position 1.

From equation 2:

$$\overline{GM}_1 = \frac{4\pi^2 I'}{g\Delta T_1^2} \qquad (23)$$

9. The metacentric height at position 1 can be corrected to that of position 10, when the weights are at the same vertical height as the vessel's own centre of gravity, by adding the difference between v an u to $\overline{GM}_1$. This then gives the initial stability of the vessel, which is the principal objective of the calculation.

$$\overline{GM} = \overline{GM}_1 + (v - u) \qquad (24)$$

THE DIFFICULTIES OF IMPLEMENTATION

The calculation described above is clearly considerably more complex than that associated with the conventional inclining experiment. It can however be easily implemented as an algorithm for a spread sheet which takes as its input the size of the weights, their five relative positions, and the associated five periods of roll. The primary output is the metacentric height, $\overline{GM}$, but vessel's vertical centre of gravity, displacement, and effective mass moment of inertia are also results of the calculation.

An implementation of such a spread sheet has demonstrated that the calculation is valid when tested against the output of a mathematical model of the roll period of a vessel. This is only to be expected as both the model and the calculation are based on the equaition describing the period of roll (Equation 2). However attempts to use this procedure to evaluate the initial stability of a model barge in a test tank produced results which were quite unacceptable, with errors on occasion in excess of 100%.

The explanation for this can be found if consideration is given to the precision required in measuring the period of roll. By deliberately introducing an error into the spread sheet calculations the impact of inaccuracies in the period of roll can be assessed. Such calculations for a hypothetical vessel with a displacement of 5 tonnes, an initial metacentric height of 1 metre, and an effective mass moment of inertia of 10 tonne metres^2 were carried out, using weights with a combined mass moment in the order of 2.5 tonne metres. The resulting error in the calculation of the metacentric height depended on the sequencing of the individual errors for each weight position, in terms of a negative or positive error from the true period of roll. If each weight position is assumed to have either the maximum or minimum error, then there are 2^5 arrangements of errors for the five weight positions, and although many of these prove to have little impact on the final result the worst cases have a severe impact, as shown in Table 2 below.

Table 2: Example of Maximum Errors

Precision of observation (seconds)	Maximum error in $\overline{GM}$ (metres)
10^{-3}	0.055
10^{-2}	0.59
10^{-1}	490

As can be seen the precision required is in the order of one thousandth of a second for acceptable results to be obtained, and if a precision of only one tenth of a second is the best that is possible then the results can be ridiculous.

Unfortunately the difficulty in obtaining the period of roll with such precision is not one of measurement. An electronic inclinometer linked to a portable PC was used in the model tests mentioned above, and has also been used to measure the period of roll of a variety of small craft in a marina. The equipment was capable of recording the period of roll to an accuracy of 5 x 10^{-4} seconds, which is clearly adequate. The difficulty arises because of the vessels, when observed to this degree of accuracy, fail to perform in a consistent manner. Regrettably a rolling vessel is far from being a perfect signal generator. In the controlled conditions of the test tank results in the order of 10^{-2} seconds is possible, however in the marina trials even a precision of 10^{-1} seconds could not be counted upon. These results when compared with the table above are in keeping with the tank test results being in error by as much as 100%. They also suggest that implementation of the minimum observation procedure is not viable in practice.

Despite the unpromising outcome of the experimental trials, they do suggest alternative procedures that may prove workable. The errors indicated in Table 2 are the maximum possible error, given the specified level of precision in recording the period of roll. In reality the probability of obtaining such an error is quite small. Clearly if the number of observations were increased the likelihood of an error of these magnitudes affecting the final result would be decreased. The increased number of observations need not be used just to obtain a better average value for each of the five weight positions, but could include observations of additional

weight positions. This would necessitate a change in the calculation, but could be used to find both Equation 12 and Equation 16 by a least squares method. Such a procedure would be amenable to a statistical analysis to identify a confidence interval associated with the resulting calculation of the metacentric height. These ideas have not yet been fully explored but are the subject of ongoing research.

Before concluding it should be noted that even if these theoretical difficulties can be resolved the practical application of this procedure would require the introduction of relatively large moments when the pair of weights are shifted. The induced changes in the period of roll are dependant on the magnitude of the change in moment due to the mass of the weights and the distances they are moved. In their highest position the weights must not cause negative stability, therefore the maximum possible vertical moment is $\Delta\overline{GM}$. For practical reasons however, it is desirable to keep the moment to a minimum in order to avoid having to support large masses at positions remote from the deck and centre line. The two outboard positions are used to find the positions where T is the same as when the weights are high up on the centre plane. For this to be achieved by interpolation the experimental position must be further outboard than the required position for constant T. If this is not the case the required position will have to be extrapolated, so exaggerating any errors introduced to the data. If this requires the weights to be placed outboard of the vessel's bulwark, consideration will have to be given as to how the weights can be supported in the correct location. As it is clear that the weights will have to be a substantial proportion of the vessel's displacement, probably between one and ten percent, both their handling and accurate positioning dictate that this procedure can only be considered viable for small craft.

Conclusion

In this paper a procedure has been described whereby the metacentric height, vertical centre of gravity, and displacement of a vessel can theoretically be established without reference to the vessel's geometry, i.e. its lines or hydrostatic data. This is achieved be a direct calculation which uses as its only input the periods of roll, measured with computer assisted precision, as a pair of weights are moved to predefined locations on and above the deck. The basis of this procedure is that as the metacentric height and mass moment of inertia are changed in a systematic way, all the unknown variables in the basic equation for the period of roll can be evaluated.

The assessment of initial stability by this method is only necessary where the hydrostatic particulars of a vessels are not available, as if this information is to hand a conventional inclining experiment could be undertaken. However the large number of older fishing and other work boats around the world for which no record of lines or hydrostatics exists suggests that such a procedure could be considered, especially as national and international bodies increasingly include smaller vessels in their regulatory requirements. It will be necessary to assess the stability of these work boats in a manner which is both practically and economically viable, otherwise the owners will try to avoid regulation by working without certification, and therefore both illegally and unsafely.

The theory behind this procedure, demonstrated conceptually, has a certain elegance which may be pleasing to the naval architect. The surveyor however will question the practicality of locating substantial weights both above the deck, and away from the centre line, possibly even outboard of the vessel's bulwark. For this reason a detailed calculation has been suggested which minimises the number of locations for which observations of the period of roll are required. However experimental observations have indicated that the precision obtainable for the period of roll in the surveyors working environment would be liable to cause an unacceptable level of error. An extension of the procedure has been outlined that would enable the level of confidence in the result of the stability assessment to also be calculated. If future work can demonstrate that such a procedure is viable it should still be noted that this method can only be considered for small craft as the weights required must be in the order of five percent of the vessel's displacement. It is however the smallest of working craft for which records of hydrostatics are least likely to exist. These therefore are the very vessels for which an inclining experiment is not immediately possible, nor the cost of taking off the lines acceptable. Further work is being undertaken to develop the theoretical procedure described in this paper such that it is both economically acceptable and practically viable.

References

1. Marchaj, C.A. 'Seaworthiness - The Forgotten Factor'. Adlard Coles, London, 1986 (p. 128).
2. Surveyor General's Organisation. 'Code of Practice for Vessels up to 24 Meters Load Line Length'. HMSO, London, 1993.
3. Muckle, w. and Taylor, D.A. 'Muckle's Naval Architecture', 2nd edition. Butterworths, London, 1987.

WATER ACCUMULATION ON THE VEHICLE DECK OF A DAMAGED RO-RO VESSEL AND PROPOSAL OF SURVIVAL CRITERIA

By
D. Vassalos and O. Turan
The Ship Stability Research Centre, Department of Ship and Marine Technology
University of Strathclyde, Glasgow, UK

SUMMARY

Recent research at the University of Strathclyde culminated in the development of a numerical procedure for assessing the damage survivability of damaged Ro-Ro vessels and, using this as a basis, new survival criteria have been proposed and submitted to IMO. This paper presents the latest results of a fundamental study aimed at enhancing the insight into the flooding process and water accumulation on the vehicle deck of a Ro-Ro vessel during progressive flooding in waves, the emphasis here being on testing the said proposal. The investigation is based on a series of experiments using a scaled model of a typical Ro-Ro vessel. The matrix considered involves a range of ship design and environmental parameters in a number of simplified damage scenarios, starting with a fixed model and progressively introducing more degrees of freedom, building up to six degrees of freedom. The results of the experiments are presented and discussed, leading to recommendations concerning the validity of the proposed survival criteria.

INTRODUCTION

Concerted action to address the water-on-deck problem in the wake of recent well publicised Ro-Ro ferry disasters led to the proposal of new stability requirements, known as the *Stockholm Regional Agreement*, or more commonly as *SOLAS '90+50*, pertaining to compliance of existing Ro-Ro vessels with SOLAS '90 requirements whilst accounting for the presence of a maximum 0.5m height of water on the vehicle deck. In view of the uncertainties in the state of knowledge concerning the ability of a vessel to survive damage in a given sea state, an alternative route has been allowed which provides a non-prescriptive way of ensuring compliance, namely the "*Equivalence*" route, by performing model experiments in accordance with the requirements of IMO Resolution 14. An attractive alternative route to tackling the water-on-deck problem in a way that allows for a systematic identification of the most cost-effective and survivability-effective solutions has been introduced by the Ship Stability Research Centre (SSRC) at the University of Strathclyde, by making use of a mathematical/numerical model, developed and validated over the past years, describing the dynamic behaviour of a damaged ship in seaway whilst subjected to progressive flooding. This model was made the basis during the Joint North West European Project (JNWEP) for formulating and proposing rational survival criteria to deal with water on deck as part of the probabilistic procedure for assessing damage stability, [1]. A relevant paper was submitted to IMO and is currently being considered by the working group on harmonisation of probabilistic standards. In the developed mathematical model and the ensuing criteria the process of water accumulation on the Ro-Ro deck as well as the actual amount of water are dominant features. In this respect, an acceptably accurate model of water ingress/egress is a prerequisite to undertaking any investigations on damage survivability.

Deriving from the above, this paper presents and discusses results from the third series of an extensive experimental programme aimed at enhancing understanding and insight of this complex

phenomenon and of producing corroborative evidence to support the proposal of the JNWEP concerning probability of survival with water on deck, a brief introduction of which is given in the following before addressing the experimental programme and derived results.

PROBABILITY OF SURVIVAL WITH WATER ON DECK

The new damage stability framework proposed by the JNWEP is based on the probabilistic concept of survival. This means that the standard of survivability is expressed in terms of the probability that the vessel will survive, given a damage with water ingress has taken place. The total probability of survival depends on two factors: the probability that a compartment is being flooded and the probability that the vessel will survive flooding of that compartment. The concept itself is simple, but it takes a great deal of effort to establish correct formulation of these two factors, particularly when it involves large scale flooding of extensive undivided deck spaces such as the vehicle deck in Ro-Ro ferries. Concerning the latter and taking into account that there are many effects causing a vessel to capsize, the probability of survival can also be divided in two different factors: the probability to survive pure loss of stability, heeling moments, cargo shift, angle of heel and progressive flooding and the probability to survive water on deck as result of wave action.

The calculation of this last factor, referred to as survival factor with water on deck, s_w, is based on a concept whereby the critical wave height at which the vessel will capsize is found, and s_w will simply be the probability that this wave height is not exceeded. In this respect, the critical task has been to formulate a connection between the critical sea state and parameters which can be readily calculated without resorting to costly, time consuming numerical simulations or physical model experiments. For this reason all model tests and simulations have been directed towards this goal, and the result is presented in [1]. A key observation from this work is that vessel capsizal occurs close to the angle where the righting moment has its maximum, i.e. θ_{max}, calculated traditionally by using the constant displacement method and allowing for free-flooding of the vehicle deck when the deck edge is submerged. This fact, coupled with observations from physical model experiments and the experience amassed from studying large numbers of numerical tests led to the development of a "*Static Equivalent Method*" which allows for the calculation of the critical amount of water on deck from static stability calculations. To this end, a flooding scenario is considered in which the ship is damaged only below the vehicle deck but with a certain amount of water on the (undamaged) deck inside the upper (intact) part of the ship. The critical amount of water on deck is then determined by the amount causing the ship to assume an angle of loll (angle of equilibrium) that equals the angle θ_{max}.

Based on this, the volume of water on deck causing the vessel to assume an angle of loll (angle of equilibrium) that equals the angle θ_{max}, was compared with the critical volume of water at the instant of capsize and a good correlation was found. The scenario described above and depicted in Figure 1, is believed to represent closely observations of the flooding process near the capsize boundary or when a stationary (steady) state is reached with the water on deck elevated at an average height, *h*, above the mean water plane, as a result of the wave action and vessel motions. It was subsequently shown that this height is a unique measure of ship survival in damaged condition - the higher the water elevation the higher the sea state needed to elevate the water to this level and the higher the capsizal resistance of the ship - that could be applied universally to all the arrangements studied, involving ship size and shape, subdivision arrangements and loading conditions. It follows, that the relationship between h and Hs will also be unique for a given ship, thus allowing the survivability of the vessel to be expressed as a function of the critical significant wave height as denoted below:

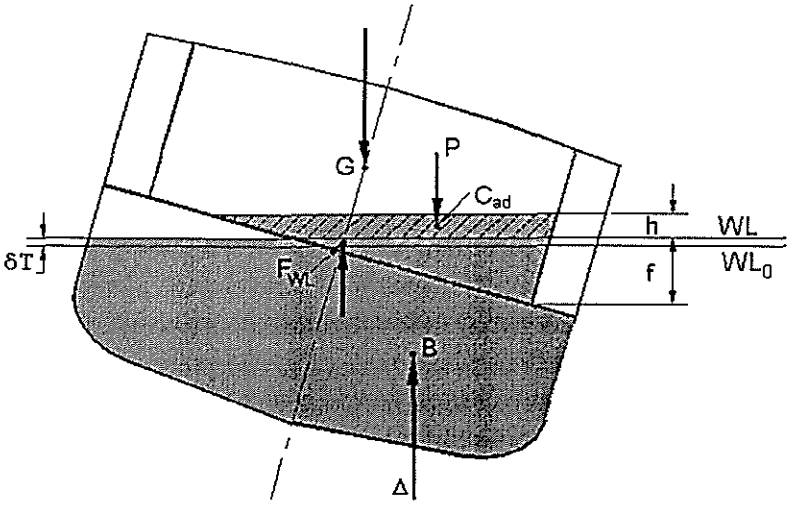

Figure 1: Stability of a Damaged Ship with Water Accumulated on Deck
(*Static Equivalent Method*)

$$h_{crit} = f(Hs) = 0.085\ (Hs_{crit})^{1.3} \qquad (1)$$

where, h_{crit} = the difference between the inner and outer waterline at the instant of capsize
Hs_{crit} = the critical significant wave height

Some additional data and a re-examination of the data presented in [1], showed that the effect of damaged freeboard had to be taken into consideration. This, in turn, led to the proposal of the following relationship, [2]:

$$h_{crit} = f(Hs, F) = 0.088\ (Hs_{crit})^{0.97+0.46F} \qquad (2)$$

At the time, it was conjectured that Hs is raised into some power other than unity as it was the significant wave height measured relative to the deck of the ship at the location of the damage opening in a way that accounts for the vessel motion (i.e., the significant relative wave height - incident) that was the parameter of interest rather than the nominal significant wave height.

EXPERIMENTAL PROGRAMME

Damage Scenarios and Test Conditions

To foster a better understanding of the water accumulation on Ro-Ro vehicle decks, a series of experiments has been planned and is taking place at the University of Strathclyde. In this paper the results of the third series of tests are presented, addressing the mean asymptotic height of floodwater on the vehicle deck *h*. The results of the first two series were presented in last year's workdhop. The additional parameters in the experimental matrix comprise wave characteristics, freeboard and KG involving the model in six degrees-of-freedom. The model used in these experiments is described in [4] and is a 1:42 scale model of a typical Ro-Ro vessel, the main particulars of which are shown in Table 1. There are two compartments open to the sea: the first is above the vehicle deck and extends from 22.25m to 97.25m from the aft perpendicular and the second between the double bottom and the vehicle deck with a length that was adjusted by inserting blocks of foam to

allow for changes in the damaged freeboard as shown in Table 2. Additional values for damaged freeboard could be obtained similarly.

Table 1: Main Particulars of the Ro-Ro Vessel Used in the Experimental Investigation

L_{BP}	(length between perpendiculars)	=	131.0 m
B	(breadth)	=	26.0m
T	(design draught)	=	6.10m
D	(depth to uppermost continuous deck)	=	18.8m
D_{bd}	(depth to bulkhead deck)	=	7.8m
D_{db}	(depth to double bottom)	=	1.6m
Δ	(displacement)	=	12200 tonnes
C_b	(block coefficient)	=	0.582

Table 2: Flooded Compartment Lengths

Length of Compartment (m)	Distance from A.P. (positive forward) (m)		Damaged Freeboard (m)
	Aft End	Forward End	
13.3	52.6	65.9	1.08
22.8	47.15	69.95	0.6
28.7	43.66	72.36	0.2

SERIES 3

In the third series of the experimental programme all three damaged freeboards of Table 2 have been considered but tests were undertaken only in irregular waves as specified in Table 4 and for damage scenario 3. Furthermore, in addition to the fixed, heaving only, rolling only and heaving and rolling modes of motion of series 1 and 2, water accumulation with the model freely drifting and capable of responding in six degrees-of-freedom is investigated in series 3. Three different loading conditions were also tested, corresponding to KG values of 9, 10, and 11 metres.

Presentation of Results and Discussion

Volume of Water on Deck

Considering this parameter, it is noteworthy that the trend observed in the previous two series, i.e., increasing the degrees of freedom results in lesser amount of water accumulated on deck is also clearly demonstratd in these results, as shown in Figure 2. Moreover, the influence of sway in affecting water accumulation deserves special attention.

Height of Water on Deck (h)

The difference between predicted and measured values concerning *h* was shown to decrease with increasing number degrees of freedom. In this respect, the measured *h* when the model is free to move in all degrees of freedom appears to be in reasonable agreement with that predicted by using

equation (1). This is shown in Figure 3, with the influence of sway being again noteworthy. In Figure 4, on the other hand, the predicted h using equation (2) is compared with the measured values for two freeboards. Again results do not appear to depend critically on freeboard in a way that clear trends emerge. More emphasis on clarifying this will be placed in the forthcoming seies 4 of this on-going experimental programme

CONCLUDING REMARKS

3ased on the results derived in Series 2, the following points are noteworthy:

- Restraining a model changes the flooding process appreciably and is not recommended, particularly when model is not allowed to sway freely.

- Corroborative evidence has now been produced in support of the proposed relationship between the seastate and the height of water on deck and of the probabilistic framework for assessing the damage survivability of passenger/Ro-Ro vessels, proposed by the NWEP.

REFERENCES

[1] Vassalos, D., Pawlowski, M. and Turan, O.: *"A Theoretical Investigation on the Capsizal Resistance of Passenger/Ro-Ro Vessels and Proposal of Survival Criteria"*, Final Report, Task 5, The Joint North West European R&D Project, March 1996.

[2] Jasionowski, A., Dodworth, K., Vassalos, D. *"Assessment of Survival Time of Damaged RO-RO Vessels"*, March 97.

[3] Letizia, L.: *"Damage Survivability of Passenger Ships in a Seaway"*, Ph.D. Thesis, Department of Ship and Marine Technology, University of Strathclyde, November 1996.

[4] DMI 88116: *"RO-RO Passenger Ferry Safety Studies Model Test for F10 - Final Report of Phase I"*, DMI Project Report to the UK Department of Transport, 1990.

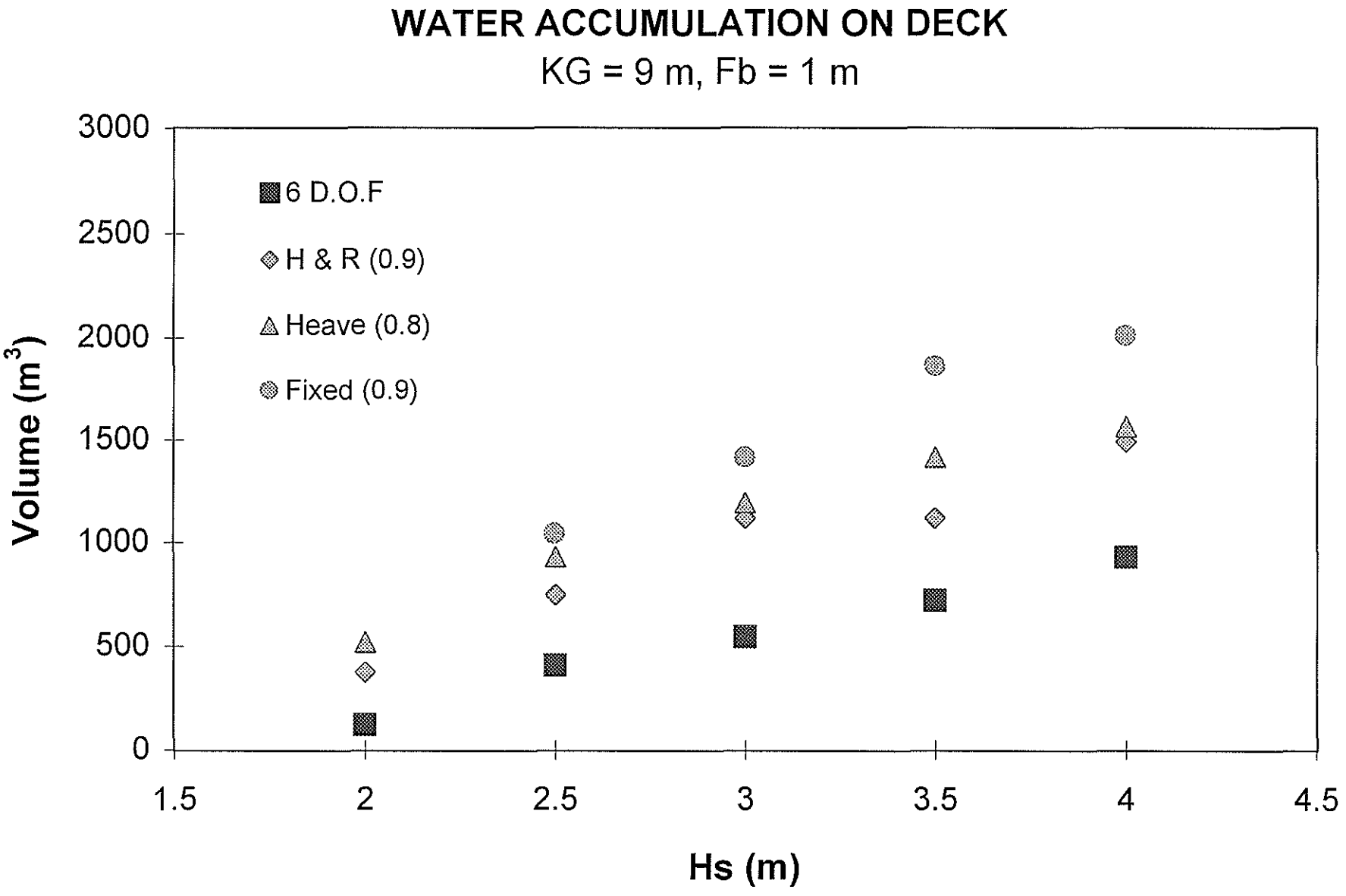

Figure 2: Effect of D.O.F. on Water Accumulation

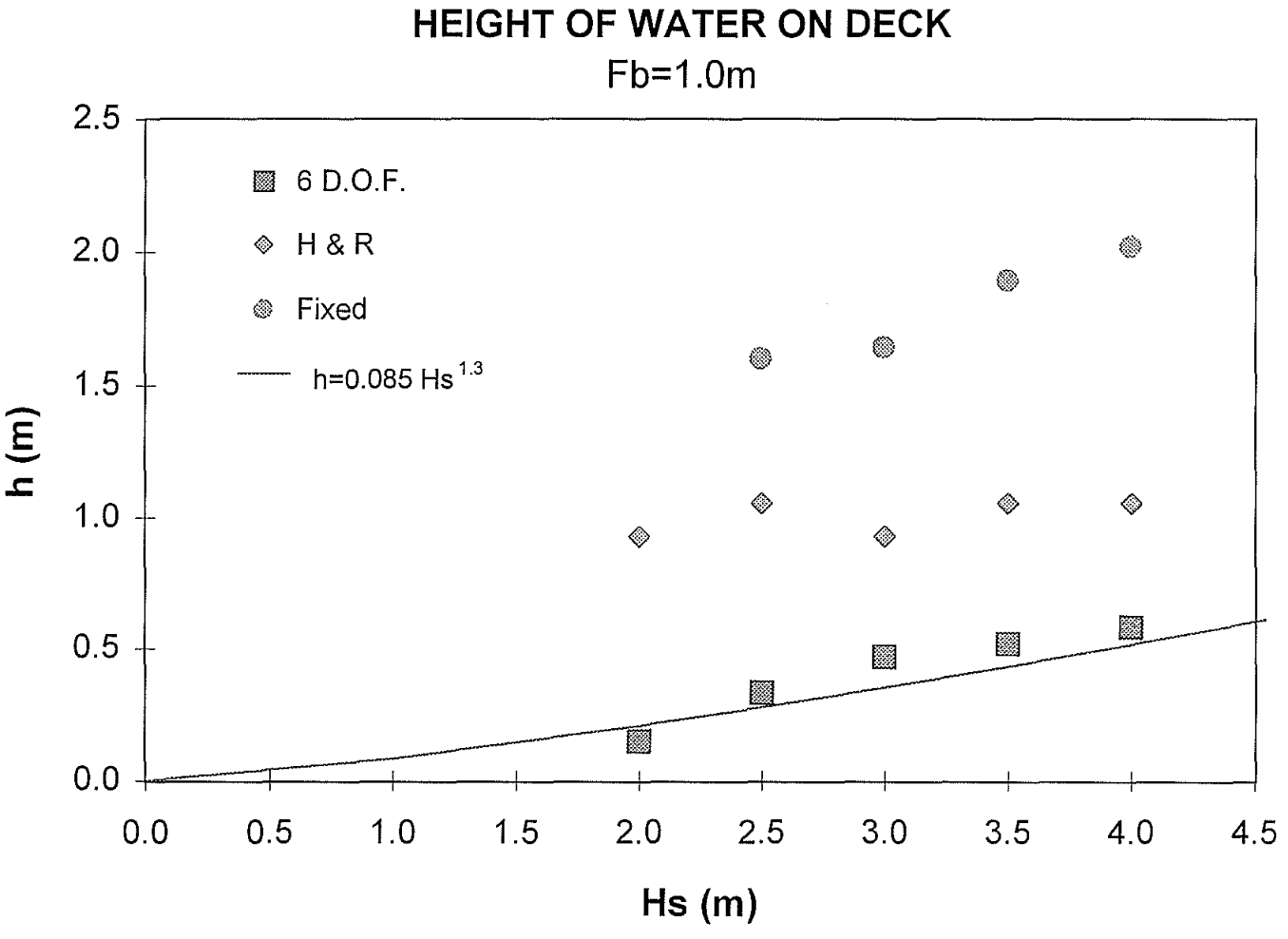

Figure 3: Effect of D.O.F. on Height of Water on Deck

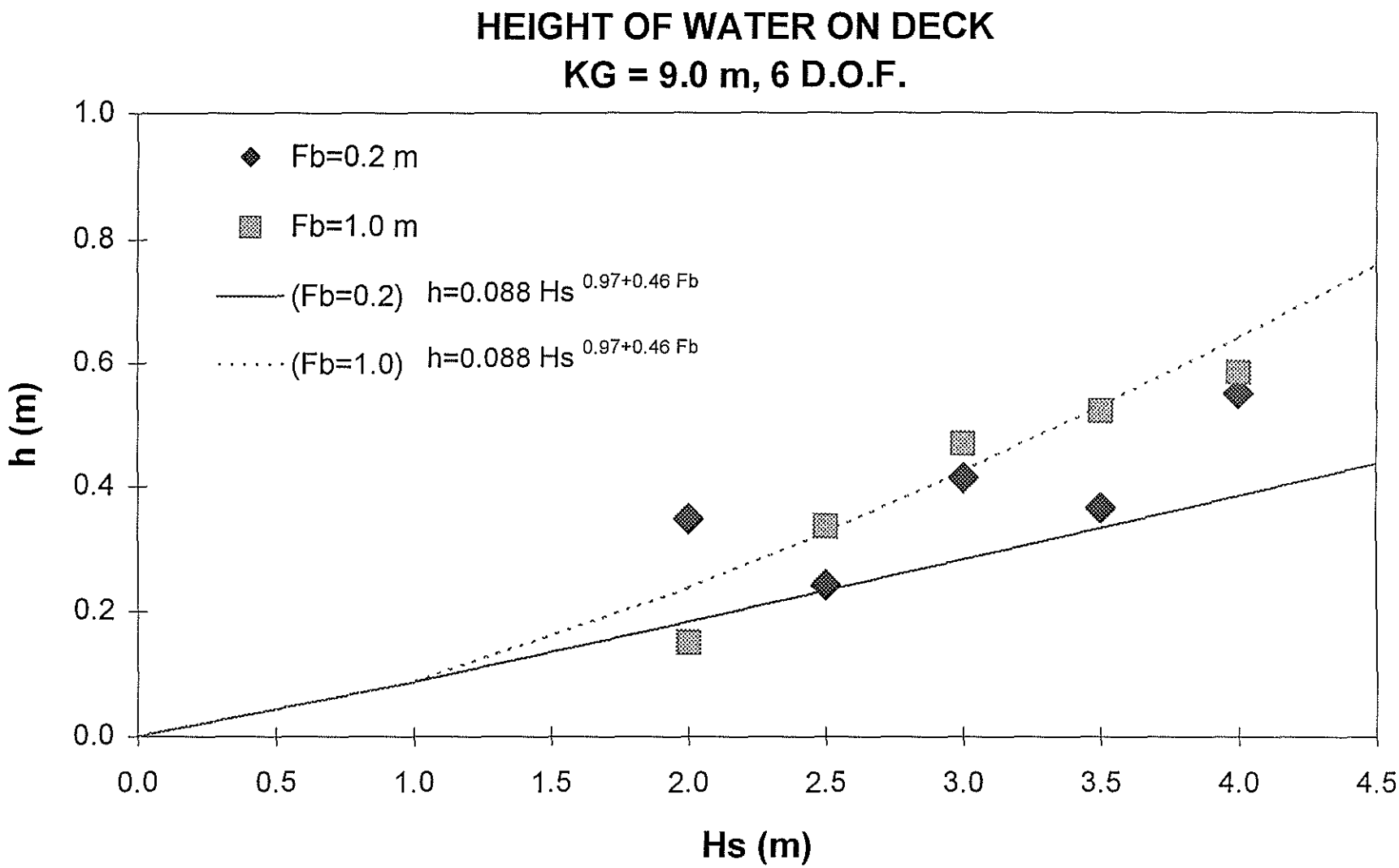

Figure 4: Effect of Freeboard on Height of Water on Deck

Exploration Of The Applicability Of The Static Equivalency Method Using Experimental Data

Andrew Kendrick[1], David Molyneux[2], Andre Taschereau[3], and Tom Peirce[4]

[1] Fleet Technology, Ltd;
[2] Institute for Marine Dynamics
[3] Transportation Development Centre
[4] Operational Dynamics

ABSTRACT

The Static Equivalency Method (SEM) developed by the Strathclyde University research team offers a simple predictor of capsize for a wide range of ship conditions. Data generated by Transport Canada's experiment program of capsize investigations was reanalyzed to investigate the validity of the predictor equations, and their range of applicability. Excellent agreement was found for cases in which the dynamic roll component of ship behaviour is small, and where internal sloshing is limited, in particular for ships with centreline casings. The SEM capsize predictor was also applied successfully to cases with freeing ports, though more work is needed to define water build-up under these conditions. Some limitations of the model predictions were highlighted, and potential sources of error identified.

Results of the project were used to provide recommendations as to how the SEM could be applied as a component of deterministic or fully probabilistic damaged stability criteria.

1. INTRODUCTION

The extensive international research which followed the ferry catastrophes of the 1980's and early 1990's led to the development of numerous proposals for ways in which safety could be enhanced in future operations. These included recommendations for new stability criteria, for design features and operational procedures. Under considerable time pressure, IMO introduced amendments to the SOLAS Convention in 1990, and then declined to make further global modifications in 1995, leading to a number of Northern European nations adopting by regional agreement their own, more stringent, requirements.

As is too often the case, the regulatory decisions were made before the researchers tasked with clarifying the issues had managed to fully disseminate, assimilate, and evaluate each other's results. In some cases, the fact that policy decisions were taken removed the support for continuing with promising research which had only yielded preliminary or inconclusive results. However, the Canadian government decided to persevere with its own program to try and provide explanations for some puzzling phenomena and indicate the most promising directions for future safety initiatives.

2. BACKGROUND

2.1 Transport Canada Research Program

Transport Canada initiated a multi-phase program of research in 1993 entitled, "Flooding Protection of RO-RO Ferries". The objective of the program was to examine the survivability of monohull RO-RO ferries, fitted with freeing ports, under various conditions of ferry loading, residual freeboard after collision damage amidships and the prevailing sea state.

Phase I of the program, which used a highly simplified model of a large Ro-Ro vessel was completed in March 1995 and a set of reports, with supporting data which confirmed the benefits of freeing ports, were provided to IMO and summarized [1] and [2] . Using the findings of Phase I and other available publications on RO-RO ferry capsize, Phase II investigated the relationships which describe the capsize phenomenon, using a more ship-shaped model of a smaller ferry. The results of this work are summarized in [3], [4] and [5], and were also provided in full to IMO. It noted that parameters other than those contained in the SOLAS 90 criteria appeared to provide better insight into safety than the SOLAS standards themselves.

Although Canada had decided to remain with the standard SOLAS 90 approach for the time being, it was recognized that both this and the SOLAS '90+50' option are imperfect predictors of safety. There was thus a continuing desire to develop a better understanding of the mechanisms causing capsizes involving water on deck, which are quite different from those which govern intact capsize under more extreme wave climates.

2.2 The Static Equivalency Method

The Static Equivalency Method (SEM) is based on a number of insights and hypotheses, some of which are common to other investigations of capsize, including the earlier phases of the Transport Canada project. References such as [6] provide more details of its workings.

It is presumed that it is the accumulation of water on the vehicle deck that causes the ship to capsize. The required capsize volume (or weight) of water on deck is assumed to be that which would cause the ship to loll to its angle of maximum GZ, θ_{GZm} , in the flooded condition. Any additional heel with this volume on deck, or any additional volume at the same heel angle, will create a larger overturning moment. This will be resisted by a smaller restoring moment. Thus, the ship will inevitably capsize.

The depth of water on deck at the critical condition corresponds to an elevation, h, above the mean external sea level, and this elevation can, in turn, be correlated with the significant wave height, H_S , through an empirical equation:

$$h = 0.085H_S^{1.3}$$

Kinetic wave energy is, in effect, transformed into potential energy.

It is assumed that the process is quasi-static, as the time frames associated with capsize are significantly longer than the wave or ship roll periods. Based on this assumption, dynamic effects do need to be accounted for either in the stability calculation approach or in the correlation of water elevation and wave height.

It is worth noting that the relationship given above has been modified, to include residual freeboard [7].

The new version is:

$$h = 0.088H_S^{(0.97+0.46F)}$$

where F is the residual freeboard.

The stability calculations needed to predict capsize water volume can be undertaken in several ways which should yield essentially identical results. None of these are 'standard' routines for commercial stability analysis software packages, but reprocessing of their normal output data allows the important quantities to be calculated with modest effort.

2.3 Project Objectives

The basic Static Equivalency Method, as outlined above, offers an appealingly simple means to predict capsize. However, the published descriptions of the method left a number of concerns, including:

i) the influence of relative motions on the accuracy of the results;
ii) the influence (if any) of sea spectrum;
iii) the influence of ship size and configuration;

iv) the ability of the method to represent adequately centre and side casing influences;
v) the potential for treating freeing port effects in the method.

As all of these variables had been explored (to varying degrees) in the Canadian experimental program. It was therefore hoped that the experimental data could be used, first, to check the basic validity of the SEM predictions, and then to examine some or all of these presumed second-order effects.

3. ANALYSES

3.1 Numerical Analyses

The predicted volumes of water associated with capsize were calculated as outlined in 2.2 above. The desired value of θ_{GZm} was first found from analysis of the damaged hulls from Phases I and II of the project. The "equilibrium" weight/volume of water on the car deck was then established for this (imposed) heel angle. Sinkage, deck edge immersion, and internal water level were supplementary outputs.

The well-known GHS program was been used for all calculations, and the basic hydrostatic calculations were checked against those from the Phase I and II projects to ensure that all input data was consistent with that used in earlier analyses. Most were within 0.1% of previous numbers. For the Phase II analyses, this was expected, as the identical data deck and program were used in both cases.

Since the SEM provides (sets of) predictions for any unique ship condition, numerical results were generated for all combinations of ship freeboard and KG which were tested in the experimental program.

3.2 Selection of Experiment Data Sets

The earlier phases of this project included considerable processing of the data traces to establish values for a number of parameters, whose influences were explored in the earlier work. In several cases, these were very similar parameters to those used in the SEM. However, they were not necessarily calculated in the same manner, or presented in an immediately useful format. The data was reprocessed to obtain a set of results aligned as closely as possible to the predictions of critical volumes, heel angles, and relative motions at the damage opening. These values were re-plotted over time periods of interest prior to capsize, and mean values the time intervals were calculated. The critical volume was picked as the highest steady volume, prior to a capsize.It was not always possible to obtain meaningful values for all of the parameters of interest, due to some data acquisition problems during the first phase of the work. Despite this, all phases of the project were found to have generated valuable data.

The data sets obtained during the earlier phases were reviewed to identify conditions expected to be most relevant to the testing of the static equivalency hypotheses. This was done both qualitatively (through the characteristics of the data traces) and quantitatively (through comparisons with the numerical analyses). Initially the selection of specific experiments was undertaken independently by the authors, searching on a variety of criteria. The resulting lists were then collated to produce an agreed set, which was confined to cases which the SEM has been developed to handle, i.e., fully-enclosed car decks, rather than those with bulwarks or open ends.

It was not considered necessary to reprocess many non-capsize runs, as the previous data analysis was expected to have provided representative mean values for the volume, heel, and motion parameters under safe conditions. However, some 'marginally safe' runs were re-examined, particularly where closely related capsize runs showed unexpected characteristics. Rapid capsizes were also excluded from reprocessing, due to the difficulty of identifying any specific critical point in the process.

3.3 Basic Capsize Prediction

As explained above, the Static Equivalency Method predicts wave height to cause a capsize by relating this to the buildup of water on deck, and assuming that the required volume on deck corresponds to the predictions of static stability calculations. Thus, the initial verification of the SEM considered its ability to predict the critical volume of water on deck and the corresponding wave height to cause a capsize. Secondly, heel angles and relative motions just prior to capsize were compared.

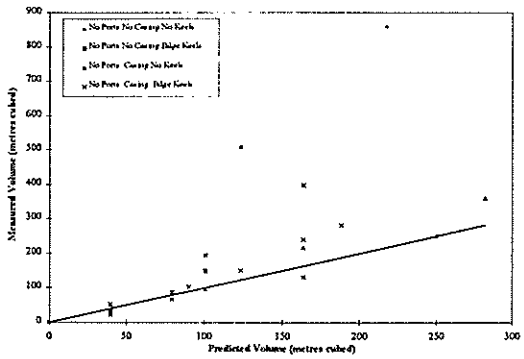

Figure 1, Phase II Volume Comparisons

Comparisons of predicted and actual volumes of water in capsize conditions for the Phase II model is shown in Figure 1. (Phase I results were similar.) As can be seen, the critical volume data shows some scatter about the expected lines, with a tendency to under predict the volumes at the higher values. Neither the scatter nor this under prediction was unexpected. As explained in [6], the capsize process is itself random in nature, and any model tests have some lack of precision. This work also observed an under prediction of survivability under conditions where the damaged ship has high residual stability.

Comparisons of measured and predicted volumes are an indication of the validity of the general methodology, but the most important question is, obviously, whether the method can accurately predict the sea conditions under which capsize can be expected to occur.

The predicted and measured capsize wave heights are compared in **Figures 2** and 3. In the experimental program, the significant wave heights were pre-determined and spaced sufficiently to obtain differences that were more than those obtained due to random nature of wave height. This provided two data points for each condition, the maximum significant wave height the model survived and the minimum significant wave height to cause a capsize. These data are shown in Figures 1 and 2 by diamonds and squares respectively. In cases where no capsize was observed during experiments, the measured data is shown with an arrow, to indicate that the capsize would most likely occur in higher waves. There were also cases where no survival was observed, and these are also marked with arrows pointing to lower wave heights.

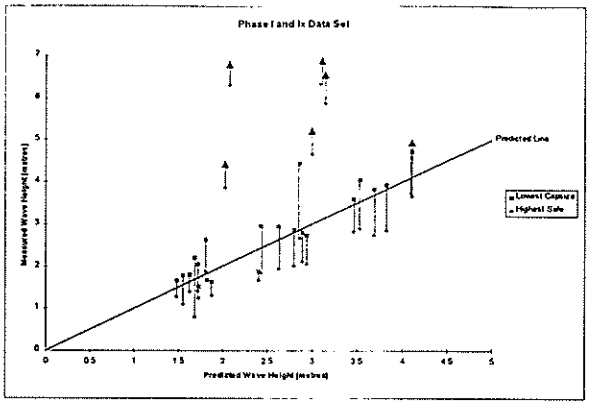

Figure 2: Predicted and Measured Capsize Wave Heights, all Phase I data

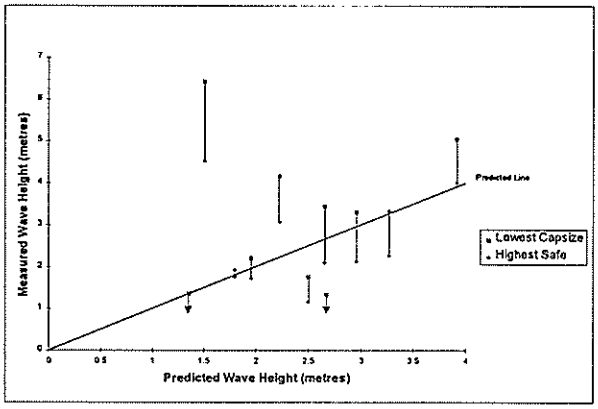

Figure 3: Predicted and Measured Capsize Wave Heights, Phase II

As can be seen, almost all the measurements bracket the predicted value for both models tested. This excellent correspondence between prediction and measurement is the key result of the project, as it demonstrates the SEM's ability to account for a range of variables in a single, simple approach to capsize prediction. The prediction capability holds good for both the large, simplified, and small 'realistic' models, answering another of the important questions regarding the method.

The data sets plotted here cover only cases with a centre casing; the set without casing is discussed at 3.4.

3.4 Effects of Supplementary Factors

Two of the factors within the SEM that the authors felt required further investigation were the regression equation linking internal water elevation and wave height, and the physical

meaning of the relationship. The capsize prediction capability appeared to provide a reasonable validation of the equation, but closer examination of the significant wave height and relative motion data indicated that the relationship was more complex than implied by the SEM's basic formula. Understanding this mechanism is important for applying the SEM to deigns outside the data set used to develop the method.

Figure 4 relates the Phase I motion data at the damage opening to the wave height, and shows that there is not a constant relationship between the two. Very similar results were observed in the original research which led to the development of the SEM. The resulting equation derived during the simulations for the SEM was

$$Hsr = 3.185\ Hs^{-0.69}$$

The values derived from the analysis of the experiment data were

$$Hsr = 3.125\ Hs^{-0.54}$$

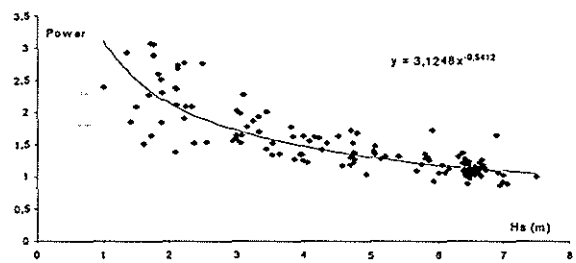

Figure 4: Regression on power p between significant height of relative motion $H_{sr} = H_s{}^p$ and significant wave height H_s for all data from Phase I. Average value of $p = 1.50$.

However, changing the formulation of the SEM to include the more complex relationship between Hsr and Hs does not significantly improve the accuracy of the predicted significant waveheight to cause a capsize. The factors modifying the influence of wave height thus remain somewhat unclear, and more extensive simulations and analyses of the phenomenon are likely to be needed to gain further insights. It is possible that the heave and roll components of the relative motion need to be considered separately, and there is a certain amount of evidence from the test series that changes in roll amplitude have relatively little effect on performance, as will be seen from discussions below.

Freeing Ports

A considerable amount of effort was used in the earlier phases of the program to investigate freeing port effectiveness in preventing capsize. Several different configurations were used, including both flapped and permanently open ports. Compared to a fully enclosed deck, the first arrangement allows more outflow for the same inflow, while the second produces both more inflow and more outflow. Flapped ports will thus generally give greater safety than permanent ports, although there are doubts about how reliable most designs would prove in actual service.

Experiments with open freeing ports were reanalyzed, with the main focus on flapped ports. The SEM was not originally intended to account for either option, though it appeared probable that it could be modified relatively easily to investigate flapped ports. Comparing the results with those for the same basic ship conditions, as shown (for example) in Figure 5, the following observations were made:

a) the volumes of water associated with capsize are essentially the same as those for the basic condition (and show even less scatter from the predicted line);
b) the wave heights at capsize for flapped freeing ports are much higher, while those for the permanent openings are more ambiguous.

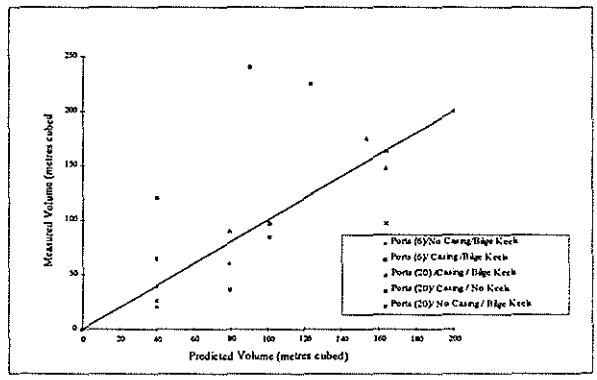

Figure 5: Phase II Volume with Ports

Unfortunately, although the first observation suggests that the basic SEM should remain applicable, insufficient time and resources were available within the project to develop a revised formulation for the wave height/water elevation relationship to account for the ports. This could probably be based on the types of inflow/outflow balancing originally proposed by Hutchison [8], but taking better account of the responses of the ship and the port flow characteristics.

Other variables investigated in the Phase I and II projects which were expected to have some influence on the capsize performance included casing location, presence/absence of bilge keels, and sea spectrum. Points associated with these conditions are identified in Figure 1 and help illustrate the results discussed below.

Sea Spectrum

A very limited number of runs were made with a spectrum other than JONSWAP, and only the most tentative of conclusions can be drawn from the data. In the two conditions tested with an ITTC spectrum, the model capsized at a higher wave height than with JONSWAP. Unfortunately, no otherwise identical conditions were tested with two spectra of equivalent significant waveheights, but it appears from the results of the non-capsize runs that the volumes of water which built up were less for any given wave height when the ITTC spectrum was used. This was an expected result, as the energy distribution of the two spectra at a given wave height differs significantly, with JONSWAP's being higher at frequencies which produce relative motions of the ship.

As one of the underlying hypotheses of the SEM is that wave energy outside the ship transforms into potential energy raising the internal water level, the regression formula defining this would also be expected to change. However, there is insufficient data to attempt to construct a new relationship at this point. The JONSWAP spectrum is representative of coastal conditions, where most collision damage is likely to occur. Therefore the relationship used in the basic SEM, which is conservative, is considered to be appropriate for most applications.

Bilge Keels/Roll Motion

The experiments in Phase II treated bilge keels fitted as the standard condition, but included a small number of runs without keels. There does not appear to be anything in the data to suggest that the build-up of water between the with and without bilge keel conditions followed different relationships, although there was some difference in relative motions due to the increase in roll motion, when the bilge keels were removed. It appears from results of these and other analyses that the SEM is relatively insensitive to the roll component of motion, as is real risk of capsize.

Casing Influences

The SEM predicts differences in the behaviour of ships with side, centre, or no casings, based on the differences in damaged hydrostatics. The test programs did not consider side casings, but devoted considerable attention to the influence of centre casing versus no casing. In general, the Canadian work indicated that no casing conditions had more survivability than conditions where the casing was present, but there were no obvious ways of quantifying the expected degree of performance improvement.

Figure 1 shows some of the differences between casing and no casing results on the standard SEM volume plots. These appear to show that there is relatively little difference between the two configurations when critical volumes are small, but much greater divergences for larger volumes when dynamic effects become significant. The magnitudes of divergence found in the experimental program for "no casings" cases were significantly larger than from previous numerical simulations [6]. The reason for this is unclear, though it may be that the treatment of internal waves in the simulation needs further refinement. This "sloshing" is a complex phenomenon, aspects of whose treatment are discussed in [9].

When dynamic effects become important, it is logical that they will be more beneficial when the flow of water across the deck is unobstructed than when the casing retains it on one side. It is questionable as to whether this type of behaviour would actually have practical meaning, as the flow of water in a real damage event is likely to be restricted by vehicles on deck, etc. This would make it more likely that the response can be treated as quasi-static, and the potential for dynamic enhancements of stability can thus be substantially discounted. In other words, it may be non-conservative to explore ways of accounting for improvements when the centre

casing is not present. However, the effect certainly warrants further exploration from a theoretical standpoint.

4. DAMAGED STABILITY CRITERIA

4.1 Deterministic Approaches

The levels (and limitations) of accuracy of the SEM are considered to be acceptable for the capsize analysis of a fairly wide range of Ro-Ro ships, in comparison with other existing or proposed methods. However, its use would involve a rather different type of criteria than those currently found in SOLAS, which would accept that safety levels for these specialized ships can be matched to expected conditions. Since the SEM matches the vessel characteristics against capsize significant wave height, the wave climate for the route needs to be known, and an appropriate limiting value needs to be selected. This limit could be selected using a variety of approaches.

One might be to compare the predicted performance of a design against other vessels assessed as being satisfactory against current criteria. Here it would only be necessary to assess all the vessels against their operational wave climates. If the "successful" designs could withstand (say) an average of 80% of the 20 year maximum wave height, then this could provide a basis for the evaluation of the questionable design. Obviously, this approach would requires the analysis of a range of ships using the SEM to establish an appropriate evaluation baseline.

4.2 Probabilistic Considerations

There is general acceptance that future stability criteria should include a much more rational treatment of risk - i.e. the probability and consequences of incidents - than existing standards. In the case of ferry stability, this should in principle consider not only the wave climate (which is relatively easy to define), but also the joint probabilities of damage (location and extent), loading condition, residual capability (e.g. the ability to keep any hole on the less dangerous leeward side), and other significant parameters. An advantage of the SEM approach is that it offers an ability to generate directly comparable results for any initial damage configurations, and thus to construct a meaningful component of any desired safety index.

5. CONCLUSIONS

The results of the two experimental phases of this program compared very well with the predictions of the Static Equivalency Method for most, though not all, of the conditions investigated. This ability of the SEM to work well over a range of ship forms and conditions means that it can provide a superior correlation with ship survivability over the current SOLAS criteria, and over any of the other simplified methods which have been published to date.

The SEM has some shortcomings, the most significant of which are summarized below. None is considered to invalidate the overall conclusions reached above, but all warrant additional investigation to enhance the current version of the method.

The method does not take full account of dynamic effects, which appear to be of increasing importance when capsizing a ship with good inherent damaged stability and when no casing or other obstructions are present to restrict the flow of water across the deck. The method errs on the side of conservatism, and so the consequences may be acceptable from a regulatory or initial design standpoint. Since the detailed numerical simulations of capsize on which the simplified SEM is based do appear to track all model test data, either model tests or simulations could be used by designers and owners to justify a relaxation in the criteria where appropriate.

The SEM is based on the relationship between static head, h, and relative motion, Hsr. Relative motion was first defined as a function of waveheight and later as a function of waveheight and residual freeboard. We should note that these two equations give different probabilities of survival. The first equation will give a 50% probability, whilst the second predicts the ship will survive for one hour. Based on the results of model experiments and simulations, it appears that relative motion is a more complex function than waveheight alone. Preliminary investigation of the data in this paper does not show a better fit to the more

complex equation than to the simple one, and so was omitted from this presentation.

In order to develop the SEM further, it may be necessary to get a better definition of the relationship between h and Hs. Physical model data alone is not sufficient for modifying this relationship with confidence. The combination of numerical simulation and physical model experiments for validation seems to be a more logical way to proceed.

The original data on the SEM does not quantify the amount of scatter in the predicted boundary between survival and capsize. This is a concern for its use in a deterministic analysis of stability, where it is important that the criteria be set near the upper bound of potential capsize behaviour. The modified version is based on a pre-determined probability of survival in a given time, which partially addresses this concern.

The effectiveness of freeing ports cannot yet be quantified using the SEM, although a promising line of approach to this has been identified. This could be carried forwards analytically, though it is probable that additional numerical simulations would also be required to bring the work to a conclusion.

ACKNOWLEDGEMENTS

The authors would like to thank Transport Canada, Ship Safety Branch and Transportation Development Centre for sponsoring this work, along with the Institute for Marine Dynamics and the Canadian Ferry Operators Association, who provided additional support.

We would especially like to acknowledge the contributions made by Prof. M. Pawlowski, from the University of Gdansk, who was working in North America at the time this analysis was carried out, as well as Mariusz Koniecki and David Cumming, who also made significant contributions to the work. In addition we would like to thank the numerous members of staff of the Institute for Marine Dynamics, Fleet Technology Limited and Polar Design Associates who all contributed to this project.

REFERENCES

[1] "Flooding Protection of Ro-Ro Ferries, Phase I", (Volumes 1 and 2), TP12310E, March 1995

[2] Stubbs, J. T. et al "Flooding Protection of RO-RO Ferries" Spring Meetings, RINA, 1996.

[3] "Flooding Protection of Ro-Ro Ferries, Phase I extension", (Volumes 1 and 2), TP12581E, October 1995

[4] "Flooding Protection of Ro-Ro Ferries, Phase II" TP12991E, March 1997

[5] Molyneux, W. D. et al "Model Experiments to Determine the Survivability Limits of RO-RO Ferries", Trans. SNAME, October, 1997.

[6] Vassalos, D. et al, "Dynamic Stability Assessment of Damaged Passenger/Ro-Ro Ships and Proposal of Rational Stability Criteria"; Marine Technology, October 1997

[7] Vassalos, D. et al "Time Based Survival Criteria for RO-RO Vessels", Spring Meetings, RINA, 1998.

[8] Hutchison et al, "Time Domain Simulation and Probability Domain Integrals for Water on Deck Accumulation", Cybernautics 1995, SNAME

[9] Z. J. Huang and C. C. Hsiung, "Experimental Study on Wave Motion Inside a Damaged Ship Compartment", Ocean Engineering International, 1997.

Analytical Studies for Water on Deck Accumulation

Maciej Pawlowski, Professor at Technical University of Gdansk
Mariusz Koniecki, Canadian Coast Guard, Fleet Services
Michel Barbahan, PhD student at Technical University of Gdansk

ABSTRACT

A mathematical model is presented for the accumulation of water on the vehicle deck of a damaged ro-ro vessel. The model leads to a simple relationship between the mean depth of water accumulated on deck, freeboard at opening (including negative freeboard) and significant height of relative motion due to heave. The two characteristic values may potentially help with the identification of the so-called point of no return for a damaged ro-ro vessel.

1. Introduction

Described in this paper are the efforts to develop a simple mathematical model for water accumulation on the vehicle deck of a damaged ro-ro ship. The theory is much the same as presented in Reference [1] but the results obtained are quite different, though the same model for water ingress has been used in both cases, as described in References [2–5]. The paper makes use of the pressure head formulation—as termed in Reference [1]—for flow rate through opening, the same as through a weir.

2. Relative motion

Consider a ro-ro ship inclined to a quasi-static angle of heel by water accumulated on the vehicle deck, as shown in Figure 1. In such a case, because of the inseparable free surface effect and a large reduction of the metacentric height, roll motion is strongly subdued and the ship can be regarded as having almost no roll at this position, performing chiefly heave in beam irregular seas. In terms of relative motions, the ship can be regarded as stationary. Therefore, the same mathematical model for accumulation of water on deck can be adopted as that developed by Hutchison for a stationary ship [1]. The only difference is that the significant wave height H_S should be replaced by a significant height of relative motion at opening H_{Sr}. The relative motion is the difference between wave elevation (at the opening) and vertical displacement of

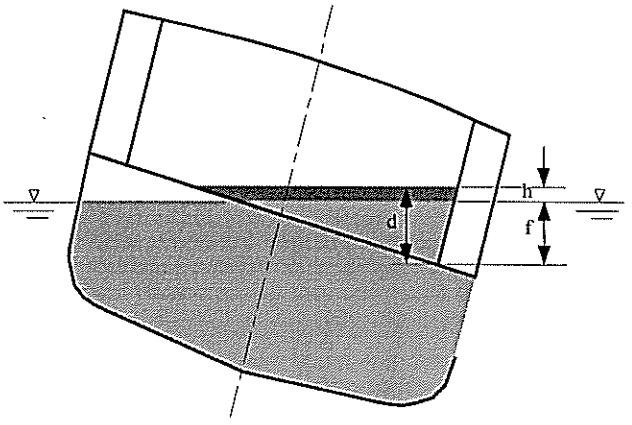

Figure 1. A damaged ro-ro ship at the point of no return

the ship, resulting both from heave and roll. Although the latter is small, it contributes significantly to relative motion, owing to large breadth of the ship.

The significant height of relative motion H_{Sr} is mainly a function of significant wave height H_S, affected also (to some extent) by tuning factors for heave and roll, described by the ratio T_o/T_z and T_o/T_ϕ, where T_z is the natural heave period, T_ϕ is the natural roll period at the point of no return, and T_o is the modal period of irregular waves. If the modal period T_o was constant, then H_{Sr} would be strictly proportional to H_S for given tuning factors. This is not the case since T_o is proportional to $H_S^{0.5}$. Therefore, H_{Sr} is a non-linear function of H_S, as shown in Table 1.

Table 1. A typical relation between significant height of relative motion H_{Sr} and significant wave height H_S.

H_S (m)	1,5	2	3	4	5	6,5
H_{Sr} (m)	2,6	3,9	5,2	5,5	5,5	5,3

For practical applications, H_{Sr} can be considered as a function of H_S only, as the effect of tuning factors is not strong. The best fit of experimental data is normally achieved by a power formulation $H_{Sr} = H_S P$, where the exponent p = 1.3 has been found by regression [4] and assumed to be constant for the sake of simplicity. All experimental data show, however, that the exponent p does depend on H_S, as shown in Figure 2 and Figure 3.

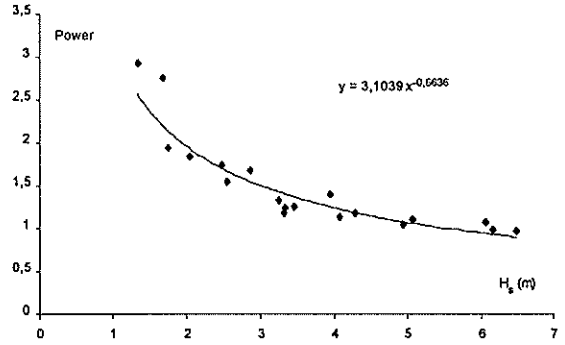

Figure 2. Regression of power p on H_S according to IMD's data, Canada, Ref. [6]. Average p = 1.49.

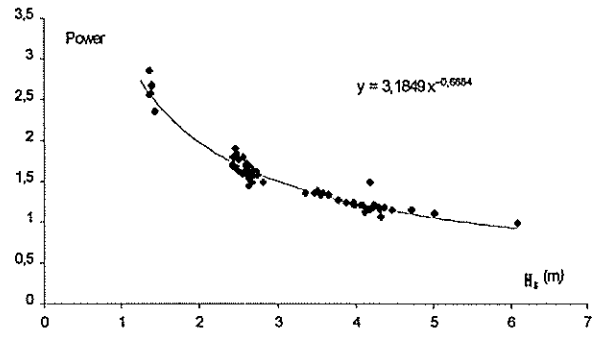

Figure 3. Regression on power p according to DMI data, Denmark. Average p = 1.54.

There is a surprising agreement between the IMD and DMI data—the two regression lines are almost identical, although they were derived for different ships at different experimental facilities. The p exponent for the two regression lines can be very well approximated by the equation

$$p = 3.144\, H_S^{-0.676}$$

where H_S is in meters. The average value of p for these data equals roughly 1.5, instead of 1.3 which is the effect of various regressions employed.

To improve further regression of H_{Sr} on H_S, the tuning factors for heave and roll motion would have to be accounted for. For practical application, however, the exponential formulation is sufficient enough.

3. Basic flow model

At each instant the flow rate of water through opening is given by the relationship

$$Q = (\operatorname{sgn} H)\, cb\sqrt{2g}\left(\tfrac{2}{3}|H|^{3/2} + d_1|H|^{1/2}\right) \qquad (1)$$

where: c – correction coefficient for non-stationary flow and resistance established experimentally
b – width of opening,
g – acceleration due gravity,
$H = \zeta - h$ – relative distance between wave profile and the free-surface at opening (positive if wave exceeds the level of water inside the ship),
d – depth of water at opening, and
d_1 – height at opening with water on both sides. The height $d_1 = d$ if $H > 0$, otherwise $d_1 = \zeta - f = d - |H|$ (the instantaneous draught of the deck edge at opening), but not less than zero.

In general, ζ is relative wave elevation, h is a height of free surface of water on deck above sea level, and f is freeboard at opening understood as distance between the deck edge and sea level, measured at the centre of damage at the inner shell of wing spaces, if any (+ if the deck is above sea level and – if it is below)—see Figure 1. For negative freeboard f, shown in this figure, the height of the free-surface on deck above sea level, h, is the same as elevation of water on deck above sea level (water head). By definition, $h > f$. The difference h and f can be interpreted as depth of water on deck, d, measured at the centre of damage at the inner shell of wing spaces, if any. Hence, $d = h - f$.

The first term in Eq. (1) is the same as for a weir, whereas the second corresponds to the flow rate

through opening in the dam below the water level. At a given instant there is either inflow of water on deck with the rate:

$$Q_{in} = \tfrac{2}{3} cb\sqrt{2g}\left(1.5\,d\,H^{1/2} + H^{3/2}\right) \qquad (2)$$

if $\zeta > h$, or outflow with the rate:

$$Q_{out} = \tfrac{2}{3} cb\sqrt{2g}\left(1.5\,d\,|H|^{1/2} - 0.5\,|H|^{3/2}\right) \quad (3)$$

if $\zeta < h$, where $|H| = h - \zeta$. A value of ζ in Eq. (2) cannot be greater than a height of the upper edge of opening above sea level measured at the centre of damage, D, while in Eq. (3) — smaller than the freeboard at opening f. If $\zeta > D$ then

$$Q_{in} = \tfrac{2}{3} cb\sqrt{2g}\left[1.5dH^{1/2} + H^{3/2} - (\zeta - D)^{3/2}\right] \quad (4)$$

If $\zeta < f$, the quantity $|H|$ in Eq. (3) assumes a maximum value $h - f = d$ and the expression in the parenthesis reduces to $d^{3/2}$. Hence, Q_{out} is then constant and independent of ζ.

4. Average global flow rate

In applications it is handy to use the flow rate averaged with respect to time, denoted by Q_{av}. If the time of averaging is long enough, then the mean value of the time averaged Q_{av} can be replaced by averaging with respect to the relative wave elevation ζ. Hence, the mean averaged flow rate through opening is given by:

$$\overline{Q} = \int_h^\infty Q_{in}\,d\zeta - \int_{-\infty}^h Q_{out}\,d\zeta \qquad (5)$$

where the first integral is $\overline{Q}_{in}$—average inflow rate, while the second one is $\overline{Q}_{out}$—average outflow rate. Applying Eqs. (2–4), yields

$$\overline{Q}_{in} = \frac{2}{3} cb\sqrt{2g}[1.5d\int_h^D H^{1/2} f(\zeta)d\zeta + \int_h^D H^{3/2} f(\zeta)d\zeta + \int_D^\infty [H^{3/2} - (\zeta - D)^{3/2}] f(\zeta)d\zeta]$$

$$\overline{Q}_{in} = \frac{2}{3} cb\sqrt{2g}[1.5d\int_h^\infty H^{1/2} f(\zeta)d\zeta + \int_h^\infty H^{3/2} f(\zeta)d\zeta - \int_D^\infty (\zeta - D)^{3/2} f(\zeta)d\zeta] \qquad (6)$$

$$\overline{Q}_{out} = \frac{2}{3} cb\sqrt{2g}[d^{2/3}\int_{-\infty}^f f(\zeta)d\zeta + 1.5d\int_f^h |H|^{1/2} f(\zeta)d\zeta - 0.5\int_f^h |H|^{3/2} f(\zeta)d\zeta] \qquad (7)$$

Since depth of water d at opening is constant over a period of time, it can be taken in front of the integrals. If height of opening is unlimited in the vertical direction (i.e., if $D \to \infty$), then the last integral in Eq. (6) vanishes. Hence, the following finally result for the average inflow and outflow rates:

$$\overline{Q}_{in} = \frac{2}{3} cb\sqrt{2g}[1.5d\int_h^\infty H^{1/2} f(\zeta)d\zeta + \int_h^\infty H^{3/2} f(\zeta)d\zeta] \quad (8)$$

$$\overline{Q}_{out} = \frac{2}{3} cb\sqrt{2g}[d^{3/2} F(\zeta = f) + 1.5d\int_f^h |H|^{1/2} f(\zeta)d\zeta - 0.5\int_f^h |H|^{3/2} f(\zeta)d\zeta] \qquad (9)$$

where $H = \zeta - h$ while $f(\zeta)$ and $F(\zeta)$ are the normal distribution density and cumulative distribution of the relative wave elevation ζ. The normal distribution density is given by

$$f(\zeta) = \frac{1}{\sqrt{2\pi}\,\sigma} e^{-\frac{1}{2}\left(\frac{\zeta}{\sigma}\right)^2}$$

where $\sigma = H_{sr}/4$ is the standard deviation (dispersion) of the relative wave elevation ζ. Integrals occurring in Eqs. (6–9) are valid for any freeboard, both positive and negative. The averaging process applied above is correct if freeboard, depth of water on deck, both measured at opening, and height of water above sea level vary slowly in the course of time which is true when a large scale flooding occurs through a relatively small opening—a typical situation for ro-ro vessels in a damaged condition.

Introducing the nondimensional random variable $t = \zeta/\sigma$, the following is obtained for the mean inflow and outflow rates:

$$\overline{Q}_{in} = Q_o q_{in}$$
$$\overline{Q}_{out} = Q_o q_{out} \qquad (10)$$

where Q_o is a constant, given by

$$Q_o = \tfrac{2}{3} c\sqrt{2g} b\sigma^{3/2} \qquad (11)$$

corresponding to flow rate through a weir of breadth b and depth of water σ at the weir, while q_{in} and q_{out} are nondimensional mean flow rates, given by

$$q_{in} = 1.5\tau \int_{t_1}^{\infty} (t - t_1)^{1/2} f(t)dt$$
$$+ \int_{t_1}^{\infty} (t - t_1)^{3/2} f(t)dt \qquad (12)$$

$$q_{out} = \tau^{3/2} F(t = t_0) + 1.5\tau \int_{t_0}^{t_1} (t_1 - t)^{1/2} f(t)dt$$
$$- 0.5 \int_{t_0}^{t_1} (t_1 - t)^{3/2} f(t)dt \qquad (13)$$

where: $f(t)$ and $F(t)$ – standard normal density function and cumulative distribution of the nondimensional relative wave elevation $t = \zeta/\sigma$;
$t_o = f/\sigma$ – nondimensional freeboard at opening;
$t_1 = h/\sigma$ – nondimensional height of the free surface on deck above sea level;
$\tau = d/\sigma$ – nondimensional depth of water on deck at opening, $\tau = t_1 - t_o$.

The mean net inflow rate $\overline{Q} = \overline{Q}_{in} - \overline{Q}_{out}$ can be presented finally in a short form:

$$\overline{Q} = Q_o (q_{in} - q_{out}) \qquad (14)$$

The two quantities q_{in} and q_{out} reflect the effect of random variations of water elevation at opening on the resultant mean flow rates. The integrals in Eqs. (12) and (13) represent moments of the order of 0.5 and 1.5 of the density function $f(t)$ with respect to $t = t_1$. These moments can be easily calculated by numerical integration, either directly or by applying the substitution $dF = f(t)dt$, and terminating integration for the inflow case when $t \approx 3.3$ or $F \approx 0.9995$. The quantities q_{in} and q_{out} are well defined since the freeboard at opening f and the height of water on deck above sea level h are known at each position of the damaged ship—see Figure 1, and the same applies to their nondimensional counterparts $t_o = f/\sigma$ and $t_1 = h/\sigma$.

With the help of moments of the density function $f(t)$, Eqs. (12) and (13) for the nondimentional flow rates can be further abbreviated, namely

$$q_{in} = 1.5\tau\, q_{0.5}(t_1) + q_{1.5}(t_1) \qquad (15)$$

$$q_{out} = \tau^{3/2} F(t_0) + 1.5\tau q_{0.5}(t_0, t_1)$$
$$-0.5 q_{1.5}(t_0, t_1) \qquad (16)$$

where, in general, moments of the order m are defined as follows

$$q_m(t_1) = \int_{t_1}^{\infty} (t - t_1)^m f(t)dt \qquad (17)$$

$$q_m(t_o, t_1) = \int_{t_o}^{t_1} (t_1 - t)^m f(t)dt \qquad (18)$$

As can be seen, since $\tau = t_1 - t_o$, both nondimensional flow rates q_{in} and q_{out} are functions of two variables. These are: $t_o = f/\sigma$ – the nondimensional freeboard at opening, and $t_1 = h/\sigma$ – the nondimensional height of the free surface on deck above sea level, where $t_o \le t_1$ and $t_1 > 0$. The variable t_1 can also be negative. Negative t_1 is, however, out of interest as it occurs when the ship is inclined beyond the angle of vanishing stability.

Moments of the standard normal density function $f(t)$ can be expressed by moments of the complements of the cumulative distribution function $1 - F(t)$ that are smaller by one order. Applying integration by parts yields

$$q_m(t_1) = m \int_{t_1}^{\infty} (t - t_1)^{m-1} (1 - F)dt$$
$$q_m(t_o, t_1) = \tau^m (1 - F_0) - m \int_{t_o}^{t_1} (t_1 - t)^{m-1} (1 - F)dt$$

5. Inflow moments

The nondimensional inflow rate q_{in} depends on two special functions of one variable $q_{0.5}(t_1)$ and $q_{1.5}(t_1)$. These are the moments of the order 0.5 and 1.5 of the standard normal density function with respect to $t = t_1$ for $t > t_1$, given by Eq. (17). Their values, obtained numerically, are shown in Table 2 and plotted in Figure 4. Excellent approximations of these functions up to about $t_1 = 3$ are polynomials of the 3rd degree, shown in this figure.

Besides regression, the inflow moments $q_m(t_1)$ can be approximated in a more analytical way, based on the mean value theorem. Namely, integration by parts in Eq. (17) yields

$$q_m(t_1) = \int_{F_1}^{1^-} (t - t_1)^m \, dF = [(t - t_1)^m F(t)]_{t_1}^{t_{max}} - \int_{t_1}^{t_{max}} F d(t - t_1)^m$$

Now, applying the mean value theorem to the integral yields a simple equation

$$q_m(t_1) \approx \delta^m [1 - F(t_1 + k\delta)] \qquad (19)$$

where: $\delta = t_{max} - t_1$ – practical extent of the integration range;
t_{max} – value of t for which $F \approx 1$, and
k – coefficient dependent on the moment $\in \langle 0, 1 \rangle$.

Table 2 Values of inflow moments q_m in terms of nondimensional height of free surface on deck above sea level $t_1 = h/\sigma$.

$t_1 = h/\sigma$	$q_{1.5}$	$q_{0.5}$	$t_1 = h/\sigma$	$q_{1.5}$	$q_{0.5}$
0	0.4300	0.4107	1.75	0.0131	0.0228
0.25	0.2951	0.3102	2	0.0066	0.0124
0.5	0.1952	0.2250	2.25	0.0032	0.0064
0.75	0.1241	0.1564	2.5	0.0014	0.0031
1	0.0756	0.1039	2.75	0.0006	0.0015
1.25	0.0441	0.0659	3	0.0002	0.0006
1.5	0.0246	0.0398	3.25	0.0000	0.0003

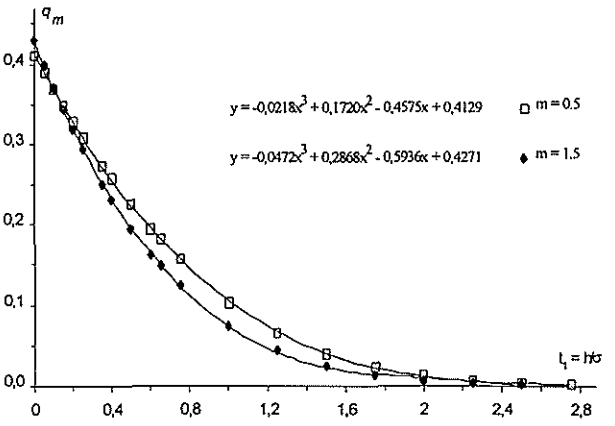

Figure 4. Inflow moments q_m for $m = 0.5$ and 1.5 versus nondimensional height of free surface on deck above sea level $t_1 = h/\sigma$.

The two constants t_{max} and k occurring in Eq. (19) can be found with the help of the least squares method. A value of $t_{max} = 2.7$ is assumed the same for all moments. On the other hand, the coefficients k is dependent on the moment, as shown in Table 3.

Table 3. Values of the coefficient k for moments of different orders m

m	k	m	k
.5	0.246	2.5	0.604
1	0.385	3	0.646
1.5	0.481	4	0.705
2	0.551	5	0.741

Equation (19) is amazingly accurate, as accurate as the approximations shown in Figure 4 — differences between the two types of approximations are invisible in this figure. Now, since the calculation of moments $q_m(t_1)$ is simple and accurate, the same applies to the nondimensional inflow rate q_{in}, given by Eq. (15). For a given value of t_1, q_{in} is a linear function of τ, starting at a value $q_{1.5}(t_1)$ for $\tau = 0$.

6. Outflow moments

As it can be seen from Eq. (16), the nondimensional outflow rate q_{out} depends on two special functions $q_{0.5}(t_o, t_1)$ and $q_{1.5}(t_o, t_1)$. These are the moments of the order 0.5 and 1.5 of the standard normal density function with respect to $t = t_1$ but for $t \in$

$\langle t_o, t_1\rangle$, as given by Eq. (18). The outflow moments $q_m(t_o, t_1)$ as functions of two variables are difficult to approximate by sheer regression. Fortunately, we can overcome this difficulty with the help of the mean value theorem. Integration by parts in Eq. (18) yields now

$$q_m(t_0,t_1)=\int_{F_0}^{F_1}(t_1-t)^m\,dF=[(t_1-t)^m F(t)]_{t_0}^{t_1}$$

$$-\int_{t_0}^{t_1}Fd(t_1-t)^m$$

Applying again the mean value theorem to the integral, we get

$$q_m(t_o, t_1) = \tau^m [F(t_o + \kappa_m\tau) - F(t_o)] \qquad (20)$$

where the factor $\kappa_m \in \langle 0, 1\rangle$. The expression in square brackets represents the area under the density function $f(t)$ between t_o and $t_o + \kappa_m\tau$. It is obvious that to get the same moment only part of the whole area can be located on the full lever τ. Contrary to the inflow case, the factor κ_m is no longer a constant—in addition, it is affected by the limits of integration t_o and t_1 which makes the approximation much more involved. In such a case, regression methods are of little use. To get versatile approximations, analytical methods have to employed.

One immediate possibility is to expand $f(t)$ in Eq. (18) into a series around $t = t_1$ and perform integration directly. We get

$$q_m(t_o, t_1) = \tau^m\left(\frac{f_1\tau}{m+1} - \frac{f_1'\tau^2}{m+2} + \frac{f_1''\tau^3}{m+3} \mp \cdots\right) \qquad (21)$$

where f_1, f_1' and f_1'' are the density function f and its derivatives f' and f'' calculated for $t = t_1$. Since $f'/f = -t_1$ and $f''/f = t_1^2 - 1$, therefore

$$q_m(t_o, t_1) = \tau^{m+1} f_1\left[\frac{1}{m+1} + \frac{t_1\tau}{m+2} + \frac{(t_1^2-1)\tau^2}{m+3} + \cdots\right]$$

The above approximation works well only for small τ. Much better results can be obtained with Eq. (20) if κ_m is approximated analytically. The easiest way, none the less still quite involved, is to compare the expressions for area inside the brackets in Eqs. (20) and (21).

$$f(1-\kappa) = \frac{f}{m+1}$$

$$f'(\kappa^2-1) + f\,2\kappa' = -\frac{2f'}{m+2}$$

$$-f''(\kappa^3-1) - f'\,6\kappa'\kappa + f\,3\kappa'' = c\frac{3!\,f''}{m+3}$$

where $1 - \kappa$, κ', and κ'' are the factor κ_m and its first two derivatives at $\tau = 0$ (notation $1 - \kappa$ for the initial value is used here just for convenience), while c is a coefficient to be established by regression. The above system defines the three initial quantities of κ_m

$$\kappa = \frac{m}{m+1}$$

$$2\kappa' = t_1\left(\frac{2}{m+2} + \kappa^2 - 1\right)$$

$$3\kappa'' = \left(t_1^2-1\right)\left(\frac{6c}{m+3} + \kappa^3 - 1\right) - 6t_1\kappa'\kappa$$

These quantities are obviously independent of τ and depend on m and t_1 only. For that reason, the factor κ_m can be approximated by a trinomial square:

$$\kappa_m = (1-\kappa) + \kappa'\tau + 0.5\,\kappa''\tau^2 \qquad (22)$$

where the initial value $(1 - \kappa) = 1/(m+1)$. A temporary guess for the fitting coefficient is 0.5. As can be seen, the factor κ_m is a function of all the three independent quantities. Despite the complexity, the parabolic approximation, with the coefficient $c = 0.5$, appears to be amazingly accurate, as illustrated in Figure 5.

Now, with the help of outflow moments, as given by Eq. (20), the nondimensional outflow rate q_{out} takes the form

$$q_{out} = \tau^{3/2}[1.5F(t_o + \kappa_{0.5}\tau) - 0.5F(t_o + \kappa_{1.5}\tau)] \qquad (23)$$

where the factors $\kappa_{0.5}$ and $\kappa_{1.5}$ are calculated by Eq.(22). Since $q_{out} < \tau^{3/2}$, therefore the expression in square brackets is less than 1 and the outflow rate can be finally presented in a short form $q_{out} = \tau^{3/2} F(t_o + \kappa_{out}\tau)$ where the factor κ_{out} is now a function of two variables t_o and t_1 and belongs to the interval $\langle 0, 1\rangle$. As can be seen, q_{out} is a non-linear function of τ, varying roughly as $\tau^{3/2}$. The highest value of t_o equals obviously t_1 for which τ and q_{out} vanish (no water on deck). On the other side, the smallest value of t_o

corresponds to a maximum asymptotic depth of water τ_∞ for which the mean outflow and inflow rates equalise. The asymptotic depth τ_∞ defines the aforementioned range of interest for flow calculations.

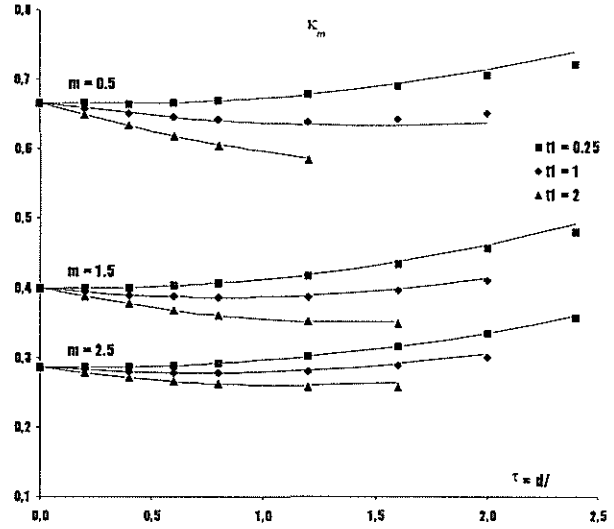

Figure 5. Factor κ_m and its parabolic approximation.

7. Asymptotic depth of water on deck

Asymptotic values of the nondimensional depth of water on deck at opening are obtained from the solution of the equation $q_{out} = q_{in}$. As follows from the previous discussion, given a value of $t_1 = h/\sigma$, the equation always yields a unique root for $\tau = d/\sigma$. Further, when t_1 approaches zero, then τ tends to infinity as the inverse of t_1. The asymptotic values of τ_∞ are shown in Table 4 and Figure 6. They were obtained numerically using exact values for q_{out} given by Eqs. (18). An excellent approximation for the nondimensional depth of water τ_∞ at the entire range of t_1 as shown in Figure 6, despite the singularity at zero. It is noteworthy that the quasi-static balance of water on deck can be achieved only for $t_1>0$.

The vertical segments between lines $y = t_1$ and $y = \tau(t_1)$ in represent the nondimensional freeboard t_0 (= $t_1 - \tau$) as a function of t_1. Hence, a point of intersection between the two lines determines point A with $t_1 \approx 0.6185$ in which freeboard f and its nondimensional counterpart $t_0 = f/\sigma$ change the sign (i.e., where the deck edge at opening immerses). Below point A, freeboard is negative and h is the same as elevation of water on deck above sea level, termed also as water head.

Table 4. Maximum mean nondimensional depth of water on deck $\tau = d/\sigma$ (at opening) versus nondimensional height of free surface on deck above sea level $t_1 = h/\sigma$.

$t_1 = h/\sigma$	$\tau = t_1 - t_0$	$t_1 = h/\sigma$	$\tau = t_1 - t_0$
0	∞	0,75	0,460
0,05	9,768	1	0,274
0,1	4,800	1,25	0,167
0,15	3,154	1,5	0,103
0,2	2,340	1,75	0,064
0,25	1,852	2	0,037
0,3	1,521	2,25	0,018
0,4	1,093	2,5	0,008
0,5	0,831	2,75	0,003

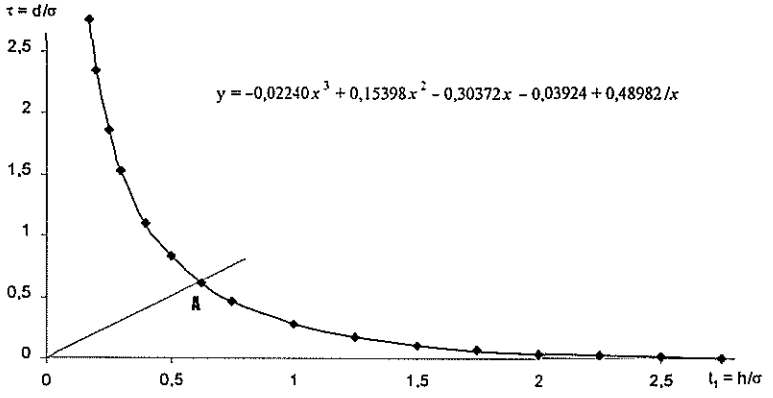

Figure 6. Maximum mean nondimensional depth of water on deck $\tau = d/\sigma$ at opening versus nondimensional height of free surface on deck above sea level $t_1 = h/\sigma$

8. Conclusions

In this paper, the problem of asymptotic depth of water on deck has been solved as a function of the height of the free surface on the deck above sea level non-dimensionalized with respect to the standard deviation of relative motion. As these two quantities are the key parameters in the Static Equivalency Method (Ref. 7), a major expansion of the method is now possible to include additional effects such as irregular dimensions of the opening, the presence of water draining devices, etc.. Now, it is also feasible to deal analytically with the fact that deck flooding is a random phenomenon and its mean value is not sufficient to describe it.

9. Disclaimer

The content of this paper reflect the views of the authors and not necessarily the official views of the Canadian Coast Guard.

10. Acknowledgements

The authors would like to thank the Marine Safety of Transport Canada for their kind permission to use Canadian experimental data in validating the theoretical approach presented in this paper. The financial support from the Canadian Coast Guard and encouragement from the members of *Flooding Protection of Ro-Ro Ferries* project team (Institute for Marine Dynamics, Fleet Technology Ltd., Operational Dynamics, and Transportation Development Centre) are also gratefully acknowledged.

11. References

1. Hutchison, B. L.: 'Water on Deck Accumulation Studies' by the SNAME ad hoc Ro-Ro Safety Panel, *Proceedings*, Workshop on Numerical and Physical Simulation of Ship Capsize in Heavy Seas, University of Strathclyde, Glasgow, July 1995, 13 pp.; see also progress papers:

- SNAME Ad Hoc Ro-Ro Safety Panel: 'Water Accumulation on the Deck of a Stationary Ship', Annex A to the second position paper submitted 28 February 1995 to the IMO Panel of Experts, 35 pp.;
- Hutchison, B. L., Molyneux, D. and Little, P.: 'Time Domain Simulation and Probability Domain Integrals for Water on Deck Accumulation', CyberNautics 95, SNAME California Joint Sections Meeting, Long Beach, Ca, April 1995, 19 pp.;
- Hutchison, B. L., Little, P., Molyneux, D., Noble, P. G. and Tagg, R. D.: 'Safety Initiatives from the SNAME Ad Hoc RO-RO Safety Panel', *Proceedings*, 13th Int. Conf. on Marine Transport Using Roll-on/Roll-off Methods RO-RO '96, BML Ltd., Lübeck, May 1996, 19 pp.

2. Vassalos, D., and Turan, O.: 'A Realistic Approach to Assessing Damage Survivability of Passenger Ships', SNAME *Transactions*, Vol. 102, 1994, pp. 367–394; see also paper: Turan, O., and Vassalos, D.: 'Dynamic Stability Assessment of Damaged Passenger Ships', RINA *Transactions*, Vol. 136, 1994, pp. 79–104.

3. Vassalos, D.: 'Capsizal Resistance of Damaged Ro-Ro Ferries: Modelling and Application', *Proceedings*, WEGEMT Workshop on Damage Stability of Ships, Danish Technical University, Copenhagen, Oct. 1995, 15 pp. + 10 figures.

4. Vassalos, D., Pawlowski, M. and Turan, O.: 'A Theoretical Investigation on the Capsizal Resistance of Passenger Ro-Ro Vessels and Proposal of Survival Criteria', Final Report, Task 5, The North West European R&D Project, March 1996.

5. Pawlowski, M.: 'Theoretical Model of Damaged Ship Behaviour', Research grant "Damaged Stability Criteria for Ro-Ro Passenger Ferries with Water on Deck", Ship Design and Research Centre—CTO, Gdansk, October 1997, 8 pp.

6. Kendrick, A., Pawlowski, M., Peirce, T.: 'Flooding Protection of Ro-Ro Ferries, Phase 3', Transport Canada Report No. TP13216, March 1998

7. Vassalos, D., Turan, O., Pawlowski, M., : 'Dynamic Stability Assessment of Damaged Passenger/RO-RO Ships and Proposal of Rational Survival Criteria', Marine Technology, October 1997.

ON THE CRITICAL SIGNIFICANT WAVE HEIGHT FOR CAPSIZING OF A DAMAGED RO-RO PASSENGER SHIP

Tomihiro HARAGUCHI*, Shigesuke ISHIDA*, Sunao MURASHIGE †

*SHIP RESEARCH INSTITUTE, Ministry of Transport
6-38-1, Shinkawa, Mitaka, Tokyo 181-0004, Japan
Fax : +81-422-41-3056, E-mail : haraguch@srimot.go.jp
† Department of Mathematical Engineering, The University of Tokyo, Japan

SUMMARY

Since the accident of Estonia, studies have been continued on the stability of RO-RO ships in damaged condition in waves. Because the phenomena are complicated and affected by many factors, studied should be conducted in various conditions. In this study experiments in beam waves were carried out, having the characteristics of Japanese ships and waves around Japan in mind. Discussions were mainly focused on the relation between the height of water on deck and the critical wave height for capsizing, and on the effect of the peak period of wave spectrum.

The main conclusions are as follows,

(1) When a ship has no initial heel angle capsizing does not occur, but an initial heel angle of as small as 2 degrees makes the ship in dangerous condition for capsizing.
(2) The critical significant wave height for capsizing is affected by the peak period of the wave spectrum. The longer the peak period is, the higher the critical significant wave height becomes.
(3) The relation between the critical height of water on deck and the critical significant wave height proposed by UK gives a good estimation in short waves. However, thinking of the waves in various locations in the world, an equation applicable to a wider range of peak period is desired.

INTRODUCTION

After the capsizing accident of Estonia occurred in the Baltic Sea in 1994, International Maritime Organization (IMO) reviewed the measures to enhance the safety of RO-RO passenger ships and amended International Convention for the Safety of Life at Sea (SOLAS) in November 1995. Subsequent to this amendment, a proposal[1)] was submitted by United Kingdom to Sub-committee on Stability and Load Lines and on Fishing Vessels Safety (SLF40) of IMO, which explicitly includes the flooded free water effect on deck to the stability.

From this background, much study has been continued on how to prevent sea water from accumulating on RO-RO deck[2], and on stability performance when flooding into the deck has occured[3)~9)].

In the experiment of this study a model of a typical RO-RO passenger ship in Japan was used because Japanese ships tend to have a different proportion from Northwest European ships and because oceanographic phenomena is a little different from Northwest Europe.

In this paper at first, the effect of initial heel angle was mentioned. Subsequently, the relation between the critical height of water on deck and the critical significant wave height for capsizing was discussed. It is because the validation of the important proposal by UK,

$$hc = 0.085\ Hsc^{1.3} \qquad (1)$$

to Japanese ships is necessary. This equation shows that a ship should have the stability performance to bear the water on deck corresponding to hc in the critical significant wave height, Hsc. At the same time, it can be explained that the critical significant wave height should cause the amount of water on deck corresponding to hc. The experimental results are shown on the effects to the relation of initial heel and of peak period of wave spectrum.

EXPERIMENT

Model Ship and Experimental Conditions

The model ship is a 1/48.6 scale model of a typical and oceangoing RO-RO passenger ship in Japan. The characteristics of the ship are larger L/B and smaller B/d ratios than that of Northwest European ships. The principal particulars and the body plan are shown in Table 1 and Fig.1 respectively. Fig.2 shows the damaged opening, flooded compartments (the central part, colored dark) and the position of 7 water level gauges on the vehicle deck, which is for measuring the amount of water on deck. For realistic modeling of the shell plating in the damaged compartment as well as the vehicle deck, the model ship was made of FRP. In accordance with SOLAS'90, two compartments are damaged with an opening in the central part of the ship and are designed to make flooding symmetrically.

Table 1 Principal Particulars in Intact and Damaged Conditions (scale ratio : 1/48.6)

	Ship		Model	
	Intact	Damaged	Intact	Damaged
Lpp(m)	170.00		3.500	
Bmld(m)	25.00		0.515	
Dmld(m)	9.50		0.196	
Mean Draft(m)	6.60	8.2	0.136	0.17
Trim(m)	0.00	-1.3	0.000	-0.0259
Condition	Full Load Departure Condition			
△(ton)	15020		0.128	
KG_0(m)	10.86		0.224	
G_0M(m)	1.41	2.8	0.029	0.057
Fbd[1)](mid)(m)	2.90	1.3	0.060	0.027
Fbd[2)](mid)(m)	2.20	0.6	0.045	0.012
Tr(sec)	17.90	13.4	2.570	1.93

1) Designed Deck Height, 2) Lower Deck Height

The experiment was performed in two different conditions that the vehicle deck height was originally designed (hereafter called the designed deck height) and that the height of the deck including the ceiling was lower than the designed one by 0.7m (hereafter called the lower deck height). GM values in both conditions were kept the same. In addition to the condition of no

initial heel angle, the conditions with initial heel angles of 2 degrees and 4 degrees were tested, assuming cargo shifting or asymmetrical flooding.

Only the condition of the lower deck height with 2 degrees of initial heel angle just does not comply with SOLAS'90 because of insufficient range of positive GZ value. The other conditions sufficiently satisfy SOLAS'90.

Measuring System

The experimental apparatus is shown in Fig.3. The model ship was placed with the damage opening facing the oncoming waves. Swaying, heaving and rolling motions were set free but yawing is loosely restricted by means of a string. The measuring time was set to be 30 minutes in the real ship scale. The carriage followed the model ship to let it drift freely, however, when the drifting speed is too large, drifting was a little controlled by the string.

Incident waves

All experiments were carried out in irregular waves with the spectrums of JONSWAP type. As for the wave period, 13.7 sec., 11.6 sec., 9.5 sec. and 7.4 sec. were used (listed in order of the discrepancy from the natural rolling period in damaged condition). The maximum ratios of wave height to wavelength are 1/25, 1/15, 1/12 and 1/12 respectively. These wave heights are the highest ones which the wave maker can generate in the tank. The significant wave heights used in the experiment are shown in Table 2.

Table 2 Significant Wave Height, Model Conditions and Occurrence of Capsize

Deck Height	Initial Heel Angle (deg)	Peak Period of Wave Spectrum (sec)			
		13.65	11.55	9.45	7.35
Designed Deck Height	0°	10.55○	12.58○	10.53○	6.37○
	2°	10.55×	9.44×	6.32×	5.10×
	2°	9.76○	8.58×	5.74○	4.50×
	2°	8.79○	7.55○	5.05○	3.82○
	4°	7.53×	7.55×	5.74×	3.82×
	4°	7.13×	6.29×	5.49×	3.47×
	4°	6.59○	5.39○	5.05○	3.06○
Lower Deck Height	0°	10.55○	12.58○	10.53○	6.37○
	0°	8.79○	9.44○	8.42○	5.10○
	2°	5.27×	4.72×	3.16×	2.55×
	2°	4.79×	4.19×	2.81×	2.18×
	2°	4.63×	4.02×	2.69×	1.91○
	2°	4.39○	3.78○	2.53○	1.53○

Numbers in the table are significant wave height (m)
○:Non-capsize ×:Capsize

EFFECT OF INITIAL HEEL

The Case without Initial Heel

In Table 2 marks ○ represent non-capsize and marks × represent capsize to 90 degrees. As shown in this table, the ship only capsized with initial heel and she did not in case of no initial heel. In the case of no initial heel, the ship heeled to lee side in both height of the vehicle deck. Consequently the deck edge of the damaged side (weather side) became higher from the mean sea level than that before flooding. Thereafter flooding into the vehicle deck stopped and that avoided capsizing. This fact agrees with the former experimental results of the authors[8].

Fig.4 shows GZ curves for the designed deck height and the lower deck height. Plus angle represents the heel to damage side (weather side). The stability performance of intact side is far superior to that of damage side. Therefore, it is natural that the ship did not capsize when she heeled to lee side. It is concluded that heeling to lee side is very safe when there is no opening in the lee side because it stops further flooding, and because righting moment itself is

large in that direction.

According to the wave statistics[11], 1/20 as the ratio of wave height to wavelength is the highest in the sea areas around Japan. Moreover, the ratios of 1/20 or over were used in this experiment, excluding the wave with the peak period of 13.7 sec. Therefore, it is concluded that this ship at the GM value in the experiment is hard to capsize without initial heel in the sea area around Japan. A circular letter issued by IMO[10] includes a provision that a ship shall be thought to have capsized when its steady heel angle exceeds 20 degrees. In this experiment steady heel angles were less than 20 degrees except for only one case, hence this ship is supposed to be hard to capsize in terms of the steady heel angle, too.

The Case with Initial Heel

On the other hand, when the model ship had an initial heel to weather side, the mean heeling direction was always weather side and she capsized in many cases. An initial heel to weather side lowered the deck edge, furthered flooding into the vehicle deck, increased steady heel to weather side and again lowered the deck edge. This chain led to capsizing. This is the same phenomenon in the case of a ship with a center casing[8], except that the stability performance reduced by the initial heel. This fact indicates that if the water flooded into the vehicle deck accumulates on the damage side, it will cause the risk of capsizing. Table 2 shows that the wave height at which the ship capsized became lower with increasing initial heel angle and with descending deck height. This is because the stability performance deteriorates with increasing initial heel and with descending deck height, as shown in Fig.4.

The ship capsized at about only 2m of the significant wave height in the condition of 2 degrees of initial heel and the lower deck height, in which the stability is slightly in short of the requirements of SOLAS'90 as stated in the former paragraph. So, it can be said that capsizing is unavoidable in this condition. However even if the deck height was raised to the designed value from this condition, in which SOLAS'90 is satisfied, capsizing took place with the significant wave height of 3.5m. It can be concluded that the risk of capsizing is very high when a ship has an initial heel to the damage side (weather side).

CRITICAL HEIGHT OF WATER ON DECK AND CRITICAL SIGNIFICANT WAVE HEIGHT

Definitions of Critical Height of Water on Deck and Critical Significant Wave Height

The height of water on deck from the outer mean sea surface is an important factor for stability in waves. The value is not zero in general even if time average for a certain period is made. Direct measurement of this quantity is very difficult, so usually it is evaluated statically as a function of the amount of water on deck and the heeling angle in calm water.

Examples of time histories of the amount of water on deck are shown in Fig.5. For evaluating the height of water on deck, the time averaged volume for a certain period in steady condition was used. In non-capsized case the period was selected at the last stage of experiment (Fig.5(a)), and in capsized case the period was just before the capsizing motion (Fig.5(b)). As for the heeling angle, time average in the same period was used.

When the ship capsized the critical height of water on deck (hcritical) was defined as the average of the heights of water on deck in two experiments, one capsized the other not, in the same conditions except significant wave height. Similarly, the critical significant wave height (Hscritical) and the critical angle for capsizing (θ critical) were defined as the averages in the two experiments. Hereafter, affixed "critical" represents the critical values obtained from the experiment with this manner.

On the other hand, another critical height of water on deck from mean sea surface should be defined (hc), which is calculated without considering waves explicitly. In calculating hc, the heeling angle is fixed to a critical value (θ c), in which the GZ curve has the maximum value in damage side. The amount of water on deck is decided to make GZ zero at the angle of θ c. Hereafter, affixed letter "c" represents the values obtained by this method. In addition, the critical significant wave height (Hsc) is defined by equation (1).

Critical Height of Water on Deck

Fig.6 shows the relationship between the critical height of water on deck and the critical significant wave height with black marks. For comparison some steady conditions of non-capsized cases (see Fig.5(a)) are also shown with empty marks. Fig.6(a) and (b) show the result of the designed deck height and the lower deck height respectively. The horizontal three lines show hc's which were calculated from GZ curves as mentioned. The solid curve represents equation (1). The results of four peak periods of wave spectrum are included.

Fig.6(a) for the designed deck height indicates that hcritical (black marks) is equivalent to or somewhat smaller than hc (horizontal lines) and that hcritical remains almost constant or goes up slightly for the significant wave height. Fig.7 shows the ratio of hcritical to hc. The ratios are ranging between 0.5 and 1.0, and capsizing especially took place at the smaller value than hc when the initial heel angle is 2 degrees. As will be mentioned later, the ratio of the critical heel angle (θ critical/ θ c) is greater than 1. The height of water on deck has a tendency to decrease when the heel angle increases, as shown in Fig.8. Consequently, it is supposed that if θ critical/ θ c approaches 1, hcritical/hc would approach 1. It is concluded that the critical height of water on deck can be roughly estimated by hc in various ship and wave conditions.

Additionally in Fig.6(a), the height of water on deck in the case of no initial heel (empty marks) shows a similar tendency, while some of them are greater than hc. This is because, being different from the case of initial heel, the ship heels to lee side (intact side), hence it has a stability great enough to bear large amount of flooded water.

Meanwhile, in Fig.6(b) for the lower deck height, the tendency of hcritical is similar to that in Fig.6(a) (designed deck height). It might seem to be strange that some hcritical values are negative. It means flooding might be still continuing at the moment of capsizing. However the discrepancies between hcritical and hc are almost the same as Fig.6(a). It is thought that the main cause is the dynamic effect and that hcritical might depend somewhat on the time histories of wave elevation. Anyway, the stability of this condition is very small as shown Fig.4(b), so the ship capsized with a small amount of water on deck.

In the case of no initial heel (no capsize) in Fig.6(b), the ship heeled to lee side as was the case with the designed deck height. The height of water on deck was lower than the one in Fig.6(a) and sometimes lower than the mean sea surface. This can be explained by the reasons that the ship was easy to heel because of the small stability as shown in Fig.4(b) and that the height of water on deck is sensitive to heel angle as shown in Fig.8. It should be noted that the smaller amount of water on deck makes the height more sensitive to heel angle and that the amount was in fact small because water ingress stopped after she heeled to lee side in a short time.

Effects of Peak Period of Wave Spectrum on Critical Significant Wave Height

Fig.9(a)~(d) show the comparisons of the results in Fig.6(a) and equation (1) for each peak period of the wave spectrum. These figures prove that when the peak period is 7 sec. the

critical significant wave height (Hscritical) is smallest and is in good agreement with equation (1). However with the increase of peak period of wave spectrum Hscritical increases. Fig.10 shows the ratio of Hscritical to Hsc for the designed deck height. It can be seen that the ratio is increasing as the peak period increases, being in agreement with the tendency in Table 2. When the peak period is 13 sec. Hscritical is greater than Hsc by twice.

As shown in Fig.6(b), the variation of Hscritical for the lower deck height is smaller than the designed deck height. But when the peak period is 13 sec., Hscritical is greater than Hsc by three times. This fact indicates that the ship can survive in higher waves than equation (1) in longer waves and that the critical value depends on wave steepness.

Critical Angle for Capsizing

Fig.11 shows the ratio of the critical angle for capsizing (θ critical) to the heel angle (θ c) at which GZ value in damage side reaches the maximum. The figure reveals that all the results are greater than 1 for either deck height, i.e. the ship capsized after the heel angle exceeded θ c. This means that capsizing occured after the mean heel angle exceeds the point of the maximum of GZ value, namely after the static capsizing moment counteracts the righting moment. It is concluded that θ c, calculated in static conditions, can roughly estimate the lower boundary of the critical angle for capsizing. As for the difference between θ critical and θ c, the effect of ship motion, motion of flooded water and so on should be considered. The mechanism of capsizing still remains to be elucidated.

COMPARISON BETWEEN PROPOSAL BY UK AND EXPERIMENTAL RESULTS

As discussed with Fig.6 and Fig.9, hcritical is small compared with equation (1) when the peak period of wave spectrum is long. Therefore, the equation (1) gives rather large amount of accumulated water, i.e. the required stability performance is higher than the necessary in reality. From the standpoint of wave height, Hscritical is 2 or 3 times as large as Hsc, i.e. the critical wave height might be underestimated in some peak period of the wave spectrum. In other words the dependence of the critical wave height on the peak period of wave spectrum is not reflected to equation (1).

Equation (1) was obtained from many simulations and experiments. The experiments were conducted in the same spectrum type as this experiment, JONSWAP type. But the peak period was from 4 sec. to 9 sec. and the significant wave height was from 1m to 8m, which was decided considering the crowded sea areas around Europe. As a result, it is convinced that the equation almost agrees with the results of this experiment up to 9sec. of the peak period. Conversely, it might be natural that the equation is not applicable to peak periods greater than 9 sec.

In order to apply the equation to various sea areas in the world, it should be considered that the critical significant wave height varies by the peak period. According to the database on waves statistics in the sea area around Japan[11], the frequency of occurrence of waves whose period is 9sec. or over has exceeded a negligible level especially in the side of Pacific Ocean. So an equation applicable to a wider range of peak periods is desired.

CONCLUSIONS

A capsizing experiment was carried out in beam seas with JONSWAP spectrum, using a model of a typical oceangoing RO-RO passenger ship in Japan. The main conclusions are as follows,

(1) The ship, which satisfies SOLAS'90, does not capsize in the condition of no initial heel even in high waves, which are rarely seen in wave statistics around Japan. However she often capsizes with a little initial heel to damage side. The critical significant wave height for capsizing is lower than that in which the ship without initial heel survives.

(2) The critical significant wave height for capsizing is affected by the peak period of the irregular wave spectrum. The longer the peak period is, the higher the critical significant wave height becomes.

(3) The relation between the critical height of water on deck and the critical significant wave height proposed by UK gives a good estimation as long as the peak period of the wave spectrum is short. However, considering of the waves around Japan and other areas in the world, the relation should include the effect of peak periods.

REFERENCES

1) SLF 40/4/5,HARMONIZATION OF DAMAGE STABILITY PROVISION IN IMO INSTRUMENTS,A Proposal on New Damage Stability Framework for RO-RO Vessels based upon Joint North West European R & D Project "Safety of Passenger/RO-RO Vessels" Submitted by Denmark, Finland, Norway, Sweden and the United Kingdom, July, 1996
2) J.H.Rousseau : Flooding Protection of RO-RO Ferries Phase II ,March 1997
3) D.Vassalos, A.Jasionowski et al. : Time-Based Survival Criteria for RO-RO Vessels, The Royal Institution of Naval Architects spring meetings 1998
4) D.Vassalos, G.Conception, I.Letizia : Modeling the Accumulation of Water on the Vehicle Deck of a Damaged RO-RO Vessel, Third International Workshop on Theoretical Advances in Ship Stability and Practical Impact, October 28-29,1997
5) D.Vassalos, M.Pawlowski and O.Turan : Joint North West European Project, Safety of Passenger RO-RO Vessels - Task 5,A Theoretical Investigation on the Capsizal Resistance of Passenger RO-RO Vessels and Proposal of Survival Criteria, University of Strathclyde Marine Technology Centre, March 1996
6) N.Shimizu, K.Roby, Y.Ikeda : An Experimental Study on Flooding into the Car Deck of a RORO Ferry through Damaged Bow Door, Journal of the Kansai Society of Naval Architects, Vol.225, September,1996
7) T.Hamano, K.Roby, Y. Ikeda : A New Approach to Damage Stability Rule (2nd report)-Experiments to Identify the Motion Characteristics of Damaged Ships, Journal of the Kansai Society of Naval Architects, Vol.228, 1997 (in Japanese)
8) S.Ishida, S.Murashige, I.Watanabe, et al. : Study on Damage Stability with Water on Deck of a RO-RO Passenger Ship in Waves, Journal of the Society of Naval Architects of Japan, Vol.179, May, 1996 (in Japanese)
9) S.Ishida, S.Murashige : STABILITY OF A RO-RO PASSENGER SHIP WITH A DAMAGE OPENING IN BEAM SEAS, Proceeding of STAB'97, September, 1997
10) AGREEMENT CONCERNING SPECIFIC STABILITY REQUIREMENTS FOR RO-RO PASSENGER SHIPS UNDERTAKING REGULAR SCHEDULED INTERNATIONAL VOYAGES BETWEEN OR TO OR FROM DESIGNATED PORTS IN NORTH WEST EUROPE AND THE BALTIC SEA, ANNEX1 "Significant wave heights", Appendix MODEL TEST METHOD, IMO Circular letter No1891, 29 April, 1996
11) I.Watanabe, H.Tomita, K.Tanizawa : Winds and Waves of the North Pacific Ocean (1974～1988) , Papers of Ship Research Institute, Supplement No14, May, 1992

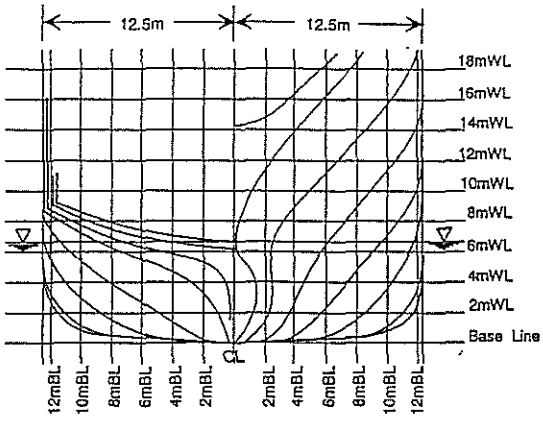

Fig.1 Body Plan

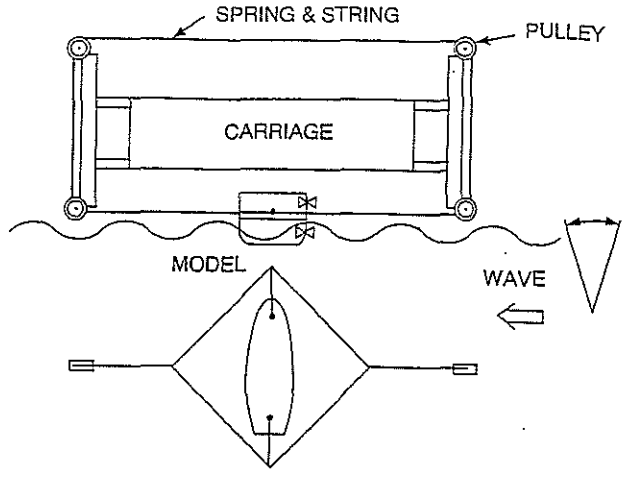

Fig.3 Experimental Apparatus

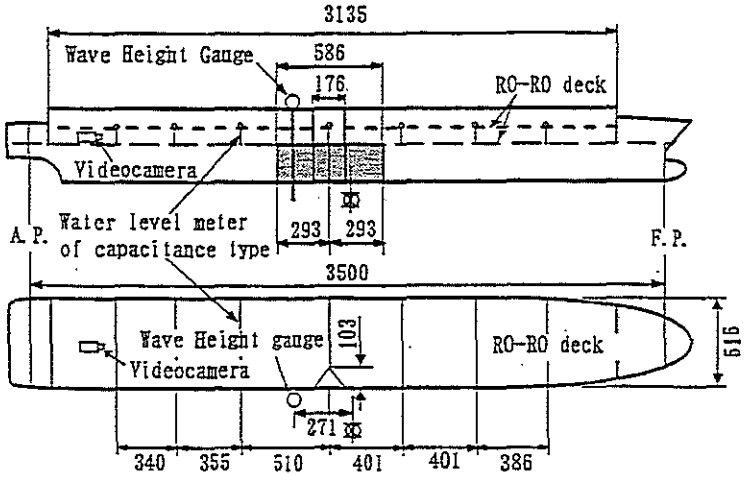

Fig.2 Damaged RO-RO Ship Model

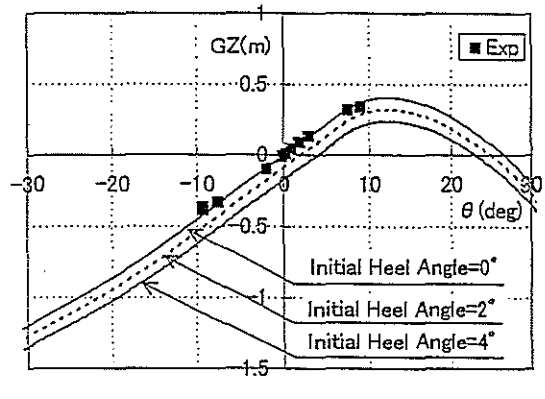

Fig.4(a) GZ Curves(Designed Deck Height)

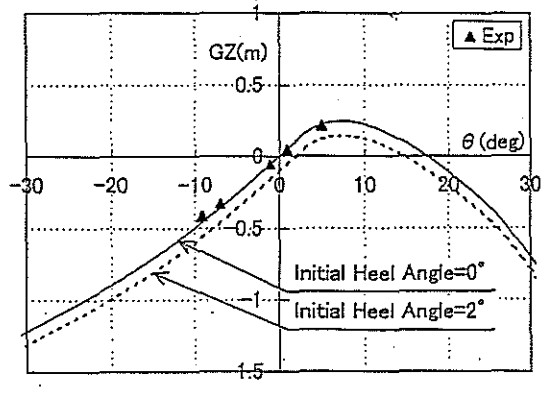

Fig.4(b) GZ Curves(Lower Deck Height)

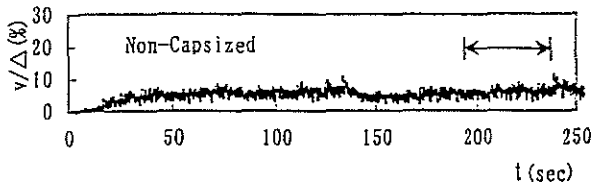

Fig.5(a) Time History of Amount of Water on Car Deck(No Capsize) (v:Amount of Water on Deck, Δ:Displacement)

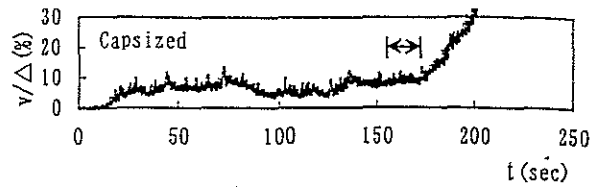

Fig.5(b) Time History of Amount of Water on Car Deck(Capsize) (v: Amount of Water on Deck, Δ: Displacement)

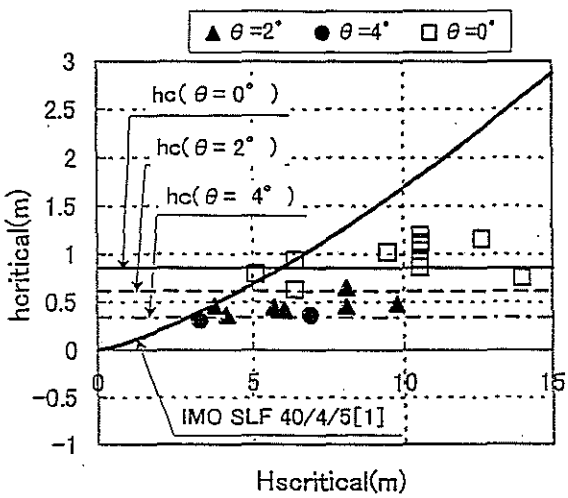

Fig.6(a) Critical Height of Water on Car Deck(Designed Deck Height) (θ :Initial Heel Angle)

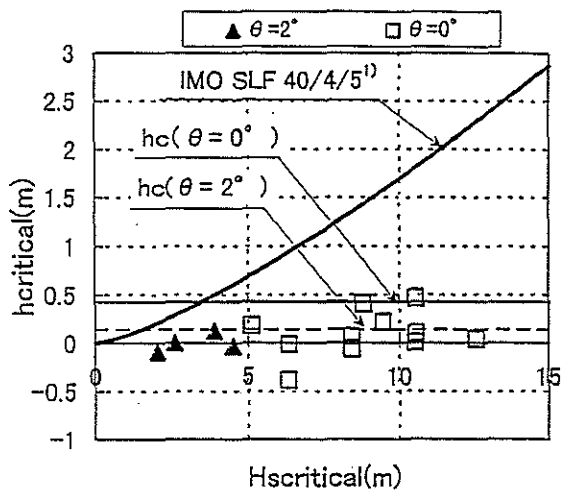

Fig.6(b) Critical Height of Water on Car Deck(Lower Deck Height) (θ :Initial Heel Angle)

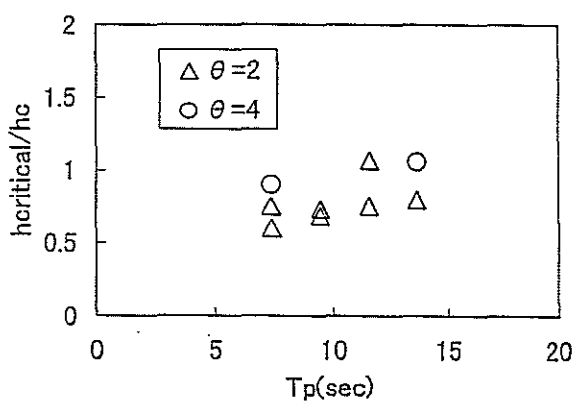

Fig.7 Critical Height Ratio of Water on Car Deck(Designed Deck Height) (θ :Initial Heel Angle, Tp:Peak Period of Wave Spectrum)

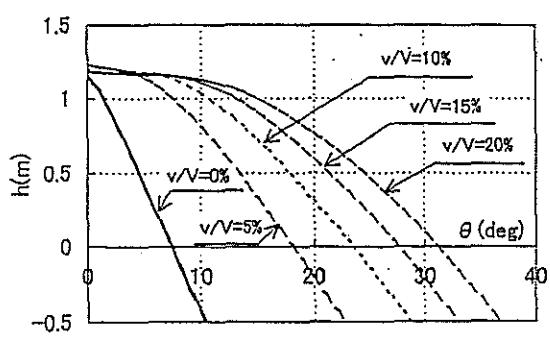

Fig.8 Relation between Height of Water on Car Deck and Heel Angle (v: Volume of Water on Deck, V: Volume of Car Deck)

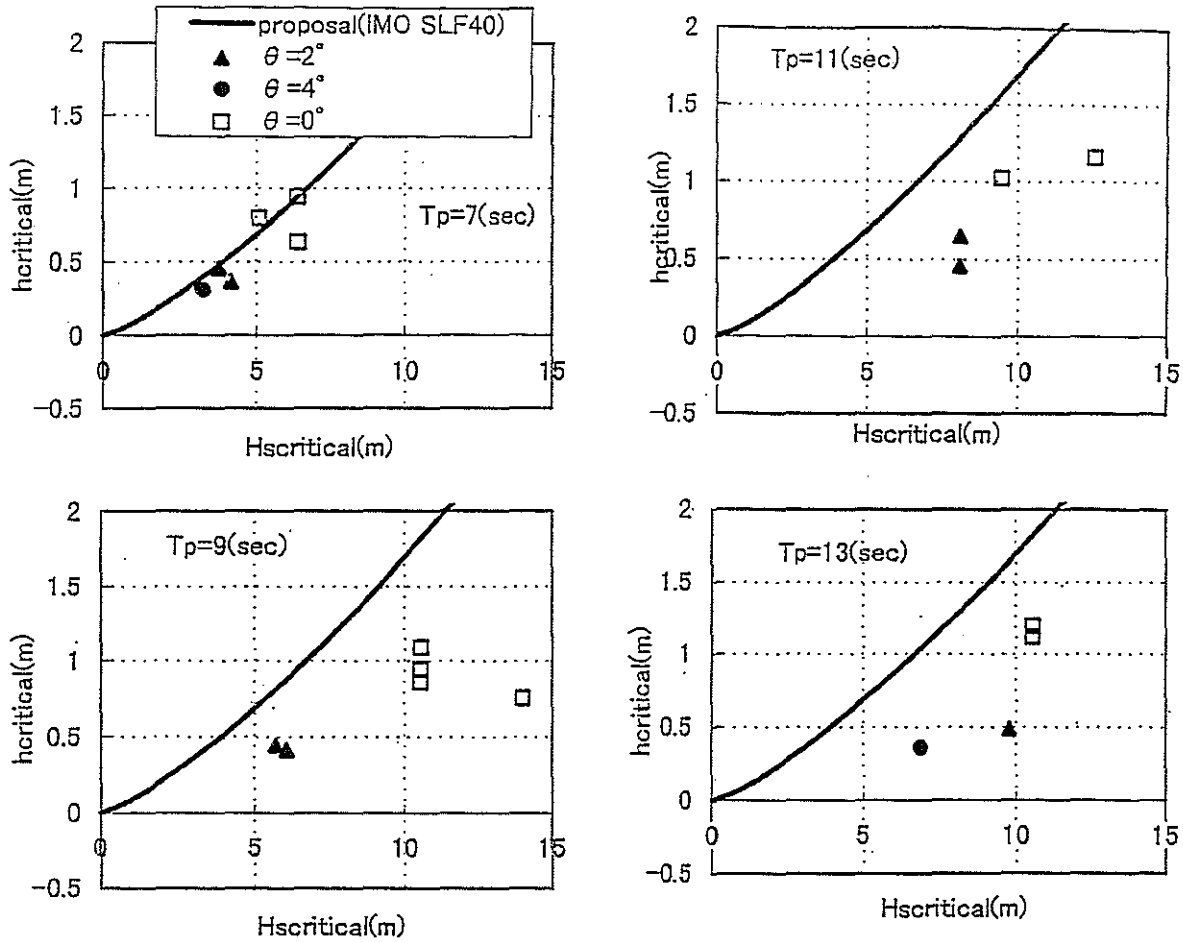

Fig.9 Effect of Peak Period of Wave Spectrum to Critical Significant Wave Height (Designed Deck Height)
(θ :Initial Heel Angle, Tp:Peak Period of Wave Spectrum)

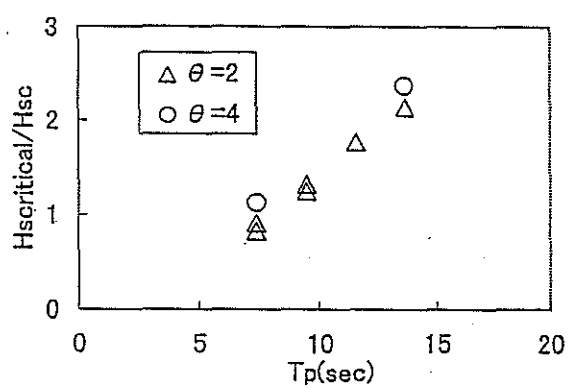

Fig.10 Ratio of Critical Significant Wave Height(Designed Deck Height)
(θ :Initial Heel Angle, Tp:Peak Period of Wave Spectrum)

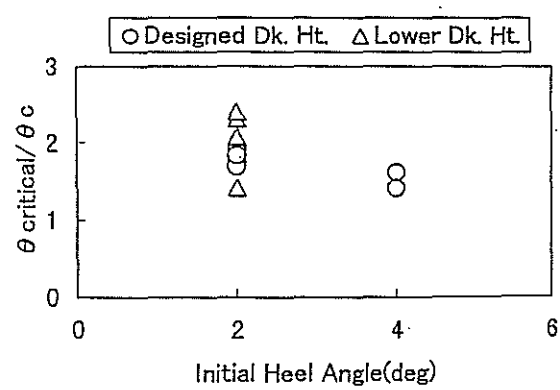

Fig.11 Ratio of Critical Heel Angle

RO-RO Passenger Vessels Survivability - a study of three different hull forms considering different RO-RO-deck subdivisions.

A. Jost

Abstract

Based on the newly defined Stockholm Agreement's water on deck criteria model tests where carried out aiming at a better understanding of the critical water height on the ro-ro deck. For this purpose three differently aged vessel types with respectively different operating freeboards have been included in this study. The results achieved are shown and discussed.

1. Background

Legislative Activities have finally calmed down that had been pushed forward by the tragic losses of ro-ro passenger the most recent of which had been the Estonia. The drastic measures newly required are being put into place now. Once they will be completely in place, time will proof their effectiveness.

Legislative tools dedicated to ro-ro passenger vessels cover other than a set of 1995 SOLAS Amendments, IMO Resolutions requiring the upgrading of shell doors scantlings and their securing as well as a Regional Agreement on a specific damage stability standard applicable to ships travelling in the North and Baltic Seas.

With regard to damage survivability it should be noted that the amended SOLAS [1] requirements and the Regional agreement [2] enforce an increase in standard that will become mandatory to both new and existing passenger vessels. One of the newly installed criteria is a survivability standard that requires to show sufficient residual stability even with accumulating water on the damaged ro-ro deck. The respective legislation does allow to chose showing compliance with this standard either by calculation or by model tests. In both cases the regional agreement does give detailed procedures which are to be complied with.

The scope of this research project (sponsored by BMBF[1]) was to find a better understanding of the critical amount of water on deck relative to the existing trading practice and eventual upgrading of the ship types. Thus three existing hull forms that had been built in accordance with different subdivision and survivability standards due to their individual keel laying and or reconstruction dates were chosen as sample ships. It was anticipated that some kind of subdivision of the ro-ro deck would become necessary during the course of the proposed upgrading and the effect of such subdivision on the survivability of these hull forms was to be studied.

[1] German Ministry for Research and Technology

2. Hydrostatic Evaluation of the Sample Ships

Today's subdivision standard is based on the SOLAS 1974 requirement that has been considerably amended after 1988. Up to 1988 for any passenger ship compliance had to proven with existing intact stability criteria the requirement of floodable lengths and certain damage stability criteria. Usually the damage stability requirements would be the crucial criteria and the designs freeboard. Both the intact stability criteria and the floodable length requirement have not been reconsidered while the damage stability criteria had been amended by a requirement of a residual stability standard. As usual this new standard became applicable to new ships and showed a remarkable influence on the designs.

Ro-ro passenger ferries operating in the Baltic and North sea areas are required to comply with a survivability standard that includes the flooding of the ro-ro (bulkhead) deck. The requirement is that acceptable residual stability standards are to be maintained even with a certain flooding height $(h_w \leq 0.5m)$. Compliance with this standard can either shown by model testing or calculation.

Technically, two different survivability standards for new and existing ro-ro passenger ferries can not be justified. Consequently the amended standard became mandatory also to existing vessels.

The vessels chosen for this project are considered to be typical representatives of the kind used in this area:

1. Ship A

   This ship was built in accordance with SOLAS 74/83 standard. Her subdivision below the bulkhead deck consists of a relative high number of transverse bulkheads combined with some longitudinal subdivision. The operating freeboard is minimised by making use of cross flooding that decrease or eliminate heeling angles in damaged condition. In this case the criteria of non-submerging the margin was the governing criteria as residual stability standards had not been imposed.

2. Ship B

   Although this ship had been built prior to ship A, with regard to survivability standards she presents a later design standard since she was completely re-built when entering a different service after the 1988 SOLAS amendments came into force. With this conversion in accordance with SOLAS 74/88 she features a very similar subdivision below the bulkhead deck, the operating freeboard was remarkably increased due to the requirement of a minimum heeling lever curve in damaged condition.

3. Ship C

   This vessel was only designed when the new standard had already been established. Her subdivision below the bulkhead deck is governed by longitudinal bulkheads located at B/5 measured from the shell. Not all of these are equipped with cross flooding ducts. Respectively heeling angles in the damaged water lines are not eliminated although they are legally limited.

The main dimensions of the vessels and some general remarks regarding the damage stability calculations are:

Main Dimensions:	Ship A	Ship B	Ship C
length L_s [m]	151.46	177.21	179.5
beam B [m]	29.00	26.00	27.2
height D [m]	8.10 /16.20	8.0 /	8.7 /
draught t [m]	6.40/ 6.20 / 5.90	5.75	6.0
trim [m]	0.0	-1.0 /0.0 / +1.0	-1.0 /0.0 / +1.0
modelled damaged Compartments	9/10 and 11/12	7/8 and 11/12	6/7 and 10/11

All three vessels are narrow and evenly subdivided below the bulkhead deck [figures 1]. All three ships had in their original configuration non watertight divided ro-ro decks.

Each one was subjected to a SOLAS 90 damage stability calculation in order to establish a governing double compartment that was taken into account regarding the "water on deck" criteria. (Figure 2 shows as an example the governing residual stability criteria for ship A at a draught of 6.2m)

The Stockholm agreement requires that unless the governing criteria is located within 10% of the mid-length a second double compartment located within this margin has to be demonstrated. Taking this into account the models of all three vessels were built to cover two SOLAS damages over the length. Where the crucial condition turned out to be within the a.m. mid length part the second damage was chosen to be near the vessels shoulder.

For vessels B and C, where the operating freeboard was considered rather large, it was understood that further increase of freeboard would only effect the survivability to become more favourable by allowing for less GM_0 values. In those cases the introduction of trim was considered to be of more interest.

Generally, for all three vessels three different ro-ro deck versions were investigated. Starting point was

Version A the open deck configuration.

In the course of this project. By calculation a variety of different deck subdivision alternatives were considered. Within the scope of this project only two further versions could be expanded on in model testing:

Version E2 with 2 full height bulkheads in transverse ship direction and

Version F with side casings.

In terms of compliance with "SOLAS 90" standard, in the damage stability investigation the side casing version was the version that seemed to best cope with the criteria.

Summarising the scope the research project covered variations of damage location, subdivision and GM as well as draughts and trims respectively.

	Version A open deck			Version E transverse bulkheads			Version F side casings		
	draught variations			trim variations			trim variations		
	6.4 m	6.2 m	5.9 m	-1.0 m	0.0 m	+1.0 m	-1.0 m	0.0 m	+1.0 m
GM variations	X	X	X	X	X	X	X	X	X
Sea State realisations	X	X	X	X	X	X	X	X	X

3. Model testing

Within the model tests the model is subjected to a long-crested irregular seaway. The damaged model is free to drift and is placed in beam seas with the damage hole facing the oncoming waves.

The survival criteria in these model tests are such that at least five experiments for each peak period need to be carried out. The test duration shall be such that a stationary state has been reached and a minimum of 30 min. in full scale time are proven. The model is considered to survive when the angles of roll do not reach more than 30° against a vertical axis occurring more frequently than 20% of the rolling cycles or the steady heeling angle becomes greater than 20°.

To cover the scope of these tests the model has to be such that the hull is thin enough in the damaged areas and the main design features such as watertight bulkheads, air escapes permeabilities and etc. above and below the bulkhead deck can be modelled to represent the real situation.

Each of the models used in this project was built accordingly in GRP and the interior for two damage locations was mostly built of ply wood in suitable size. These two damage locations were chosen in accordance with the SOLAS damage stability as described above. The damage holes were opened successively. Each one sized in accordance with the SOLAS damage and a penetration depth of B/5. Both of the damage locations per ship were subjected to draught or trim variations and to address the critical wave height the GM_L was continuously decreased in order to find the boarder line between safe and capsizing.

This borderline is of course subject to uncertainties that are usually involved in methods that include statistics. The results cover for each tested GM_L the observation survived/ not survived. This statement of result does not cover the residual margin that might exist versus an exact limiting condition on the edge of capsizing. For this reason it would be necessary to evaluate many more runs in testing such capsizing margins to finally achieve the answer to a question of critical "water on deck"-height.

4. Computer Simulations

The scope of this investigation covered also a computer simulation of the relative motions of the damaged ro-ro passenger vessels in the seaway. The software utilised in this respect is based on methodologies developed at the Institut für Schiffbau, Hamburg. (Kröger [3] and Petey [4]) which was expanded and adapted to such model tests by Chang [5]

As an example table 4 and 5 cover the results of simulations for ship A, tables 6 and 7 ship B and tables 8 and 9 ship C respectively. The simulation confirm the outcome of the model testing.

In order to get an improved understanding of the boarder line between safe and unsafe in this context the simulations covered the same scope of GM variations, only in much smaller steps.

5. Conclusions

The realisation of the seaway and the accumulated water on deck is shown in figures 3. Due to the a.m. uncertainties the measured accumulated water heights can not be considered representing the critical water height on deck. The scheme of water height measurements are shown in figures 3a.

In order to produce a better understanding of such critical height of water and in conjunction with earlier survivability test made at the HSVA model basin, it is proposed that the residual stability lever curve is employed to help judge the residual stability margin. It is proposed that the residual area of the heeling lever curve of the respective damage case beyond the measured heeling and rolling angle is used to represent survivability borders. (figure 4)

With regard to improving safety of such existing vessels, and in order to limit the necessary increase in GM to a practicable margin further subdivision versions on the ro-ro deck were investigated. As described above three versions per ship were tested.

As an example the scope of the tested configurations is shown in the following table:

Initial draught	Original configuration Version A		With additional bulkheads Version E2		With side casings Version F	
	L 11/12 GM_L	L9/10 GM_L	L 11/12 GM_L	L9/10 GM_L	L 11/12 GM_L	L9/10 GM_L
6.4 m	-	4.2 m	-	2.3 m	-	2.4 m
6.2 m	3.5 m	4.2 m	1.3 m	2.0 m	1.8 m	2.4 m
5.9 m	2.6 m	3.2 m	1.4 m	1.7 m	1.6 m	1.9 m

The conclusion to be drawn from such result can be summarised as follows:

- the increase in freeboard effects a drastic decrease in GM requirement of the damage case.
- For this vessel not built in accordance with "SOLAS 90" standard the requirement in GM in the original configuration becomes impracticably high.

- Any subdivision introduced on the ro-ro deck significantly influences the survivability of the vessel in damaged condition.
- Other than the calculation the test show better results by the introduction of the proposed two full height bulkheads.

A graphical evaluation of the maximum allowable KG-values are shown in figure 5, 6 and 7.

In case of ship B and ship C the freeboard effect was not considered of the same predominance. A result of the trim variations, however is that obviously small trim angles do have some effect on the GM-requirement.

This is shown for ship B:

Initial trim	Original configuration Version A		With additional bulkheads Version E2		With side casings Version F	
	L 11/12 GM_L	L 7/8 GM_L	L 11/12 GM_L	L 7/8 GM_L	L 11/12 GM_L	L 7/8 GM_L
-1.0 m	2.73 m	-	0.78 m	-	1.54 m	-
0.0 m	2.30 m	1.13 m	1.11 m	1.21 m	1.19 m	1.29 m
1.0 m	-	1.37 m	-	0.96 m	-	1.60 m

The evaluation of Ship C had the following outcome:

Initial trim	Original configuration Version A		With additional bulkheads Version E2		With side casings Version F	
	L 10/11 GM_L	L 6/7 GM_L	L 10/11 GM_L	L 6/7 GM_L	L 10/11 GM_L	L 6/7 GM_L
1.06 m	0.71 m	1.92 m	0.54 m	-	1.11 m	-
0.0 m	1.02 m	1.94 m	1.07 m	1. 24 m	1.20 m	1.83 m
-1.07 m	-	2.10 m	-	1.29 m	-	2.00 m

An overview of the survivability results are shown in table 1, table 2 and table 3

The ship motion, the relative motion between the damage opening and the water surface and the water height on deck were measured during the tests. The most important information is the roll-response which indicates whether or not the vessels is regarded as capsizing or not. Figures 3a show as a section of the measured time and water height records such a typical capsizing. Encountering a group of high waves the vessel is forced to heel to a rather large angle by the load introduced by the collected water on deck. In the following calmer period the vessels recovers very slowly to a more upright position. Another group of larger waves approaching again increases the heeling continuously to lead to the eventually observed capsize. Provided the initial GM is slightly larger the vessel shows better recovering times before encountering the next group of high waves.

Once the critical KG/GM values had been generated as describing the limit between safe and unsafe, the residual stability parameters were calculated. Accordingly the respective maximum lever arms and stability ranges were derived.

The results indicate clearly that the "open deck" Version iterates a larger requirement of residual stability. Both of the subdivided Versions (side casings and two transverse bulkheads), however, showed requirements in a similar order.

Based on the known dependency of the stability parameters on B/T and the observation that the deck area involved (i.e. length and beam of the wetted ro-ro cargo area) and trim have large impact. Therefore, it is proposed to use these geometric features to describe the residual stability characteristic.

$$GZ^* = GZ_{MAX} * \frac{T}{B} * \frac{1}{(1.368 - \exp(-(A_{RO} / bL)^2)) * (0.2 + \exp(-(57.3 * \Delta T / L)^2))}$$

$$F_b^* = (F_b + B/2 * \sin\Phi_{Stat}) / \varsigma_{\omega sig}$$

For Version A all three hulls are shown in figure 4a versus the freeboard.

7. References

[1] The International Convention.for the Safety of Life at Sea (SOLAS) 1974 including all relevant amendments

[2] Regional Agreement concerning specific stabilty requirements for ro-ro passenger ships ("Stockholm Agreement") published as IMO Circ. Letter 1891 dated 29th April 1996.

[3] Kröger, H.P., Rollsimulation von Schiffen, Schiffstechnik 33 (1986)

[4] Petey, F., Ermittlung der Kentersicherheit lecker Schiffe im Seegang, Schiffstechnik 35 (1988), 155-172

[5] Chang Bor-Chau, On the capsizing safety of damaged ro-ro ships by means of motion simulation in waves, Int. Symposium Ship Safety in a Seaway: Stability, Manoeuverability, Nonlinear Approach, Kaliningrad 1995.

Water Discharge From An Opening In Ships

S. M. Calisal[1], M. J. Rudman[2] , A. Akinturk[1], A. Wong[1] and B. Tasevski[1]

Abstract

Water trapped on ship decks can play an important role in the safety of ships in terms of stability. The goal of this study is to understand the governing factors and to model the discharge mechanism of water from an opening e.g. freeing-ports onboard of ships. This paper presents the initial results obtained by experimental and numerical studies done at the University of British Columbia and Melbourne University, respectively.

In the formulation of the discharge flow from a flooded deck two major problems exist. One is the form and location of the free surface, the other discharge rate and how it is connected to the rest of the form of the free surface. In the study of water-on-deck flows without freeing ports, only the form of the water-on-deck is of interest. The problem of water-on-deck with discharge can be reduced to a water-on-deck without freeing ports if a relationship between the discharge rate and the free surface form can be established. This is the starting point of this research. The proposed method and approach consists of both the numerical and the experimental study of water discharge from the open deck of a ferry or a fishing vessel through permanently open freeing ports or freeing ports with a flap cover. A two-dimensional model of the discharge was built during the summer of 1997 to visualize the free surface and to measure the flow discharge from a flat bottom. The model has four different lengths corresponding to the width of the ship and the initial water height used before the discharge was changed in order to determine the importance of the level of accumulated water on deck. The discharge flow pattern and free surface form were recorded with a digital camera. The frames were captured on a computer and the location and the form of the free surface established. From knowledge of the free surface the change in volume, discharge rate velocity at the freeing port and various parameters of the discharge kinematics were calculated. The experimental results will be studied to generate numerical algorithms that can be used to calculate the discharge rates from freeing ports.

Numerical modelling and preliminary results are also given in this paper. Initial results suggest a very good agreement between the experimental and numerical results.

[1] University of British Columbia, Department of Mechanical Engineering, Canada
[2] Melbourne University, Advanced Fluid Dynamics Laboratory, Australia

1. Introduction

Some Canadian ferries operating in British Columbia in relatively sheltered areas have open car decks. Water could possibly collect on deck of these ferries by the scooping action in waves, or as a result of an accident thus causing loss of stability by a process which is generally known as the "free surface" effect. Various researchers in Canada have studied the possibility of water on deck and its drainage from freeing ports. The authors participated in the experimental study of water accumulation on a ferry model in head seas, Roddan et al. (1995). In this study the model was in moderate waves and a procedure was developed to estimate the minimum freeboard required to avoid water accumulation on deck for a given sea state, Calisal et al. (1997). This procedure consists of experimental and numerical results. During the summers of 1997 and 1998, discharge from a two-dimensional model of a section of a ferry was experimentally studied. The model, initially full of water was drained by instantaneously opening a freeing port. The measurement of the form of the water surface on board and the discharge rates were the primary objectives of this preliminary study. This preliminary experimental study allowed us to measure and document the variation of the free surface and discharge rates of water from the freeing ports during the draining phase. An optical measurement system was developed for this purpose, which uses a video camera, a frame grabber and specialized software developed in-house to calculate the location of the free surface during draining. The data collected are currently under study. This paper presents some of the preliminary results and comparison of the experimental results with the numerical predictions. The visualization showed that in addition to the expected gradual drop in the free surface, some traveling waves are also present on deck. The objective of this study is to develop a numerical procedure for calculating the water collection and discharge rates from the open deck of a ferry or a fishing vessel. The numerical procedures will be validated in experimental work and suitable design procedures and algorithms will be developed for the time-domain calculations of ship stability. The requirement of an estimate of the discharge rate is essential for the numerical calculations, and the use of such an algorithm permits the definition of the boundary conditions necessary for the application of numerical methods such as Boundary Element Method. The defining of a boundary condition supported by experimental work is expected to increase the numerical accuracy of the computed flow field, therefore of the critical discharge time. This in turn is expected to permit relatively fast evaluation of damaged stability of open deck vessels in time domain.

Another important objective is the establishment of a "closure" relationship for the completion of the potential flow formulation. That is, knowledge of the discharge rates for unsteady flow is necessary in order to assign the normal velocity boundary condition for the potential flow formulation (BEM). Work done on steady waterfalls suggests that the depth-Froude number of the flow should be equal to one (Fr = 1). However, our recent experimental work with a constant model length but with various initial water heights suggests that the Froude number of the flow discharging from the decks is time dependent and starts at a value of zero. The Froude number then increases to a value of approx. 0.7 and then starts to decrease continuously back to zero. We will study various model lengths and model roll frequencies to establish if numerical algorithms can be developed to predict the discharge velocity from knowledge of the instantaneous water height. Of course, the form of the water surface will remain an unknown and will be calculated by a numerical procedure. The overall objectives can be listed as:

- Establishment of a relationship between water height and discharge speed.
- We expect to find a time domain expression for the Froude number for unsteady free-surface flows. This algorithm is expected to improve the performance of existing codes on water deck flows as it will permit a relatively easy and accurate calculation of the discharge rates.
- This result will also be important for the understanding of free-surface flows such as waterfalls, where for steady conditions, the depth-Froude number is usually assumed to be equal to one.

The development of a numerical code to establish water accumulation and discharge volume rates for different ship conditions such as rolling, and stationary, and with and without

list, will permit the study of the dynamic stability of damaged ferries.

The study will give design criteria for the minimum free board necessary for open-deck ferries, as this height determines the amount of water which will accumulated on deck for a given wave height condition. As this rate must be smaller than the discharge rate for the number of available freeing ports, a design procedure based on a design wave height, freeboard height and number and size of freeing ports will result from this study.

2. Experiments

The experimental apparatus consisted mainly of the following items: water discharge tank, data acquisition devices including a high speed camera, VCR, and data analysis devices including video frame grabber, imaging software, and a surface scanner program.

A discharge tank was constructed with 1/2' clear Plexiglas (see Figure 1). The inner dimensions of the tank are 6 feet long by 1.5 feet tall by 1 feet wide, or 72 x 18 x 12 inches respectively. The tank is closed on one end and water is only allowed to drain out of the other end. A height adjustable gate was installed on the open end such that the opening area of discharge port can be changed between 0 and 12 inches. An elastic cord mousetrap like device was used to open the piano hinged door to start the discharge very quickly.

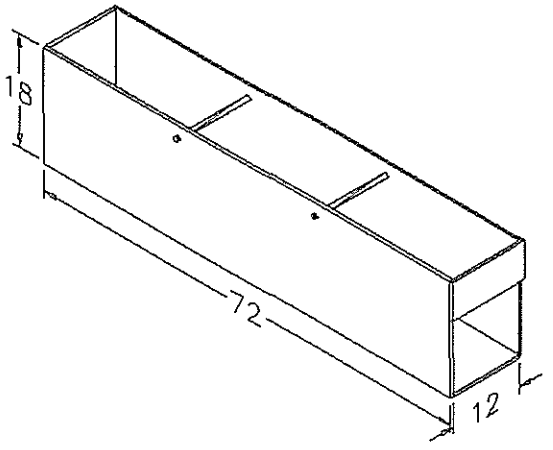

Figure 1. Plexiglas discharge vessel dimensions

A dexion table with four height adjustable feet was also constructed to support the tank. The adjustable feet allowed us to properly adjust the height such that the tank could be perfectly level.

For experiments where shorter tank length was required, a piece of 1/2-inch removable Plexiglas divider was placed at the desired location (see Figure 2). The divider was supported by an angle plate and a 2 x 6 lumber to prevent it from sliding back when the other side was filled with water. A non-permanent rubber gasket tape was also added at the edges to prevent leakage.

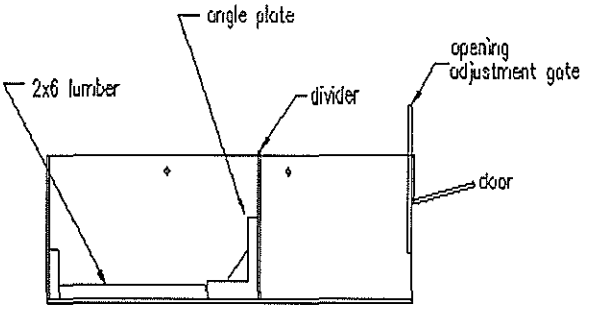

Figure 2. Side-view of discharge vessel

2.1 Data Acquisition Devices

The Optikon MotionScope High Speed Video System was used to capture the discharging water profile near the opening of the gate (see Figure 3). The system is a simple to "point" and "shoot" device, with a built-in 5" monochrome CRT video display and a separate video camera. The system has the capability to capture 60, 120, 180, 250, 300, 400, and 500 frames per second. The electronic shutter is also user adjustable and can be set from 1X to 20X of the set recording rate. The images captured were stored temporary in the system's buffer, with a capacity to store up to 2,048 full frames.

The lens which came with the MotionScope was removed and a Cosmicar CCTV 1/2-inch manual-iris c-mount lens was used as a replacement (see Figure 4). This lens was used because the software that was used to analyze the captured data had previously been calibrated for distortion with this particular lens. With the irregularity of the MotionScope's camera however, some problems were encountered

with the lens geometrical specifications. For one, the Cosmicar lens was located too closely to the CCD of the camera, which caused the lens to provide a very large field of view (FOV) which cannot be focused properly. A 5mm CS to C mount adapter ring, which was supplied with the MotionScope, must be installed onto the lens mount of the sensor head assembly before the c-mount lens could be mounted. However, with the use of the adapter ring, the lens was moved too far away from the CCD which gave us a very small FOV (5.64 degrees). Nonetheless, this set up was used because no other options were available if the MotionScope was to be used. The small FOV was compensated for by moving the camera further away from our water tank.

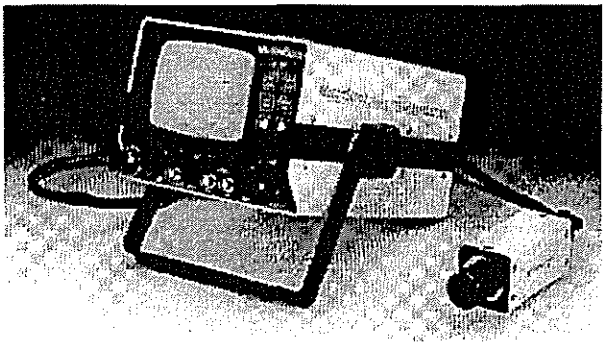

Figure 3. Optikon MotionScope High Speed Video System

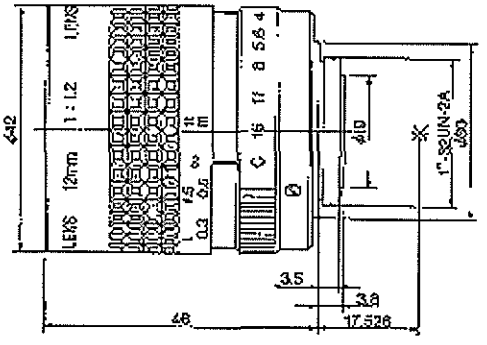

Figure 4. Cosmicar CCTV 1/2inch manual-iris c-mount lens

2.2.1 TV and VCR

A TV and VCR combo was required due to the lack of permanent storage on the MotionScope. The data from the MotionScope was played back through it's RS-170 (NTSC compatible) video output and recorded onto a videocassette in the VCR. If a PC computer with a frame-grabbing card was available, then the TV and VCR would not be required as we could directly save the MotionScope playback images as a bitmap on the computer.

A schematic of the experimental setup is shown in Figure 5. The camera was placed in such a way that the line passing through the center of the lens and its focal point is perpendicular to the side of the disharge tank. With the current distance (S), it was able to capture the floaded length of the discharge tank.

In this initial study, there were three parameters that were planned to change, t, height of the opening, h, initialwater height in the tank and l, floaded length of the tank. For the results presented in this paper, only initial water height was varied as 6, 10 and 14 inches. The floaded length was 2 feet and height of the opening for water discharge was 4 inches.

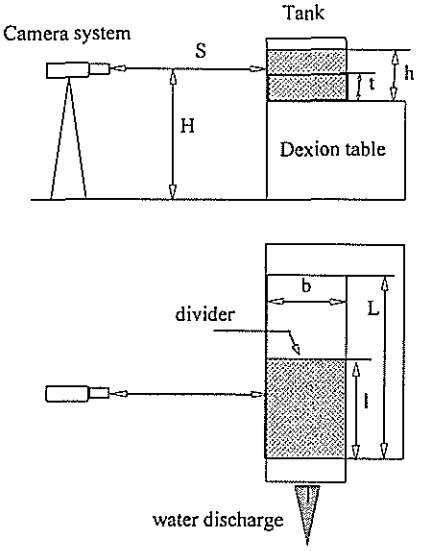

Figure 5: Experimental setup

3. Numerical Method

The numerical method used to simulate the flow of water through the dam sluice gate is the volume tracking method of Rudman (1998). The method is based on the Volume-of-Fluid (VOF) method introduced by Hirt and Nichols (1981) and improved by Youngs (1982). A brief overview of the method is given here, but details of the implementation are beyond the scope of this paper and may be found in Rudman (1998).

The gas-liquid system is treated numerically as a single incompressible fluid whose density and viscosity vary rapidly in the vicinity of physical interfaces. The incompressible Navier-Stokes equations for a variable density fluid are written:

$$\frac{\partial(\rho U)}{\partial t} + \nabla\cdot(\rho\, UU) = -\nabla P + \rho\, g + F_S + \nabla\cdot \mathrm{T}, \quad (1)$$

$$\nabla\cdot U = 0 \quad (2)$$

$$\frac{\partial C}{\partial t} + \nabla\cdot(U C) = 0 \quad (3)$$

where ρ is the density, U is the velocity vector, P is the pressure, g is the gravity vector, F_S is the surface tension force and $\mathbf{T}$ is the stress tensor defined as:

$$\mathrm{T}_{ij} = \mu\left(\frac{\partial U_i}{\partial x_j} + \frac{\partial U_j}{\partial x_i}\right) \quad (4)$$

The fractional volume function C is a function that takes a value of one inside the liquid and zero inside the gaseous phase. In computational cells through which the interface passes, the value of C varies between 0 and 1. Local densities are calculated from C using:

$$\rho = C\rho_G + (1-C)\rho_L \quad (5)$$

And local values of the dynamic viscosity μ are determined in a similar manner. The equations are discretised on a rectangular Cartesian mesh.

The numerical method is second order in time and space. It uses the Flux-Corrected Transport (FCT) ideas of Zalesak (1979) to calculate the advective terms in the momentum equations and a multigrid pressure solver based on the Galerkin coarse grid approach of Wesseling (1992) to solve for pressure and enforce incompressibility. Accurate determination of surface tension forces is often an important part of the solution of free surface flow problems and is achieved here using a kernel-based variant of the Continuum Surface Force (CSF) method of Brackbill et al. (1992). In this method, a continuously varying body force approximates the exact discontinuous surface force over a thin transition region near the interface. Volume tracking (Eqn 3) is undertaken using a Volume-of-Fluid method based on that of Youngs (1982). VOF methods are designed to maintain very thin numerical interfaces, with the transition from gas to liquid occurring across just one mesh cell in most instances. The advantage of VOF methods over more common approaches for interface problems (such as Boundary Integral Methods) is the ability to accurately simulate arbitrarily complicated problems of fluid coalescence and fragmentation without the need of purpose-built algorithms. In the code used here, the only difference to the method discussed in Rudman (1998) is the inclusion of obstacle cells that allow arbitarily complex internal boundaries to be included in a computation. These obstacle cells are included in the same way as in the original Marker and Cell (MAC) method of Welch et al. (1965)

The basic first-order in time algorithm on which the second-order method is based is as follows:

1. Estimarte new values of C:
$$C^{n+1} = C^n - \delta t\,(\nabla\cdot U^n C^n)$$
2. Estimate new densities and viscosities, ρ^{n+1}, ρ^{n+1}, using Eqn 5.
3. Estimate new velocities using old timestep velocities and pressures:
$$\rho^{n+1} U^* = \rho^n U^n + \delta t\,(-\nabla\cdot\rho^n U^n U^n - \nabla P^n + \rho^n g + F_S^n + \nabla\cdot \mathrm{T}^n)$$
Calculate the pressure correction ρP required to enforce incompressibility:
$$\nabla\cdot\left(\frac{1}{\rho}\nabla\delta P\right) = \frac{1}{\delta t}\nabla\cdot U^*$$
4. Adjust velocities and pressure:
$$U^{n+1} = U^* - \frac{1}{\rho^{n+1}}\nabla\delta P$$
$$P^{n+1} = P^n + \delta P$$

The second-order in time algorithm used in this study performs two passes of steps 1-5. On the first pass, steps 1-5 are performed using a half timestep. In the second pass, steps 1-5 are performed again with a full timestep, the only other difference being that the pressures and velocities on the right-hand side of step 5 are replaced by the half time estimates calculated in the first pass.

The computational domain was discretised on a uniform mesh of 256 × 192 grid cells with physical dimensions 1000mm × 750mm. The holding tank (dimensions 601mm × 425mm) was then numerically 'constructed' by placing a horizontal row of obstacles cells at a height of 200mm above the domain bottom (forming the tank base) and a vertical row 601mm from the left wall of the domain (forming the tank wall). The additional part of the domain outside the tank was required in order to allow the fluid to drain from the tank in a natural way without enforcing arbitrary (and possibly incorrect) boundary conditions on the draining process. The initial condition had the tank filled to a depth of 356mm. The initial velocities were zero and the pressure was set to be equal to the hydrostatic pressure equilibrium that would exist if the tank gate were closed. At zero time, the gate is instantaneously removed and the water flows out of the opening under gravity.

4. Results

As mentioned earlier, after the discharge gate opens, a travelling wave is observed as the free surface level drops gradually. Figure 6 shows the drop in the free surface level and the formation of the travelling wave as the time progresses. The discharge end of tank corresponds to the location around 0.6 meters in the figure. Numerical results are shown as lines. "x" marks the experimental results in the figure. Generally, there is a very good agreement between the two results. In both of the results travelling wave phenamonon was apparent.

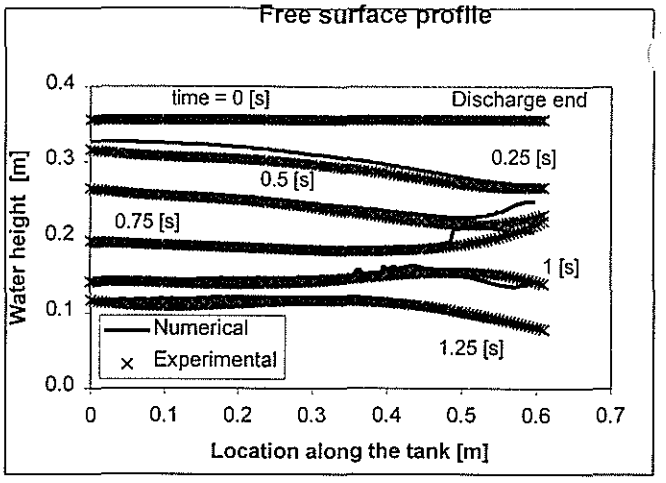

Figure 6: Comparison of the free surface profiles inside the discharge tank at different times

In Figure 7 discharged volumes for both numerical and experimental study are compared. Initially, the agreement is very good between the numerical and experimental volume data. However, as the free surface level decreases considerably, there appaers to be some differences between the two cases (see Figure 7).

Figure 8 shows the effects of initial water height on the Froude number (Fn). The definition of Fn is as follows:

$$Fn = \frac{(Q/A)}{\sqrt{g * Hr}}$$

Where Q is the discharged volume per unit time, A is the exit cross sectional area, g is the gravitational acceleration and Hr is the water height at the rear end of the floaded section. As shown in the figure, Froude number initially starts from 0, increases to a certain value (less than 1) and drops to zero as the amount of water reduced in the discharge tank. From the figure, it seems that as the initial water level in the tank increases so as the maximum Froude number for each experiment. Maximum Froude numbers for the experiments with 14, 10 and 6 inches of initial water heights are approximately 0.7, 0.6 and 0.3 respectively.

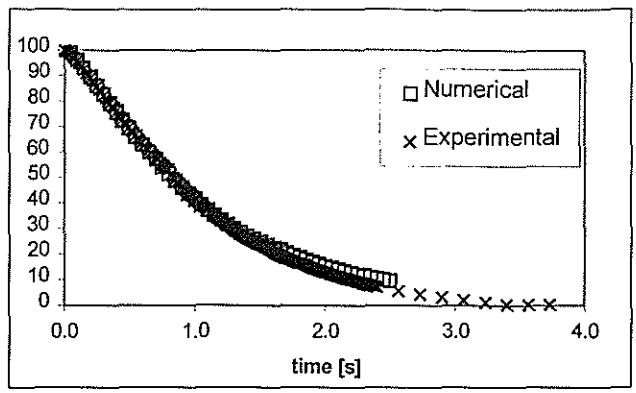

Figure 7: Remaining volume in the discharge tank as the percentage of the initial water volume

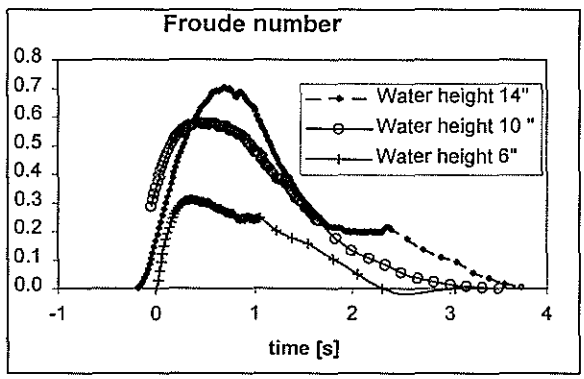

Figure 8: The effects of initial water height on the Froude number

5. Summary

Up to now two model lengths (length of the floaded section in the discharge tank) have been used and discharge data for them at various initial water heights stored. However, the results presented in this paper correspond to 60.96 cm model length only. The discharge tank was filled with water at a prescribed level and the discharge gate was opened to simulate the freeing ports with a flap cover. The discharge flow pattern and free surface form were recorded with a digital camera. The frames were captured on a computer and the location and the form of the free surface established. From knowledge of the free surface the change in volume, discharge rate velocity at the freeing port and various parameters of the discharge kinematics were calculated. In addition to using horizontal bottom conditions we intend to study discharge from listing and periodically rolling decks both with permanently open freeing ports and with freeing ports that have flapped covers. The experimental results will be studied to generate numerical algorithms that can be used to calculate the discharge rates from freeing ports. Time domain results will also be used to validate the numerical studies.

Initial numerical calculations done by Rudman showed that a very good representation of flow can be predicted by his formulation including wave formation by the opening of the gate. This type of wave formation was observed during the experiments and was successfully predicted using this code.

After completion of the two- dimensional studies we intend to model symmetric, three- dimensional flows and study them experimentally and numerically.

6. References

Brackbill JU; Kothe DB; Zemach C (1992) A continuum method for modelling surface tension. *J. Comput Phys.* **100**: 335–354

Hirt CW; Nichols BD (1981) Volume of Fluid (VOF) Methods for the dynamics of free boundaries. *J. Comput. Phys.* **39**: 201–225

Rudman, M (1998) A Volume-tracking method for simulating multi-fluid flows with large density variations. *Int. J. Numer. Methods Fluids* **28** 357-378.

Welch, JE, Harlow, FH, Shannon, JP and Daly, BJ (1965) The MAC method: A computing technique for solving viscous, incompressible, transient fluid-flow problems with free surfaces, Los Alamos Scientific Laboratory Report LA-3425.

Wesseling P (1992) *An introduction to multigrid methods.* John Wiley and Sons. Chichester U.K.

Youngs DL (1982) Time-dependent multi-material flow with large fluid distortion, in *Numerical methods for fluid dynamics*. Morton and Baines (eds), Academic Press, New York: 273-285

Zalesak ST (1979) Fully multi-dimensional Flux Corrected Transport algorithms for fluid flow. *J. Comput. Phys.* **31**: 335–362

DESIGN ASPECTS OF SURVIVABILITY OF SURFACE NAVAL AND MERCHANT SHIPS

APOSTOLOS PAPANIKOLAOU[1], EVANGELOS BOULOUGOURIS[2] ,

[1] Professor, Head of Ship Design Laboratory, National Technical University of Athens, Department of Naval Architecture & Marine Engineering, Greece, *papa@deslab.ntua.gr*
[2] PhD. cand., National Technical University of Athens, Department of Naval Architecture & Marine Engineering, Ship Design Laboratory, Greece, *vboulg@deslab.ntua.gr*

Abstract. The paper addresses various design aspects of survivability for surface naval and merchant ships through a common probabilistic methodology. In the essence, the suggested methodology is based on earlier work of Kurt Wendel introduced in the early sixties on a probabilistic approach to the damage stability of surface ships. This method was adopted by SOLAS 1974 in the regulatory framework of IMO through Res. A.265 (VIII) as an alternative to the deterministic SOLAS criteria for passenger ships and finally by SOLAS 1992 for the evaluation of stability of new cargo ships. The method is currently under review by relevant working groups of IMO for application to all types of merchant ships in the framework of harmonization of all existing stability rules. On the other side, the method found recently access into the design process of modern naval ships. The declining defence budgets world-wide and the reduced manning requirements bound the size and thus the payload of modern naval ships, required in addition to operate in an increased dangerous warfare environment. Thus, one way to efficiently proceed is the introduction of a new naval ship design philosophy, namely the introduction of rather small naval ships of *enhanced survivability*. Most designer decisions, associated with survivability, as compartmentation and arrangements, are taken at the preliminary design stage and are very difficult and costly to change, if at all, in latter stages. Therefore, a proper guidance in the preliminary design stage would greatly help to design the next generation surface combatants, as it is expected from the design of merchant ships, to comply with future more stringent survivability and safety requirements. The paper addresses the fundamental aspects of survivability and introduces this relatively new probabilistic approach for assessing the damage stability and survivability properties of both naval and merchant ships.

Keywords. Survivability, damage stability, probabilistic stability method, A.265-IMO, vulnerability, lethality, susceptibility, modelling, simulation, simulation based acquisition (SBA).

1. INTRODUCTION

Introduction

One might wonder what is common between the design of a naval surface combatant and a Ro-Ro passenger ship. The answer is simultaneously easy and complex: they both *have to* survive in case of damage, for obvious reasons, however under quite different constraints, external damage threats and environmental conditions. For surface combatants, although the probability of damage is very high and it should be a significant factor in their design, there was never before a

systematic examination and assessment of their survivability. On the other hand, many tragic events occurred recently in passenger shipping, turning the attention of the public to the inherent safety of Ro-Ro Passenger Ferries. The public outcry stressed the need for enhancing the inherent survivability of this type of ships in case of damage by efficient design measures. In the following, a consideration of possible common methodologies for the survivability analysis of these two totally different ship types is attempted.

The Naval Ship Dimension

Modern naval warfare is characterised by highly sophisticated weapon systems. Surface combatants have to counter a great number of air, surface and underwater weapons guided with various sensors: radar, infrared, electroptic, or laser-guided. In order to accomplish their mission they have to carry a large arsenal and a complicate suit of advanced (but nevertheless sensitive) electronics. All these have increased their acquisition and operational cost and have reduced the size of the fleets operated by various Navies. On the other hand the need for a high payload to displacement ratio has driven the designers to a reduction of the shell plate thickness for keeping the structural weight as low as possible. It was a change in the philosophy of designing naval ships: a shift *from enhanced armour to sensor capability*. The so made naval ship designs were more vulnerable as could be proven in the *Falkland Islands* Conflict, in the *USS Stark* (FFG-31) incident and during the *Gulf War* Naval Operations. It becomes obvious that an effective solution to this problem is the adoption of a rather a new design philosophy, namely *Design for Enhanced Survivability.*

Nature makes its creatures adaptive to their environment for survival. In the same way, ships should be designed with an inherent ability to survive in the threat environment they have to operate. For naval ships survivability is the capability to continue to carry out their missions in the combat lethal environment. This is obviously first of all a function of their ability to prevent the enemy from detecting, classifying, targeting, attacking or hitting them. The *inability* to "intercept" any of the above threats is a measure of their *susceptibility.* In case the later proves to be insufficient for eliminating the threat to the ship and an enemy hit succeeds, then the ship's survival depends on the extend of degradation as result of the damage it suffers. The degree of impairment characterises the ship's *vulnerability.* The product of *susceptibility* and *vulnerability* defines the *killability* of the combatant. Mathematically this can be expressed by the following global formula:

$$\textit{Killability} = \textit{Susceptibility} \times \textit{Vulnerability}$$

or in terms of the respective probabilities

$$P_K = P_H \times P_{K/H} \qquad (1)$$

Thus the probability of survival S is expressed by:

$$S = 1 - P_K \qquad (2)$$

It is obvious that *in order to maximise the naval ship's survivability we have to minimise its susceptibility and vulnerability.*

The susceptibility of a naval combatant is dependent on its *signature* characteristics. Signature reduction measures will decrease the chance of being detected and classified. These measures include the minimisation of the radar cross section, infrared and noise, magnetic and electro-optical signature.

The vulnerability reduction measures must be addressed in the early design phase in order to maximise the results. These measures include arrangements, redundancy, protection, and equipment hardening as well as damage containment.

If we restrict our analysis only to conventional (high explosive) anti-surface weapons then there are two main damage effects that threat the survival of a combatant: **flooding** and **fire**. Though both are equally essential we will limit our survivability analysis herein only to the first one. The reason is first of all that the second aspect (fire) can be effectively performed only at advanced stages of design. Besides for any ship we have to counter a fire onboard, it is assumed that it is staying afloat and upright. Mathematically this means that we consider flooding and fire as *independent* events:

$$P_K[Hit \cap (Flooding \cup Fire)] = P_K[(Hit \cap Flooding) \cup (Hit \cap Fire)] =$$
$$= P_K[Hit \cap Flooding] + P_K[Hit \cap Fire] - P_K[Hit \cap Flooding] \times P_K[Hit \cap Fire]$$

which also means that in the following we will be assuming that the probability of loss after a hit due to fire, given the progressive flooding due to the same hit, is zero, i.e. $P_K[(Hit \cap Fire) \mid (Hit \cap Flooding)]=0$. Therefore for the rest of this paper we will be referring to the survivability of naval ships by meaning just *flooding survivability* and by calculating the $P_K[Hit \cap Flooding]$.

The Passenger Ship Dimension

Since the early seventies (SOLAS 1974) the International Maritime Organisation (IMO) has adopted probabilistic methodologies for the assessment of survivability of passenger ships. We refer to the regulation A.265 (VIII) of IMO setting an equivalent to the deterministic stability criteria, namely part B of Chapter II of the International Convention for the Safety Of Life At Sea, 1960 (SOLAS 60). The vast number of the required calculations for a full probabilistic assessment of a ship under consideration, was, in those days of limited computer hard- and software, a serious drawback that led to only limited applications to actual ships. This was one serious reason for the further development of the deterministic criteria (SOLAS 90, 92 & 95), whereas the results of the probabilistic approach (or a simplified version thereof) was only used as an indicator for the implementation of new regulatory schemes to existing ships (phase-in procedure). However, it is a taken decision of IMO to formulate[1] and approve a "harmonised" new probabilistic stability framework for all types of ships, possibly by the SOLAS conference in the year 2000.

According to IMO Res. A.265, and following the fundamental concept of K. Wendel [1], there are the following probabilities of events in the framework of damage stability:

1. The probability that a ship compartment or group of compartments *may be flooded (damaged)*, **p**.
2. The probability of *survival after flooding* the ship compartment or group of compartments under consideration, **s**.

The total probability of survival is expressed by the attained subdivision index **A** which is given by the sum of the products of $\mathbf{p_i}$, and $\mathbf{s_i}$ for each compartment and compartment group, **i**, along the ship's length:

$$\mathbf{A} = \sum_i \mathbf{p_i} \cdot \mathbf{s_i} \qquad (3)$$

The regulations require that this attained subdivision index should be greater than a required subdivision index **R**, which is determined as a function of the number of passengers the ship is carrying and the extent of life-saving equipment onboard. This value is a measure for the acceptable risk of the ship for not surviving a random damage and it is obvious that this value increases with the number of passengers onboard the ship. The factors in the formula determining **R** are so selected to correspond to the mean values of the attained subdivision indexes of a sample of existing ships with *acceptable* stability characteristics. This is, of course, a point for lengthy discussions, because the safety standards of passenger ships have significantly changed over the years, therefore the basis for the evaluation of **R** must be updated to account for these changes.

In order to determine how we can increase the survivability of the RoRo passenger ships we have to specify the "threats" (or better the "risks") they have to counter. Similar to naval vessels, passenger ships face mainly two major threats: Flooding and Fire. It is obvious, that for A.265 the survivability is virtually identical to the vulnerability in case of flooding. The regulation does not take into consideration either the *vulnerability* in case of fire or the *susceptibility* of the ship. However, it is formally not difficult and probably advisable to incorporate *susceptibility* to the survivability of Ro-Ro passenger ships, as it has been suggested for naval ships. This concept is more or less adopted in the formulation of the "Safety Assessment", or "Formal Safety Assessment (FSA)"[2]. In this way we can

[1] See, SLF39, SLF 40, SLF 41, forthcoming SLF 42

formulate a unified scheme model (methodology) for assessing the survivability of both naval surface combatants, passenger Ro-Ro ships and any other type of ship. The main difference to naval ships is in the formulation of the anticipated risks, namely in case of passenger ships, and of merchant ships in general, we should be considering flooding due to one of the following impact events [2]:

1. Ship to ship (collision)
2. Ship to berth/breakwater (contact)
3. Ship to bottom (grounding/stranding).
4. Explosion
5. Terrorist act
6. Material Failure
7. Human Error

The probability of a passenger ship loss in case of flooding or fire is calculated by the formula:

$$P_L[\text{ Flooding} \cup \text{Fire}] = P_L[\text{Flooding}] + P_L[\text{Fire}] - P_L[\text{Flooding}] \times P_L[\text{Fire}]$$

As has been noted above, we should herein discuss only the probability of loss in case of flooding, namely P_L[Flooding].

2. OUTLINE OF POSSIBLE SHIP DAMAGE CONSEQUENCES

It is obvious that between the intact condition and the total loss of a ship there are many intermediate stages. Though these stages can be defined in various ways a very common characteristic is the one relating them to a *functional hierarchy* [3].

According to this in case of a **naval ship** we may have, in descending order, one of the following damage extents:

- **Total Kill** when the ship is considered lost entirely because of sinking (foundering) or completely damaged by fire (or other phenomenon).
- **Mobility Kill** if immobilisation or loss of controllability of the ship occurs.
- **Mission Area Kill** if a mission area (e.g. AAW capability) is considered lost for the ship.
- **Primary or Combat System Kill** in case of one or more vital systems of the ship, such as a propulsion engine or a CIWS, are damaged.
- **Hull, Machinery or Electrical (HM&E) Support System Kill** if one or more components supporting a primary/combat system of the ship are damaged (e.g. the cooling water system).

Apparently a *combat system kill* can lead to a *mission area kill* or a *mobility kill* or even a *total kill*. Likewise a *mission area kill* may decrease to a *combat system kill* after the crew makes necessary repairs. Our primary target is herein to confine damage extent to the lowest possible level.

Accordingly, in case of a **Ro-Ro passenger ship** we may have:

- **Loss of stability** (Intact or damage ship capsizing)
- **Loss of floatability** (progressive flooding, foundering)
- **Loss of power**
- **Loss of mobility** (controllability)

Loss of stability and of floatability, though they might have the same outcome, namely the foundering of the ship, they might be addressed separately, because of the different time scales available for evacuation of the ship. With the loss of power and controllability we consider herein the outcome of damage of the ship's main machinery and vital equipment compartments, and not of an isolated failure incident of the ship's equipment.

3. FUNDAMENTALS OF NAVAL SHIP DESIGN

Compared to a merchant ship, the design of a naval ship is a very complicate task. There is a vast number of requirements -many of them contradicting- and additionally a large number of constraints. Our effort to develop ships of enhanced survivability imposes further constraints to the naval ship design. This means penalties associated with cost, weight and impact on other features. It is generally recognised that during a naval ship development program, though the expenditure at the early design stage amounts only 6% of the total cost, related decisions concern 80% of

the final realisation cost and should be taken with great care [4]. Thus it is important in the early stages of design to have a methodology to assess the survivability of the proposed vessel, to identify shortcomings and to explore feasible improvements. Furthermore, it seems that simulation methods and the development of virtual demonstrators will be indispensable approaches to ship design for the 21st century [5]. Within such approaches, the *Survivability Performance Analysis* is an indispensable design tool, to be briefly addressed in the following.

In order to properly assess the survivability of a naval ship we have first to identify the major threats it has to counter. Considering only conventional weapons, which are the most widely used, we can focus on the consideration of a threat posed by a radar guided missile. The same type of analysis can obviously be modelled for other type of weapons, sensors and threats in general.

4. SURVIVABILITY PERFORMANCE ANALYSIS FOR NAVAL SHIPS

This analysis is based on the modelling of the event sequence from the enemy's arrival to ship's operational area up to the moment at which a hit might strike the vessel. Thus we have the detection, classification, target acquisition and launch of an enemy attack. The ship's response is to jam, attempt to deceive, or to destroy the enemy's incoming weapons.

The probability of ship's detection is a function of the threat's sensor, its range and the ship's signature. A first estimation of the RCS of a surface combatant can be taken from the formula [6]:

$$\sigma = 52 \cdot \sqrt{f} \cdot \sqrt[3]{Disp^2} \qquad (4)$$

where: = ship's RCS in m^2
f = incident radar frequency in MHz
Disp = ship's displacement in tons.

The range at which the ship will be detected from the enemy's radar is given by the equation [7]:

$$R_{max} = \left[\frac{P_T G^2 \lambda^2 \sigma}{(4\pi)^3 P_{min}} \right]^{1/4} \qquad (5)$$

where:
R_{max} = maximum detection range
P_T = transmitter's power
G = antenna gain
= radar's operating wavelength
= ship's Radar Cross Section (RCS)
P_{min} = minimum detectable received signal from the enemy's sensor

Obviously the lower the RCS of the ship, the closer the enemy has to come for detecting it. An optimization of the RCS is nowadays possible by application of STEALTH technology.

P_{min} depends on the enemy radar characteristics and also on the environmental conditions. By the later we mean temperature, sea condition as well as jamming. Increase of any of these parameters results to an increase of P_{min} and eventually decrease of the R_{max}.

Following the vessel's detection it is up to the enemy to decide on the tackle of the target he has picked up. In case he does, classification, targeting and the release of missiles will follow.

Assuming that the missile is radar-guided, its course to the target will also depend on ship's RCS. The path, it will follow, depends very much on its accuracy. This property for weapons engaging surface combatants can be expressed by their Linear Error Probability (LEP). Knowing (or assuming) missiles' LEP we may assume that the missile's position relatively to ship's profile follows a normal distribution with standard deviation σ, related to the LEP by the formula [8]:

$$LEP = 0.6745\sigma. \qquad (6)$$

At this phase the ship will try (if it has not started at a previous stage, assuming it knows that it is under attack) jamming the missile's radar. Because of its higher power, the ship's jamming device will block the missile's radar until it reaches a certain distance from its target. This distance depends on the power ratio

between the radar and the jamming device. At the moment the missile regains a lock on the ship it depends on its aerodynamic characteristics (i.e. maximum turning acceleration and speed) whether it will allow it to turn to the vessel's direction. If not, it will miss the target vessel. To be successful, the missile's minimum turning radius has to be less than its distance from the ship at that moment, namely [6]:

$$\text{Missile Radius} = \frac{V_m^2}{N \cdot g} \leq R_{regain} \qquad (7)$$

Where:

V_m missile's velocity.

N maximum turning acceleration of missile in [g].

g gravitational acceleration.

The range at which the missile will regain a clear picture of the ship's location is given by the formula [6]:

$$R_{regain} = \sqrt{\frac{P_M}{P_J} \cdot \frac{\sigma}{4\pi}} \qquad (8)$$

where P_M/P_J power ratio between the missile seeker and the jammer.

Thus the effectiveness of jamming can be expressed by the integral of the normal distribution from the ship's either end to a distance R_{max}—R_{regain} towards the centre of the ship.

The next step in the above ship-missile struggle includes the use of decoys. Their performance depends also on their RCS. If it is higher than that the ship it will allow the "throw off" the threat. If it is the same, there is a 50% probability that the missile will follow the decoy.

In case of the ship's arsenal includes a "close in" weapon system (CIWS) it will try to destroy the incoming missile. Its probability of success is usually known from trial experiments and it can be incorporated into the model. If there are also missiles that can be used against the incoming threat, their contribution must be also included.

The above can be estimated relatively easily by computer. The problem is that in order to assess the survivability of a ship design we have to estimate the ship's vulnerability and in particular her single hit kill probability. Therefore we have to calculate:

- the probability of "hit of a particular point of the ship".
- the probable "damages extent given a hit at that point".
- the probability of "ship's survival given the hit point and extent".

5. VULNERABILITY - ADVANCED PROBABILISTIC DAMAGE STABILITY (APDS) FOR NAVAL SHIPS

The impact of a hit can be at any point of the ship's length. The target point of the missile guidance system depends on its type, sensor type and guidance system characteristics. For instance, an *Exocet* missile will aim at the ship's waterline, while a *Harpoon* missile will try to enter the ship higher at the ship's superstructure. Likewise, the longitudinal point of impact will depend on the shape that the signature of the ship presents to the particular threat sensor. An IR (infrared) missile will target at the ship's machinery that is an intense hit source. On the other hand a radar-guided missile will probably aim at the ship's radar image centre. For simplicity and generality, we may assume that the impact location is described by a normal probability distribution with its centre at the ship's centre and a linear error probability (LEP) equal to $0.5 \cdot L_{WL}$.

The damage extent can be taken from a Log-Normal Damage Function. This is given by the function [8]:

$$d(r) = 1 - \int_0^r \frac{1}{\sqrt{2\pi}\beta r} \exp\left[-\frac{\ln^2(r/a)}{2\beta^2}\right] \cdot dr \qquad (9)$$

where:

$$= (R_{SK} R_{SS})^{0.5}$$

$$= \frac{1}{2\sqrt{2} z_{SS}} \ln\left(\frac{R_{SS}}{R_{SK}}\right)$$

R_{SK} "dead-sure kill radius"

R_{SS} "dead-sure surviving radius"

which correspond to 98% and 2% probabilities of damage respectively. Their values can be derived from empirical data for the threat missiles considered. Herein we will assume a R_{SK} diameter equal to the U.S. Navy standards namely $15\%L_{BP}$ [9]. The "sure-save" diameter will be taken as $0.24 \cdot L$ as in the A.265 IMO-SOLAS regulations for merchant ships. This results in a ratio of R_{SK}/R_{SS} equal to 0.625. The variation of the log-normal damage function is shown in the following figure.

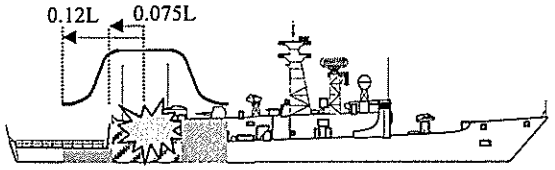

Having defined the first two probabilities namely hit at a particular point and damage extent given the impact point, we are left to define the probability that the ship will survive given the damage location and extent.

A rational methodology for this evaluation can be based on the survival criteria of the U.S. Navy [9], considering that the latter:

- are based on extensive World War II damage reports, though many changes occurred in naval warfare.
- have been proved quite reliable, because they refer to a large number of events during almost 40 years of use. Even though several ships of the U.S. Navy suffered serious combat damages, none of them was lost due to the lack of stability or floatability.
- include dynamic effects though in a "quasi-static" way.

The philosophy for transforming these deterministic criteria into a set of rational probabilistic approach criteria will be based on A.265 IMO-SOLAS regulations for merchant ships.

It is well established that in all relevant criteria there is an underlying assumption that the sea conditions at the time of damage are "moderate". This constraint could be lifted if we knew (or we could assume) a specific operational sea spectrum for the ship design in question. Thus, we could calculate the probability that waves will not exceed the wave height considered as basis for the current deterministic U.S. Navy criteria, namely a sign. wave height of 8 feet. This wave height was the relevant one for the determination of $_{roll}$, namely the roll amplitude due to wave action. It was also the underlying assumption behind the guidelines for establishing the watertight features/closures to prevent progressive flooding. Thus, any attempt to change the wave amplitude must take into account changes in both $_{roll}$ as well as the margin line. Another important environmental parameter is the wind speed. Given the small probability of exceeding the values given by the U.S. Navy standards (namely, about 33 knots for a 3500 tons frigate), this value could be left unchanged.

We can propose, as a first step, the following guidance for the formulation of **survival criteria** to be applied in the frame of a probabilistic approach to the survivability of **naval ships**:

$S = 1$ ($_{roll}$) =25 deg.
Wind speed : acc. to USN-DDS-079-1
Min Freeboard $\geq$ 3in + 0.5×(H_S(0.95)-8 ft)
$A_1 \geq 1.4\ A_2$

$S = P(H_S<8\ ft)$ if the ship meets the current (deterministic) damaged stability criteria of the U.S. Navy.

$S = 0$ ($_{roll}$) =5 deg.
Wind speed $\leq$ 11 knots
$A_1 \leq 1.05\ A_2$
Margin line immerses.

For intermediate stages, interpolant values could be used.

It is obvious, that some systematic experimental and theoretical work is needed in order to specify in a more rigorous way the calculation of the ***S*** value for naval ships. In any case, the calculation of the probability distributions of wave exceedence in the area of

operation are necessary. For instance, the $P(H_S<8\ ft)= 0.60$ holds for the North Atlantic, but $P(H_S< 8ft)= 0.90$ for the Mediterranean Sea. Thus, a combatant, meeting the U.S. Navy criteria, should have, according to the criteria formulated above, a 60% probability of survival for any 2-compartment damage in the North Atlantic and a 90% probability of survival in the Mediterranean Sea [10,11].

The above procedure for assessing the damage stability component of the vulnerability could form an important element of a new *Advanced Probabilistic Damage Stability* method for naval ships. It makes possible the assessment of damage cases, where multiple hits of non-adjacent compartments can occur. This increases the flexibility of the designer. It makes also the damage stability of the vessel a property of the design and not just a requirement that has to be met later on.

6. THE RO-RO SHIP DESIGN PROCEDURE

The existing probabilistic method A.265 is a rational but complicate and non transparent procedure for assessing the probability of survival of a ship. On the other hand, the ship specific survivability characteristics should be reflected in a clear way in its survivability index for possible design optimization. By use of modern hardware and software computing tools, an optimization appears today feasible, as it will be outlined in the following.

As far as the possible risks for passenger ships are concerned, it has been noted at the stage of definition of the various possible damage cases for Ro-Ro vessels that multiple stages of damage prior to the total loss of ship can be considered. The probability of loss of controllability, or of power (black out) should be actually also considered. Piping transferring cold water for cooling vital machinery or power transfer lines passing through the damaged compartment should be identified. The probability of their damage has to be considered and properly included in the calculations. Additionally, the time required to evacuate the ship must also be taken into account. This would encourage ship designers to consider arrangements and efficient equipment for the safe evacuation of passengers and crew, beyond the least requirements set by the regulations. Recent work by D. Vassalos [12] stresses the need for assessing the available evacuation time in case of damage and prior to capsizing or foundering. Existing regulations specify the maximum time available for evacuation but no special care is given to consider the ship damage conditions that might affect this time. Large heel or trim may increase the evacuation time significantly especially for children, elderly or persons with mobility problems. Thus damage cases with large heel or significant trim have to receive reduced weights even though the stability requirements are met.

The consideration of the particular significance of the various ship spaces can be incorporated in the regulations by assigning them so-called *"vitality"* coefficients as it has been already done with the variation of space permeability. Thus spaces with vital machinery or equipment will receive more weight in the survivability analysis. This will account for the fact that even though the ship stays afloat, in case of damage, the associated risks are greater compared to the same post-damage condition after damage of non-vital spaces. The Attained Subdivision Coefficient formula should be therefore modified as following:

$$A = \sum_i p_i \cdot s_i \cdot w_i \qquad (10)$$

where w_i is a properly defined vitality coefficient for compartment i. The vitality coefficients ($w_i \leq 1.0$) of the various compartments should be in descending order to their significance. As defined above, vitality of course depends on the existence of redundant equipment. Also, if for a damage case involving multiple compartments, both the primary and the emergency equipment are contained in the damage extent, the vitality coefficient has also to be reduced. The above procedure calls for the introduction of innovative machinery and equipment arrangement concepts (multiple machinery spaces, redundancy of equipment, etc.) as, e.g., has been indicated in recently published work by M. Kanerva [13].

Specific values cannot be proposed in this

paper because more work has to be done in this area. It should involve both damage statistics and actual machinery arrangements of existing ships.

The above revision of the Attained Subdivision Coefficient formula calling for special consideration of vital spaces can be incorporated in a more general Ro-Ro ship design optimization scheme, as outlined in the attached chart. The procedure considers the optimization with respect to the Local Subdivision Index, as proposed earlier by P. Sen and M. Gerigk [14] and properly modified, as given above to account for the vitality of spaces.

7. CONCLUSIONS

The paper addressed the survivability of naval and merchant ships (here: Ro-Ro passenger ships) through a common ("harmonized") probabilistic procedure. Possible risks for naval and passenger ships have been outlined. Special attention has been paid to the formulation of survival criteria for naval ships. At present, at the authors' knowledge, all known damage stability criteria for naval ships are deterministic. They all assume a specific extent of damage and require that the ship achieves certain values of metacentric height, or maximum righting levels (GZ), at certain heel angles. The only probabilistic method known to the authors at this stage is that of the German Navy, but only for those ships which do not satisfy the set deterministic criteria. Therefore the authors suggest, herein, specific survival criteria for naval ships, to be included into a formal probabilistic assessment of survival of naval ships. Finally, following general design concepts of naval ships, a modification of the formula of the Attained Subdivision Index of passenger ships has been proposed accounting for the vitality of specific ship compartments, securing the powering, electric supply and controllability of the ship after damage.

The increased importance of modelling and simulation methods in modern ship design requires the development of more rational concepts. Though the above methodology is, at this stage, not complete, it is suggested as a first step to a new design direction. It is of course obvious that much work is still needed to test and to fully verify the proposed procedures. A framework for discussion of the suggested design procedures for Ro-Ro passenger ships is the Thematic Network SAFER-EURORO [15] supported by DG XII of the European Commission. Their financial support is herein acknowledged.

REFERENCES

1. K. Wendel, "Die Wahrscheinlichkeit des Ueberstehens von Verletzungen", Journal Schiffstechnik, 1960, p. 47-61.
2. J. Spouge, "Safety assessment of passenger/Ro-Ro vessels", Int. Seminar n the Safety of Passenger Ro-Ro Vessels, RINA, London, 1996.
3. R. E. Ball & C. N. Calvano, "Establishing the Fundamentals of Surface Ship Survivability Design Discipline", Naval Engineers Journal, January 1994.
4. M. T. Van Hees, *Quaestor: Expert governed parametric model assembling*, PhD Thesis, Technische Universiteit Delft, February 1997.
5. *Technology for the U.S. Navy and Marine Corps, 2000-2035:Becoming a 21st Century Force*, National Research Counsil study.
6. D. A. Rains, "Methods For Ship Military Effectiveness Analysis", Naval Engineers Journal, March 1994.
7. C. H. Goddard, D. G. Kirkpatrick, P. G. Rainey and J. E. Ball, "How much STEALTH?", Naval Engineers Journal, May 1996.
8. J. S. Przemieniecki, "Mathematical Methods in Defense Analyses", AIAA, Washington, DC, 1994.
9. S. W. Surko, "An Assessment of Current Warship Damaged Stability Criteria", Naval Engineers Journal, May 1994.
10. A. D. Papanikolaou et al., *Study on the Practical Implications of the Proposed New SOLAS Regulations on Existing Greek Ro-Ro Passenger Ships and Critical Review of the Proposed New Regulations*, NTUA Report, Athens, September 1995.
11. G. Athanassoulis, M. Skarsoulis, *Wind and Wave Atlas of the North-Eastern Mediterranean Sea*, NTUA-SMHL Publ., Athens 1992.
12. D. Vassalos et al., "Time Based Survival Criteria for Ro-Ro Vessels ", The Royal

Institution of Naval Architects, Spring Meetings 1998.
13. M. Kanerva, "Fundamental Rethinking of Passengership Design for Economic Operation by Owners and Construction by Shipyards", Cruise & Ferry 97, London, 1997.
14. P. Sen & M. Gerigk, "Some Aspects of a Knowledge-Based Expert System for Preliminary Ship Subdivision Design for Safety", Proc. PRADS'92, Vol. 2, pp. 1187-97, 1992.
15. D. Vassalos et al., *The Thematic Network SAFER-EURORO, Ro-Ro Design for Safety*, European Commission Network, DG XII, 1996-2000.

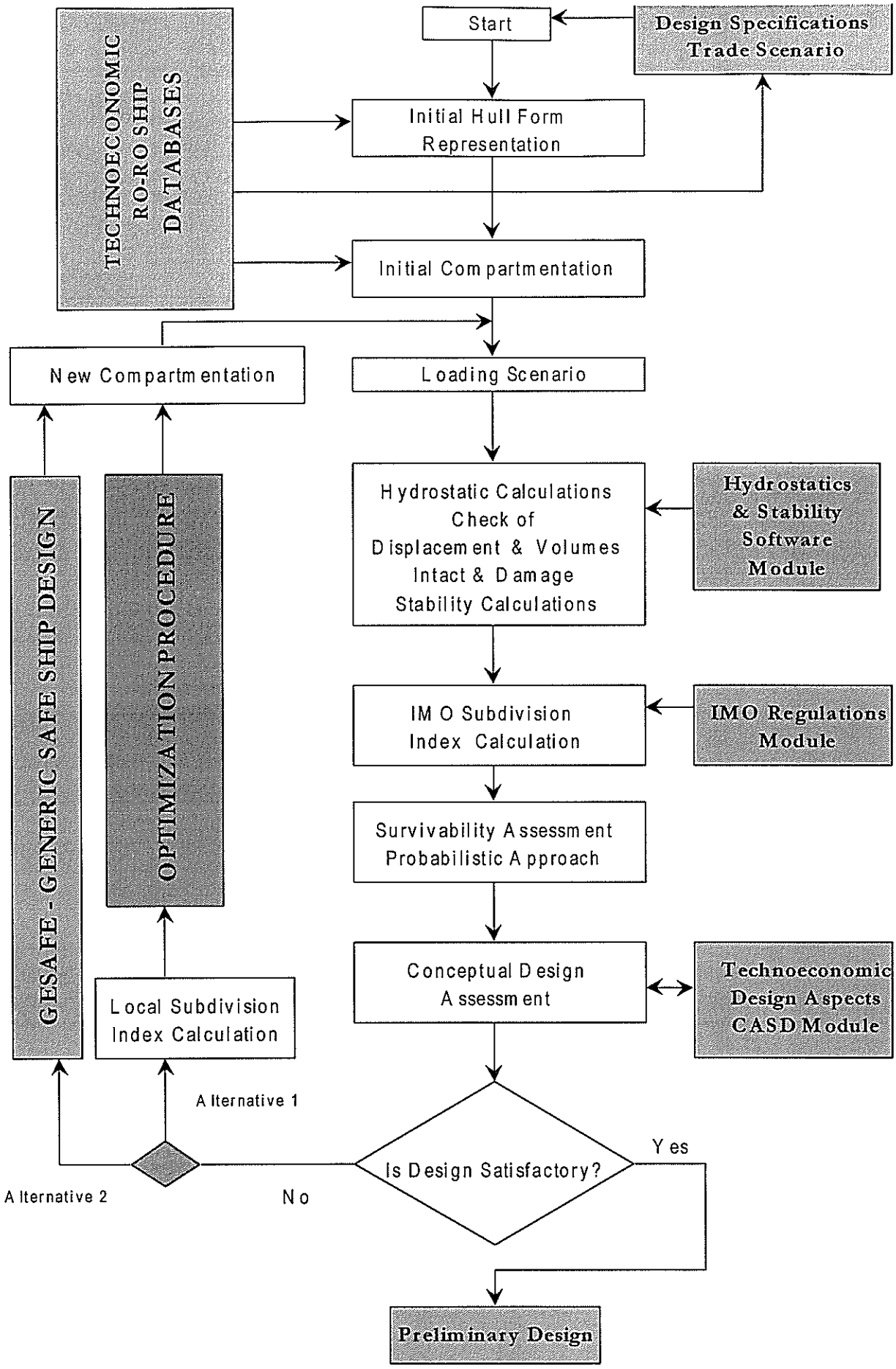

SAFER-EURORO: COMPUTER-AIDED SAFE FERRY DESIGN PROCEDURE

A Realisable Concept of a Safe Haven Ro-Ro Design

By
Dracos Vassalos
The Ship Stability Research Centre, Department of Ship and Marine Technology
University of Strathclyde, Glasgow, UK

SUMMARY

A considerable amount of effort has been expended, particularly over the recent past, towards enhancing the safety of Ro-Ro vessels. The routes followed include proposals for a stricter regulatory regime, improvements on operational procedures, effective training of personnel onboard and the introduction of more efficient life saving and evacuation appliances and approaches. However attractive (and sometimes necessary) these measures might be, they do not address the root of the problem - namely the ship design concept itself. In this respect, it is particularly alarming to see proposals that undermine the meaningful evolution of the Ro-Ro concept, the most commercially successful ship design. With design-for-safety in mind this paper re-iterates the use of sheer and camber in the design of the Ro-Ro car deck as an efficient means to enhancing survivability drastically and cost-effectively. Two applications of this idea are considered: the first involving a combination of positive sheer with positive camber (PSPC) and the second negative shear with negative camber (NSNC) whilst employing the use of intelligent wash ports (IWP). The impressive enhancement of damage survivability is demonstrated by means of numerical simulation using the suite of software developed at SSRC. The latter is currently being extensively applied by the ferry industry for upgrading, retrofitting and design purposes in the strife of this industry to meet the new demanding survivability standards in the most effective way possible. Following a brief background and a description of the proposed survivability enhancing design ideas, the mathematical/numerical model used to perform the comparative study is briefly explained. The features of the Ro-Ro design and of the damage cases used in the analysis are described next before presenting and discussing the results for the basis ship flat deck (BSFD) design and the two alternatives considered.

BACKGROUND

The Ro-Ro concept provides the capability to carry a wide variety of cargoes in the same ship, thus being able to offer a competitive turn-around frequency with minimum port infrastructure or special shore-based equipment. Short sea routes are dominated by Ro-Ro ships with lorries, trailers, train wagons, containers, trade cars and passengers being transferred from the "outer" regions (UK, Ireland, Scandinavia and Finland) to the "main" land (continental Europe). In the Southern Europe corridors, the Ro-Ro freight service is progressively increasing in volume. The case for a long-distance Ro-Ro service to provide a European maritime highway has also been made several times before. This is particularly relevant and important in respect of fast sea transportation where again Ro-Ro ferries play a prominent role. As a result, the world fleet of Ro-Ro ships has steadily increased over the last 15 years to some 5,000. Over the same period there has been an encouraging reduction in the annual vessel casualty rate. However, the large number of serious casualties for this ship type and the overall loss of life have not shown the same improvement as the casualty rate. The maritime industry is acutely aware of recent shipping casualties involving Ro-Ro ferries,

which have resulted in severe loss of life. These led to safety becoming the main concern with Ro-Ro vessels. Standards for Ro-Ro ship configuration, construction and operation have undergone close scrutiny and new legislation has been put into place aimed at improving the safety of these vessels, notably SOLAS '90, [1] as the new global standard for all existing ferries. However, since the great majority of Ro-Ro passenger ships were designed and built prior to the coming-into-force of SOLAS '90, it is hardly surprising that few of them comply with the new requirements. Furthermore, concerted action to address the water-on-deck problem in the wake of the *Estonia* tragedy led IMO to set up a panel of experts to consider the issues carefully and make suitable recommendations. Following considerable deliberations and debate, a new requirement for damage stability has been agreed among north-western European Nations to account for the risk of accumulation of water on the Ro-Ro deck. This new requirement, known as the *Stockholm Agreement* [2], demands that vessels satisfy SOLAS '90 standards (allowing only for a minor relaxation) with, in addition, a constant height of water on deck. The net effect of these developments in legislation is a massive increase in survivability standards to a level many believe to be unattainable without destroying the very concept industry is extremely keen to defend.

Deriving from this, haphazard attempts to improve Ro-Ro safety by introducing ineffective survivability enhancement devices must give way to rational approaches. The ingenuity of designers must be called upon, and be nurtured, to pave the way towards practical designs for cost-effective safety, in order to ensure both the survival and a meaningful evolution of Ro-Ro ships in the future. Attempting to demonstrate that simple, cost-effective ideas, capable of ensuring the survivability of Ro-Ro vessels whilst retaining the Ro-Ro concept intact are there to be discovered, this paper features two configurations of the main deck, which if optimised could render Ro-Ro ships a safe haven. The analysis presented in the following provides ample evidence that such a concept can be realised and demonstrates beyond doubt the survivability effectiveness of one of the most traditional naval architecture design practices.

THE PROPOSED SURVIVABILITY ENHANCING DESIGN IDEAS

Earlier studies have clearly shown that the decisive factor affecting Ro-Ro damage survivability is the water accumulated on the main deck, [3]. Therefore, any measures to prevent or limit the water accumulation would result in a vessel with enhanced survivability. Should such measures prove effective with the ship damaged at high sea states, it could then be suggested that staying onboard the vessel would be the safest alternative in case of an accident that results in breaching of the hull. This is the idea of a safe haven ship. In the investigation considered here, the level of damage survivability aimed at is $H_s = 4$m over the whole range of feasible loading conditions. This is in accordance with the most severe damage stability requirement currently in force. The idea being advocated here is that of using a curved Ro-Ro deck, rather than a flat deck, (Figure 1), with or without intelligent wash ports as a means of channelling the water on deck to flow out. More specifically, the following two alternatives are examined:

Alternative 1 (PSPC) – Figure 2: Ro-Ro deck with positive sheer and positive camber.

Perceived advantages offered by this idea include:

- In the case of midship damage any water finding its way on the Ro-Ro deck would tend to concentrate in the vicinity of the damage opening because of the fore-and-aft sheer on the deck and flow out.

- In the case of damage forward or aft, the increased freeboard resulting from the deck sheer will ensure that less water reaches the Ro-Ro deck and hence survivability will be improved. Normally, the ensuing trim forward or aft, following respective damages will be conducive to water accumulation towards the vicinity of the damage opening and hence to water egress from the deck.

- Irrespective of the damage location, the presence of positive deck camber potentially provides two additional benefits. Water may flow towards the intact side of the ship resulting in an increased damaged freeboard and hence enhanced survivability. If the ship is inclined towards the damage, the presence of camber in principle impairs water inflow whilst assisting water outflow.

Alternative 2 (NSNC + IWP) – Figure 3: Ro-Ro deck with negative sheer and negative camber together with intelligent wash ports.

Intelligent wash ports are freeing ports with flaps, which passively allow only water outflow, their opening or closing depending on the pressure difference on either side of the flap. The use of these ports has been considered and abandoned on the basis of inconclusive research showing that the overall area of the freeing ports necessary to ensure effective outflow would be too large to offer an attractive solution. The idea put forward here is aimed at minimising the area of opening of the IWP's by utilising again a curved Ro-Ro deck. In a damage scenario resulting in progressive flooding of the Ro-Ro deck, there is a slow build up of water accumulation with the ship heel increasing equally slowly until a point is reached where the heeling effect of the water on deck exceeds the restoring capacity of the vessel. Beyond this point, capsize is inevitable and happens very quickly. Considering the above, if the capacity of IWP's were such as to offset the net inflow of water on deck for the range of loading and environmental conditions the ship is likely to operate in, survivability would be ensured and a safe haven ship could be realised.

Perceived advantages deriving from the idea include:

- Negative deck camber assists in water accumulating near the ship centreline and hence reducing the ship heeling. This is very important, as the damaged freeboard is a critical parameter affecting ship survivability.

- Negative deck sheer assists water flow towards the ship ends where the heeling effect is further reduced due to reduced beam. Additionally, by locating IWP's at the ends water can flow out.

- Negative deck sheer results in increasing damaged freeboards particularly amidships where the ship is the most vulnerable when damaged at this location without having to raise the whole deck which would adversely affect the overall stability of the ship.

- The presence of IWP's would give a Ro-Ro ship a chance in case of accidents similar to the *Herald of Free Enterprise* and the *Estonia* where bow damage with forward speed rendered capsize inevitable and catastrophic.

To assess the survivability and effectiveness of these ideas, use is made of the North West European R&D Project on the "Safety of Passenger/Ro-Ro Vessels" and of the

mathematical/numerical models developed at the Department of Ship and Marine Technology of the University of Strathclyde over the past 10 years.

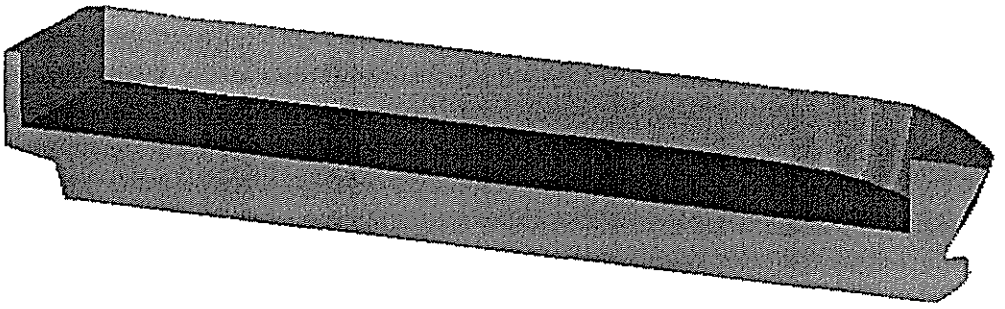

Figure 1 – Basis Ship Flat Deck (BSFD)

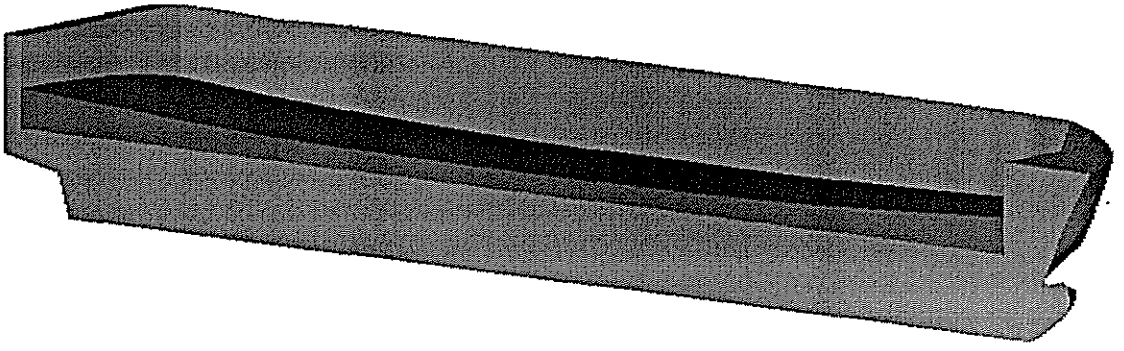

Figure 2 – Positive Sheer Positive Camber (PSPC)

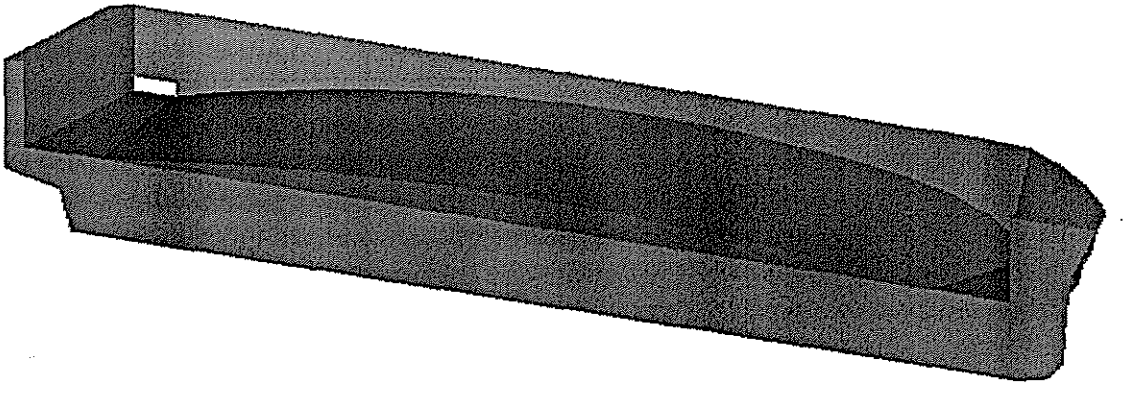

Figure 3 – Negative Sheer Negative Camber + Intelligent Wash Ports (NSNC + IWP)

MATHEMATICAL/NUMERICAL MODELS

Since the dynamic behaviour of the damaged vessel and the progression of the flood water through the damaged ship in a random seaway are ever changing, rendering the dynamic system highly non-linear, the technique used to study such behaviour is time simulation. The numerical experiment considered assumes a stationary ship, beam on to the oncoming waves, with progressive flooding taking place through the damage opening which could be of any shape, longitudinal and transverse extent and in any location throughout the vessel. The simulation begins with pre-defined initial conditions after which the damaged ship starts moving under the action of random beam waves. Instantaneous water ingress is considered by taking into account the wave elevation and ship motions, which are also estimated at each time step. For each case under investigation simulations are carried out for different loading conditions while the sea state used in the calculations is progressively increased to a limit where the ship capsizes systematically, thus allowing for a definition of survival boundaries. The complexity of the problem at hand dictates that several simplifications are adopted in both the mathematical formulation of the damaged vessel motions and of the water ingress in order to derive engineering solutions. The mathematical/numerical models developed at the

University of Strathclyde during the UK Ro-Ro Research Programme and subsequently the North-West European R&D Project have clearly demonstrated that acceptable accuracy could be attained with what appears to involve a high degree of simplification. In the majority of cases considered, a coupled sway-heave-roll model with instantaneous sinkage, heel and trim will normally suffice. Essentially this relates to a three-degree-of-freedom non-linear seakeeping model and a hydraulic water ingress model that allows for water inflow and outflow and associated gravitational forces in a semi-empirical manner, applicable to multiple-compartment flooding and to any vessel subdivision and deck arrangement.

The model considered comprises the following:

$$\{[M(t)] + [A]\} \{\ddot{Q}\} + [B] \{\dot{Q}\} + [C] \{Q\} = \{F\}_{WIND} + \{F\}_{WAVE} + \{F\}_{WOD}$$

with, $[M(t)]$: Instantaneously varying mass and mass moment of inertia matrix.
$[A]$, $[B]$: Generalised added mass and damping matrices, calculated once at the beginning of the simulation at the frequency corresponding to the peak frequency of the wave spectrum chosen to represent the random sea state.
$[C]$: Instantaneous heave and roll restoring, taking into account ship motions, trim, sinkage and heel.
$\{F\}_{WIND}$: Regular or random wind excitation vector
$\{F\}_{WAVE}$: Regular or random wave excitation vector, using 2D or 3D potential flow theory.
$\{F\}_{WOD}$: Instantaneous heave force and trim and roll moments due to floodwater.

The latter is assumed to move in phase with the ship roll motion with an instantaneous free-surface parallel to the mean waterplane. This assumption is acceptable with large ferries since, owing to their low natural frequencies in roll, it is unlikely that flood water will be excited in resonance which is further spoiled as a result of progressive flooding. Indeed, when the water volume is sufficiently large to alter the vessel behaviour, small phase differences are expected between the flood water and ship roll motions. During simulation, the centre of gravity of the ship is assumed to be fixed and all subdivisions watertight.

Considerable effort has been expended to ensure the validity of the numerical simulation program in its ability to predict the capsizal resistance of a damaged vessel in a random sea whilst accounting for progressive flooding, over the whole range of possible applications. These include vessel type and compartmentation (above and below the bulkhead deck), loading condition and operating environment and location and characteristics of damage opening. Such claims have been substantiated by the impressive agreement achieved between theoretical and experimental results spanning a wide range of parameters, [3]. Typical results from ten ships, tested through the "Equivalent Safety" route by numerical and physical model experiments are shown in Figure 4 where the agreement between physical model tests and numerical tests is very convincing, [4]. This is a clear indication of the ability of the mathematical model used to accurately assess the capsizal resistance of a damaged Ro-Ro vessel subjected to large scale flooding. This derives from the accurate modelling of the dynamic system behaviour in the capsize region. This might at first sound surprising, considering how complex the processes involved are, but can be easily explained by the hydrostatically dominated nature of the capsize phenomenon relating to an extensively flooded vessel. With the exception of very few cases the results from both approaches are identical.

In general the agreement between numerical and experimental results has reached a level where any discrepancy of more than 0.25m in critical Hs between the two is considered unacceptable and is normally the cause of a thorough investigation until a satisfactory explanation is found. Typical cases include discrepancies, which are the result of differences in deck permeability of the order of 10% and in heel angle in the order of 0.5^0. The level of confidence in the results of numerical tests is clearly being demonstrated by some ferry owners/operators who proceed with retrofitting plans on the strength of numerical predictions. Efforts are currently under way to collect this and other relevant evidence to prepare a working paper for submission to IMO, aiming for approval to utilise numerical simulation as an alternative route to compliance with damage survivability standards.

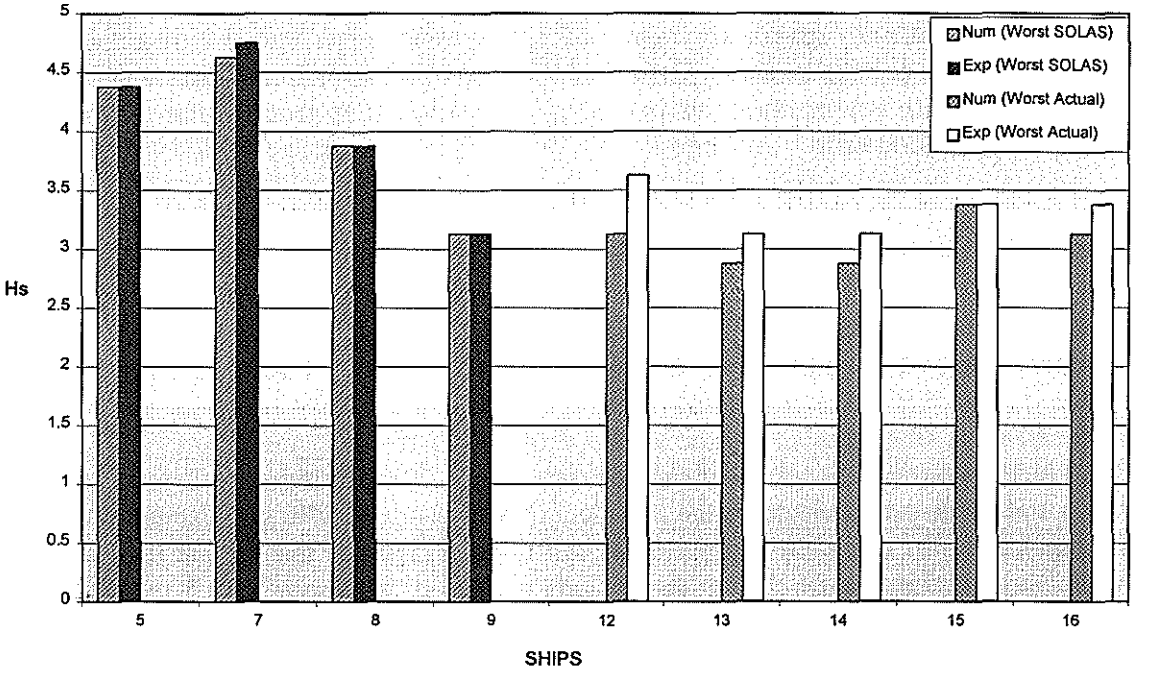

Figure 4 - Comparison Between Numerical and Experimental Results – Critical Hs

CASE STUDY

The case study presented here considers as a basis ship, the flat open deck Ro-Ro vessel NORA which is a generic design used in the North West European R&D Project. The two alternatives explained in the foregoing are also described in detail in this section, following a description of NORA. All three alternatives are illustrated in Figure 5.

Basis Ship

The principal design particulars of NORA are shown in Table 1 and the outline design with the original car deck configuration is illustrated in Figure A.1 of Appendix A.

Table 1: Principal Design Particulars of NORA

Length, $\mathbf{L_{BP}}$	130.00 m
Beam, **B**	25.50 m

Depth to Car Deck, **D**	8.35 m
Draught, **T**	5.75 m
Displacement, Δ	12,000 tonnes
Block Coefficient, C_B	0.612
Intact **KM**	14.26 m
Intact Freeboard, **F**	2.60 m

Alternative 1 (PSPC)

Details of this arrangement are shown in Figure A.2 of Appendix A. The sheer considered is parabolic in shape with maximum values of 1.0 m at the ends and 0.0 m amidships. The camber is also of parabolic shape with a maximum value of 0.2 m at the centreline of the vessel. This choice was made by taking the ratio of maximum sheer to maximum camber in proportion of the L/B ratio.

Alternative 2 (NSNC + IWP)

Details of this arrangement are shown in Figure A.3 of Appendix A. The negative sheer has now a maximum value of 0.8 m amidships at the side of the car deck reducing to 0.0 m at the location of the IWP. The maximum camber is again 0.2 m but with the negative camber considered here, this would correspond to a drop of 0.2 m along the ship centreline with the deck at side following the shape of the negative sheer. This configuration provides therefore for two flat deck portions along the ship length where the IWP's are located. The freeing ports considered in this case study are located at both sides of the ship at the stern and the bow as illustrated in Figure 5 with dimensions of 10.0 m in length by 0.5 m in height. The 20.0 m reduction in the sheered Ro-Ro deck length is the reason for considering a maximum camber of 0.8 m in this alternative rather than 1.0 m as in alternative 1. No optimisation study has been made to determine the most effective dimensions or location of the IWP's for the damage scenarios considered.

Figure 5 – Case Study Alternatives

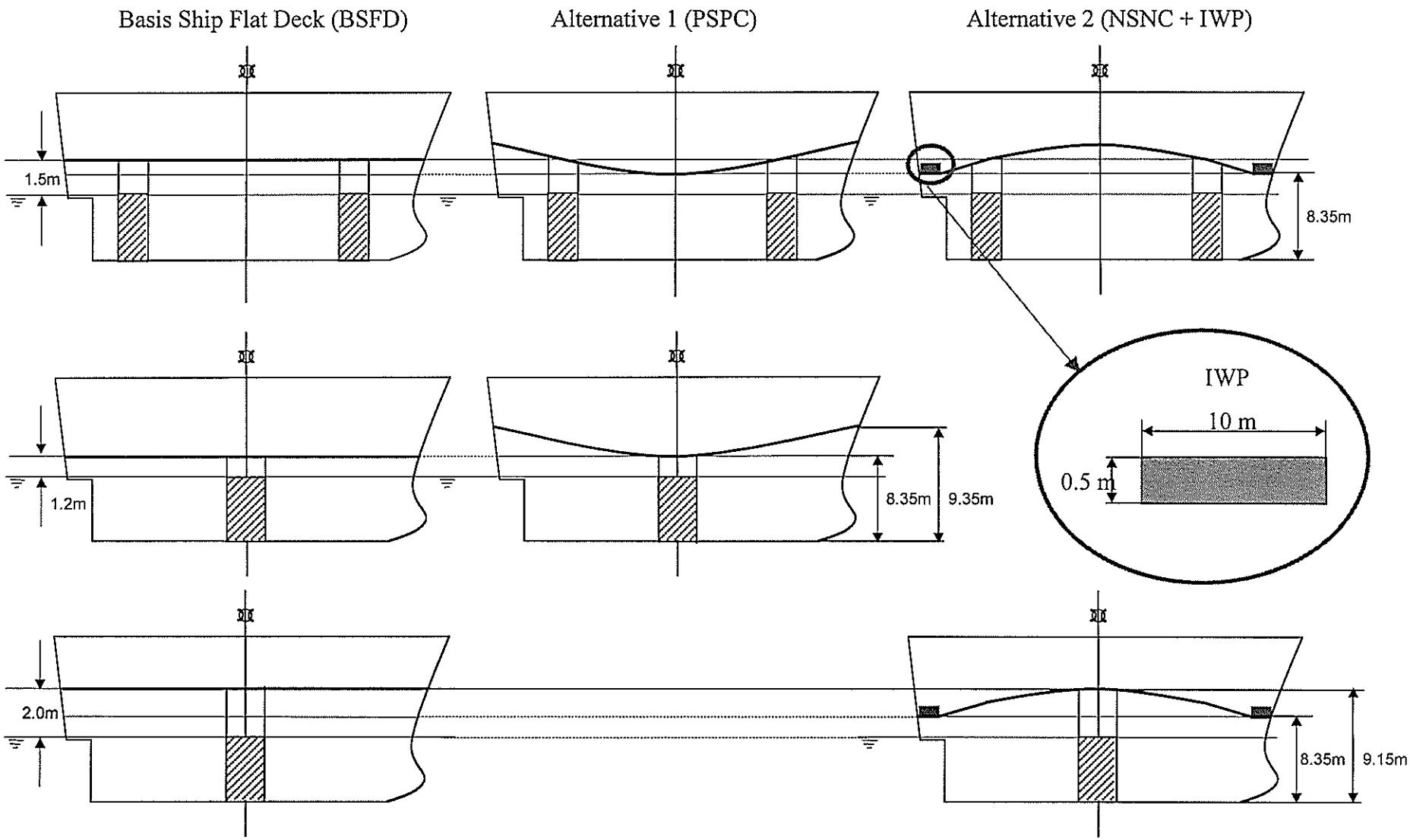

Particulars of Damage

To evaluate the effectiveness of the proposed ideas in enhancing Ro-Ro damage survivability, it was thought appropriate to consider a relatively low damaged freeboard for the basis ship, for ease of illustration of the survivability enhancing effect of the proposed ideas. To this end, the basis ship damaged freeboard was taken to be 1.2 m. Furthermore to eliminate any bias in the results deriving from the difference in the damage freeboards due to the presence of deck sheer, it was considered appropriate to compare the survivability of the various alternatives at the same damaged freeboard. This was achieved by raising in each case the car deck artificially to the right level. In this respect, it is to be noted that the damaged freeboard for both the fore and aft damages at the location of damage is approximately 1.5 m in both alternatives whilst for the midship damage of alternative 2 the damaged freeboard is 2.0 m.

Deriving from the above, the damage cases considered in this case study are given in the Table 2 below referring to all the alternatives and are illustrated in Figure A.4 of Appendix A.

Table 2: Particulars of Damaged Cases

Damage Case	Damaged Freeboard (m)	Damaged Compartment Length (m)	Compartment Location (m)	Damaged KM (m)
Aft	1.5	18.00	-47.00 ÷ -29.00	13.71
Midship	1.2	29.20	-22.43 ÷ 10.00	13.45
	2.0	29.20	-13.80 ÷ 0.50	
Forward	1.5	19.30	19.65 ÷ 43.35	13.23

Parametric Investigation

Considering the damage cases described in the foregoing over the range of possible operational and environmental conditions leads to the test matrix shown in Table 3. With the operational KG at 11.5 m, a ± 0.5 m variation was thought to be representative for the KG operational envelop appropriate to this vessel.

Table 3: Test Matrix

	FLAT DECK			ALTERNATIVE 1		ALTERNATIVE 2	
KG (m)	Damaged Freeboard (m)			Damaged Freeboard (m)		Damaged Freeboard (m)	
	1.2 amidships	1.5 fore &aft	2.0 amidships	1.2 amidships	1.5 fore & aft	1.5 fore & aft	2.0 amidships
11.0	X	X	X	X	X	X	X
11.5	X	X	X	X	X	X	X
12.0	X	X	X	X	X	X	X

WAVE ENVIRONMENT

The wave environment used in the numerical simulations is representative of the North Sea and is modelled by using a JONSWAP spectrum as shown in the table below.

Table 4: Sea States (JONSWAP Spectrum with γ=3.3)

Significant Wave Height $\mathbf{H_s}$ (m)	Peak Period $\mathbf{T_p}$ (s)	Zero-crossing Period $\mathbf{T_0}$ (s)
1.0	4.00	3.13
1.5	4.90	3.83
2.0	5.66	4.42
2.5	6.33	4.95
3.0	6.93	5.42
4.0	8.00	6.25
5.0	8.95	6.99

$$H_s/L_p = 0.04\ (L_p = 25\,Hs);\ T_p = \sqrt{\frac{2\pi L_p}{g}}\ (T_p = 4H_s^{1/2});\ T_0 = \frac{T_p}{1.279}$$

Numerical survivability tests have been undertaken for a significant wave height resolution of 0.25 m. Limiting Hs in the derived results represents the maximum sea state that can be survived repeatedly in each damaged case considered. The norm adopted in presenting the results of numerical simulations and model experiments is to provide a capsize region rather than a capsize boundary to correctly reflect the fact that, because of the random nature of all the parameters determining a capsize event, a single boundary curve does not exist.

RESULTS AND DISCUSSION

The results are presented as survivability bands in the form of critical Hs (i.e. significant wave height characterising a limited sea state from survivability point of view) versus KG, allowing for comparisons between the basis ship and the two alternatives proposed at the corresponding KG and freeboard.

Flat Deck (BSFD) Vs Alternative 1 (PSPC)

Midship Damage – Figure 6a

For open deck Ro-Ro vessels, damage amidships is the most onerous and hence it constitutes the critical damage concerning survivability. This is clearly demonstrated in Figure 6 where the basis ship appears to have very low capsizal resistance, barely managing to survive 3.0 m Hs, even at low KG's. Introducing positive sheer and camber on the deck at levels that could easily be realised, however, results in increasing the damage survivability of the vessel over the required 4.0 m Hs, even at high KG's.

Fore & Aft Damages – Figures 6b & 6c

For open deck Ro-Ro vessels fore and aft damages are normally less onerous than midship damage, as indicated above. It is interesting, however, to demonstrate that even by increasing the damaged freeboard of the basis ship at a level corresponding to the height of the sheered deck at the damage location, alternative 1 still results in a clear improvement of survivability for both damage cases.

Flat Deck (BSFD) Vs Alternative 2 (NSNC + IWP)

Midship Damage – Figure 7a

The importance of freeboard in improving damage survivability is clearly demonstrated in Figure 6, where by increasing the damaged freeboard of the basis ship to 2.0 m, the vessel is capable of surviving over 4.0 m sea states almost throughout the range of possible loading conditions. This example explains clearly and justifies in a way the drive inherent in recent criteria and approaches for assessing survivability towards higher freeboards. However the introduction of curved decks as described in alternative 2 together with moderately sized freeing ports improves survivability beyond these levels by an average of 1.0 m Hs over the whole range considered.

Fore & Aft Damages – Figures 7b & 7c

The potential advantages deriving from alternative 2 are clearly demonstrated in Figure 7 where survival to extreme sea states appears to be realisable, throughout the possible range of interest and well above the survival levels offered by alternative 1.

Figure 6a - MIDSHIP DAMAGE
Freeboard = 1.20 m

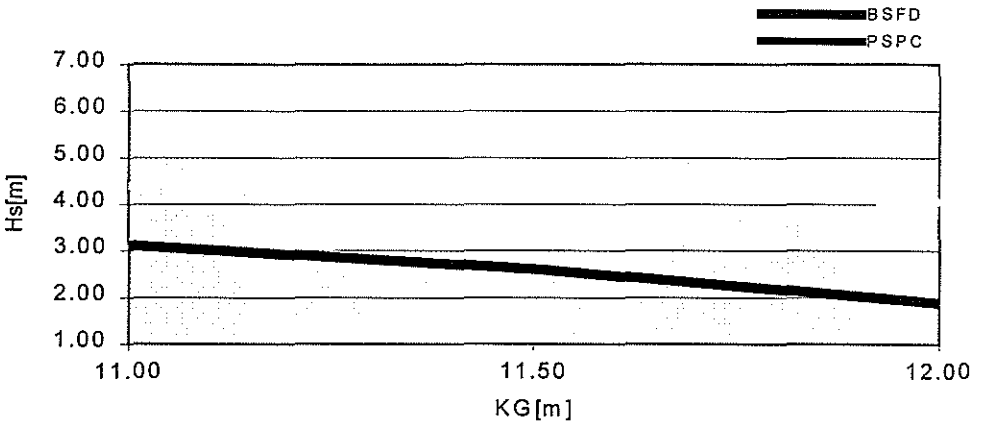

Figure 6b - AFT DAMAGE
Freeboard = 1.50 m

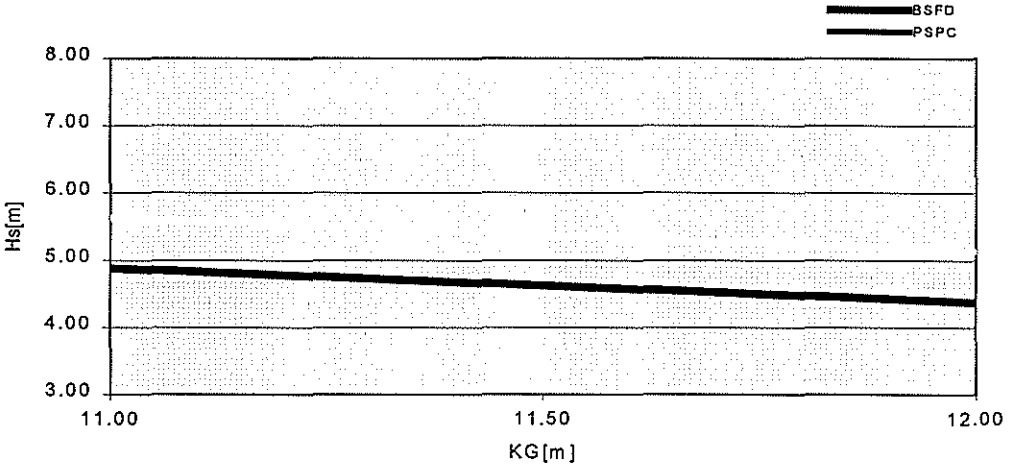

Figure 6c - FORWARD DAMAGE
Freeboard = 1.50 m

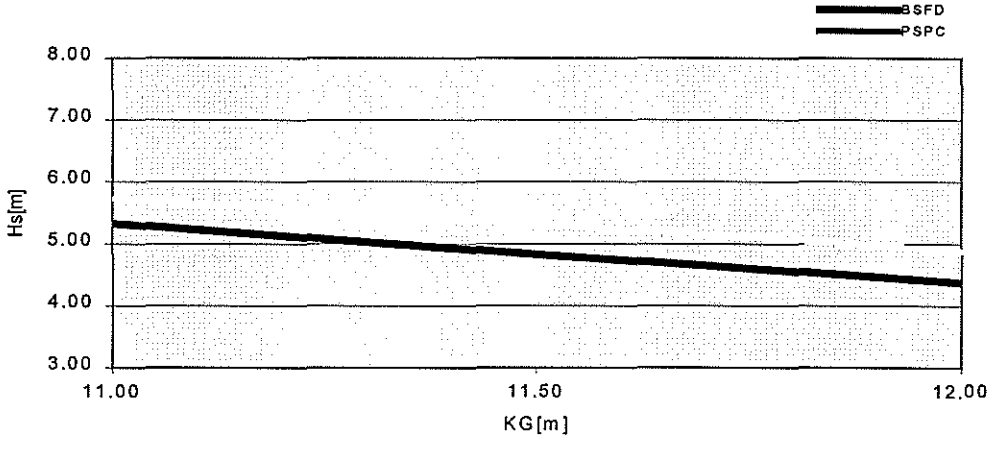

Figure 6 – Comparison Between Basis Ship (BSFD) and Alternative 1 (PSPC)

Figure 7a - MIDSHIP DAMAGE
Freeboard = 2.00 m

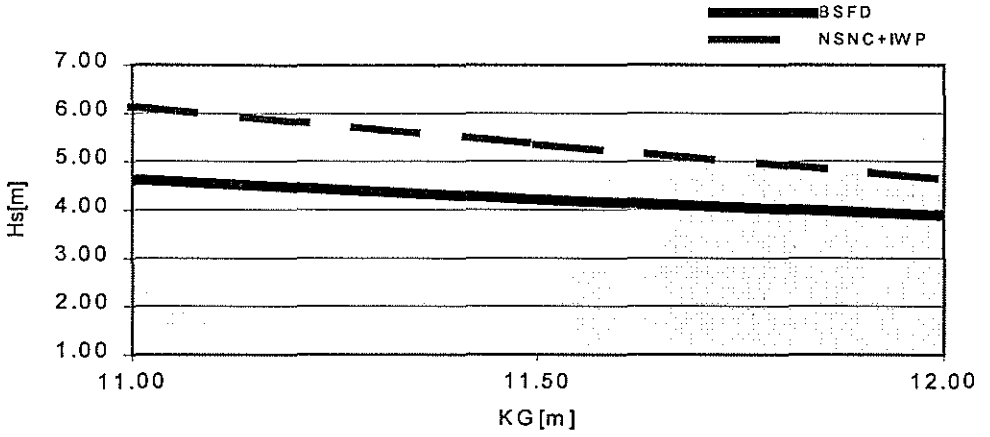

Figure 7b - AFT DAMAGE
Freeboard = 1.50 m

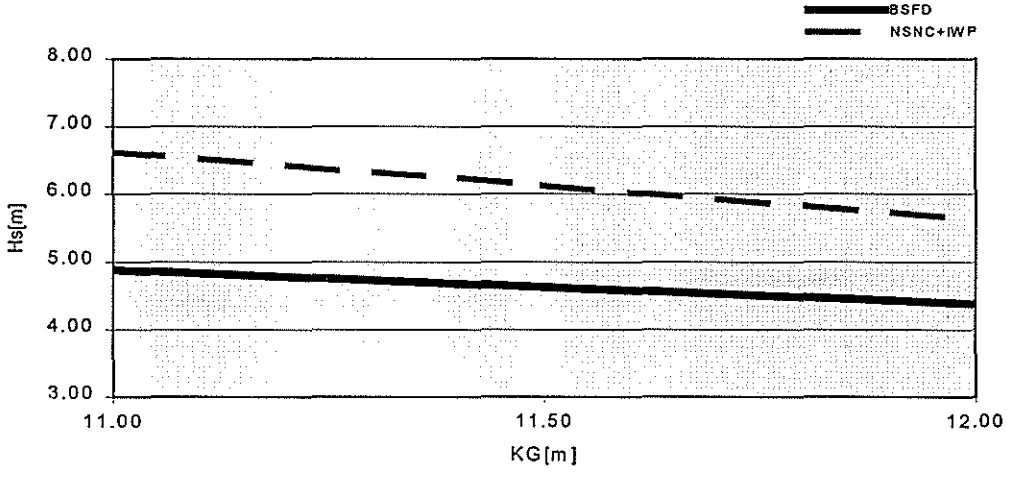

Figure 7c - FORWARD DAMAGE
Freeboard = 1.50 m

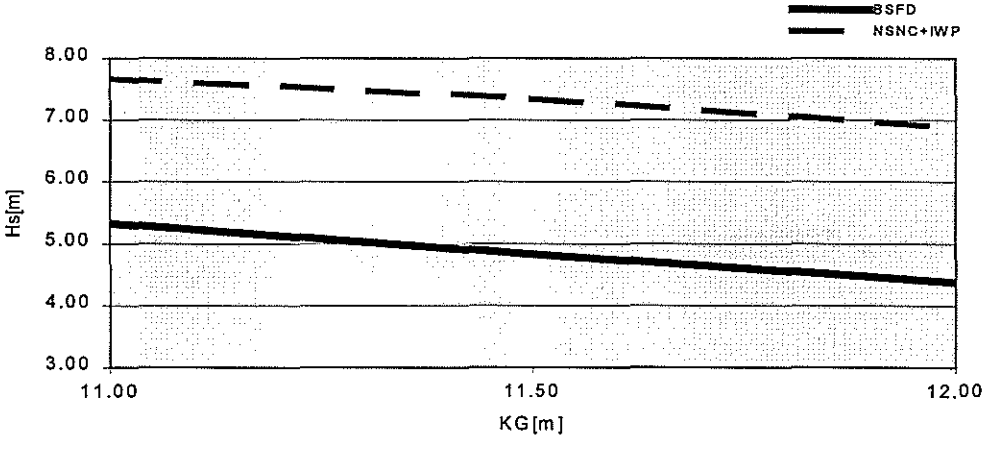

Figure 7 – Comparison Between Basis Ship (BSFD) and Alternative 2 (NSNC + IWP)

CONCLUDING REMARKS

Considering that the proposed design alternatives have not been optimally applied and hence the potential improvements on Ro-Ro damage survivability could be even more pronounced renders the results achieved from the introduction of such simple ideas even more impressive. The parametric investigation undertaken in the foregoing leaves little doubt that curved decks optimally designed to resist flooding and assist outflow could help realise Ro-Ro designs which can achieve acceptably high levels of survivability when damaged whilst preserving the flexibility and operational advantages offered by the open undivided Ro-Ro decks.

The results presented in this study help demonstrate to all concerned that cost-effective ship safety cannot be achieved solely by regulations, particularly when the latter derive from lack of understanding, experience or knowledge of the problem at hand.

Give the designers a chance and they will pave the way to safer ships!

REFERENCES

[1] **IMO Resolution MSC.12 (56) (Annex),** "Amendments to the International Convention for the Safety of Life at Sea, 1974: Chapter II-1 – Regulation 8", adopted on 28 October 1988.

[2] **IMO Resolution 14,** "Regional Agreements on Specific Stability Requirements for Ro-Ro Passenger Ships" – (Annex: Stability Requirements Pertaining to the Agreement), adopted on 29 November 1995.

[3] **Vassalos, D, Pawlowski, M, and Turan, O:** "A Theoretical Investigation on the Capsizal Resistance of Passenger RoRo Vessels and Proposal of Survival Criteria", Final Report, The Joint North West European Project, University of Strathclyde, Department of Ship and Marine Technology, March 1996.

[4] **Vassalos, D:** "Damage Survivability of Passenger/Ro-Ro Vessels by Numerical and Physical Model Testing", WEMT'98, Rotterdam, May 1998.

APPENDIX A

DESCRIPTION OF DESIGN ALTERNATIVES AND DAMAGED CASES

Figure A.1: Basis Ship

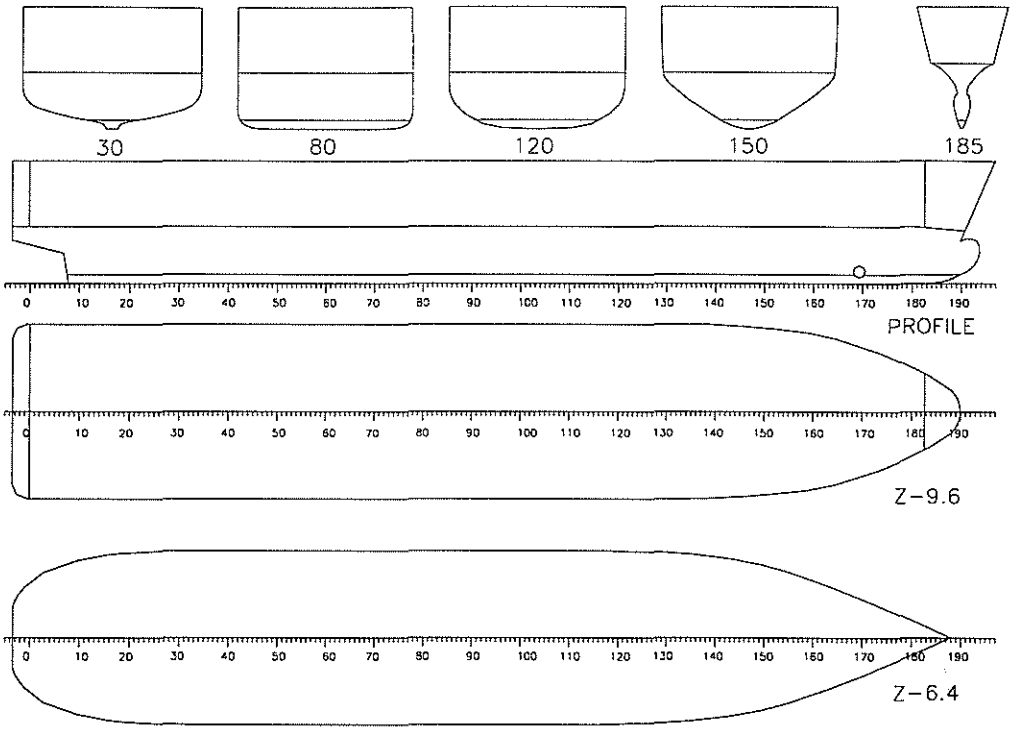

Figure A.2: Alternative 1

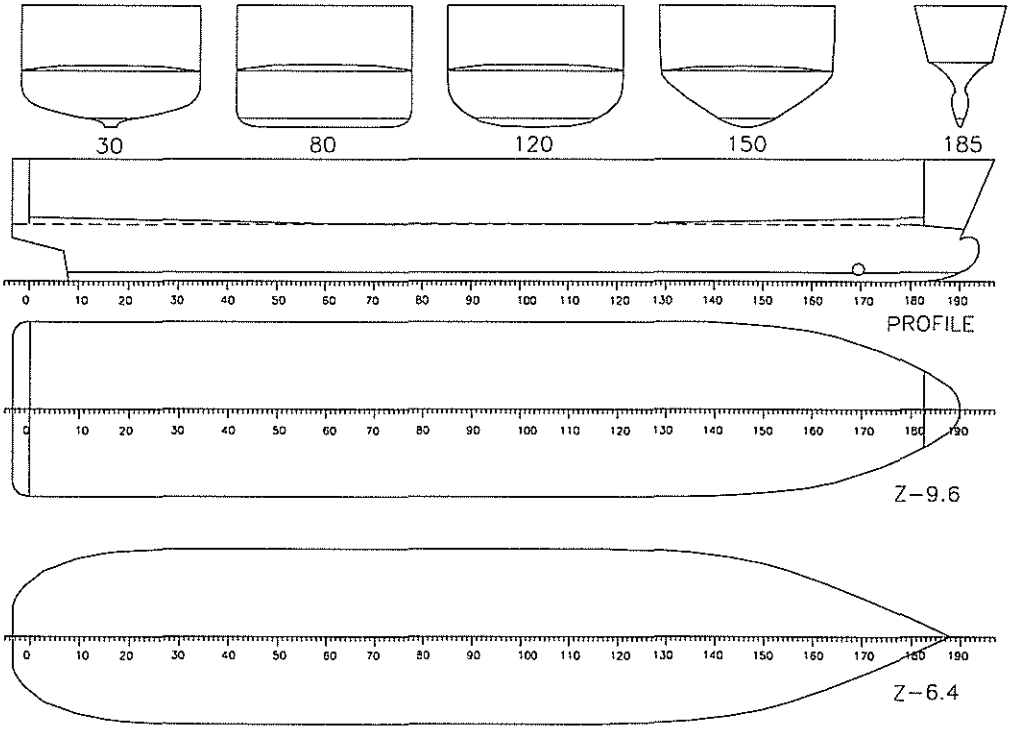

Figure A.3: Alternative 2

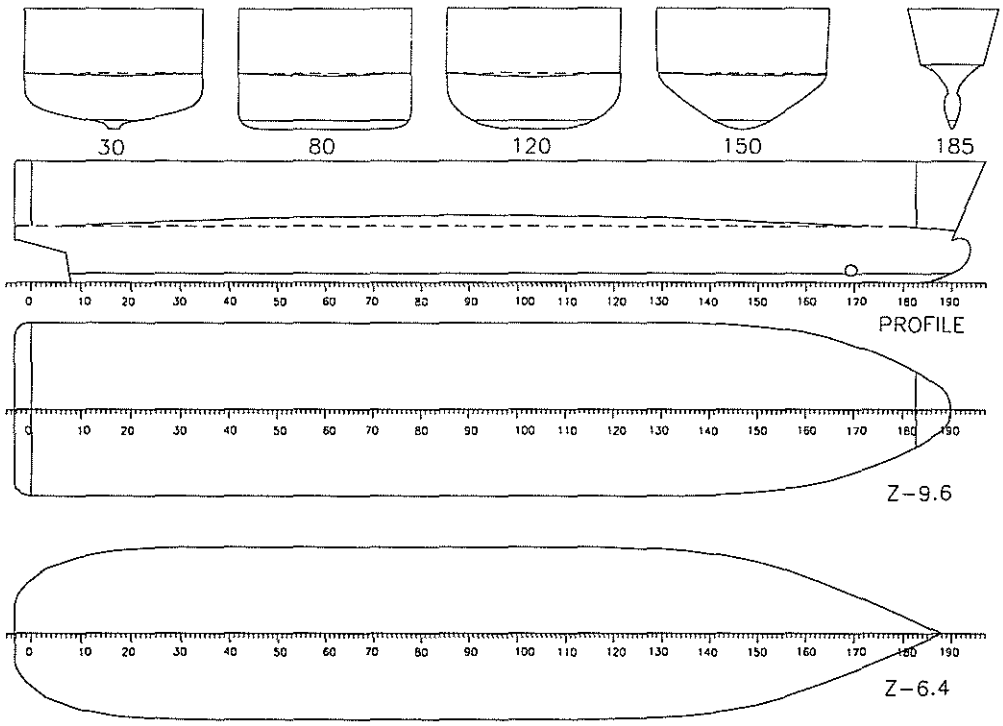

Figure A.4: Damage cases - Aft, Midship and Forward